U.S.NRC
United States Nuclear Regulatory Commission
Protecting People and the Environment

NUREG/CR-7288
Volume 1

Evaluation of In-Service Radon Barriers over Uranium Mill Tailings Disposal Facilities

Office of Nuclear Regulatory Research

AVAILABILITY OF REFERENCE MATERIALS IN NRC PUBLICATIONS

NRC Reference Material

As of November 1999, you may electronically access NUREG-series publications and other NRC records at the NRC's Library at www.nrc.gov/reading-rm.html. Publicly released records include, to name a few, NUREG-series publications; *Federal Register* notices; applicant, licensee, and vendor documents and correspondence; NRC correspondence and internal memoranda; bulletins and information notices; inspection and investigative reports; licensee event reports; and Commission papers and their attachments.

NRC publications in the NUREG series, NRC regulations, and Title 10, "Energy," in the *Code of Federal Regulations* may also be purchased from one of these two sources:

1 **The Superintendent of Documents**
U.S. Government Publishing Office
Washington, DC 20402-0001
Internet: www.bookstore.gpo.gov
Telephone: (202) 512-1800
Fax: (202) 512-2104

The National Technical Information Service
5301 Shawnee Road
Alexandria, VA 22312-0002
Internet: www.ntis.gov
1-800-553-6847 or, locally, (703) 605-6000

A single copy of each NRC draft report for comment is available free, to the extent of supply, upon written request as follows:

Address: **U.S. Nuclear Regulatory Commission**
Office of Administration
Digital Communications and Administrative Services Branch
Washington, DC 20555-0001
E-mail: distribution.resource@nrc.gov
Facsimile: (301) 415-2289

Some publications in the NUREG series that are posted at the NRC's Web site address www.nrc.gov/reading-rm/doc-collections/nuregs are updated periodically and may differ from the last printed version. Although references to material found on a Web site bear the date the material was accessed, the material available on the date cited may subsequently be removed from the site.

Non-NRC Reference Material

Documents available from public and special technical libraries include all open literature items, such as books, journal articles, transactions, *Federal Register* notices, Federal and State legislation, and congressional reports. Such documents as theses, dissertations, foreign reports and translations, and non-NRC conference proceedings may be purchased from their sponsoring organization.

Copies of industry codes and standards used in a substantive manner in the NRC regulatory process are maintained at—

The NRC Technical Library
Two White Flint North
11545 Rockville Pike
Rockville, MD 20852-2738

These standards are available in the library for reference use by the public. Codes and standards are usually copyrighted and may be purchased from the originating organization or, if they are American National Standards, from—

American National Standards Institute
11 West 42nd Street
New York, NY 10036-8002
Internet: www.ansi.org
(212) 642-4900

Legally binding regulatory requirements are stated only in laws; NRC regulations; licenses, including technical specifications; or orders, not in NUREG-series publications. The views expressed in contractor prepared publications in this series are not necessarily those of the NRC.

The NUREG series comprises (1) technical and administrative reports and books prepared by the staff (NUREG–XXXX) or agency contractors (NUREG/CR–XXXX), (2) proceedings of conferences (NUREG/CP–XXXX), (3) reports resulting from international agreements (NUREG/IA–XXXX),(4) brochures (NUREG/BR–XXXX), and (5) compilations of legal decisions and orders of the Commission and the Atomic and Safety Licensing Boards and of Directors' decisions under Section 2.206 of the NRC's regulations (NUREG–0750).

U.S.NRC
United States Nuclear Regulatory Commission
Protecting People and the Environment

NUREG/CR-7288
Volume 1

Evaluation of In-Service Radon Barriers over Uranium Mill Tailings Disposal Facilities

Manuscript Completed: November 2021
Date Published: March 2022

Prepared by:
M. Williams[2]
M. Fuhrmann[3]
M. Stefani[1]
A. Michaud[1]
W. Likos[1]
C. Benson[1]
W. Waugh[2]

[1]Geological Engineering, University of Wisconsin-Madison
1415 Engineering Drive
Madison, WI 53706 USA

[2]RSI EnTech, LLC
Grand Junction CO 81503

[3]U.S. Nuclear Regulatory Commission

Mark Fuhrmann, NRC Project Manager

Office of Nuclear Regulatory Research

ABSTRACT

Earthen final covers over uranium mill tailings and associated wastes were investigated at four sites that had been in service for approximately 20 years: Falls City in Texas, Bluewater in New Mexico, Shirley Basin South in Wyoming, and Lakeview in Oregon. Test pits were excavated, radon fluxes were measured, soil morphological observations made, and samples were collected to determine saturated hydraulic conductivity, soil water characteristic curves, Pb-210 concentrations, and related properties. Similar procedures were conducted at natural analogue sites – nearby locations of undisturbed natural ground used as an indicator of the very long-term state of the covers. Saturated hydraulic conductivity of the Rn barriers at three of the four sites typically fell within the range recommended to represent long-term in-service conditions (1.0×10^{-7} to 5.0×10^{-6} m/s), regardless of depth or thickness of the cover or radon barrier. These saturated hydraulic conductivities are 2 to 3 orders of magnitude higher than the common 1.0×10^{-9} m/s design criterion established for low-conductivity Rn barriers. One Rn barrier was an exception, with some hydraulic conductivities as low as 10^{-11}m/s. A slight increase over the as-built Rn flux was evident for some of the barriers. However, the intentionally biased sampling procedure and differences between the methods used in this study for measuring Rn flux relative to those used in the as-built condition precluded making inferences regarding sitewide in-service Rn fluxes. Rn fluxes were higher in regions where woody vegetation (mesquite, salt bush, and bitterbrush) or aggressive insects had established on the cover, suggesting that the vegetation and insects affected the performance of the barrier in these locations. These higher fluxes are attributed to soil structure induced by root activity and insect burrowing in the Rn barrier, as well as higher Rn diffusion coefficients associated with lower water saturation in areas influenced by root water uptake. A method to use Pb-210 concentration profiles to quantify long-term (decades) Rn-222 fluxes was developed. Soil morphology within the covers is evolving toward a more structured condition, and in some places appears to be approaching a state comparable to the natural analogues.

TABLE OF CONTENTS

LIST OF FIGURES

LIST OF TABLES

EXECUTIVE SUMMARY

Compacted soil materials used to build covers over waste disposal cells do not retain 'as built' properties after being in service for time periods as short as 9 years. This observation resulted from an earlier NRC research project on engineered covers published in December 2011 as NUREG/CR-7028, "Engineered Covers for Waste Containment: Changes in Engineering Properties and Implications for Long-Term Performance Assessment." That report was limited in scope and did not conduct any radon (Rn) studies at uranium mill tailing disposal sites. The NRC subsequently formed the NRC Engineered Covers Technical Group (ECTG) to discuss and review the implications of the findings in NUREG/CR-7028. Following their recommendations, the current project expands upon this earlier research and investigates changes in cover soil properties and on Rn and water transport through engineered covers at uranium mill tailing disposal sites.

A study was conducted to evaluate changes in properties of radon (Rn) barriers in earthen final covers at four disposal facilities for uranium mill tailings that had been in service for approximately 20 yr: Falls City in Texas, Bluewater in New Mexico, Shirley Basin South in Wyoming, and Lakeview in Oregon. Rn barriers are engineered fine-textured earthen barriers placed within final covers that are used to control egress of gaseous Rn emitted from the waste and ingress of water from precipitation. The study was conducted to evaluate how abiotic and biotic processes (e.g., wet-dry cycling, freeze-thaw cycshg1ling, biota intrusion) occurring while the final covers were in service affected the saturated hydraulic conductivity and gaseous diffusivity of the Rn barriers, and how changes in these engineering properties are related to the development of soil structure. The anticipated very long-term naturalized condition was assessed by studying a natural analogue nearby each facility. Descriptions of the sites that were studied are in Section 2.

Test pits were excavated at each site to collect samples and to measure Rn flux. Overburden and protective layers above the Rn barrier were removed to expose the surface of the Rn barrier. Rn flux measurements were made on the surface of the Rn barrier using flux chambers, with the Rn concentration buildup curves measured with an electronic radon monitor (ERM). After the flux measurements on the Rn barrier were completed, samples were collected from the Rn barrier and soil morphological surveys were conducted. Large diameter (400 mm) block samples were collected for saturated hydraulic conductivity and soil water characteristic curve measurements. When possible, samples were collected in a vertical profile to capture conditions existing as a function of depth. Additional samples were collected to determine moisture content, dry unit weight, index properties, and root characteristics. After sampling, excavation into the Rn barrier continued until the surface of the tailings was exposed. Rn flux measurements were made directly on the surface of the tailings for comparison with fluxes measured on the surface of the Rn barrier. At least five test pits were excavated at each site, and as many as eight flux measurements were made in each test pit. After sampling and testing, the final cover was restored to the specifications employed at the time of construction.

Test pits were located in areas where greater change likely occurred to the Rn barrier while in service (e.g., in areas with woody vegetation or insect burrowing), which biased the findings. In some cases, pairs of nearby test pits were excavated to compare areas likely to have greater impact (e.g., areas with woody vegetation) to areas that with less impact (e.g., areas with mowed grass cover). A systematic survey was not conducted to determine a site-wide average Rn flux. Details on site selection, criteria used to select locations of the test pits, and the

conditions that were tested are in Section 2. The inferences made in this report reflect the biased sampling methodology, and may not reflect site-wide conditions.

Hydraulic properties of the Rn barriers are reported in Section 3. Saturated hydraulic conductivities of the Rn barriers ranged from 3.9×10^{-6} to 1.2×10^{-9} m/s for the Falls City site, 4.7×10^{-6} to 1.5×10^{-8} m/s for the Bluewater site, 1.1×10^{-7} to 2.4×10^{-11} m/s for the Shirley Basin site, and 3.2×10^{-6} to 1.1×10^{-7} m/s for the Lakeview site. A limited number of SWCCs were measured. For those that were measured, the saturated water content ranged from 0.29 to 0.50, van Genuchten's α ranged from 0.0018 to 0.30 kPa^{-1}, and van Genuchten's n ranged from 1.14 to 1.36. The saturated hydraulic conductivities for all but the Shirley Basin site fall within the range of 1×10^{-7} to 5×10^{-6} m/s recommended in NUREG/CR-7028 for use in performance assessments. The hydraulic conductivities at Shirley Basin are approximately one to four orders of magnitude lower than the lower bound recommended in NUREG CR-7028, with some approaching 10^{-11} m/s, which is comparable to sodium bentonite. For all sites, the saturated hydraulic conductivities generally are similar regardless of depth of sampling or type of surface (vegetated or rock armored). Saturated hydraulic conductivities of samples from the analogue sites were comparable to or modestly higher than saturated hydraulic conductivities of the blocks removed from each site, and generally were near the upper bound recommended in NUREG CR-7028. The analogue at Shirley Basin was an exception, with saturated hydraulic conductivities ranging from 1.4×10^{-9} to 9.8×10^{-9} m/s.

The Rn-222 fluxes and associated diffusion coefficients computed from the data are in Section 4. Rn-222 fluxes on the surface of the Rn barriers ranged from 0.005 to 1.28 $Bq/m^2/s$ at the Falls City site, 0.002 to 1.26 $Bq/m^2/s$ at the Bluewater site, 0.004 to 0.226 $Bq/m^2/s$ at the Shirley Basin site, and 0.002 to 0.040 $Bq/m^2/s$ at the Lakeview site. The fluxes at Shirley Basin were low despite very high fluxes from the surface of the underlying tailings (up to 397 Bq/m^2-s). Fluxes from the surface of the Rn barrier at the Lakeview site were much lower than at the other sites because the underlying waste contains only a small quantity of Ra-226, and the waste closer to the Rn barrier had low activity.

Fluxes from the surface of the Rn barriers varied with surface treatment (e.g., riprap vs. vegetated) and the surface condition (e.g., woody species present, ephemeral ponding). For example, the geometric mean Rn fluxes on the top deck at the Falls City site was 0.254 $Bq/m^2/s$, whereas geometric mean flux on the side slope was 0.011 $Bq/m^2/s$ (23 times lower). The Rn barrier beneath the apron and on the side slope at Falls City was moist and plastic, whereas the Rn barrier on the top deck was drier and more friable. Similarly, areas where woody and deep-rooted plants had established generally exhibited greater variability in fluxes. For example, in one test pit at the Bluewater site, the Rn-222 flux ranged from 0.11 to 1.26 $Bq/m^2/s$ at separation distances on the order of a meter, suggesting local zones of preferential Rn transport. Comparison of distributions of the in-service fluxes measured in this study relative to distributions of the as-built fluxes indicated that some in-service fluxes as the Falls City and Bluewater sites were higher than any as-built flux. In contrast, at the Shirley Basin site, the in-service and as-built distributions of flux were comparable. However, because the sampling method was deliberately biased, inferences cannot be made regarding the in-service condition relative to the as-built condition.

Diffusion coefficients were determined from the flux data using RAECOM, a 1-D model that calculates the Rn flux based on diffusive transport in the Rn barrier. Diffusion coefficients are computed from the Rn fluxes measured on the surface of the Rn barrier and the surface of the underlying waste. Steady-stay gaseous diffusive transport is assumed. Diffusion coefficients for Rn barriers in RAECOM and other models used for design and analysis are assumed to vary

consistently with water saturation. The findings in this study suggest that this relationship is not valid if preferential pathways developed for Rn transport.

A method to determine the long-term average Rn-222 flux from activity profiles of Pb-210 in the Rn barrier is described in Section 5. Pb-210 is a progeny of Rn-222, with a half-life of 22.3 yr. The method provides a relatively simple technique to assess long-term average Rn fluxes based on Pb-210 present in the upper 100-200 mm of the Rn barrier. Samples for Pb-210 analysis could be collected by drilling and sampling, direct push techniques, or hand auger, precluding the need for disruptive test pits and flux chambers. Because the approach is sufficiently rapid and unobtrusive, the technique could be used for periodic assessment of Rn barriers.

Soil morphology and soil chemistry of the earthen. materials in the test pits and at the analogue sites are described in Section 6. Morphological properties that were determined include horizon/material thickness, boundary, Munsell color, pedality/structure (size, shape and grade, consistence), root morphology per unit area (abundance, diameter, class), shape and size of void structures or animal excavations, rupture resistance, and descriptions of inclusions. Anomalous morphologies were also recorded. Gravimetric moisture content profiles were also determined. Soil samples were collected from each horizon from at least five locations for measurements of organic matter content, total carbon, nitrogen, hydrogen, macro- and micronutrients, nitrogen speciation, calcium carbonate, electrical conductivity (EC), pH, and particle size.

Soil structure developed in all of the Rn barriers in response to plant root growth, volume change due to root water uptake, and biota intrusion (e.g., insect burrowing). With few exceptions, roots were observed throughout the depth of the Rn barriers. Roots were found near the bottom of the Rn barrier at each site. Deep-rooted woody plants and harvester ants contributed to greater structural development than other biota. For example, in the vegetated section of cover at the Falls City site, the Rn barrier was drier and friable, containing remnant soil structure from the borrow area with clods of mixed sizes delineated by hairline fractures that served as preferred sites for water flow, iron precipitation, and root mats. At the Shirley Basin site, the Rn barrier is composed of a montmorillonite rich clay with little structure. Although fine roots did penetrate the barrier, the root development was less extensive than at other sites, resulting in less soil structure, lower Rn flux, and lower saturated hydraulic conductivity. Root growth at Shirley Basin apparently was tempered by acidic conditions within the Rn barrier. Similar conditions were observed at the analogue sites.

Morphological characteristics at each site and each analogue were quantified using the soil morphological development score (SMDS), which incorporates texture, pedality, macroporosity, root density, and water content. The SMDS ranged from as low as 5 (Falls City site) to as high as 10,688 (Bluewater site), with higher SMDS corresponding to greater structure. The scoring system was used to assess the impact of soil morphology on the saturated hydraulic conductivity and Rn diffusion coefficients. Generally, as the SMDS increased, the hydraulic conductivities and Rn diffusion coefficients also increased.

ACKNOWLEDGMENTS

The authors are grateful for the many persons who contributed to this project. They include Joseph Kanney, Michael Salay, Hans Arlt, Sarah Tabatabai, and Karen Dickey (USNRC), Jiannan Chen (U. Central Florida), Xiaodong Wang (U. Wisconsin), Laurel Larsen (U. California Berkeley) David Dander, Ray Johnson, Anthony Martinez, Aaron Tigar, and Chris Holmes.

This report was peer reviewed by: Nicholas Kiusalaas (RSI Entech/DOE-Legacy Management Support), Stephen Dwyer (Dwyer Engineering, LLC) and William Albright (Desert Research Institute, emeritus). Peer review, by four anonymous reviewers, for the sections on Pb-210 and radon flux also resulted from the publication of two journal articles. We thank all those reviewers.

This research is a collaboration between the DOE Office of Legacy Management (LM) and the Nuclear Regulatory Commission with funds provided by both agencies. Investigators are from the University of Wisconsin, University of Virginia, University of California at Berkeley, Navarro Research and Engineering Inc. (the former DOE/LM contractor), RSI Entech/DOE-Legacy Management (the current DOE/LM contractor) and NRC. Additional support was provided by DOE/EM through the Consortium for Risk Evaluation with Stakeholder Participation (CRESP).

ABBREVIATIONS AND ACRONYMS

ASTM	American Society for Testing and Materials
Bq/g	becquerels per gram
$Bq/m^2/s$	becquerels per meter square per second
CFR	*Code of Federal Regulations*
cm	centimeters
cm/s	centimeters per second
CMB	compacted mineral barrier
D	diffusion coefficient (m^2/s)
D_{Rn}	diffusion coefficient for radon
DOE	U.S. Department of Energy
DOE/EM	U.S. Department of Energy/Environmental Management
DOE/LM	U.S. Department of Energy/Legacy Management
EC	electrical conductivity
ECTG	Engineered Covers Technical Group
EPA	U.S. Environmental Protection Agency
ET	evapotranspiration
K_{sat}	saturated hydraulic conductivity
LM	Office of Legacy Management
LTS&M	long-term surveillance and maintenance
LMS	Legacy Management Support
LTSP	long-term surveillance plan
MDA	minimum detectable activity
mm	millimeters
NRC	U.S. Nuclear Regulatory Commission
NRCS	Natural Resources Conservation Service
Pb	lead (isotope)
$pCi/m^2/s$	picocuries per square meter per second
PNV	potential natural vegetation
$_pSMDS$	partial soil morphological development score
Ra	radium (isotope)
RAECOM	Radiation Attenuation Effectiveness and Cover Optimization with Moisture Effects
RCRA	Resource Conservation and Recovery Act of 1976
Rn	radon (isotope)
SMDS	soil morphological development score
SWCC	soil water characteristic curve

$_{t}$SMDS	total soil morphological development score
S_r	soil moisture saturation (%)
SOM	soil organic matter
UMTRCA	Uranium Mill Tailings Radiation Control Act
USDA	U.S. Department of Agriculture

1 INTRODUCTION

The Radon Barriers Project (formally called *Effectiveness of Surface Covers for Controlling Fluxes of Water and Radon at Disposal Facilities for Uranium Mill Tailings*) is a research program created to study the effects of changes in the properties of in-service engineered earthen covers over uranium mill tailings as these covers age. The purpose of this study is to evaluate the effects of soil structure formation by abiotic and biotic processes on the hydraulic conductivity and gaseous diffusivity of radon barriers, how structural development varies with depth and thickness of the radon barrier, and how structure influences transmission of radon and seepage of water through radon barriers. This research is a collaboration between the DOE Office of Legacy Management (LM) and the NRC, with investigators at the University of Wisconsin, University of Virginia, University of California at Berkeley, and Legacy Management Support (LMS, the DOE contractor). Additional support was provided by DOE/EM through the Consortium for Risk Evaluation with Stakeholder Participation (CRESP).

The research team visited four uranium mill tailing sites: Falls City in Texas, Bluewater in New Mexico, Shirley Basin South in Wyoming, and Lakeview in Oregon. Small areas on these sites were excavated, radon fluxes were measured, numerous observations were made, and samples were taken for a variety of parameters, such as saturated hydraulic conductivity, root counts, moisture, density, lead (Pb)-210 concentrations, soil texture, chemistry, and nematode counts. This report provides the findings of that work.

1.1 Regulations

Congress passed the Uranium Mill Tailings Radiation Control Act (UMTRCA) of 1978 (PL 95-604) to provide for the safe and environmentally sound disposal and long-term stewardship of uranium mill tailings. Under UMTRCA, Congress (1) directed the U.S. Environmental Protection Agency (EPA) to establish cleanup performance standards and to mandate remedial actions in accordance with the standards, (2) assigned the U.S. Nuclear Regulatory Commission (NRC) responsibility as the federal regulator to license the disposal facilities, and (3) assigned the U.S. Department of Energy (DOE) responsibility for custody and long-term care of uranium mill tailings sites. In 1983, EPA issued performance standards for the cleanup of inactive uranium mill sites (Title 40 *Code of Federal Regulations* Section 192 [40 CFR 192], subparts A, B, and C). In 2003, DOE created the Office of legacy Management (LM) to manage licensed UMTRCA sites and other World War II and Cold War environmental waste legacy sites.

In 1985, the 10th Circuit Court of Appeals set aside the groundwater provisions of UMTRCA and remanded them to EPA. In 1987, EPA published draft groundwater standards in response to the 1985 ruling. In April 1989, DOE began incorporating the draft performance standards for water quality under the assumption that the standards would soon become final. In 1995, EPA replaced existing provisions with 40 CFR 192.20[a][2] and [3] which requires that remedial action be conducted to ensure that the amounts of radioactive and associated hazardous constituents in groundwater derived from uranium mill tailings meet certain concentration standards.

UMTRCA defined two types of sites. Sites designated as Title I were inactive (milling had ceased and their milling licenses had been terminated before 1978 when UMTRCA was passed). Sites designated as Title II had active milling licenses in 1978 or were issued a license

after 1978. Congress assigned DOE responsibility for remediating Title I sites and assigned the licensee responsibility for remediating Title II sites.

Separate general licenses are established for Title I and Title II sites. NRC regulates remediated Title I sites under 10 CFR 40.27, and regulates remediated Title II sites as stipulated in 10 CFR 40.28. Both require that monitoring, maintenance, and emergency measures be established in site-specific Long-Term Surveillance Plans (LTSPs). When NRC concurs that a remedial action is complete and accepts the site specific LTSP, DOE assumes responsibility for custody and long-term care of the UMTRCA disposal site under the general license. For Title II sites, the licensee provides funding for inspections, monitoring, and maintenance. DOE then develops an LTSP and accepts title to the site for custody and long-term care. Finally, if processing-related groundwater contamination is present beneath a disposal site, the site will not be fully licensed until groundwater quality satisfies the applicable EPA standards.
Several license criteria in 10 CFR 40, Appendix A, are relevant with respect to the objectives of the Radon Barrier Study:

- The "general design goal or broad objective in siting and design decisions is permanent isolation of tailings and associated contaminants by minimizing disturbance and dispersion by natural forces, and to do so without ongoing maintenance."
- A "full, self-sustaining vegetative cover or rock cover [is required] to reduce wind and water erosion to negligible levels."
- An earthen cover (or approved alternative) over wastes is required to control radioactive and other hazardous for up to 1000 years, to the extent reasonably achievable, and, in any case, for at least 200 years.
- Cover designs are required to provide reasonable assurance that releases of radon-222 (^{222}Rn) from residual radioactive material to the atmosphere will not (1) exceed an average release rate of 20 picocuries per square meter per second, or (2) increase the annual average concentration of ^{222}Rn in air at or above any location outside the disposal site by more than one-half picocurie per liter. These averages apply over the entire surface of the disposal site and over at least a 1-year period.
- Remediation designs are also required to provide reasonable assurance of conformance with groundwater protection standards imposed by EPA under 40 CFR 192, Subparts D and E; and groundwater monitoring is required.

Additional information can be found at https://www.nrc.gov/reading-rm/doc-collections/fact-sheets/mill-tailings.html and https://www.energy.gov/lm/articles/us-department-energy-office-legacy-management-2015-umtrca-title-i-and-title-ii-disposal.

1.2 Overview of the Radon Barriers Project

1.2.1 Drivers and Objectives

A major impetus for much of this work was NUREG/CR-7028, "Engineered Covers for Waste Containment: Changes in Engineering Properties and Implications for Long-Term Performance Assessment," issued in December 2011. The report assesses the performance of engineered covers in terms of percolation of water through the covers at disposal sites that were not UMTRCA facilities. All of the covers documented in the report (27 test sections at 12 sites) were vegetated with a mixture of annual and perennial grass mixtures. No covers were studied with a riprap surface or without vegetative root systems. Changes in cover hydraulic properties (saturated hydraulic conductivity and the alpha parameter for the soil water characteristic curve) both increased, indicating the formation of larger pores as a result of pedogenic processes such

as wet-dry and freeze-thaw cycling. These changes were observed on materials that had been in place for time periods of 3.8 to 8.9 years.

The NRC established the Engineered Covers Technical Group (ECTG) to discuss and review the implications of NUREG/CR-7028. Their review is documented in Arlt et al. (2011), which noted that an important conclusion of the report is that "compacted soil materials used in cover materials do not retain 'as built' properties over the period of regulatory interest as assumed in most performance assessments. The properties of these materials change to values typical of surrounding soils within 5 to 10 years after installation. For some properties the change may be several orders of magnitude, which may potentially lead to increased water infiltration and augmented radon flux out of the system." However, the sites discussed in that report were generally not uranium mill tailing sites and all were vegetated, whereas most mill tailing sites have rock covers.

No radon studies were conducted or reviewed for NUREG/CR-7028; in fact, few, if any, studies of radon emissions after the initial closure survey have been conducted at mill tailings disposal sites. However, that report showed that hydraulic conductivity of barrier materials increases over time. A reasonable inference is that radon emissions may also increase, as discussed in Chapter 5, "Potential for Increased Radon Release due to Processes Documented in NUREG/CR-7028," of Arlt et al. (2011). The ECTG made a number of suggestions, and some of these evolved into the Radon Barriers Project.

1.2.2 Radon Barriers Project Sites

The Radon Barriers Project team assembled a list of 24 sites that were evaluated as potential research sites using parameters, such as climatic influence, vegetation, barrier vulnerability, source activity, and NRC priority, derived from Arlt et al. (2011). Four sites were selected; Table 1-1 gives some of their general properties and details are presented in Chapter 2, showing: their locations, climate information, images of the sites, test pit descriptions, and plant ecology information for each site.

Table 1-1 Radon Barriers Project Research Sites

Site	Title	Closure Date	Cover Area Acres	Type of Cover	Waste Tons	Waste Activity (curies of radium-226)
Falls City	I	1994	127	Veg	7,100,000	1277
Bluewater	II	1995	354 main cell	Rock	23,000,000	11200
Shirley Basin S	II	2000	142	Veg	5,300,000	974
Lakeview	I	1988	16	Rock/Veg	926,000 cubic yards	42

LMS staff prepared an extensive field work plan document for the work to be conducted at each site. These plans include maps and cover diagrams and the field workflow for excavation, sampling, measurements, and site restoration to the original construction criteria. They also contain sections on safety and health, training requirements, and environmental management. The NRC staff conducted a National Environmental Policy Act review in accordance with NUREG-1748, "Environmental Review Guidance for Licensing Actions Associated with NMSS Programs," issued August 2003, and concluded that the actions were categorically excluded under 10 CFR

51.22(c)(6). As such, the NRC staff did not prepare an environmental assessment; a categorical exclusion checklist provided documentation. Field work was planned at analogue sites for each location. If needed, a cultural resources survey (archeological reconnaissance (Phase III)) was conducted.

After completion of the field research, each pit was refilled with the various soil types that had been excavated and saved in separate piles. The radon barrier material was restored to the required density, and moisture content and a radon flux check was conducted. Closure reports were prepared by LMS staff, documenting the test results to demonstrate that the excavations had been closed to the required criteria.

1.3 References

Arlt, H., R.L. Johnson, D. Mandeville, G. Alexander, M. Meyer, J. Philip, J. Kanney, M. Fuhrmann, and T. Johnson, "Documentation of the Engineered Covers Technical Group (ECTG) Activities by U.S. NRC Staff," 2011 (ADAMS Accession No. ML112300105), U.S. Nuclear Regulatory Commission, Washington DC.

NUREG-1748, "Environmental Review Guidance for Licensing Actions Associated with NMSS Programs," 2003, U.S. Nuclear Regulatory Commission, Washington DC.

Benson, C,H. W.H. Albright, D.O. Fratta, J.M. Tinjum, E. Kucukkirca, S.H. Lee, J. Scalia, P.D. Schlicht, and X. Wang, 2011, NUREG/CR-7028, "Engineered Covers for Waste Containment: Changes in Engineering Properties and Implications for Long-Term Performance Assessment," 2 volumes, U.S. Nuclear Regulatory Commission, Washington DC.

2 BACKGROUND INFORMATION, STUDY SITE SELECTION, AND PLANT ECOLOGY

2.1 Introduction

This section contains background information, descriptions of the methods developed for selecting disposal sites and test pit sampling locations on disposal cell covers, brief histories of selected disposal sites, and discussions of the attributes of disposal sites and sampling locations that led to their selection. Background information includes the regulatory setting, an overview of uranium mill tailings disposal sites and cover designs, and routine long-term stewardship activities. The section also describes the selection process for and attributes of natural analogue sites (natural areas that can provide clues about potential long-term changes in engineered covers), and descriptions of vegetation on covers and at analogues sites.

2.2 Background

2.2.1 UMTRCA Disposal Sites and Engineered Covers

Although UMTRCA Title I and Title II sites occur throughout the United States, the majority are in the western states (Figure 2-1). In 1978, Congress designated 22 inactive uranium-ore processing sites for remediation under Title I of UMTRCA. Many of these sites were essentially abandoned when UMTRCA was passed in 1978. Remediation of the 22 sites resulted in the creation of 19 engineered disposal cells that contain uranium mill tailings and associated contaminated material. Tailings and contaminated material from three sites were relocated and placed in other disposal cells. In 2001, when the licensee became insolvent, Congress directed DOE to remediate the Atlas mill site near Moab, Utah, under Title I. Moab was originally a Title II site. As of August 2019, DOE/LM manages 19 Title I and 6 Title II disposal sites. NRC anticipates licensing Moab as a Title I disposal site and another 24 Title II sites by 2050.

Figure 2-1 Map of Current and Anticipated Title I and Title II UMTRCA Sites Managed by Office of Legacy Management as of August 2019

2.2.1.1 Early Designs

Before EPA promulgated groundwater quality criteria for UMTRCA sites, the design process for engineered covers focused on radon attenuation and longevity standards. These early designs consisted basically of three layers: (1) a compacted clayey soil layer or "radon barrier" overlying the tailings, (2) either a rock riprap or planted soil layer at the surface for erosion control, and (3) a bedding layer of coarse sand or gravel underlying the riprap.

Radium-226 (^{226}Ra) and ^{222}Rn are daughter progeny of uranium-238. Radon-222 is a colorless, odorless, radioactive gas with a half-life of 3.8 days. Conceptually, with a low radon barrier diffusion coefficient, ^{222}Rn would decay several half-lives, significantly reducing in concentration as it travels to the surface. NRC accepted calculations of ^{222}Rn attenuation using the computer program RAECOM, later called RADON (NRC 1989), as a basis for compliance. The mathematical model implemented in RAECOM describes one-dimensional, steady-state radon diffusion through a two-phase multilayer system. The properties that most influence ^{222}Rn flux are the soil moisture content of the radon barrier, the radon diffusion coefficient for the radon barrier, ^{226}Ra activity in the tailings, and the ^{222}Rn emanation fraction for the tailings (Smith et al. 1985). At drier sites, ^{222}Rn flux is particularly sensitive to the radon barrier water content and porosity; ^{222}Rn diffusion is elevated when interconnected pore spaces are filled with air (NRC 1989). NRC considers the long-term soil water content of the radon barrier to be the parameter that introduces the greatest uncertainty in ^{222}Rn attenuation calculations. In the absence of field data, NRC accepts the soil water content at −1500 kilopascals (−15 bar) of suction pressure, often defined as the permanent wilting point, as a reasonable value of the long-term soil water content of the radon barrier (DOE 1989). The thickness of the radon barrier is computed by a

trial-and-error procedure until the calculated ^{222}Rn flux at the surface is less than 20 picocuries per square meter per second (pCi/m^{2}s) (0.74 becquerel per square meter per second; Bq/m^{2}s). The necessary thickness of the radon barrier can be minimized if materials with low ^{226}Ra activity are placed as the waste layer directly underlying the radon barrier.

The rock riprap armoring most UMTRCA covers was designed to protect the underlying radon barrier and tailings from erosion. The design process for the rock riprap centered on the erosion potential and the 1000-year longevity standard. The rock armor was sized to prevent erosion of underlying layers given a probable maximum precipitation event, the most severe combination of meteorological and hydrological conditions possible at a site (DOE 1989). The selection of stone for the riprap layer was based on conservative rock durability standards and tests provided by NRC (2002) to ensure survivability of the armor.

2.2.1.2 Low-Permeability Designs

After EPA published draft groundwater quality standards, DOE refined the cover design process and placed greater emphasis on designing "low-permeability" radon barriers (DOE 1989). DOE informally adopted a standard specified in the Resource Conservation and Recovery Act of 1976 (RCRA) for designing low-permeability caps for disposal of hazardous waste in shallow-land burial facilities. RCRA guidance requires a compacted soil layer with a saturated hydraulic conductivity less than 10^{-9} meters per second (m/s) and that is equal to or less permeable than the liner material underlying the tailings (EPA 1989). The latter requirement was intended to prevent water from ponding, or "bath tubbing," in the tailings. DOE design guidance indicated that low conductivity could be achieved with either highly compacted native soil or bentonite-amended soil (DOE 1989). The new guidance also provided a framework or checklist for selecting and designing cover components based on site-specific needs. This approach gave options for adding components to the original design including a thick "protection layer" intended to isolate the radon barrier from processes that could increase permeability such as freeze-thaw cracking and biointrusion.

After DOE adopted 10^{-9} m/s as a design target for the radon barrier, an increasing body of literature suggested that the saturated hydraulic conductivities of compacted soil layers achieved in the field were much greater than that predicted by laboratory tests. Processes that initiate these changes include freeze-thaw and desiccation cracking (Kim and Daniel 1992; Benson and Othman 1993; Albrecht and Benson 2001), retention of borrow soil structure during construction (NRC 2011; Albright et al. 2006), and biointrusion (Hakonson 1986; Suter et al. 1993; Bowerman and Redente 1998).

2.2.2 Long-Term Surveillance and Maintenance Activities

LM conducts long-term surveillance and maintenance (LTS&M) activities under the general license granted by NRC in accordance with 10 CFR 40.27 for Title I sites and 40.28 for Title II sites. LTS&M activities at these sites include site inspections; maintenance; monitoring; institutional controls; corrective actions; and administrative functions such as records management, stakeholder relations, and regulatory interactions. LTS&M of disposal cells consists of annual inspections, groundwater monitoring (in most cases), maintenance, and corrective actions in accordance with the site-specific LTSPs. LTSPs contain methods and procedures established by DOE and approved by NRC to verify compliance with license requirements. Guidance for site inspections, monitoring, and maintenance is based on the assumption that disposal cells are designed to be effective for 200 to 1000 years and are

constructed so that “ongoing active maintenance is not necessary to preserve isolation” of radioactive material (DOE 2012).

2.2.3 Site Inspections

LTSPs require site inspections to document the visible condition of the disposal cell; identify changes or new conditions in surface features that may affect the long-term performance of the disposal cell; and identify any problems that may require maintenance, follow-up inspections, or corrective actions with respect to the condition of visible surface features (DOE 2012). Inspections are also intended to detect progressive changes in surface features over several years that may occur as a result of natural processes. This is accomplished by comparing sequences of inspection results to baseline conditions as recorded in the completion reports. NRC regulations (10 CFR 40; NRC 2003) require follow-up inspections in response to unusual observations from routine inspections and extreme natural events. Results of follow-up investigations have led to revisions of LTSPs. The Burrell, Pennsylvania, Disposal Site is an example. At Burrell, the LTSP required annual herbicide applications to control plant encroachment on the cover. A follow-up investigation found that root intrusion had indeed increased the saturated hydraulic conductivity of the cover. However, a subsequent risk-based performance assessment found that the increased hydraulic conductivity was highly unlikely to increase risks to human health and the environment (DOE 1999). As a result, NRC accepted a revised LTSP that allows plants to grow without further intervention, thus significantly reducing annual maintenance costs.

2.2.3.1 Performance Monitoring

LTSPs also describe “long-term environmental monitoring activities that are necessary to maintain and demonstrate protectiveness, and comply with applicable regulatory requirements” including groundwater monitoring “to determine if the cell is performing as designed” (DOE 2012). However, LTSPs do not require direct monitoring of cover performance (protectiveness) with respect to radon attenuation or rainwater percolation. Groundwater monitoring is an indirect means of determining if the disposal cell is functioning as designed with respect to limiting water movement into tailings. This strategy assumes that detection of elevated levels of tailings constituents in groundwater samples could indicate that the cover is allowing rainwater to pass into tailings. This retrospective approach (after-the-fact detection) does not provide an early warning if natural processes acting on cover soil layers were to cause unacceptable increases in water percolation (Waugh 2006).

2.2.3.2 Routine Maintenance and Emergency Measures

The stated purpose for site maintenance is “to preserve site function and conditions (i.e., to ensure protection of human health and the environment)” (DOE 2012). Routine activities are primarily custodial such as road maintenance, grass mowing, and control of noxious weeds. Repairs are related to observations of changes in surface features such as erosion and rock riprap degradation. LTSP guidance also includes provisions for emergency measures to correct severe damage to disposal cells such as from erosion and differential settlement. However, guidance for routine maintenance and emergency measures does not address possible changes in subsurface features of disposal cells. Specifically, the guidance does not address natural changes in the engineering properties of low-permeability radon barriers that could reduce protectiveness with respect to radon diffusion and rainwater percolation.

2.2.4 Study Site Selection Objectives and Bias

The study site selection process evolved to address several objectives that can be summarized as sets of general questions:

Soil morphology: Can we identify and quantify soil-forming processes that are changing as-built engineering properties of UMTRCA covers? How does soil formation vary for ranges of cover thicknesses, soil types, ecological conditions, and climates? Is soil formation in covers systematic, predictable, and depth-dependent?

Soil engineering: Can we measure depth-dependent effects of soil formation on radon diffusion, radon flux, and hydraulic properties of radon barriers? Can we improve field monitoring and modeling of radon flux and water percolation in covers that have been altered by soil-forming processes?

Long-term performance: Can we project the long-term effects of ecological and soil-forming processes on radon flux and water percolation in radon barriers?

To achieve these objectives, selection of uranium mill tailings disposal sites and test locations on disposal cell covers was not random but intentionally biased. The selection process identified disposal sites and test locations on covers where researchers anticipated the greatest changes in cover performance—the worst case conditions, not the average conditions. Disposal sites were selected (1) that generally scored high with respect to propensity for radon diffusion and hydraulic conductivity, and (2) that encompassed a broad range of cover designs, climates, and ecological conditions. The process for selecting test conditions and sampling locations on disposal cell covers incorporated a combination of as-built design data, radiological data, and observations of surface ecology. Researchers used this information to identify areas on disposal cells where they anticipated the greatest changes in soil morphology and related engineering properties and the highest radon flux rates. Selection methods and results for disposal sites and for test conditions on disposal cells are in Sections 2.3 and 2.4, respectively.

2.3 Disposal Site Selection

The process for selecting UMTRCA disposal sites for study advanced through two phases: (1) an initial ranking of all Title I and II sites based on attributes such as design vulnerability, climatic influence, vegetation, source activity, and regulatory priority, and (2) a follow-up selection that emphasized contrasting environments (climates and ecologies) and different cover designs. The Bluewater, New Mexico, Disposal Site scored highest in the initial ranking (Phase I) and also had the greatest variety of cover designs. Three additional disposal sites scored relatively high in the initial ranking and offered the greatest opportunity to compare sites with different designs and environments (Phase II): Falls City, Texas; Shirley Basin South, Wyoming; and Lakeview, Oregon.

2.3.1 Phase I Methods: Initial Ranking

All UMTRCA Title I and II disposal sites within the LM portfolio were included in the initial ranking. Each site was graded as high, medium, or low for eight attributes (Appendix A) with the hierarchy in context of propensity for radon flux (a high score corresponded to potentially high radon flux). Sites were also graded with regard to their proximity to urban areas. Finally, each site received an Overall Opportunity grade based on an average attribute score, with each attribute given a numerical score of 3 for high, 2 for medium, and 1 for low. Average attribute

scores were tallied both including and excluding Urban Proximity (Table 1). Sites were assigned an Overall Opportunity grade of high for an average score ≥ 2.3, low for an average score ≤ 1.7, or medium otherwise. The four highest scoring disposal sites (including and excluding Urban Proximity) were Bluewater (2.78, 2.75); L-Bar, New Mexico (2.33, 2.38); Mexican Hat, Utah (2.33, 2.38); and Ambrosia Lake, New Mexico (2.11, 2.25). Bluewater was selected as the first study site.

2.3.2 Phase II Methods: Contrasting Designs and Environments

The three highest scoring sites in the initial ranking after Bluewater (L-Bar, Mexican Hat, and Ambrosia Lake) are all similar to Bluewater with respect to cover designs, climates, and ecologies, and are all located in the Southwest within a 270 kilometer radius of Bluewater. Researchers reasoned that the study would have broader applicability if sites with contrasting environments and cover designs were compared. Therefore, as an alternative to studying four similar sites, researchers modified the selection process to include sites that encompassed broad ranges of cover designs and environments within the DOE/LM portfolio.
Appendix B lists site attribute categories and selection rationale for cover designs, climates, soils, and vegetation that researchers considered when selecting contrasting sites. Only sites with an initial ranking of medium or high (both with and without urban proximity) in Phase I (Appendix A) were considered for Phase II.

2.3.3 Attributes of Selected Sites

An assessment of site attributes compiled in Appendix C led to selection of three additional sites that were thought to provide the greatest opportunity for comparisons of different designs in the same environment and of similar designs in different environments, and that encompassed a broad range of UMTRCA designs and disposal cell environments: Falls City, Shirley Basin South, and Lakeview (Table 2-2). The cover design and climate for Falls City contrasted most with Bluewater. Shirley Basin South and Falls City have similar cover designs but very different climates and ecologies. Shirley Basin is cold and semiarid while Falls City is humid and subtropical. Lakeview and Bluewater also have similar cover designs but different climates and ecologies. The following sections compare the features of the four sites that led to their selection. Appendix D provides brief histories of uranium ore processing and remedial actions at the four sites.

2.3.3.1 Cover Designs

Bluewater is a Title II site with several disposal cells (Table 2; Appendix D; ARCO 1996). The three largest are the main, carbonate, and acid cells. The main and acid disposal cells have relatively thin 2-layer cover designs (Figure 2-2). The main cell (by far the largest at 143 hectares) has a 50–75 centimeter (cm) thick low-permeability radon barrier overlying sand tailings on the southern portion of the cell and a 50 cm thick radon barrier overlying slime tailings on the northern portion of the cell. A layer of low-activity windblown tailings and soil was placed above the slime tailings (below the radon barrier) on the norther portion of the cell. The term “slime tailings” is used here to refer to the finer particle tailings that settle out last in solution and are generally observed in down gradient locations in legacy tailings piles. The radon barrier on the carbonate disposal cell, constructed to fill and level the undulated surface that resulted from the disposal of building debris and other rubble, varies in thickness from less than 30 cm overlying the highest points to greater than 300 cm overlying the deepest swales. The main and carbonate cell covers are armored with 10–30 cm of basalt riprap. The top deck of the cover for the relatively flat acid disposal cell along the northwest edge of the main tailings

cell has a 20 cm thick radon barrier and 20 cm of topsoil. The topsoil was seeded with warm-season native grasses for erosion protection.

Falls City is a Title I disposal cell with different covers on the top deck and side slope (Table 2; Appendix D; DOE 1996). Whereas the Bluewater main and acid cells have the simplest and thinnest UMTRCA covers managed by LM, the Falls City top deck is one of the more complex and thickest. The top deck cover design consists of a 90 cm thick, compacted clay, low-permeability radon barrier; a 75 cm layer of soil considered to be suitable as a plant growth medium and protection layer; and a 15 cm layer of topsoil that was seeded with a mixture of native and introduced warm-season hay grasses (Figure 2-2). The side-slope cover has a 60 cm thick clay radon barrier overlain with a 15 cm layer of gravel bedding material and a 40 cm layer of rock riprap.

Shirley Basin South is a Title II site (Table 2-2; Appendix D; Petrotomics 2001). Shirley Basin and Falls City have similar top deck and side slope covers but very different climates (see Section 2.4.3.2). The Shirley Basin disposal cell has top deck covers sloped at about 20:1 on two large terraces separated by a rock-armored, interior embankment sloped at about 5:1. The top deck cover has a 60 cm compacted clay radon barrier, a 60 cm silty sand overburden or protection layer, and a 25 cm topsoil layer (Figure 2-2). The topsoil was seeded with a mixture of cool-season native and introduced forage grasses. The interior slope cover has the same radon barrier and protection layer design but with a 12 cm thick granite riprap armor overlying a 10 cm filter (bedding) layer instead of topsoil and vegetation.

Lakeview is a Title I site with a disposal cell cover similar to Bluewater (Table 2; Appendix D; DOE 1991) and a climate similar to Shirley Basin South (see Section 2.4.3.2). The top deck and side slope covers have a 45 cm thick low-permeability radon barrier placed over contaminated materials, a 15 cm sandy gravel bedding layer placed over the radon barrier, and a 30 cm thick basalt riprap armor (Figure 2-2). DOE placed a 15 cm topsoil layer above the riprap on the top deck and seeded it with a mixture of cool season grasses. Soil has since moved into rock interstices in some places.

2.3.3.2 Climates

The four study sites are located in different regions of the West that collectively span a broad range of climate indices and parameters (Table 2-2; Figure 2-3). Bluewater, in the desert Southwest, has a cold semiarid climate, one of the drier UMTRCA sites and the driest of the four study sites. Seasonal precipitation is dominated by the North American Monsoon System (https://www.climate.gov/news-features/blogs/enso/north-american-monsoon) with nearly half of annual precipitation arriving during the growing season: July, August, and September (Figure 2-3). In sharp contrast, Falls City has a humid, subtropical climate, one of the wetter and warmer UMTRCA sites and the wet

Table 2-1 Attributes of UMTRCA Title I and Title II Sites Considered for Field Evaluation of Radon Flux From an In-Service Cover

Site	Urban Proximity	Climatic Influence		Vegetation	Barrier Vulnerability	Source Activity	Depth to Source	Borrow Source	NRC Priority	Overall Opportunity			
		Aridity	Seasonality							With Urban		Without Urban	
Ambrosia Lake	Low	High	High	Low	High	Low	High	Medium	Medium	Medium	2.11	Medium	2.25
Bluewater	***High***	***High***	***Medium***	***Medium***	***High***	***High***	***High***	***High***	***High***	***High***	***2.78***	***High***	***2.75***
Burrell	High	Low	Low	High	High	Medium	High	Low	Medium	Medium	2.11	Medium	2.00
Canonsburg	High	Low	Low	High	High	Medium	--	--	Medium	Medium	2.11	Medium	2.00
Durango	High	Medium	Medium	Medium	Medium	High	Medium	Medium	Low	Medium	2.11	Medium	2.00
Green River	High	High	Medium	Low	High	Low	High	Medium	Low	Medium	2.11	Medium	2.00
Grand Junction	High	High	Medium	Medium	Medium	High	Low	Medium	Low	Medium	2.11	Medium	2.00
Gunnison	High	High	Medium	Low	Medium	Medium	Medium	High	Low	Medium	2.11	Medium	2.00
Edgemont	High	Medium	Medium	Medium	High	Medium	High	--	Low	Medium	2.22	Medium	2.13
Falls City	High	Low	Medium	High	High	Medium	Low	High	Medium	Medium	2.22	Medium	2.13
L-Bar	Medium	High	Medium	High	High	Medium	Medium	High	Low	High	2.33	High	2.38
Lakeview	High	Medium	High	High	High	Medium	Low	High	Medium	High	2.44	Medium	2.25
Lowman	Low	Low	Medium	Medium	High	Medium	High	--	Low	Medium	1.89	Medium	2.00
Maybell	High	Medium	Medium	Low	Medium	Medium	Medium	Low	Low	Medium	1.78	Low	1.63
Maybell West	High	Medium	Medium	Low	Medium	Low	Medium	Low	Low	Low	1.67	Low	1.50
Mexican Hat	Medium	High	Medium	Low	High	High	Medium	Medium	High	High	2.33	High	2.38
Naturita	High	Medium	Medium	Low	Medium	Low	High	Medium	Low	Medium	1.89	Medium	1.75
Rifle	High	High	Medium	Low	Low	Medium	Medium	Low	Low	Medium	1.78	Low	1.63
Salt Lake	Low	Medium	High	Low	Low	Medium	High	Medium	Low	Medium	1.78	Medium	1.88
Sherwood	Low	High	High	Medium	Low	Low	--	Medium	Low	Medium	1.78	Medium	1.88
Shiprock	High	High	Medium	Low	Low	Medium	--	High	Medium	Medium	2.11	Medium	2.00
Shirley Basin S.	Low	High	Medium	Medium	High	Medium	--	--	Low	Medium	2.00	Medium	2.13
Slick Rock	High	Medium	Medium	Medium	Medium	Low	Medium	Medium	Low	Low	1.67	Medium	1.75
Tuba City	High	High	Medium	Low	High	Low	Low	Medium	High	Medium	2.11	Medium	2.00

Note: Overall opportunity is based on the average total score for site, with each attribute scored 3 for high, 2 for medium, and 1 for low (urban proximity excluded). A score of 2 was assigned to attributes without a qualitative score. An overall score of high was assigned to sites with an average score ≥ 2.3, low for an average score ≤ 1.7, and medium otherwise.

Table 2-2 Contrasting Cover Designs, Climates, and Ecologies of Uranium Mill Tailings Sites Selected for the Study

Site	Title[1]	Top Deck Cover Designs[2]	Climate Class[3]	Ann Temp Max/Min (°C) Precip (mm)[4]	Soil Regime[5]	Potential Natural Vegetation[6]	Deep-Rooted Plants[7]	Vegetation Development Score[8]	Tailings Activity/ Dry Tons[9]
Bluewater, New Mexico	II 1995	Rock/ Barrier (20/76) NP	Arid, Cold Steppe (Semiarid)	21.3/1.4 267	Aridic-Ustic/ Mesic	Grama Galleta Steppe	ATCA ULPU 3%	High (8.0)	11,200 $2.3x10^7$ (4.87)
Falls City, Texas	I 1994	Soil/ Rooting/ Barrier (15/76/91) P	Temperate, Hot Summer Without Dry Season	26.9/14.3 721	Udic-Ustic/ Hyper thermic	Mesquite/ Acacia Savanna	PRGL 2%	Low (3.5)	1277 $7.1x10^6$ (1.80)
Shirley Basin S., Wyoming	II 2000	Soil/ Rooting/ Barrier (25/61/61) P	Arid, Cold Steppe (Semiarid)	11.3/-5.1 279	Ustic-Aridic/ Frigid	Grama/ Needlegrass/ Wheatgrass	ASCI ATCA 1%	Low (2.5)	974 $5.3x10^6$ (1.84)
Lakeview, Oregon	I 1988	Soil/Rock/ Bedding/ Barrier (15/30/15/46) P	Continental, Hot Dry Summer	15.5/0.8 374	Xeric/ Frigid	Sagebrush Steppe	PUTR ARTR ERNA 5%	High (8.5)	42 $9.3x10^5$ (4.52)

[1] Uranium Mill Tailings Radiation Control Act (UMTRCA) Title I or Title II and the year the disposal cell was completed.

[2] Climate classes are from an updated Koppen-Geiger climate map (Peel et al., 2007).

[3] Mean annual maximum and minimum temperatures (°C) and mean annual precipitation in millimeters (mm) (www.usclimatedata.com).

[4] Cover layer types and thicknesses in centimeters (cm) from the surface down to tailings: Rock = rock riprap layer, Bedding = course sand or gravel bedding for rock, Rooting = rooting medium or protection layer overlying the radon barrier, Barrier = low-permeability radon barrier. NP = not planted and P = planted. All four sites had two or more cover designs. The table shows top deck designs and the Main Tailings Cell cover for Bluewater. Other designs are listed below.
Bluewater Carbonate Cell: rock/barrier (20 cm/varying thickness up to 240 cm), NP.
Bluewater Acid Cell: soil/barrier (15/20), P
Falls City Side Slope: rock/bedding/barrier (41/15/61), NP
Shirley Basin Terrace Slope: rock/bedding/rooting/barrier (15/10/61/61), NP
Lakeview Side Slope: rock/bedding/barrier (30/15/46), NP

[5] Soil moisture/temperature regimes (nrcs.usda.gov/wps/portal/nrcs/detail/soils/use/maps/).

[6] Potential natural vegetation (PNV) types are from a 2000 version of the Kuchler (1964) PNV map (firelab.org/document/potential-natural-vegetation-groups-v2000).

[7] Genus and species for potentially deep-rooted plants growing on disposal cell covers are from the U.S. Department of Agriculture Plants Database (www.plants.usda.gov). Plant acronyms are the first two letters of the genus followed by the first two letters of the species: ATCA (*Atriplex canescens*, fourwing saltbush), ULPL (*Ulmus pumila*, Siberian elm), PRGL (*Prosopis glandulosa*, honey mesquite), ASCI (*Astragalus cicer*, chickpea milkvetch), PUTR (*Purshia tridentata*, antelope bitterbrush), ARTR (*Artemisia tridentata*, big sagebrush), ERNA (*Ericameria nauseosa*, rubber rabbitbrush). Percent cover values are estimates from 2014 site inspection reports (www.lm.doe.gov).

[8] The vegetation development score was calculated based on a combination of changes in plants species (e.g., grasses to shrubs) and changes in plant abundance on the cover, form the time of construction.

[9] Total curries of ^{226}Ra in the disposal cell, dry tons of tailings and other materials (e.g., mix of windblown tailings and soil), and ^{226}Ra activity per dry ton in parentheses.

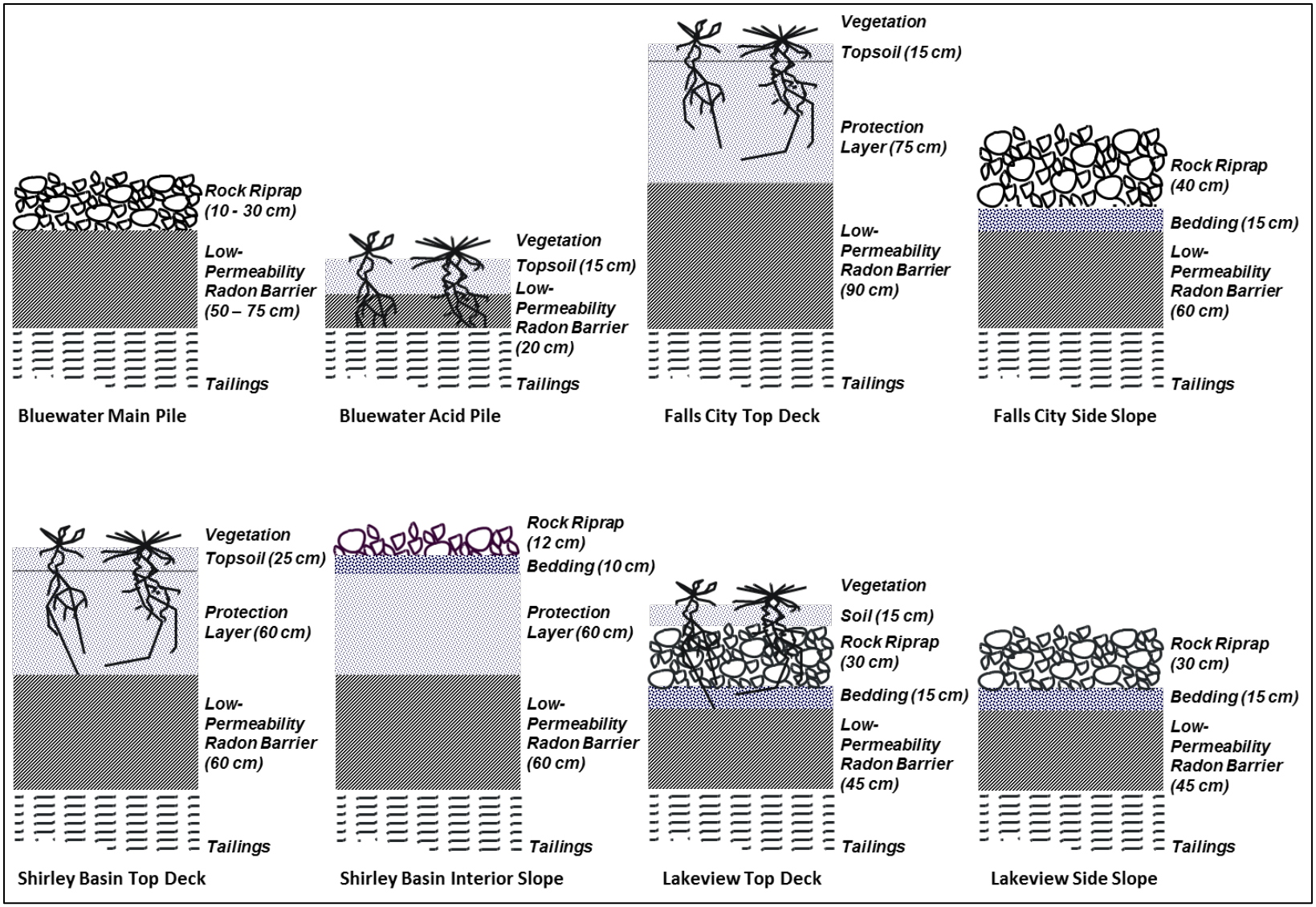

Figure 2-2 Cross Sections of Engineered Cover Designs at the Four Sites Selected for Study

and warmest of the four study sites. Falls City receives more than 2.5 times the average annual precipitation as Bluewater and is an average 9.2 °C warmer. Falls City precipitation peaks in late spring and again in early fall (Figure 2-3). Shirley Basin South, the coldest UMTRCA site, has a cold semiarid (bordering on a boreal continental) climate. Shirley Basin is an average 6.3 °C colder than Bluewater and 15.5 °C colder than Falls City. Annual precipitation is similar to Bluewater but with a much weaker summer monsoon peak. Lakeview has a continental (bordering on a cold semiarid) climate with a dry summer. Lakeview is more than 100 millimeters (mm) per year wetter than Bluewater but with no summer monsoon. Precipitation at the Lakeview site peaks seasonally as winter snow; summers are dry.

2.3.3.3 Soils

The four study sites also have contrasting soil types and soil moisture and temperature regimes. Researchers used UMTRCA site completion reports and online U.S. Department of Agriculture (USDA) soil surveys (https://websoilsurvey.sc.egov.usda.gov/App/HomePage.htm) to compare and contrast the taxonomic classes of soils "borrowed" to construct radon barriers for the four sites. The USDA soil classifications reflect the dominant factors active during soil formation at a particular location. Comparable to the Linnean system used in biology, the USDA system of soil taxonomy (Soil Survey Staff 1999) consists of a hierarchy of six levels (in order from most general to most specific): Order, Suborder, Great Group, Subgroup, Family, and Series. Hence, the Orders and taxonomic classes (Table 3) of soils borrowed to construct radon barriers contain information about soil properties and formation such as texture (particle size distribution), minerology, activity of clay surfaces, climate, and stage of soil development. Soil moisture regime names (Table 2-4) indicate the presence or absence of soil water available for use by plants. Soil temperature regime names reflect mean annual soil temperatures and seasonal temperature differences at a depth of 50 cm, which also greatly influence plant habitat.

The Sparank-San Mateo Complex at Bluewater consists of very deep, well drained, very to moderately slowly permeable soils that formed in fan and stream alluvium derived from shale and siltstone. The silt clay soils are slightly effervescent; strongly alkaline; and, as Entisols, have little horizon development. As aridic-ustic mesic soils, they are either dry or with limited moisture present at 50 cm depth at times when conditions are suitable for plant growth, and have a mean annual soil temperature of 8 °C or higher but lower than 15 °C with more than 6 °C difference between mean summer and mean winter soil temperatures. The Torida Clay at Falls City is also a well-drained, very slowly permeable soil. However, in sharp contrast with Bluewater, these smectitic vertisols formed in clayey material overlying weathered mudstone and sandstone containing volcanic ash and shards, and have moderately developed blocky structure in thick illuviation horizons. Also, in sharp contrast with Bluewater, soils are udic-ustic hyperthermic, usually have adequate plant-available water at 50 cm depth, and have a mean annual soil temperature of 22 °C or higher with more than 6 °C difference between mean summer and mean winter soil temperatures. Drews Loam at Lakeview is also a very deep, well-drained soil, but that formed in alluvium and some lacustrine sediments weathered from basalt, tuff, and rhyolite. As a mollisol, Drews Loam has distinct horizonation and thick illuviation layers of clay and clay loam with medium platy, prismatic, and blocky structure. Soils are dry in summer and moist in winter (xeric moisture regime) but are colder than at Bluewater, with a mean annual temperature lower than 8 °C at 50 cm with more than 6 °C difference between mean summer and mean winter soil temperatures (frigid temperature regime). Shirley Basin South soils have a moisture regime similar to Bluewater, although a bit drier in the summer, with a temperature regime similar to Lakeview.

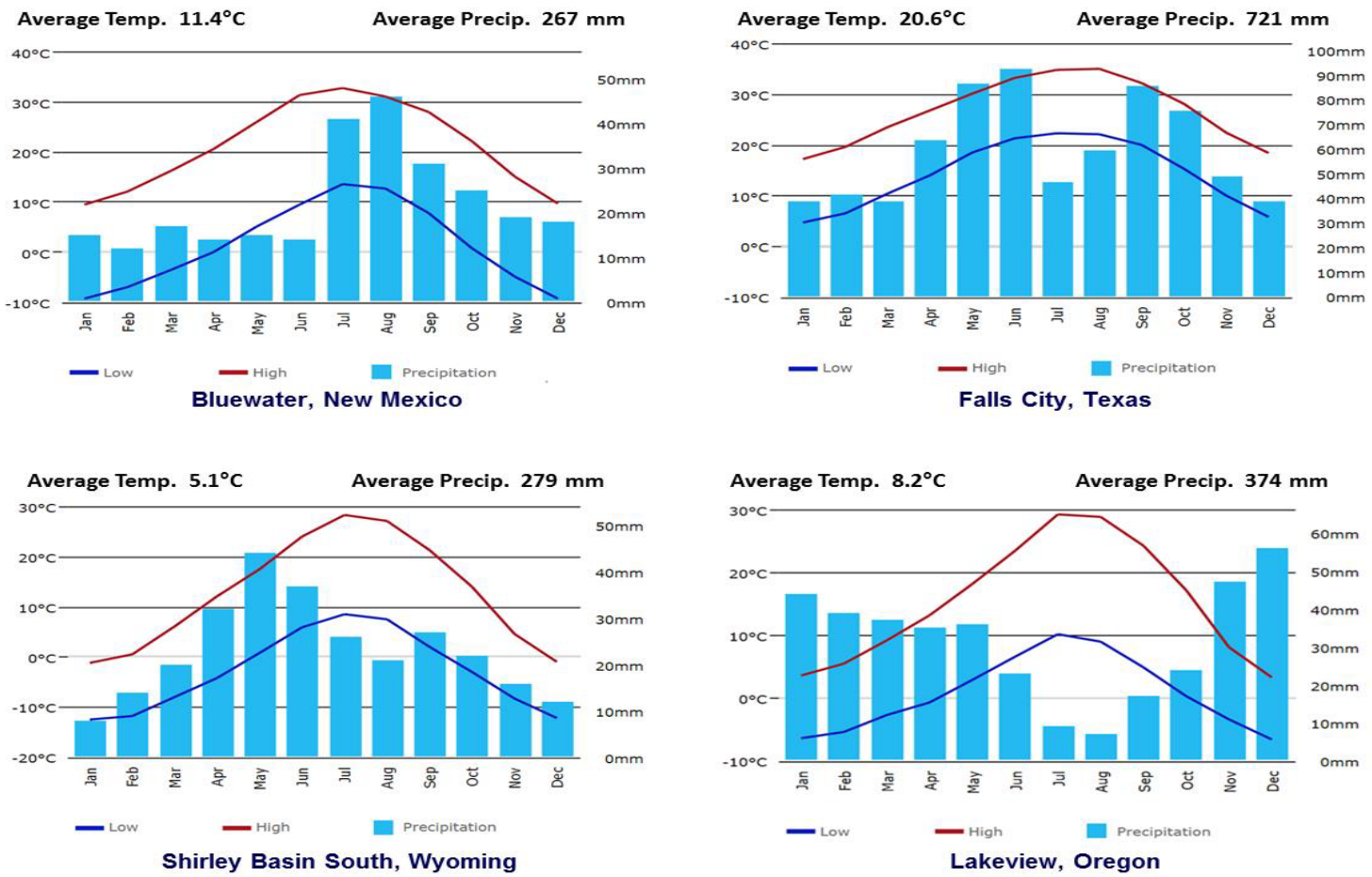

Figure 2-3 Annual and Monthly Temperature and Precipitation Data for the Four Study Sites (www.usclimatedata.com) Bluewater and Shirley Basin South data are for Grants, New Mexico, and Medicine Bow, Wyoming, respectively. Grants is about 15 kilometers (km) southeast of the Bluewater disposal cells. The town of Falls City, Texas, is about 13 km northeast of the Falls City cell. Medicine Bow is about 48 km south of the Shirley Basin South cell. The town of Lakeview, Oregon, is about 12 km southeast of the Lakeview cell.

Table 2-3 Taxonomic Classification for Radon Barrier Borrow Soils at Disposal Sites Selected for Study

Site	Map Unit[1]	Order[2]	Classification[3]	Parent Material	Source[4]
Bluewater, New Mexico	Sparank-San Mateo Complex	Entisol	Fine, mixed, superactive, calcareous, mesic Ustic Torrifluvents	fan alluvium derived from shale and siltstone	Bluewater completion report (ARCO 1996).
Falls City, Texas	Torida clay	Vertisol	Fine, smectitic, hyperthermic Typic Haplusterts	clayey alluvium	Falls City completion report (DOE 1996).
Lakeview, Oregon	Drews Loam	Mollisol	Fine-loamy, mixed, mesic Pachic Argixerolls	gravelly sedimentary rock and/or gravelly rhyolite	Lakeview completion report (DOE 1991).
Shirley Basin S, Wyoming	Shirley Basin	Aridisol	Fine, mixed, superactive, frigid Ustic Paleargid	Alluvium from tuffaceous sedimentary mudstone	USDA Web Soil Survey[4]

[1] A soil map unit is a collection of areas with common soil components and delineated as different than other areas. Map unit areas were borrow locations for radon barrier soil.

[2] The most general level of classification in the USDA system of Soil Taxonomy. Soil orders are defined by a dominant characteristic affecting soils in that location such as the prevalent vegetation, the type of parent material, or climate variables: (1) Entisols have little profile (horizon) development. (2) Vertisols have a high content of clay minerals that shrink and swell as they change water content. (3) Mollisols are mineral soils that developed with vegetation, have extensive fibrous root systems, and are characteristically dark and rich with organic matter.

[3] USDA soil taxonomic classification (Soil Survey Staff 1999).

[4] Sources: Locations of soil borrow areas were from Completion Reports. USDA soil survey data was from https://websoilsurvey.sc.egov.usda.gov/App/HomePage.htm for that location.

Table 2-4 Soil Moisture Regimes[1]

Regime	Description
Aridic	Aridic moisture regimes include those soils that have moisture control sections completely dry more than one-half of the time and never moist in any part for as long as 90 consecutive days when the soil temperature at 50 cm averages more than 8 °C. In the United States, these areas are mainly in the desert Southwest.
Ustic	Ustic moisture regime soils have moisture control sections that are dry in some parts more than 90 cumulative days in 6 out of 10 years. If the mean annual soil temperature is less than 22 °C and mean summer and winter temperatures differ by more than 5 °C (9 °F), they are not dry in all parts for more than 45 days in the 4 months following the summer solstice in as much as 6 out of 10 years. These areas of the United States are in the western part of the Great Plains.
Xeric	Xeric moisture regime soils have completely dry moisture control sections more than·45 consecutive days in the 4 months following the summer solstice in at least 6 out of 10 years and are not aridic. Most of these areas are in California, Oregon, and Washington.
Udic	Udic moisture regime soils have moisture control sections that are not dry, in any part, as long as 90 cumulative days in most years and not dry throughout for as much as 45 consecutive days within 4 months after the summer solstice in more than 6 of 10 years when the soil temperature is above 5 °C. In the United States these areas are generally east of 95° longitude.

[1] Soil Survey Staff (1999).

Table 2-5 Soil Temperature Regimes[1]

Soil Temperature Regime	Description
Hyperthermic	Mean annual soil temperatures of 22 °C or more and a difference between mean summer and mean winter soil temperatures of less than 5 °C at 50 cm below the surface.
Mesic	Mean annual soil temperatures of 8 °C or more, but less than 15 °C, and the difference between mean summer and mean winter soil temperatures is greater than 5 °C at 50 cm below the surface.
Frigid	Mean annual soil temperatures of greater than 0 °C, but less than 8 °C, with a difference between mean summer and mean winter soil temperatures greater than 5 °C at 50 cm below the surface, and warm summer temperatures.

[1] Soil Survey Staff (1999).

2.3.3.4 Vegetation

The potential natural vegetation (PNV) at the four study sites, types of deep-rooted plants present, and vegetation development scores (Table 2-2) span the range of vegetation conditions found at Western UMTRCA sites. PNV is the vegetation that would be expected at a site without human intervention or other disturbances given environmental constraints of climate, geomorphology, and soil type. PNV assumes current climate and atmospheric carbon dioxide concentrations. Researchers determined PNV for UMTRCA sites using an online interactive version of Kuchler (1964). By comparison, Section 2.6 includes information on current vegetation growing on disposal cells and at analogue sites as observed by researchers during field investigations. Vegetation development scores were calculated using information found in annual inspection reports for the sites (https://www.energy.gov/lm/office-legacy-management). Vegetation development scores reflect changes in plant species and plant abundance on the cover since construction.
Table 6 lists common PNV species at the four study sites. All PNV plant associations include woody shrubs and perennial grasses. A key difference between the southern two sites (Bluewater and Falls City) and the northern two sites (Shirley Basin South and Lakeview) is the photosynthetic pathway for perennial grasses. Southern site grasses are primarily C4 (warm season), and northern site grasses are primarily C3 (cool season). C4 species grow during warmer periods (late spring to early fall) and use soil moisture more efficiently than cool-season species. C3 species grow during cool weather (late spring to early summer and at higher elevations) and may re-green in the fall if soil moisture is adequate. At all four sites, woody plants growing on covers (Table 2-2) are capable of sending roots through the cover profile and into tailings (Table 2-7).

Researchers used annual LM inspection reports to calculate vegetation development scores for UMTRCA sites (Appendix C; Table 2). Annual input data included separate estimates of plant abundance for grasses/forbs and deep-rooted woody plants, and separate estimates of percentage change in abundance for planted covers and unplanted covers. The four sites selected for study had divergent scores. Bluewater (unplanted) and Lakeview (planted) had the highest vegetation development scores. High scores indicate greater overall increases in plant abundance over time and greater increases in abundance of deep-rooted plants. Falls City and Shirley Basin South, both planted, had low scores. The abundance of planted grasses on these two sites remained little changed over time, and very few deep-rooted plants have established.

Table 2-6 Potential Natural Vegetation Types and Associated Common Plants at Disposal Sites Selected for Study

UMTRCA Site	Potential Natural Vegetation[1]	Common Plants[2]		
		Genus Species	Common Name	Growth Form
Bluewater, New Mexico	Grama Galleta Steppe	*Pascopyrum smithii*	western wheatgrass	C3 perennial grass
		Atriplex canescens	fourwing saltbush	evergreen shrub
		Bouteloua gracilis	blue grama	C4 perennial grass
		Panicum obtusum	obtuse panicgrass	C4 perennial grass
		Pleuraphis jamesii	James' galleta	C4 perennial grass
		Sporobolus airoides	alkali sacaton	C4 perennial grass
		Sporobolus wrightii	giant sacaton	C4 perennial grass
Falls City, Texas	Mesquite Acacia Savanna	*Bouteloua curtipendula*	sideoats grama	C4 perennial grass
		Trichloris crinite	false Rhodes grass	C4 perennial grass
		Panicum obtusum	vine mesquite	C4 perennial grass
		Bothriochloa barbinodis	cane bluestem	C4 perennial grass
		Eriochloa sericea	Texas cupgrass	C4 perennial grass
		Eragrostis intermedia	plains lovegrass	C4 perennial grass
		Buchloe dactyloides	buffalograss	C4 perennial grass
		Setaria vulpiseta	plains bristlegrass	C4 perennial grass
		Prosopis glandulosa	honey mesquite	perennial tree/shrub
		Vachellia rigidula	blackbrush acacia	perennial tree/shrub
Shirley Basin S., Wyoming	Grama Needlegrass Wheatgrass	*Bouteloua gracilis*	blue grama	C4 perennial grass
		Pascopyrum smithii	western wheatgrass	C3 perennial grass
		Hesperostipa comata	needleandthread	C3 perennial grass
		Pseudoroegneria spicata	bluebunch wheatgrass	C3 perennial grass
		Artemisia tridentata ssp. wyomingensis	Wyoming big sagebrush	evergreen shrub
		Artemisia frigida	fringed sagebrush	spreading sub-shrub
		Carex filifolia	threadleaf sedge	perennial sedge
Lakeview, Oregon	Sagebrush Steppe	*Festuca idahoensis*	Idaho fescue	C3 perennial grass
		Pseudoroegneria spicata	bluebunch wheatgrass	C3 perennial grass
		Purshia tridentata	antelope bitterbrush	perennial shrub
		Achnatherum thurberianum	Thurber's needlegrass	C3 perennial grass
		Leymus cinereus	basin wildrye	C3 perennial grass
		Poa secunda	Sandberg bluegrass	C3 perennial grass
		Artemisia tridentata ssp. vaseyana	mountain big sagebrush	evergreen shrub

[1] PNV types are from a 2000 version of the Kuchler (1964) potential natural vegetation map (firelab.org/document/potential-natural-vegetation-groups-v2000).

[2] Lists of common plants are for soil mapping units from https://websoilsurvey.sc.egov.usda.gov/App/HomePage.htm. Genus, species, common names, and growth form are from the USDA Plants Database (https://plants.usda.gov/home).

Table 2-7 Rooting Depths of Woody Plants Growing on Cell Covers Selected for Study

UMTRCA Site	Acronym	*Genus Species*	Common Name	Max. Root Depth (m)	References
Bluewater, New Mexico	ATCA	*Atriplex canescens*	fourwing saltbush	12.0	Stromberg 2013
	ULPL	*Ulmus polumis*	Siberian elm	4.9	Sprackling & Read, 1979
Falls City, Texas	PRGL	*Prosopis glandulosa*	honey mesquite	5.5	Gibbens & Lenz, 2001
Shirley Basin S., Wyoming	ATCA	*Atriplex canescens*	fourwing saltbush	12.0	Stromberg 2013
Lakeview, Oregon	PUTR	*Purshia tridentata*	antelope bitterbrush	3.0	Klepper et al. 1985
	ARTR	*Artemisia tridentate*	big sagebrush	3.0	Link et al. 1994
	ERNA	*Ericameria nauseosa*	rubber rabbitbrush	4.0	Stromberg 2013

2.4 Selection of Test Conditions

Effects of natural processes on near-term and long-term radon barrier performance were evaluated in test pits on disposal cell covers and at analogue sites. Sections 2.4.1 and 2.4.2 review methods for selecting test conditions and test pit locations. Sections 2.4.3 – 2.4.6 describe the conditions selected. Section 2.5 compares plant communities on disposal cells and at analogue sites.

Field work plans prepared by LM for the four study sites laid out the sequence of field activities; listed required equipment and materials; and described safety, health, and environmental management requirements: Bluewater (DOE 2016b), Falls City (DOE 2016c), Shirley Basin South (DOE 2017a), and Lakeview (DOE 2017b). LM also documented the restoration of test pits excavated on disposal cell covers and at analogue sites: Bluewater (DOE 2019), Falls City (DOE 2018a), Shirley Basin South (DOE 2018b), and Lakeview (DOE 2018c).

2.4.1 Selection Methods for Test Pits on Covers

Test pits were excavated within disposal cell radon barriers to characterize effects of ecological and soil-forming processes on hydraulic properties, radon diffusion, and radon flux. The selection of test pit conditions and locations was purposefully biased. The objective was not to determine average properties of radon barriers and changes since construction at selected sites. The objective was not to demonstrate compliance with the radon flux criterion which is based on the average flux applied over the entire surface of the disposal cell cover and over at least a 1-year period (see Section 2.1). Rather, the objective was to select test conditions on the four study sites that provided opportunities for measuring the highest radon fluxes and the greatest changes in engineering properties since construction. Table 2-8 lists the types of information, rationale, and sources of information researchers used to select test pit conditions on disposal cell covers.

The process identified areas on covers where surface conditions had changed the most since construction, with emphasis on ecological change, and identified areas where as-built radon flux was high. Test locations were also selected that generated opportunities to compare different cover designs in the same environment, to measure depth-dependent changes in soil morphology and soil engineering properties (including soil hydraulic properties), and to compare different combinations of conditions. Researchers searched site completion reports for

information on as-built cover designs and radon flux measurements, and then conducted reconnaissance trips to the four study sites. Researchers walked the covers to observe, record current surface conditions, and flag candidate locations.

The timing of sampling events was also biased. Researchers scheduled sampling events when they anticipated seasonally high radon flux rates: near the end of a period of high evapotranspiration (ET) following a period of historically low precipitation for a site when the radon barrier would likely be seasonally driest.

2.4.2 Selection Methods for Analogue Sites

The language in 10 CFR 40 Appendix A addresses longevity of engineered disposal cell covers (see Section 2.2.1). General design goals include permanent isolation: minimizing dispersion of contaminants by natural forces without ongoing maintenance. Cover designs are required to isolate radioactive and other hazardous materials in tailings for 200 to 1000 years.
For practical purposes, LM assumes that stewardship of disposal sites will last indefinitely (www.lm.doe.gov). However, the four engineered covers in this study were only between 15 and 30 years old when sampled. Hence, the results from sampling in test pits on disposal cells are but an early snapshot in the trajectory of natural processes acting on cover performance. Given the uncertainty associated with long-term soil change and service lives in hundreds to thousands of years, studies of natural analogue systems can provide an understanding of future soil conditions that cannot be adequately evaluated from short-term experiments or computer modeling (Waugh et al. 1997). Researchers studied analogue sites to gain an understanding of possible long-term changes in the performance of disposal cell covers. Researchers characterized and sampled analogue sites (1) for evidence of potential long-term effects of ecological and soil-forming processes on cover engineering properties, and (2) to begin to define possible future performance scenarios. For the purposes of this study, ideal analogue sites had undisturbed profiles of the same soil type as that used to construct the radon barrier, and undisturbed (late-seral) vegetation. Researchers relied on completion reports, soil surveys, site visits, and test holes to acquire information needed to identify candidate analogue sites. Table 2-9 lists the types of information, rationale, and sources of information researchers used to select analogue sites.

Soil-forming factors (see Appendix H) at the four sites on the top-deck, side-slope, and natural analogues are summarized in Table 2-10. A variety of soil-forming factors are present at each site, and between sites. With a few exceptions, the top-deck conditions and analogues share similar material properties and setting. In contrast, slope and surface cover are disparate between the side-slope profiles and the analogues (rock riprap versus topsoil). Therefore, the analogues provide reasonable comparisons of the long-term condition for the top deck, but poor comparisons for the side-slopes at these facilities.

Table 2-8 Test Conditions and Rationale for Selecting Test Pit Locations on Covers

Test Condition[1]	Selection Rationale[2]	Sources of Informtion[3]
As-Built Cover Design	Select locations that provide opportunities (1) to compare different cover designs and materials in the same environment and in different environments, and (2) to evaluate depth-dependent changes in soil morphology and engineering properties. For example, compare vegetated and rock-armored surfaces, and thin and thick radon barriers.	Completion Reports[4] and Site Fact Sheets[5] (www.lm.doe.gov)
As-Built Radon Flux	Select locations where as-built radon flux values and/or radium activity in tailings were high. Also compare areas with and without low-activity material overlying higher-activity tailings. At most sites, contractors systematically sampled radon flux soon after construction using activated charcoal canisters sealed to the surface of the radon barrier.	Completion Reports (www.lm.doe.gov)
Surface Condition	Select locations where observations of surface conditions provide evidence of changes in subsurface conditions. For example, select locations where mid to late seral deep-rooted plants have established. Researchers recognize that plant succession is likely a driver of pedogenic changes in radon barrier engineering properties. Other surface conditions that may indicate subsurface changes include animal burrows, aeolian soil filling riprap interstices, ponded water, and wetland vegetation.	Site Reconnaissance[6]
Seasonally Dry Climate	Schedule sampling when the radon barrier is likely seasonally driest based on monthly precipitation and temperature records for nearby towns. Radon diffusion coefficients are higher for air than for water. Therefore, radon flux is likely seasonally high when the radon barrier is dry: during warmer months and near the end of a period of low precipitation and high evapotranspiration.	Western Regional Climate Center (wrcc.dri.edu) U.S. Climate Data (usclimatedata.com)
Paired Plots	Select locations that provide opportunities to isolate effects of a particular test condition using paired plots. For example, isolate effects of deep-rooted plants by selecting a location with a rock-armored thin radon barrier and high as-built radon flux, and then excavate one test pit where deep-rooted shrubs grow and a second test pit at an adjacent location that is devoid of vegetation.	Combinations of the above sources
Replicate Plots	For a subset of test plots, excavate replicate plots for the same combination of test conditions to be able to evaluate sampling variability.	Combinations of the above sources

[1] Test conditions researchers considered in the process of selecting test pit locations on disposal cell covers.

[2] Rationale for the selection of locations on a disposal cell cover to test for a specific condition.

[3] Sources of site-specific information about selected test conditions.

[4] Remediation contractors documented as-built conditions in Completion Reports as evidence that disposal cells were constructed in accordance with approved design and performance criteria.

[5] LM produces fact sheets that provide a summaries of the history, regulatory setting, compliance strategy, disposal cell designs, and surveillance and maintenance activities for UMTRCA disposal sites.

[6] Resarchers walked the surface of disposal cells in advance of sampling events to observe surface conditions and mark candidate locations for test pits.

Table 2-9 Test Conditions and Rationale for Selecting Analogue Sites and Test Pit Locations

Type of Information[1]	Selection Rationale[2]	Source of Information[3]
Soil Borrow Source	Ideally, find undisturbed areas adjacent to known radon barrier soil borrow areas. An objective of analogue studies was to characterize soil morphology and soil engineering properties in an undisturbed profile of the same soil type used to construct the radon barrier.	Completion Reports[4] (www.lm.doe.gov)
Soil Survey	Use published soil survey data to determine the extent of soil types (soil survey mapping units) within which radon barrier borrow sources were located. An objective was to locate applicable soil mapping units within disposal site boundaries to expedite the approval process for excavation.	Web Soil Survey, Natural Resource Conservation Service[5]
Soil Profile Augering	Hand auger pilot holes to determine if the soil profile, layer thicknesses, and layer depths are similar to the radon barrier profile.	Site Reconnaissance[6]
Plant Ecology	Select locations with late successional vegetation growing in the soil type used to construct the radon barrier. An objective was to compare plant communities on disposal cells and at undisturbed analogue sites to interpret current seral stages of disposal cell vegetation and begin to define long-term performance scenarios.	Site Reconnaissance[6]
Ground Surface	Ideally, find analogue sites with surface conditions similar to the disposal cell covers. For example, undisturbed borrow soil capped with desert pavement may be a better analogue of a rock-armored engineered cover than a profile without desert pavement.	Site Reconnaissance
Land Use History and Disturbance	Determine current and historical land uses and disturbances. Examples of disturbances that influence plant ecology and soil morphology include livestock grazing, past cultivation, haying, surface soil removal, and past land leveling. Land use has bearing on interpretations of plant succession and the development of long-term performance scenarios.	Completion Reports and Site Reconnaissance

[1] Information researchers acquired in the process of selecting locations for analogue site test pits.

[2] Rationale for the application of this information in the process of selecting analogue sites.

[3] Sources of site-specific information related to analogue site selection.

[4] Locations and properties of radon barrier soil borrow sources were documented in completion reports by DOE for Title I sites and by remediation contractors for Title II sites.

[5] https://websoilsurvey.sc.egov.usda.gov/App/HomePage.htm

[6] Resarchers conducted field reconnaissance of candidate analogue sites, surveyed plant communities, and hand augured pilot holes in advance of sampling events.

Table 2-10 Summary of Soil-Forming Factors at Four Engineered Covers for Waste Containment and Natural Analogues

		Cover Design / Material Properties / Setting					Climate		Biota[a]		Management	Time
	Setting	Type	Barrier Depth (*range*)	Texture (clay %) (*range*)	Mineralogy (2:1 clay %) (*range*)	Slope	Soil Moisture Regime	Soil Temperature Regime	Flora	Fauna	Strategy	*years*
Falls City	Top deck	Vegetated	0.97-1.54 m	38-51%	57-70%	1-2%	Udic-Ustic	Hyperthermic	Managed grassland	*Limited*	Mowing	[b]22
	Side-slope	Rock riprap	0.47-0.94 m	43%	59%	20%			Mixed/sparse	*Limited*	Hand removal of trees/shrubs	
	AN-1	n/a	n/a	43% at ~1.0 m	58% at ~1.0 m	1-4%			Mixed woodland	Cattle	Cattle grazing	[c]<30,000
Bluewater	Top deck main cell	Rock riprap	0.14-0.85 m	13-41%	37-45%	2-4%	Aridic-Ustic	Mesic	Kochia, squirreltail grass, fourwing saltbush	Ants, Rodents	Hand removal of trees	[b]21
	AN-3	n/a	n/a	31% at ~0.5 m	48% at ~0.5 m	1-3%			High altitude steppe	Elk, Rodents, Ants	Wildlife	[d]<15,000
	AN-6	n/a	n/a	29% at ~0.5 m	51% at ~0.5 m	4%			High altitude steppe	Elk, Rodents, Ants	Wildlife	[e]<15,000
Lakeview	Top deck	Vegetated	0.59-1.10 m	8-22%	52-71%	2-5%	Xeric	Frigid	Sagebrush, rabbitbrush, bitterbrush, mixed grasses	Ants, Rodents	Hand removal of trees	[b]28
	Side-slope	Rock riprap	0.5-0.85 m	16%	-	20%			Grasses/sparse	Rodents	Hand removal of trees	
	AN-2	n/a	n/a	27% at ~0.8 m	[f] 5% at ~0.8 m	2-7%			Sagebrush steppe	Deer, rodents	Wildlife	[g]<20,000
Shirley Basin	Top deck	Vegetated	0.99-1.52 m	37-66%	58-76%	1-3%	Aridic-Ustic	Mesic	Mixed grasses, sparse fourwing saltbush	Rodents, Cattle, antelope	Grazing, hand removal of noxious weeds	[b]17
	Side-slope	Rock riprap	1.17-1.80 m	55%	-	20%			Mixed grasses/sparse	Rodents	Hand removal of noxious weeds	
	AN-4	n/a	n/a	69% at ~1.3 m	55% at ~1.3 m	1-3%			High altitude grassland/steppe	Ants, rodents, badgers	Wildlife	[h]<15,000

2.4.3 Bluewater, New Mexico

2.4.3.1 Disposal Cell

Bluewater provided the best opportunities of all UMTRCA disposal sites to compare (1) different cover designs in the same environment, (2) thin and thick radon barriers constructed of the same materials, (3) different types of tailings, (4) high and low as-built radon fluxes, and (5) vegetation and no vegetation (Table 2-11). The A/B designation for some test pit names indicate duplicate radon flux measurements. Seven locations on the top slope of the main tailings disposal cell, two locations on the top slope of the carbonate tailings disposal cell, and one location on the top slope of the acid tailings disposal cell were selected for study (Figure 2-4). All fieldwork was conducted in June 2016 following six months of historically low precipitation and high ET (Figure 2-3, Section 2.4.3.2).

Some test locations were paired to isolate effects of particular conditions (Table 2-10). Test locations 1A/B and 2A/B were selected to isolate effects of seasonal ponding. Both locations overlie slime tailings and a thin radon barrier relative to other sites investigated. Location 1A/B was in a bare depression that formed as a result of dewatering and settlement of the slimes tailings, whereas 2A/B was on the edge of the depression in an area with squirreltail grass (*Elymus elymoides*). Test locations 4 and 5A/B and test locations 7 and 8 were selected to isolate effects of fourwing saltbush (*Atriplex canescens*), a deep-rooted woody plant (Table 2-7). Locations 4 and 5A/B both overlie sand tailings in an area on the main tailings disposal cell that had high as-built radon flux values. Mature fourwing saltbush plants were rooted in the cover at 5A/B. Location 4, adjacent to 5A/B, was bare. The remaining test locations on the main disposal cell included an area with a high as-built radon flux value and sparse vegetation (3A/B), and an ant mound with a relatively high as-built radon flux value (Table 2-11). Locations 7 and 8 on the Carbonate disposal cell both had a thick radon barrier and low as-built radon flux values. Fourwing saltbush grew at location 7 but not at location 8. These two locations, with the thickest radon barriers in the study (2.5 meters), were selected to evaluate depth-dependent changes in soil morphology and soil engineering properties. The one test location on the grass-covered acid disposal cell was selected for the combination of a relatively thin radon barrier and the highest as-built radon flux value at Bluewater (2.47 Bq/m^2s).

2.4.3.2 Analogue Sites

Two analogue sites were selected for study at Bluewater (Figure 2-4). Pit 3 was an undisturbed area on the eastern edge of the borrow area where ARCO had excavated Sparank-San Mateo soil (Table 2-3) to construct the radon barrier (ARCO 1996). Pit 3 was within the disposal site fence, and, therefore, vegetation had likely been protected from grazing for a least 20 years. Researchers also selected Pit 6, an area with basalt desert pavement overlying fine soil northwest of the Acid disposal cell (Figure 2-4), as a natural analogue of the rock-armored cover on the main tailings disposal cell. Vegetation at Pit 3 may have been disturbed during the many years of ore processing and then remediation of the site.

Table 2-11 Disposal Cell Cover Conditions at Test Locations, Bluewater, New Mexico

Test Pit	Disposal Cell	Tailings	As-Built Rn Flux[1,2] (Bq/m^2s)	Rn Barrier Thickness[3] (meters)	Surface	Ecology
1A/B	Main	slimes	0.13, 0.12	0.58	riprap, ponding	sparse vegetation
2A/B	Main	slimes	0.10, 0.05	0.61	riprap, no ponding	grasses and forbs
3A/B	Main	sands	0.65, 0.22	0.79	riprap	sparse vegetation
4	Main	sands	0.65, 0.22	0.71	riprap	no saltbush
5A/B	Main	sands	0.65, 0.22	0.73	riprap	saltbush
6	Main	sands	0.21, 0.22	0.70	riprap	ant mound
7	Carbonate	mixed	0.02, 0.02	2.50	riprap	saltbush
8	Carbonate	mixed	0.02, 0.02	2.50	riprap	no saltbush
9A/B	Acid	mixed	2.47, 0.55	0.21	soil	seeded grasses

[1] As-built radon flux values for the sample point closest to the test pit followed by the geometric mean of the four closest sample points.

[2] Overall mean as-built radon flux values on the surface of the radon barrier were 0.10 Bq/m^2s for the Main and Acid disposal cells and 0.05 Bq/m^2s for the Carbonate disposal cell (ARCO 1996).

[3] As-built radon barrier thicknesses for sample points closest to the test pit (ARCO 1996).

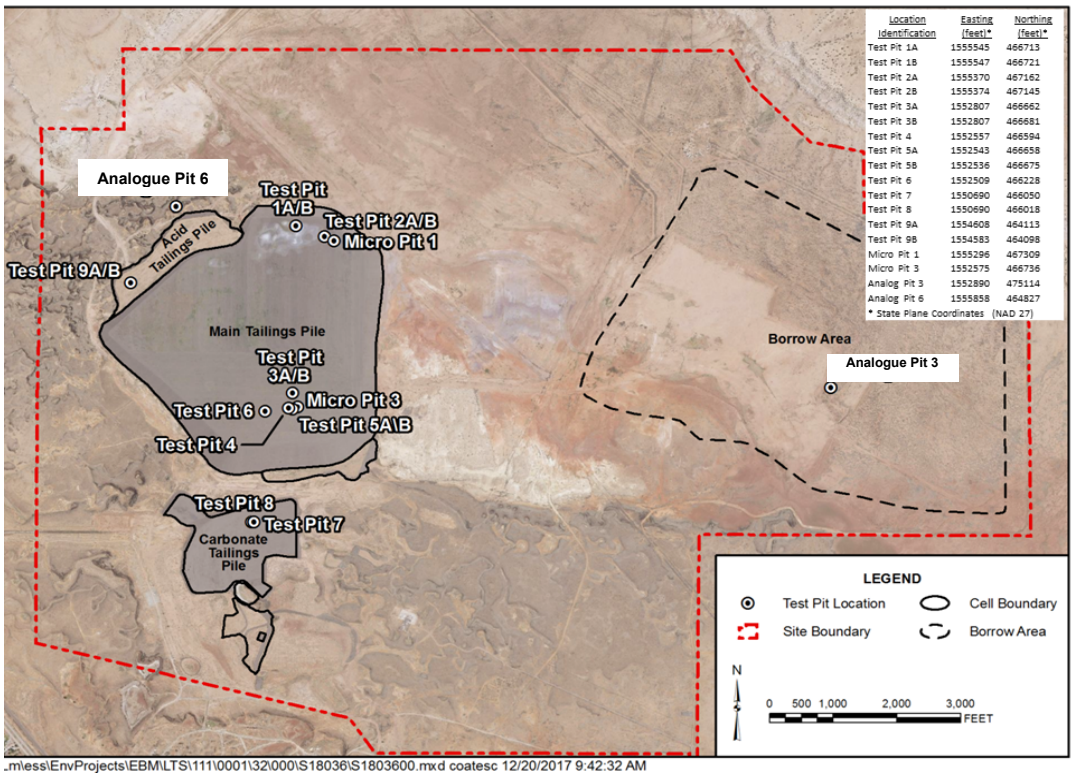

Figure 2-4 Test Pit Locations on the Disposal Cells and at Analogue Sites for Bluewater, New Mexico

2.4.4 Falls City, Texas

2.4.4.1 Disposal Cell

Selection of test pits on the Falls City disposal cell cover paired locations (1) with and without woody plants, (2) with high and average as-built radon flux values, (3) with planted soil and rock-armored surfaces, and (4) with thicker and thinner radon barriers (Figure 2-5; Table 2-12). The top deck is mowed seasonally for hay, preventing typically deep-rooted honey mesquite (*Prosopis glandulosa*) trees from maturing. TP1 (mesquite and grass) and TP2 (grass only) were in an area with the highest as-built radon flux values on the planted top deck. TP3 and TP4 were similarly paired in an area with average as-built radon flux. Researchers reasoned that the larger than average mesquite root crown at TP3 might indicate a more developed and potentially deeper root system. TP5 (rock apron) and TP6 (rock side slope) were in an area that had the highest as-built radon flux values for riprap surfaces on the disposal cell. Test pits on the disposal cell and at an analogue site were excavated and sampled in April 2016 following several months of historically low precipitation (Figure 2-3; Section 2.4.3.2).

2.4.4.2 Analogue Site

There were no undisturbed surfaces in the vicinity of the disposal cell that researchers considered to be good candidates for an analogue study. However, after consulting with a local landowner familiar with disposal cell construction, researchers selected a location southwest of the disposal cell on a slope adjacent to the protection layer borrow area (Figure 2-5). The landowner indicated that although the vegetation had been disturbed during periods of ore processing and remediation, the soil profile had likely remained undisturbed. The analogue site falls within the Bryde fine sandy loam soil taxonomic mapping unit with typically up to 40% clay in over 90 cm of argillic (Bt) horizons (https://websoilsurvey.sc.egov.usda.gov/App/HomePage.htm).

Table 2-12 Disposal Cell Cover Conditions at Selected Test Locations, Falls City, Texas

Test Pit	Location on Disposal Cell	As-Built Radon Flux[1,2] (Bq/m2/s)	Rn Barrier Thickness[3] (meters)	Surface	Vegetation
TP1	top deck	0.11, 0.06	0.91	soil/vegetation	mesquite/grass
TP2	top deck	0.08, 0.07	0.91	soil/vegetation	grass only
TP3	top deck	0.03, 0.02	0.91	soil/vegetation	mesquite/grass
TP4	top deck	0.03, 0.02	0.91	soil/vegetation	grass only
TP5	apron	0.16, 0.08	0.61	rock riprap	no plants
TP6	side slope	0.16, 0.08	0.61	rock riprap	no plants

[1] As-built radon flux values for the sample point closest to the test pit followed by the mean of the four closest sample points.

[2] Overall mean as-built radon flux on the surface of the radon barrier was 0.03 Bq/m^{2}s (DOE 1996).

[3] Design radon barrier thicknesses for the top deck and side slope (DOE 1996).

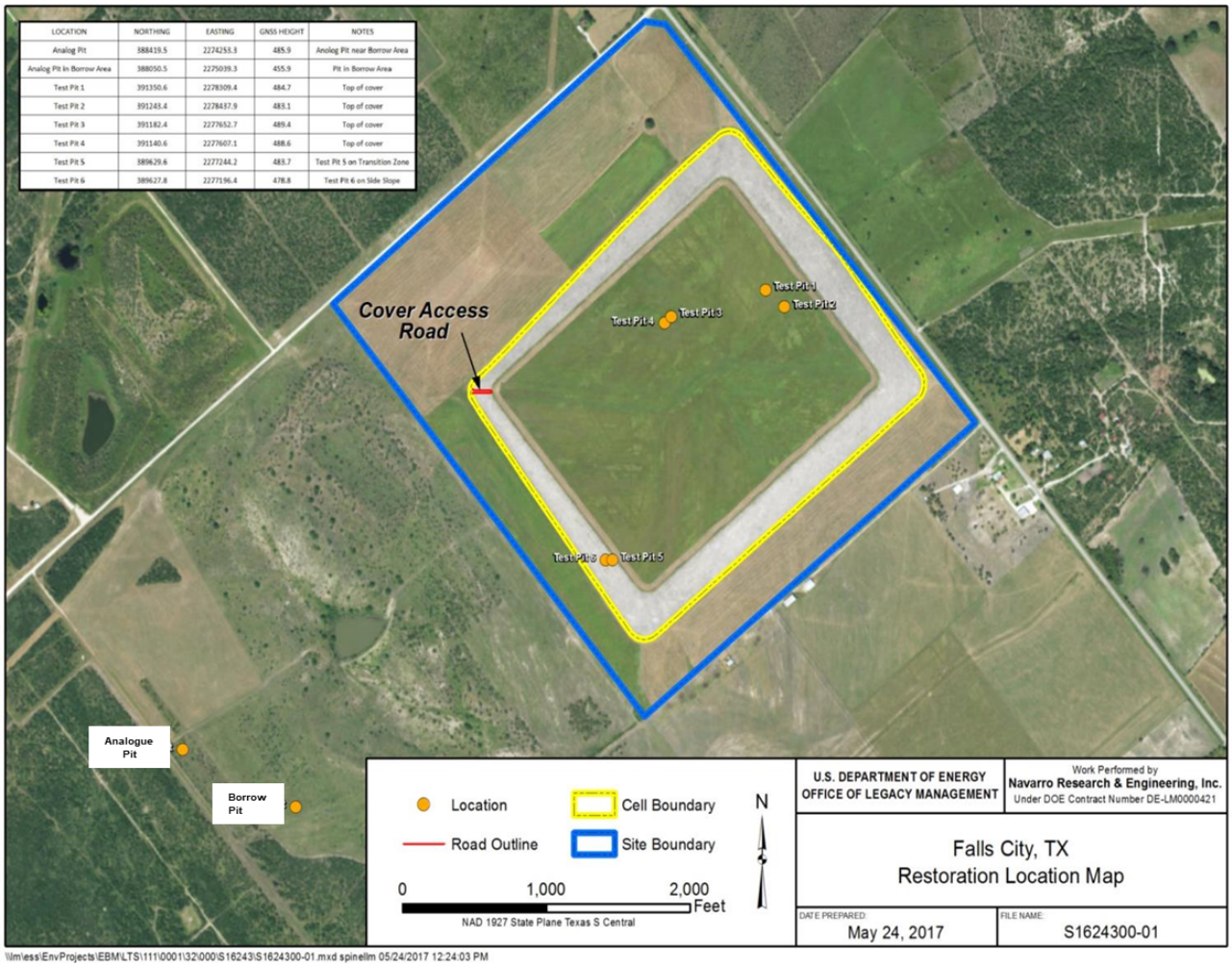

Figure 2-5 Test Pit Locations on the Disposal Cell Top Slope and Side Slopes and at an Analogue Site for Falls City, Texas

2.4.5 Shirley Basin South, Wyoming

2.4.5.1 Disposal Cell

Conditions selected for study on the Shirley Basin South disposal cell included (1) high and low as-built radon flux; (2) potentially deep-rooted plants; (3) rock riprap filled with aeolian soil deposits; and (4) a low-lying area with seasonal ponding of water, wetland soil, and wetland vegetation (Figure 2-6; Table 2-13). Test pit locations with high and average as-built radon fluxes were on the grass-planted top decks both with (DC-4 and DC-5) and without (DC-2 and DC-3) potentially deep-rooted plants. Test pits in wetland soil (DC-1) and on the soil-filled riprap slope (DC-6) were in areas with below average as-built radon flux values. Test pits on disposal cells were excavated and sampled in September 2017 following a season of historically low precipitation (Figure 2-3; Section 2.4.3.2).

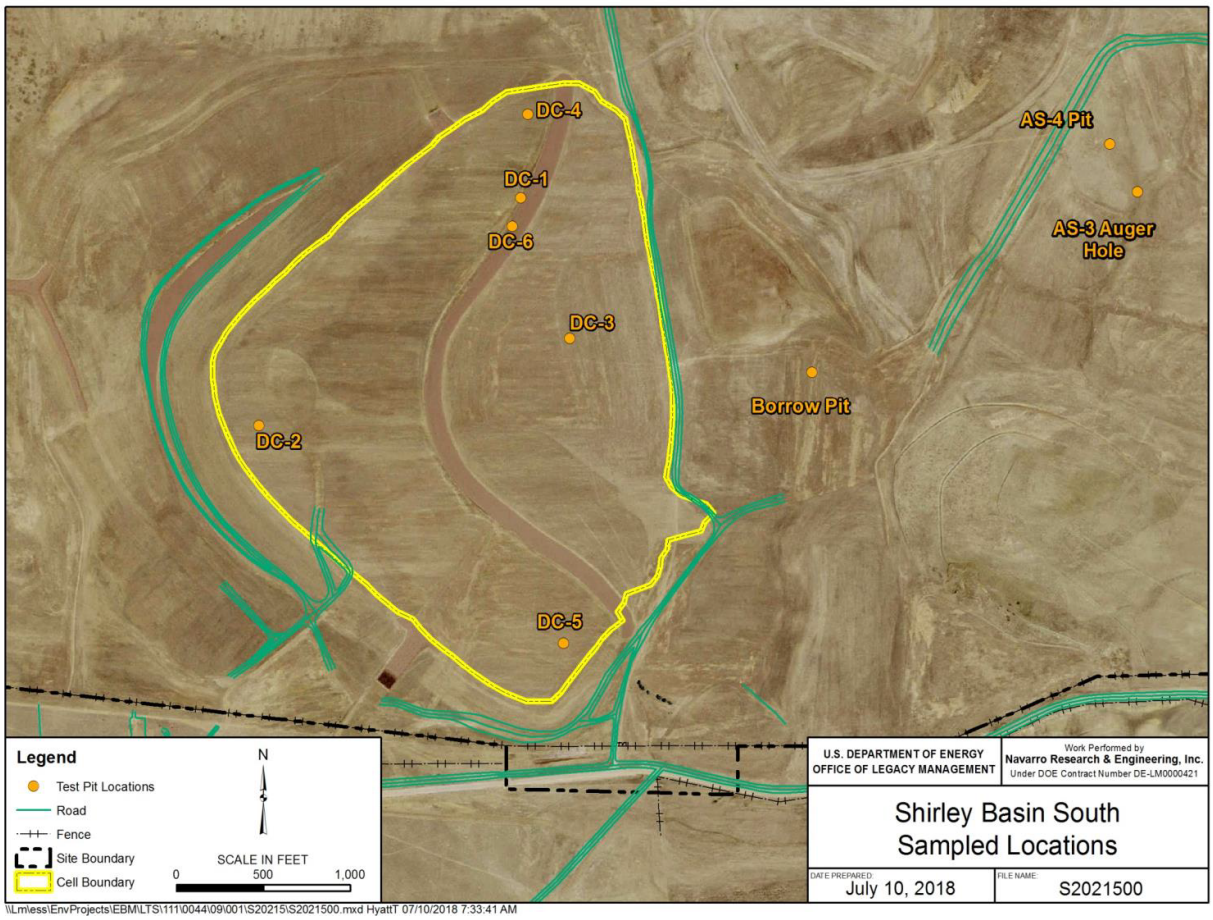

Figure 2-6 Test Pit Locations on the Disposal Cell Top-Deck Terraces, Interior Slope, and at an Analogue Site (AS) for Shirley Basin South, Wyoming

2.4.5.2 Analogue Site

Researchers had to rely primarily on-site reconnaissance to find a suitable analogue site. Most of the land surface within the site boundary had been extensively reworked during remediation, and the UDSA soil survey for northern Carbon County was incomplete. Soil map units from the northwestern quadrant of Albany County were used to estimate taxonomic classification of borrow materials based on soil forming factors. Researchers applied a knowledge of the area plant ecology to identify a small, relatively undisturbed parcel northeast of the radon barrier borrow area for excavation and characterization. The parcel is moderately grazed by livestock. Researchers located a deep clay soil profile comparable to the cover design after augering several test holes. Reconnaissance sampling occurred in September 2017 and again in March 2018. Researchers excavated and sampled the test pit at AS-4 in June 2018.

Table 2-13 Disposal Cell Cover Conditions at Selected Test Locations, Shirley Basin South, Wyoming

Test Pit	Location on Disposal Cell	As-Built Rn Flux[1,2] (Bq/m^2s)	Surface	Vegetation
DC-1	lower terrace	0.02, 0.02	wetland soil	grass/sedge
DC-2	lower terrace	1.20, 0.63	soil/vegetation	grass
DC-3	upper terrace	0.08, 0.06	soil/vegetation	grass
DC-4	lower terrace	0.11, 2.1	soil/vegetation	milkvetch/grass
DC-5	lower terrace	0.06, 0.06	soil/vegetation	saltbush/grass
DC-6	interior slope	0.03, 0.03	rock riprap/soil	grass/forb

[1]As-built radon flux values for the sample point closest to the test pit followed by the mean of the four closest sample points.

[2] Overall mean as-built radon flux on the surface of the radon barrier was 0.5 Bq/m^2s (Petrotomics 2001).

2.4.6 Lakeview, Oregon

2.4.6.1 Disposal Cell

The unique cover design at Lakeview, Oregon, with a thin soil layer placed over rock riprap (Figure 2-2; Section 2.4.3.1), provided opportunities to evaluate effects of a more diverse plant community and more advanced plant succession than at the other sites. The selection of test conditions compared (1) the top deck and side slope, (2) deep-rooted woody shrubs and sparse herbaceous vegetation, (3) animal burrows and no burrows, and (4) loamy and sandy topsoil. There were no as-built radon flux data for Lakeview (Figure 2-7; Table 2-14). Disposal cell test pits were excavated and sampled in late October 2017 following a historically dry summer (Figure 2-3; Section 4.3.2).

Three deep-rooted shrub species grow on the Lakeview top deck: antelope bitterbrush (*Purshia tridentata*), big sagebrush (*Artemisia tridentata*), and rubber rabbitbrush (*Ericamerisa nauseosa*). Researchers selected locations with bitterbrush (DC-2 and DC-11), a late seral shrub, and rabbitbrush (DC-5 and DC-12), an early seral shrub, to compare with nearby grass areas (DC-4, DC-10, and DC-13). The animal burrows at DC-5 may have been excavated by Great Basin pocket mice (*Perognathus parvus*). Two locations provided opportunities to evaluate soil morphology and engineering properties along gradients. DC-2 was excavated along a gradient from a mature bitterbrush to herbaceous vegetation on the top deck. DC-4 was excavated along a gradient from clumps of thickspike wheatgrass (*Elymus lanceolatus*) to no vegetation on the rock riprap side slope.

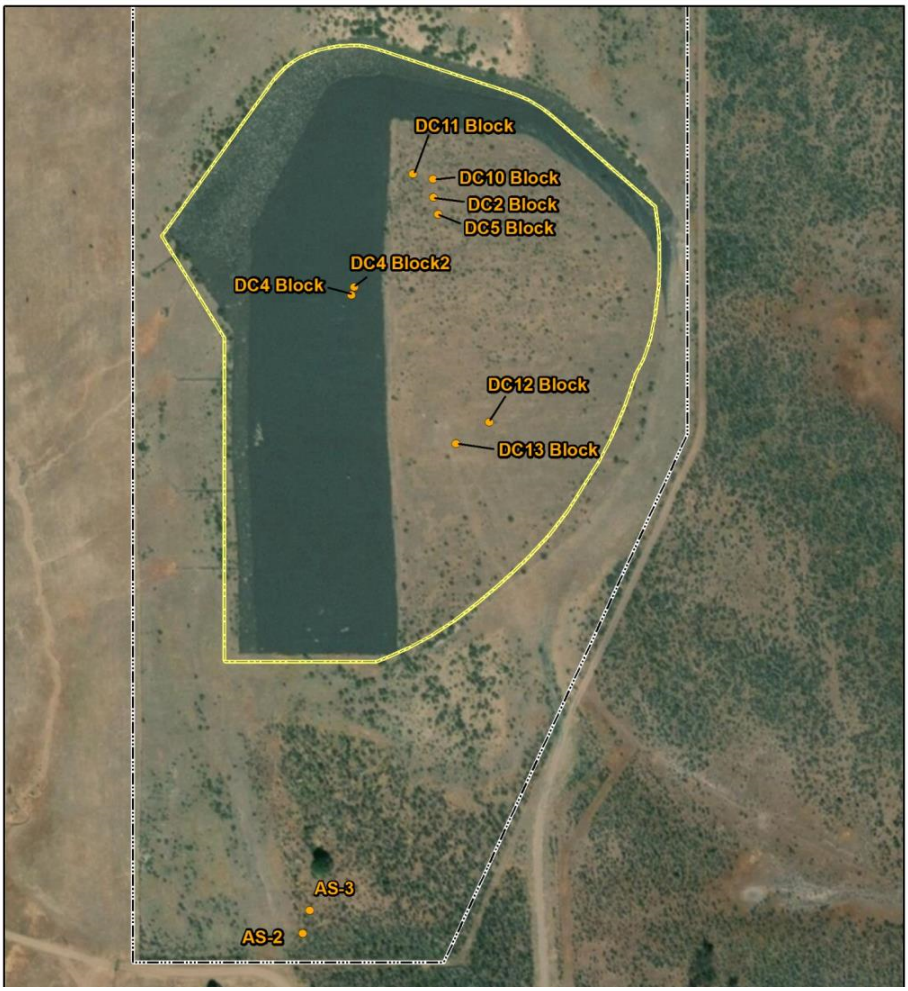

Figure 2-7 Test Pit Locations on the Disposal Cell Top-Deck, Side Slope, and at Analogue Sites (AS) for Lakeview, Oregon

Table 2-14 Conditions for Test Pits on the Disposal Cell Cover at Lakeview, Oregon

Test Pit	Disposal Cell Area	Surface	Vegetation	Other
DC-2	top deck	soil/riprap	bitterbrush/grass	gradient[1]
DC-4	side slope	riprap	grass	gradient[1]
DC-5	top deck	soil/riprap	rabbitbrush/grass	animal burrows
DC-10	top deck	soil/riprap	sparse grass	loam topsoil
DC-11	top deck	soil/riprap	bitterbrush	loam topsoil
DC-12	top deck	soil/riprap	rabbitbrush/grass	sandy topsoil
DC-13	top deck	soil/riprap	sparse grass	sandy topsoil

[1] Test pits were excavated along a gradient in surface condition from a mature bitterbrush shrub to grass at DC-2 and from grass growing in rock riprap to riprap with no grass at DC-4.

2.4.6.2 Analogue Site

The analogue sites studied at Lakeview (AS-2 and AS-3) were located within the site boundary south of the disposal cell (Figure 2-7). Both occur within the Drews loam mapping unit. Researchers observed a thick Bt horizon in an exploratory auger hole at AS-2. The disposal cell had been excavated in Drews loam (https://websoilsurvey.sc.egov.usda.gov/App/HomePage.htm), and researchers assumed that the radon barrier material had come from Bt horizons from a lower lacustrine clay deposit. Vegetation in the area had remained undisturbed during remediation and has been protected from grazing for about 30 years. Researchers conducted reconnaissance sampling at Lakeview in April 2017 and again in October 2017. The analogue test pits were excavated and sampled in June 2018.

2.5 Plant Ecology of Disposal Cells and Analogue Sites

Earthen UMTRCA covers are engineered ecosystems. An LTS&M goal is to understand and project long-term ecological scenarios, linked changes in the morphology and engineering properties of UMTRCA cover soil profiles, and effects on the long-term performance of disposal cells. Ecological processes that impact cover performance encompass interactions of all organisms (plants, animals, and microorganisms) and the physical environment of the cover and of contiguous areas. Defining and evaluating long-term performance scenarios (future conditions of the cover) will involve a combination of modeling, monitoring, and natural analogue studies (Albright et al. 2010).

Plant succession is a key ecological driver of pedogenic changes in radon barrier engineering properties. Plant succession is a directional change in species composition or structure over time following a disturbance or, in our case, following construction of an engineered cover. Understanding future plant succession (seral) stages and their role in future performance scenarios for specific UMTRCA covers will be a challenge. The best source of evidence for succession trajectories will be repeated evaluations of plant ecology over years and decades. However, indirect methods will be needed for longer time frames—to understand potential seral stages and performance scenarios over the 200–1000 year design life of a disposal cell. An indirect approach ecologists use to understand temporal dynamics involves chronsequences. A chronosequence is a set of sites formed from the same parent material but that differ in the time since they formed. A chronosequence approach would be appropriate when there is evidence that analogue sites of different ages are following similar or convergent trajectories and to compare aspects of soil formation for temporally linked sites (e.g., Walker et al. 2010). The appropriateness of using natural analogue sites in the context of chronsequences to define future ecological and soil morphological conditions as components of long-term performance scenarios will be more fully addressed in a later report. This section, as a starting point, simply compares the plant ecology of the four disposal cell covers and of their analogue sites selected for study (Sections 2.5.3–2.5.6).

2.5.1 Methods

Researchers used a modified, semi-quantitative releve' method (Barbour et al. 1999) to characterize plant species composition, plant abundance, and seral stages for different surfaces on the four disposal cells and at analogue sites. Ecologists familiar with the plant ecology of each disposal site noted the different plant communities, identified and listed all plant species observed within each community, visually estimated the foliar cover of each species, and then categorized species by abundance. Abundance classes and percentages of foliar cover varied by site. Ecologists also categorized three general seral stages of species: (1) mid-to-late

(native), (2) pioneer (native) or invasive (non-native weeds), and (3) introduced (e.g., planted non-native hay and forage plants). Total percent foliar cover in a plant community was calculated as the sum of percent cover values for all species within a seral stage. Plant data for the four disposal sites were from baseline environmental surveys (DOE 2013; 2015; 2016a) and from observations recorded by researchers during radon barrier study field campaigns. Nomenclature follows the USDA Natural Resources Conservation Service (NRCS) PLANTS Database (www.plants.usda.gov), and information on ecological roles of plant species is from the PLANTS Database and the U.S. Forest Service (www.fs.fed.us/database).

2.5.2 Results and Discussion

Contrasts in species composition, percent foliar cover, and seral stages for plant communities on dissimilar surfaces of disposal cell covers and at analogue sites are depicted in Figure 2-8. The contrasts, discussed below, reflect differences in potential natural vegetation at the sites, in cover designs and materials, and in land management practices. This discussion focuses on the more common species. See Appendix E for complete lists of species, cover classes, and seral stages.

2.5.2.1 Bluewater

Plant communities on the Main and Carbonate disposal cell covers at Bluewater are indicative of early-succession vegetation on disturbed land. These covers were not designed to have vegetation. Regular herbicide applications have limited total foliar cover to less than 10% (10 to 20% of the analogue site foliar cover) consisting primarily of the pioneer and invasive species bottlebrush squirreltail (Elymus elymoides), burningbush (Bassia scoparia), and Russian thistle (Salsola tragus). Two relatively deep-rooted shrubs also grow on these cell covers: Siberian elm (Ulmus pumila) and fourwing saltbush (Atriplex canescens). Siberian elm is an invasive tree (does not occur at the analogue sites) and may have established in response to a relatively wet habitat created by the rock mulch surface. In contrast, fourwing saltbush is an early to late seral native shrub that also occurs at the analogue sites and will likely be a common and lasting component of the Main and Carbonate cell plant communities. Hence, researchers selected locations with fourwing saltbush for test pits on these cells (Section 2.5.3).

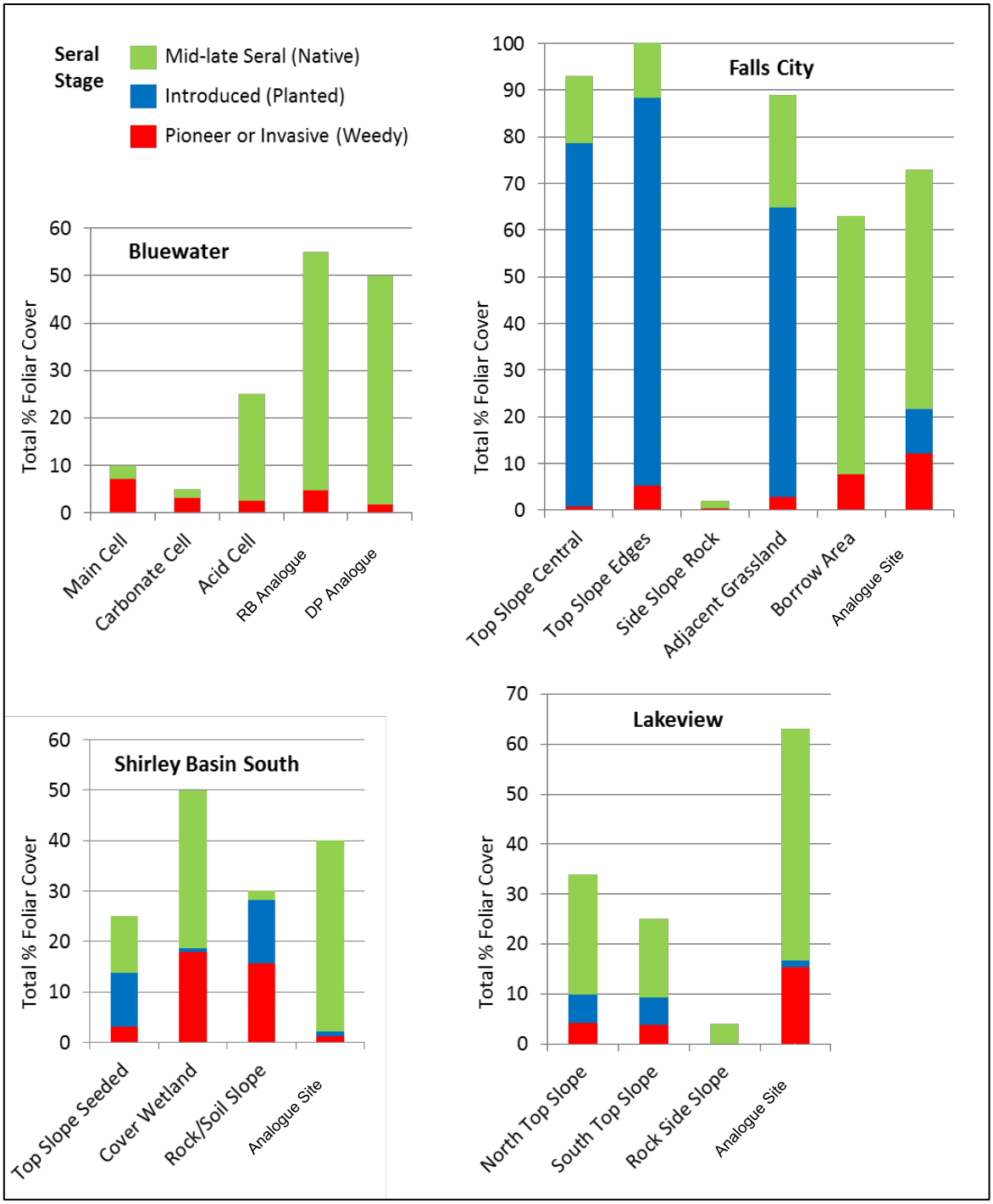

Figure 2-8 Estimated Percent Foliar Cover By Seral Stage for Plant Communities on Dissimilar Disposal Cell Surfaces and at Analogue Sites for Bluewater, Falls City, Shirley Basin South, and Lakeview

By comparison, researchers observed 25% total foliar cover on the planted Acid disposal cell; about 50% of the analogue site foliar cover. The two dominant planted grasses, blue grama (*Bouteloua gracilis*) and sand dropseed (*Sporobolus cryptandrus*), as mid to late seral species, are also abundant at the analogue sites and will likely persist. Using these metrics, researchers judged revegetation of the Acid cell to be successful and resilient.

The analogue sites at Bluewater are reasonable examples of the potential natural vegetation both with (Desert Pavement, DP Analogue site) and without (Radon Barrier, RB Analogue site) a rock-armored surface. High values for species richness, species diversity, total foliar cover, foliar cover of mid to late seral species, and low values for pioneer and weedy species are all indicative of a natural area that has been protected from grazing and other disturbances. The DP Analogue Site had fewer species (28) and slightly less foliar cover (50%) than the RB Analogue Site (41 and 55%). The two analogue sites otherwise share many of the same dominant and secondary species (Appendix E). DOE/LM can use the analogue site plant communities at Bluewater as revegetation targets, for clues about potential future changes in vegetation, and to evaluate future management options (e.g., discontinue spraying herbicides and manage and monitor as an ET cover). For example, ET values for these analogue landscapes could be input to water balance models of future hydrologic performance.

2.5.2.2 Falls City

With a humid subtropical climate, total foliar cover on the Falls City top deck, at 90–100%, was the highest of all plant communities in the study. In contrast, total foliar cover on the side slope was the lowest. DOE seeded non-native hay grasses on the top deck of the disposal cell and in adjacent areas that were disturbed during remediation. These areas have nearly become monocultures of King Ranch bluestem (*Bothriochloa ischaemum var. songarica*), a grass introduced to Texas in 1924 that is now considered to be an invasive species in natural areas because it greatly reduces diversity of insects, birds, and small mammals. The native shrub or small tree, honey mesquite (*Prosopis glandulosa*) in the Fabaceae (Legume) family, was the only deep-rooted plant on the disposal cell. The historical spread and increased density of honey mesquite on south Texas grasslands has reduced available herbaceous forage for livestock. Mesquite would likely increase on the disposal cell if the haying operation ceased. Researchers included locations with honey mesquite for test pits.

Less total foliar cover at the analogue site (73%) and borrow area (63%) than on the disposal cell can be attributed to livestock grazing. Although the invasive Bermuda grass (*Cynodon dactylon*) and weed bedstraw (Gallium sp.) are present, the native perennial grasses cane bluestem (*Bothriochloa barbinodis*) and Texas winter grass (*Nassella leucotricha*) are dominant. The most common woody plant at the analogue site is blackbrush acacia (*Vachellia rigidula*), also a shrub or small tree in the Fabaceae (Legume) family. Although blackbrush acacia has some browse value for wildlife, it increases in disturbed and overgrazed areas and has become a rangeland management problem in south Texas. Researchers considered the analogue site to be an uncertain reference for a future disposal cell plant community. The current plant community is a poor proxy for the PNV, the invasive King Ranch bluestem will likely persist on the disposal cell, and the future of management practices such as hay production and livestock grazing are unknown.

2.5.2.3 Shirley Basin South

Researchers observed three different plant communities on the Shirley Basin South disposal cell: grassland on the top decks or terraces (25% total foliar cover), a weedy rock-armored

interior slope that had filled with aeolian fines (30% cover), and a wetland at the base of the interior slope (50% cover). Like Falls City, the remediation contractor seeded the top decks. Unlike Falls City, the seed mix included both native and introduced grasses, and the vegetation is managed for seasonal livestock grazing and not hay production. The two most abundant native grasses, thickspike wheatgrass (*Elymus lanceolatus*) and Western wheatgrass (*Pascopyrum smithii*), and the two most abundant introduced grasses, crested wheatgrass (*Agropyron cristatum*) and smooth brome (*Bromus inermis*), are historically common and persistent revegetation species on central Wyoming plateaus and grasslands. Researchers selected top deck locations with the relatively deep-rooted plants fourwing saltbush and chickpea milvetch (*Astragolus cicer*) for test pits.

Researchers also selected locations on the soil-filled rock slope and wetland for test pits. Although crested wheatgrass and chickpea milkvetch were common, cheatgrass (*Bromus tectorum*), a highly invasive weed, was the dominant species on the rock-armored slope. The more common plants in the wetland community, the native species analogue sedge (Carex simulata) and mountain rush (*Juncus arcticus ssp. littoralis*) and the weedy species creeping bentgrass (*Agrostis stolonifera*) and foxtail barley (*Hordeum jubatum*), are indicative of ephemeral saturation.

Mining and remediation activities at Shirley Basin did not disturb the analogue site soil, and although subsequent moderate livestock grazing has altered the plant community, researchers considered the analogue site to be a useful PNV proxy, revegetation target, and future ecological scenario. Foliar cover was higher (40%) at the analogue site than on the top deck (25%). The lower species richness at the analogue site (17) than on the top deck (29) can be attributed to fewer weedy and introduced species (5 compared to 17 on the top deck). Most analogue site plants were mid to late seral species. The dominant plant was black sagebrush (*Artemisia nova*), a low shrub. Other common native grasses were pullup mulhy (*Muhlenbergia filiformis*), slender wheatgrass (*Elymus trachycaulus*), prairie junegrass (*Koeleria macrantha*), and Sandberg bluegrass (*Poa secunda*).

2.5.2.4 Lakeview

Researchers selected Lakeview as a study site in part due to a high vegetation development score—large increases in overall plant abundance and in abundance of deep-rooted plants since construction (Section 2.4.3.2; Tables 2-3 and 2-4). Existing plant ecology on the top deck reflects a DOE design change during the final stages of construction. The original conventional design had a surface layer of rock riprap overlying a bedding layer (Section 2.4.3.1; Figure 2-2). After construction of this rock surface, DOE decided to add a 15 cm topsoil layer seeded with native and introduced cool-season grasses (DOE 1991). The abundance of seeded grasses has remained much lower on the top deck than in surrounding revegetated areas due to inadequate shallow soil water storage as needed to establish a resilient stand of grasses. Snowmelt storage deeper in the cover (Waugh et al. 2007) creates a favorable habitat for shrubs including rubber rabbitbrush (*Ericameria nauseosa*), antelope bitterbrush (*Purshia tridentata*), and big sagebrush (*Artemisia tridentata*) (Appendix E). Researchers selected top deck locations with mature rubber rabbitbrush and antelope bitterbrush for test pits.

An area with a soil type similar to the radon barrier and with vegetation that remained undisturbed and ungrazed by livestock during and since construction of the disposal cell was selected for analogue site test pits (Figure 2-7). As a consequence, the site had high values for species richness, species diversity, total foliar cover, and foliar cover of mid-late seral species. Total foliar cover (63%) was higher at the analogue site than on the top deck (25–34%).

Researchers considered the analogue site to be a good reference area for the PNV and a reasonable future ecology scenario for cover performance evaluations. Given that the top deck had relatively high foliar cover of mid-late seral species (Figure 2-8)—plant succession has been allowed to proceed unimpeded on the top deck for over 30 years—and the analogue site is considered to be representative of potential long-term ecology, Lakeview would be a good case study for management of a conventional cover as an ET cover.

2.6 References

10 CFR 40. U.S. Nuclear Regulatory Commission, "Domestic Licensing of Source Material," *Code of Federal Regulations*.

40 CFR 192. "Health and Environmental Protection Standards for Uranium and Thorium Mill Tailings," *Code of Federal Regulations*.

Albrecht, B., and C. Benson. 2001. "Effect of desiccation on compacted natural clays," *Journal of Geotechnical Geoenvironmental Engineering* 127(1):67–76.

Albright, W.H., C.H. Benson, G.W. Gee, T. Abichou, E.V. McDonald, S.W. Tyler, and S.A. Rock, 2006. "Field performance of a compacted clay landfill final cover at a humid site," *Journal of Geotechnical Geoenvironmental Engineering* 132(11):1393–1403.

Albright, W.H., C.H. Benson, and W.J. Waugh, 2010. *Water Balance Covers for Waste Containment: Principles and Practices*, ASCE Press, Reston, Virgina.

ARCO, 1996. *Completion Report for Reclamation of the Bluewater Mill Site*, Atlantic Richfield Company, Grants, New Mexico.

Barbour, M.G., J.H. Burk, W.D. Pitts, F.S. Gilliam, and M.W. Schwartz, 1999. *Terrestrial Plant Ecology, Third Edition*, Benjamin/Cummings Publishing Company, Menlo Park, California.

Benson, C., and M. Othman, 1993. "Hydraulic conductivity of compacted clay frozen and thawed in situ," *Journal of Geotechnical Geoenvironmental Engineering* 119(2):276–294.

Bowerman, A.G., and E.F. Redente, 1998. "Biointrusion of protective barriers at hazardous waste sites," *Journal of Environmental Quality* 27:625–632.

DOE (U.S. Department of Energy), 1989. *Technical Approach Document*, Revision 2, UMTRA-DOE/AL 050425.0002, Uranium Mill Tailings Remedial Action Project,Albuquerque, New Mexico.

DOE (U.S. Department of Energy), 1991. *Lakeview, Oregon, Final Completion Report*, Albuquerque Operations Office.

DOE (U.S. Department of Energy), 1992. *Vegetation Growth Patterns on Six Rock Covered UMTRA Project Disposal Cells*, UMTRA–DOE/AL 400677.0000, Uranium Mill Tailings Remedial Action Project, Albuquerque, New Mexico.

DOE (U.S. Department of Energy), 1996. *Falls City, Texas, Final Completion Report*, Albuquerque Operations Office.

DOE (U.S. Department of Energy), 1999. *Plant Encroachment on the Burrell, Pennsylvania, Disposal Cell: Evaluation of Long-term Performance and Risk*, GJO-99-96-TAR, Environmental Sciences Laboratory, Grand Junction, Colorado.

DOE (U.S. Department of Energy), 2012. *Guidance for Developing and Implementing Long-Term Surveillance Plans for UMTRCA Title I and Title II Disposal Sites*, LMS/S00336, Office of Legacy Management.

DOE (U.S. Department of Energy), 2013. *Baseline Soil and Vegetation Characterization of the Shirley Basin South, Wyoming, UMTRCA Title II Disposal Site*, LMS/SBS/S09890, Office of Legacy Management.

DOE (U.S. Department of Energy), 2015. *Baseline Soil and Vegetation Characterization of the Bluewater, New Mexico, UMTRCA Title II Disposal Site*, LMS/BLU/S12764, Office of Legacy Management.

DOE (U.S. Department of Energy), 2016a. *Baseline Soil and Vegetation Characterization of the Falls City, Texas, Disposal Site*, LMS/FCT/S14591, Office of Legacy Management.

DOE (U.S. Department of Energy), 2016b. *Effects of Soil-Forming Processes on Cover Engineering Properties, Field Work Plan Bluewater Disposal Site, New Mexico*, LMS/BLU/S13276, Office of Legacy Management.

DOE (U.S. Department of Energy), 2016c. *Effects of Soil-Forming Processes on Cover Engineering Properties, Field Work Plan Falls City Disposal Site, Texas*, LMS/FCT/S13744, Office of Legacy Management.

DOE (U.S. Department of Energy), 2017a. *Effects of Soil-Forming Processes on Cover Engineering Properties, Field Work Plan Shirley Basin South, Wyoming, Disposal Site*, LMS/SBS/S15950, Office of Legacy Management.

DOE (U.S. Department of Energy), 2017b. *Effects of Soil-Forming Processes on Cover Engineering Properties, Field Work Plan, Lakeview, Oregon, Disposal Site*, LMS/LKD/S15951, Office of Legacy Management.

DOE (U.S. Department of Energy), 2018a. *Effects of Soil-Forming Processes on Cover Engineering Properties, Study Restoration Report, Falls City, Texas, Disposal Site*, LMS/FCT/S15952, Office of Legacy Management.

DOE (U.S. Department of Energy), 2018b. *Effects of Soil-Forming Processes on Cover Engineering Properties, Study Restoration Report, Shirley Basin South, Wyoming, Disposal Site*, LMS/SBS/S18029, Office of Legacy Management.

DOE (U.S. Department of Energy), 2018c. *Effects of Soil-Forming Processes on Cover Engineering Properties, Study Restoration Report, Lakeview, Oregon, Disposal Site*, LMS/LKD/S18030, Office of Legacy Management.

DOE (U.S. Department of Energy), 2019. *Effects of Soil-Forming Processes on Cover Engineering Properties, Study Restoration Report, Bluewater, New Mexico, Disposal Site*, LMS/BLU/S15953, Office of Legacy Management.

EPA (U.S. Environmental Protection Agency), 1989. *Technical Guidance Document: Final Covers on Hazardous Waste Landfills and Surface Impoundments*, EPA/530-SW-89-047, Office of Solid Waste and Emergency Response, Washington, D.C.

Gibbens, R.P. and J.M. Lenz, 2001. "Root systems of some Chihuahuan Desert plants," *Journal of Arid Environments* 49(2):221-263.

Hakonson, T.E., 1986. *Evaluation of Geologic Materials to Limit Biologicallintrusion into Low-Level Radioactive Waste Disposal Sites*, LA–10286–MS, Los Alamos National Laboratory, Los Alamos, New Mexico.

Kim, W.H., and D.E. Daniel, 1992. "Effects of freezing on the hydraulic conductivity of compacted clay," *Journal of Geotechnical and Geoenvironmental Engineering* 118(7):1083–1097.

Klepper, E. L., K. A. Gano, and L. L. Cadwell, 1985. *Rooting Depth and Distributions of Deep-Rooted Plants in the 200 Area Control Zone of the Hanford Site*, PNL-5247, Pacific Northwest Laboratory, Richland, Washington.

Kuchler, A. W., 1964. "Manual to accompany the map of potential natural vegetation of the conterminous United States," American Geographical Society, Special Publication No. 36, Library of Congress Catalog Card Number 64-15417.156 p.

Link, S. O., W. J. Waugh, and J. L. Downs, 1994. "Effects of coppice dune topography and vegetation on soil water dynamics in a cold-desert ecosystem," *Journal of Agricultural Research* 27:265–278.

NRC (U.S. Nuclear Regulatory Commission), 1989. *Calculation of Radon Flux Attenuation by Earthen Uranium Mill Tailings Covers*, Regulatory Guide 3.64, Office of Nuclear Regulatory Research, Washington, D.C.

NRC (U.S. Nuclear Regulatory Commission), 2002. "Design of Erosion Protection for Long-Term Stabilization," NUREG-1623, Washington, D.C.

NRC (U.S. Nuclear Regulatory Commission), 2003. "Standard Review Plan for the Review of a Reclamation Plan for Mill Tailings Sites Under Title II of the Uranium Mill Tailings Radiation Control Act of 1978," NUREG-1620, Revision 1, Office of Nuclear Material Safety and Safeguards, Washington, D.C..

NRC (U.S. Nuclear Regulatory Commission), 2011. "Engineered covers for waste containment: Changes in engineering properties and implications for long-term performance assessment," NUREG/CR-7028, Washington, D.C.

Peel, M.C., B.L. Finlayson, and T.A. McMahon, 2007. "Updated world map of the Köppen-Geiger climate classification," *Hydrology and Earth System Sciences* 11:1633–1644.

Petrotomics, 2001. *Tailings Reclamation Construction Completion Report, Shirley Basin South, Wyoming*, Petrotomics Company, Casper, Wyoming.

PL 95-604, Uranium Mill Tailings Radiation Control Act of 1978, Public Law.

Smith, W.J., R.A. Nelson, and K.R. Baker, 1985. "Sensitivity analysis of parameters affecting radon barrier cover thickness," in Proceedings of the Seventh Symposium on Management of Uranium Mill Tailings, Low-Level Waste, and Hazardous Waste, Colorado State University, Fort Collins, Colorado.

Soil Survey Staff, 1999. *Soil Taxonomy: A Basic System of Soil Classification for Making and Interpreting Soil Surveys*, Agriculture Handbook Number 436, Natural Resources Conservation Service, U.S. Department of Agriculture, Washington, D.C.

Sprackling, J.A., R.A. Read, 1979. *Tree Root Systems in Eastern Nebraska*, Nebraska Conservation Bulletin 37, Conservation and Survey Division, Institute of Agriculture and Natural Resources, University of Nebraska–Lincoln, Lincoln, Nebraska.

Stromberg, J., 2013. "Root patterns and hydrogeomorphic niches of riparian plants in the American Southwest," *Journal of Arid Environments* 94:1-9, Appendix A, "Rooting data for herbaceous plants."

Suter, G.W., II, R.J. Luxmoore, and E.D. Smith. 1993. "Compacted soil barriers at abandoned landfill sites are likely to fail in the long term," *Journal of Environmental Quality* 22:217–226.

Walker, L.R., D.A. Wardle, R.D. Bardgett, and B.D. Clarkson, 2010. "The use of chronsequences in studies of ecological succession and soil development," *Journal of Ecology* 98:725–736.

Waugh, 2006. *Sustainable Disposal Cell Covers: Legacy Management Practices, Improvements, and Long-Term Performance* (White Paper), DOE LM/GJ1156-2006, U.S. Department of Energy Office of Legacy Management.

Waugh, W.J., G.M. Smith, B. Danforth, G.W. Gee, V. Kothari, and T. Pauling, 2007. "Performance evaluation of the engineered cover at the Lakeview, Oregon, uranium mill tailings site," in Proceedings of Waste Management 2007 Symposium, Phoenix, Arizona.

3 HYDRAULIC PROPERTIES OF BARRIER MATERIALS

3.1 Introduction

Fine-grained engineered barrier layers used in final covers to control migration of gases and liquids are altered over time in response to environmental stresses such as wet-dry cycling, freeze-thaw cycling, and biota intrusion (Chamberlain et al. 1994; Othman et al. 1994; Albrecht and Benson 2001; Benson et al. 2007; Meer and Benson 2007; Scalia and Benson 2011; Scalia et al. 2017). Properties of barrier layers continue to change until the barrier is in equilibrium with the surrounding environment, or "naturalized." Benson et al. (2011) provide guidance on the hydraulic properties of naturalized barriers in NUREG CR-7028, including recommended ranges of hydraulic properties for final cover soils to use in performance assessments when simulating long-term "naturalized" conditions. This guidance is based on an integration of historical research findings and data collected during decommissioning of a network of full-scale final cover test sections constructed and monitored as part of the Alternative Cover Assessment Program (ACAP) (Albright et al. 2004).

The final covers evaluated by Benson et al. (2011) typically were associated with containment facilities for municipal or hazardous solid waste, which can be thinner than final covers for uranium mill tailings disposal facilities. The covers evaluated by Benson et al. (2011) had been in service less than a decade and may not have represented fully naturalized conditions. Whether alterations in hydraulic properties similar to those reported in Benson et al. (2011) occur in engineered barriers at greater depths, in thicker covers, or over longer in-service periods remains unknown.

Both of these issues were addressed in this study while conducting radon emission assessments at the four field sites described in Section 2. Large intact block samples were collected from the radon barrier in each cover profile from test pits representing different surface conditions that could influence alteration of the radon barrier (Figures 3-1 and 3-2). Block sampling was also conducted at analogue sites to capture what may exist for very long-term and fully naturalized conditions. Saturated hydraulic conductivity of each block sample was determined, and soil water characteristic curves (SWCCs) were measured on a subset of the block samples. Index properties and mineralogy were also measured to provide interpretative data. This chapter describes the findings from this part of the study.

3.2 Methods

3.2.1 Block Sampling

Block samples were collected from the cover profile and from the analogue sites using the procedure described in ASTM D7015. When possible, samples were collected in a vertical profile to capture conditions existing as a function of depth. Locations where the samples were collected are shown in Figure 3-1 for Falls City and Bluewater, and Figure 3-2 for Shirley Basin South and Lakeview.

The samples were collected in polyvinyl chloride (PVC) sampling rings with an inside diameter and height of 400 mm (Figure 3-3a). The procedure consisted of excavating a trench around the soil to be sampled (Figure 3-3a), followed by gradually trimming away soil around the periphery

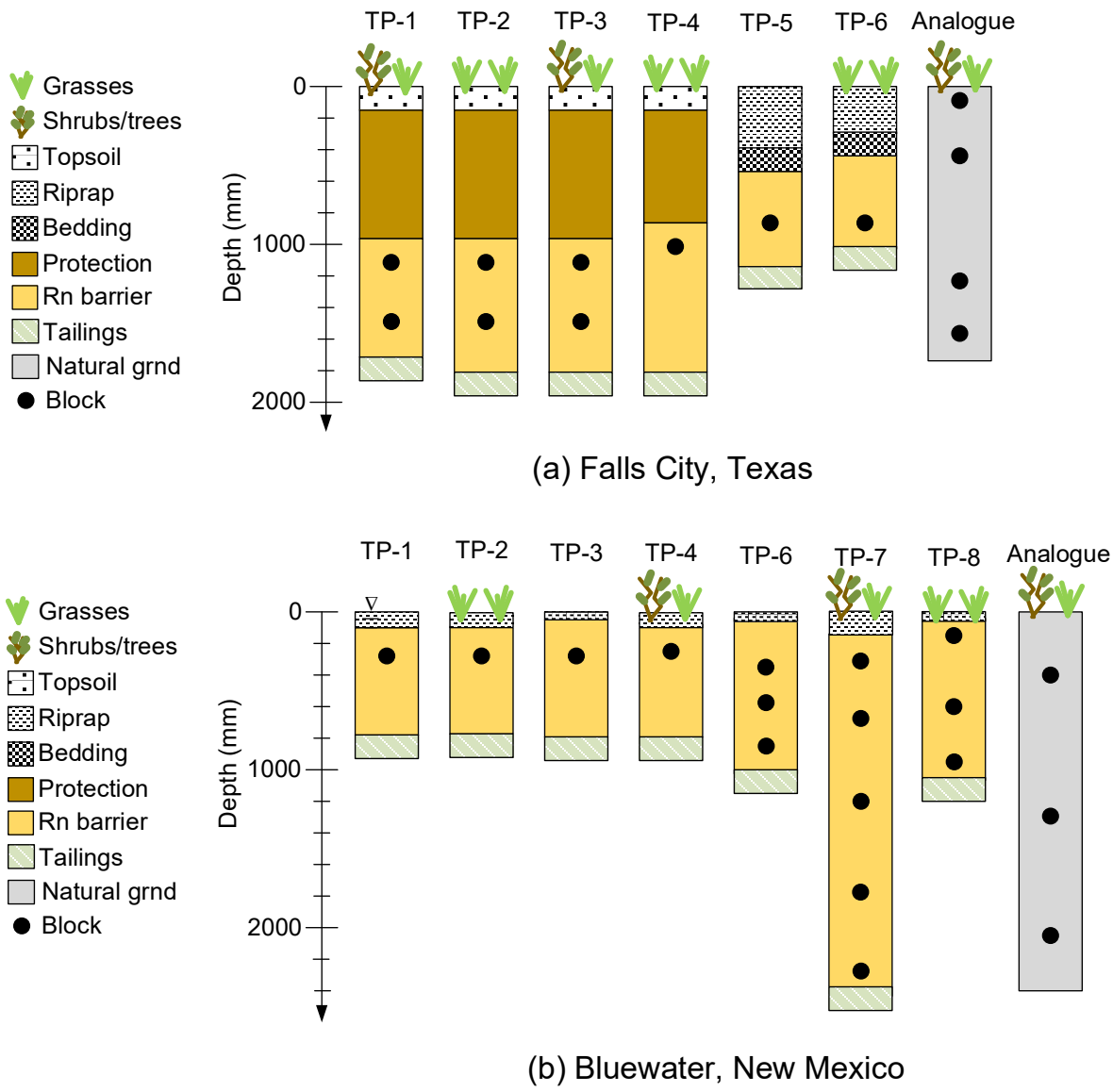

Figure 3-1 Cover Profiles from Which Block Samples Were Collected: (a) Falls City, Texas and (b) Bluewater, New Mexico Block Sampling Locations Shown With Solid Circles.

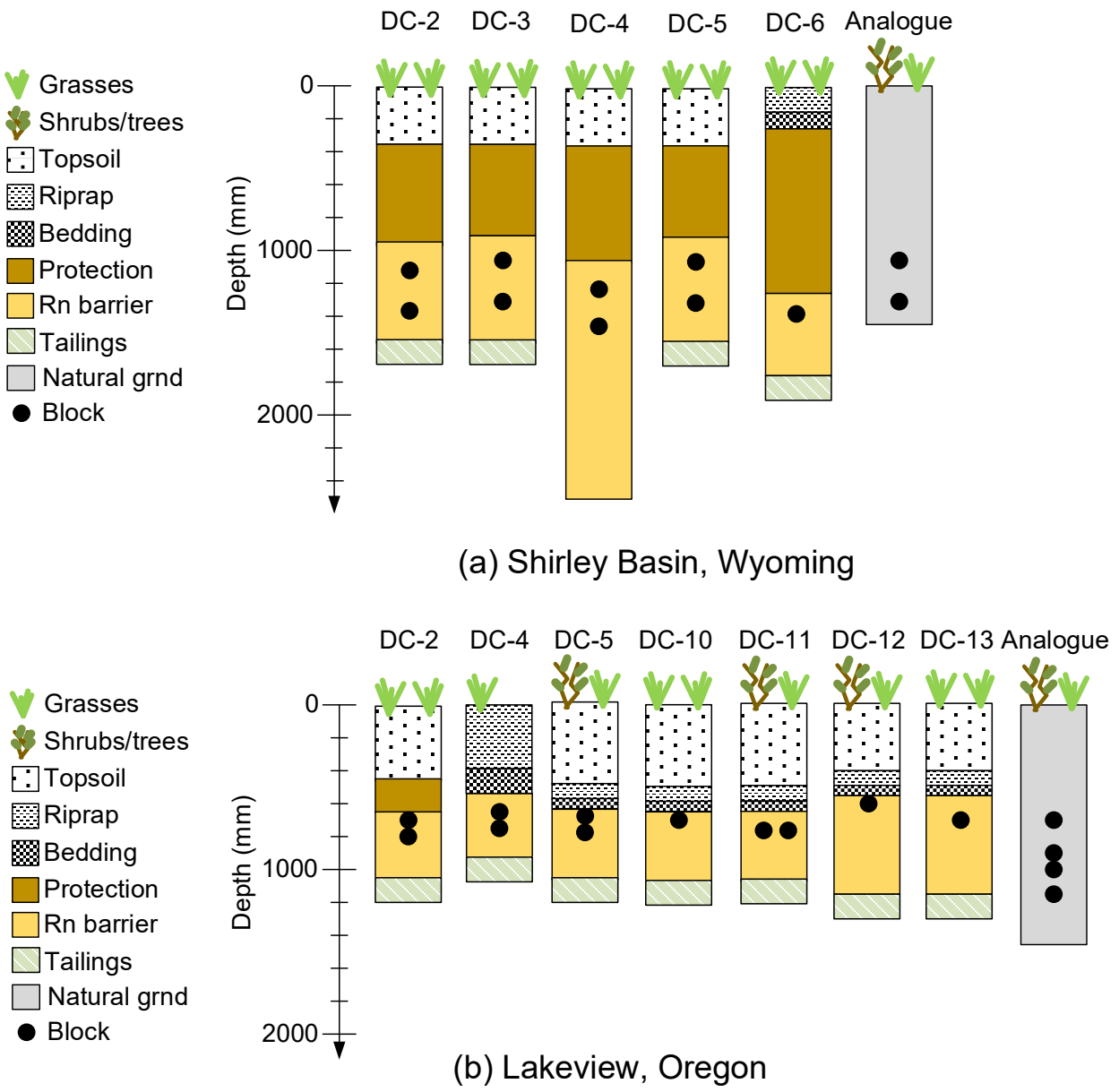

Figure 3-2 Cover Profiles from Which Block Samples Were Collected: (a) Shirley Basin, Wyoming and (b) Lakeview, Oregon Block Sampling Locations Shown With Solid Circles.

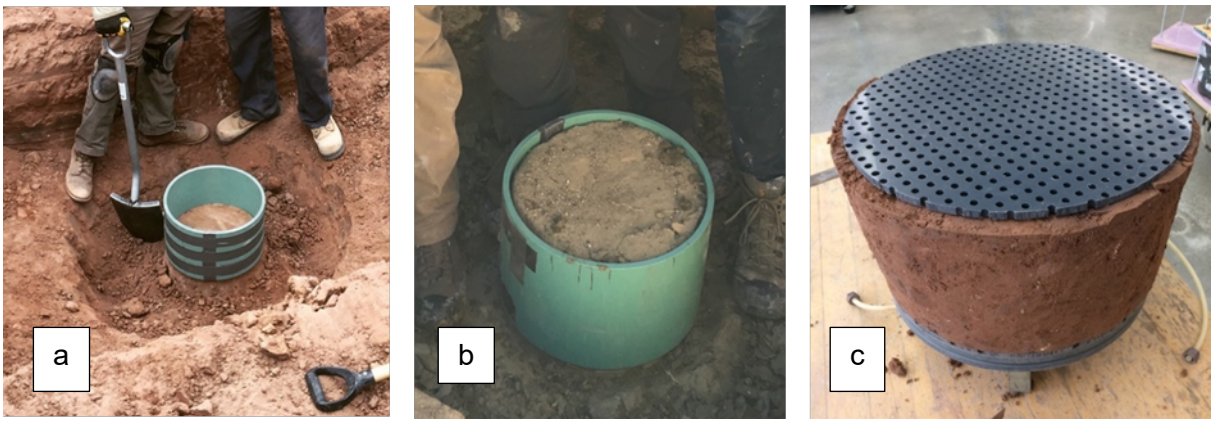

Figure 3-3 Block Samples from Radon Barriers to Characterize Hydraulic Properties: (a) trimming block sample into containment ring, (b) block sample within PVC containment ring, and (c) block sample trimmed to 305 mm diameter in the laboratory for hydraulic properties testing.

until the PVC sampling ring could be slipped over the sample while maintaining contact with the soil for confinement (Figure 3-3b). The samples were carefully sealed with plastic after being trimmed into the rings, packed in individual protective pallets, and shipped to the laboratory for testing.

3.2.2 Hydraulic Properties

Saturated hydraulic conductivity of each block sample was measured in a large-scale flexible-wall permeameter using the procedure in ASTM D5084. Test specimens were trimmed from the samples by hand to a diameter of 305 mm and aspect ratio of 1. An example of a trimmed specimen ready to be placed in a flexible-wall permeameter is shown in Figure 3-3C.

Testing was conducted using an effective stress of 21 kPa, backpressure of 280 kPa, and hydraulic gradient of approximately 10. Permeation continued until the hydraulic conductivity was steady and inflow equaled outflow, as defined in ASTM D5084.

SWCC tests were conducted on a subset of the hydraulic conductivity test specimens after permeation was complete. Specimens for SWCC testing were trimmed to a thickness of 25 mm from specimens used for hydraulic conductivity testing.

All SWCC tests were conducted following the methods in ASTM D6836. The wet end of the SWCC was measured in large-scale (300 mm diameter) pressure plate extractors similar to those described in Benson et al. (2011) following Method B in ASTM D6836. The dry end of the SWCC was determined using a chilled mirror hygrometer following Method D in D6836. A typical SWCC is shown in Figure 3-4.

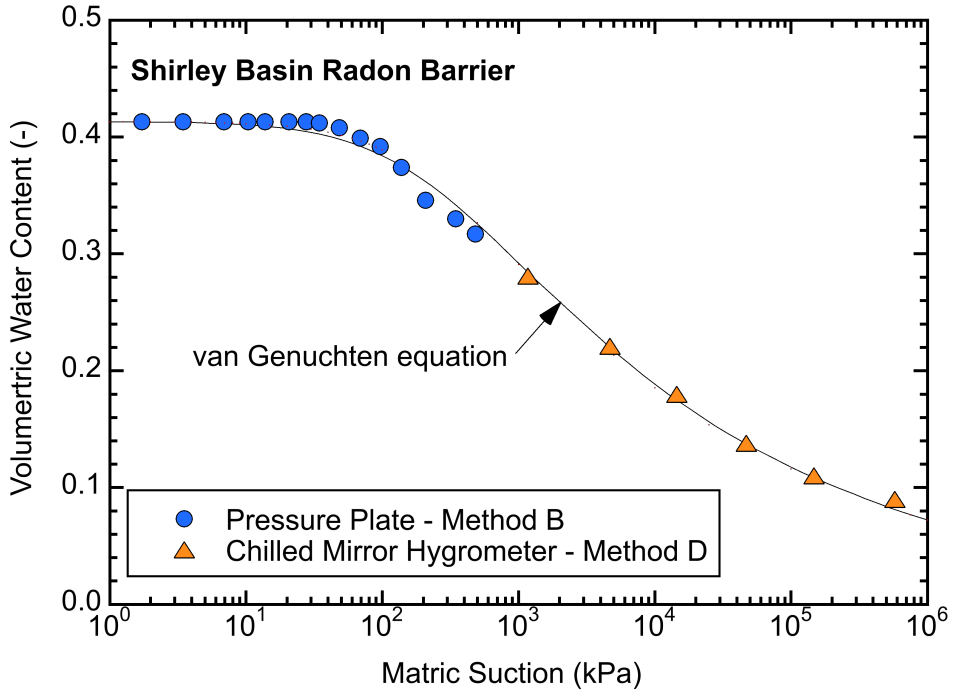

Figure 3-4 Soil Water Characteristic Curve for Radon Barrier at the Shirley Basin Site Measured With a Large-Scale Pressure Plate (Wet End – Method B) and a Chilled Mirror Hygrometer (Dry End – Method D) Following the Procedures in ASTM D6836. Solid Line is Fit of van Genuchten's Equation to the SWCC Data

The SWCC data were fit with van Genuchten's equation using a non-linear least squares regression:

$$\theta = \theta_r + (\theta_s - \theta_r)\left[\frac{1}{1+(\alpha\psi)^n}\right]^{1-\frac{1}{n}} \quad (3\text{-}1)$$

In Eq. 3-1, θ is the volumetric water content, θ_s is the saturated volumetric water content, θ_r is the residual water content, ψ is suction pressure, and α and n are the van Genuchten parameters.

3.2.3 Other Properties

Particle size distribution (ASTM D6913), Atterberg limits (ASTM D4318), and mineralogy were measured on each sample for interpretive purposes. Mineralogy was determined by X-ray diffraction following the methods in Moore and Reynolds (1989) and Scalia et al. (2014).

3.3 Results

Saturated hydraulic conductivities of the block samples are reported in Tables 3-1 and 3-2. The index properties are summarized in Table 3-3, and the mineralogy is summarized in Table 3-4. Saturated and residual water contents, α, and n are reported in Table 3-5. Soils used to

construct the radon barriers are similar to those used for engineered barriers at the sites described in NUREG CR-7028 – clayey sands and sandy clays and silts of low to high plasticity (Benson and Gurdal 2013).

3.3.1 Saturated Hydraulic Conductivity

Saturated hydraulic conductivity of the block samples is shown in Figure 3-5 as a function of depth for each of the four sites. The data points are distinguished by different symbols to represent type of cover surface (vegetated or rock armor) and data from analogue sites. The vertical dashed lines in Figure 3-5 represent the lower and upper bounds (1.0×10^{-7} to 5.0×10^{-6} m/s) of the range recommended in NUREG CR-7028 to represent naturalized conditions in performance assessments.

Saturated hydraulic conductivities for the Falls City, Bluewater, and Lakeview sites generally fall within the range recommended in NUREG CR-7028, with some points modestly below the recommended lower bound. In contrast, all but one of the saturated hydraulic conductivities for the Shirley Basin site fall approximately one to four orders of magnitude below the lower bound recommended in NUREG CR-7028. Some of the samples from Shirley Basin have saturated hydraulic conductivity approaching 10^{-11} m/s, which is comparable to sodium bentonite (Jo et al. 2001).

For all sites, no systematic trend exists between saturated hydraulic conductivity and depth or saturated hydraulic conductivity and type of surface treatment (vegetated or rock armored). Additional discussion of mechanisms affecting the hydraulic conductivity are in Section 7. Saturated hydraulic conductivities of samples from the analogue sites representing the naturalized condition are comparable to or modestly higher than saturated hydraulic conductivities of the blocks removed from each site. Saturated hydraulic conductivities for the analogue sites generally fall towards the higher end of the range recommended in NUREG CR-7028, except those from the analogue at Shirley Basin.

A definitive reason has not been identified for the much lower saturated hydraulic conductivities at Shirley Basin. The radon barrier at Shirley Basin is constructed of highly plastic clay, with montmorillonite as the predominant clay mineral. The montmorillonitic clays in Wyoming typically are sodic, which are known to swell sufficiently during wetting to close cracks and other macroscopic features that contribute to higher hydraulic conductivity. Composition of the exchange complex was not assessed in this study, but hydraulic conductivities on the order of 10^{-11} m/s for some of the samples from Shirley Basin are strongly indicative of sodic conditions (Lin and Benson 2020). The clay at Shirley Basin also was acidic, which impedes root development (see Section 7). Consequently, the radon barrier may not have been exposed to the same degree volume change and structural development as other sites, and the impacts of any structure may have been ameliorated by swelling during wetting.

Montmorillonitic clay was also used to construct the radon barrier at the Falls City site (Tables 3-3 and 3-4), and most of the samples collected from the Falls City site were from comparable depth as those at Shirley Basin (~ 1.0 to 1.5 m bgs). However, the samples from Falls City had much higher hydraulic conductivity. Both sites had surfaces comprised of vegetated soil or rock armor (Figure 3-5 a, c). However, Falls City had much more extensive vegetation with greater root penetration into the radon barrier. Falls City also had woody species that had rooted into the radon barrier, providing greater opportunity for volume change and structural change induced by

Table 3-1. Summary of Physical Properties and Saturated Hydraulic Conductivities for Bluewater and Falls City Sampling Location Corresponds to Fig. 3-1

Site and Area	Sampling Location	Depth Below Ground Surface (m)	Depth to Top of Rn Barrier (m)	Water Content (%)	Dry Unit Wt. (kN/m^3)	Porosity	Saturated Hydraulic Conductivity (m/s)
Falls City Top Deck	TP-1	1.12	0.99	37.6	12.7	0.51	$1.2x10^{-9}$
	TP-1	1.47	0.99	38.9	11.4	0.56	$2.1x10^{-7}$
	TP-2	1.11	0.98	39.6	11.8	0.55	$4.2x10^{-7}$
	TP-2	1.46	0.98	40.5	15.6	0.40	$9.4x10^{-9}$
	TP-3	1.08	0.95	39.4	15.7	0.40	$1.1x10^{-7}$
	TP-3	1.43	0.95	38.4	12.3	0.53	$5.4x10^{-7}$
	TP-4	1.03	0.90	37.9	11.0	0.58	$3.9x10^{-6}$
Falls City Apron/ Slope	TP-5	0.92	0.79	39.7	11.6	0.56	$2.0x10^{-7}$
	TP-6	0.52	0.39	44.1	11.8	0.55	$1.0x10^{-6}$
	TP-6	0.87	0.39	39.3	11.4	0.56	$2.4x10^{-7}$
Falls City Analogue	Analogue	0.13	-	30.1	12.1	0.54	$1.5x10^{-7}$
	Analogue	0.48	-	30.1	14.2	0.45	$1.4x10^{-6}$
	Analogue	1.35	-	11.0	15.5	0.40	$1.4x10^{-6}$
	Analogue	1.60	-	37.9	12.2	0.53	$4.1x10^{-6}$
Bluewater Top Deck	TP-1	0.24	0.11	12.9	19.0	0.27	$1.3x10^{-8}$
	TP-2	0.22	0.09	10.6	17.6	0.32	$2.8x10^{-6}$
	TP-3	0.21	0.08	8.1	17.6	0.32	$2.4x10^{-6}$
	TP-4	0.19	0.06	12.7	19.1	0.27	$4.7x10^{-8}$
	TP-6	0.25	0.12	10.2	17.0	0.35	$4.7x10^{-6}$
	TP-6	0.86	0.12	12.7	17.1	0.34	$1.2x10^{-6}$
	TP-7	0.27	0.14	7.2	16.7	0.36	$1.6x10^{-6}$
	TP-7	0.60	0.14	12.6	17.6	0.32	$2.2x10^{-6}$
	TP-7	1.18	0.14	11.3	16.2	0.38	$3.5x10^{-8}$
	TP-7	1.72	0.14	12.8	16.9	0.35	$7.5x10^{-8}$
	TP-7	2.33	0.14	11.5	16.2	0.38	$1.5x10^{-8}$
	TP-8	0.17	0.04	10.7	16.9	0.35	$4.9x10^{-7}$
	TP-8	0.58	0.04	16.8	15.3	0.41	$1.8x10^{-6}$
	TP-8	1.01	0.04	11.9	17.4	0.33	$7.8x10^{-7}$
Bluewater Analogue	Analogue	0.28	-	8.6	14.4	0.45	$3.7x10^{-6}$
	Analogue	1.35	-	3.3	15.4	0.41	$4.4x10^{-6}$
	Analogue	2.06	-	8.8	16.0	0.38	$4.2x10^{-6}$

Note: Hyphen indicates data not available or undefined.

Table 3-2. Summary of Physical Properties and Saturated Hydraulic Conductivities for Shirley Basin and Lakeview Sampling Location Corresponds to Fig. 3-2

Site and Area	Sampling Location	Depth Below Ground Surface (m)	Depth to Rn Barrier Surface (m)	Water Content (%)	Dry Unit Wt. (kN/m^3)	Porosity	Saturated Hydraulic Conductivity (m/s)
Shirley Basin Top Deck	DC-2	1.07	0.95	27.20	14.2	0.45	$1.1x10^{-7}$
	DC-2	1.39	0.95	20.90	13.7	0.47	$4.9x10^{-9}$
	DC-3	1.02	0.90	27.60	14.3	0.45	$1.5x10^{-9}$
	DC-3	1.30	0.90	20.00	16.5	0.36	$6.6x10^{-9}$
	DC-4	1.22	1.09	25.00	15.6	0.40	$1.1x10^{-8}$
	DC-4	1.55	1.09	20.60	15.8	0.39	$5.9x10^{-11}$
	DC-5	1.09	0.97	32.00	14.8	0.43	$3.2x10^{-11}$
	DC-5	1.37	0.97	29.60	14.2	0.45	$1.2x10^{-10}$
Shirley Basin Slope	DC-6	1.38	1.25	26.50	14.9	0.43	$2.4x10^{-11}$
Shirley Basin Analogue	Analogue	1.05	-	13.40	18.1	0.30	$1.4x10^{-9}$
	Analogue	1.35	-	17.60	17.0	0.35	$9.8x10^{-9}$
Lakeview Top Deck	DC-2	0.64	0.64	42.0	13.2	0.49	$3.2x10^{-6}$
	DC-2	0.76	0.64	27.2	14.2	0.45	$1.1x10^{-7}$
	DC-5	0.64	0.64	37.2	13.9	0.46	$1.6x10^{-6}$
	DC-5	0.76	0.64	37.2	13.9	0.49	$1.0x10^{-6}$
	DC-10	0.67	0.64	31.7	12.3	0.53	$1.3x10^{-7}$
	DC-11	0.76	0.64	37.1	12.5	0.52	$1.3x10^{-6}$
	DC-11	0.76	0.64	43.8	11.9	0.54	$5.2x10^{-7}$
	DC-12	0.55	0.55	30.4	13.0	0.50	$1.7x10^{-7}$
	DC-13	0.64	0.51	16.0	14.9	0.43	$1.4x10^{-6}$
Lakeview Slope	DC-4	0.61	0.48	16.3	14.1	0.46	$3.4x10^{-7}$
Lakeview Analogue	Analogue	0.70	-	14.0	14.3	0.45	$3.2x10^{-6}$
	Analogue	0.95	-	15.6	15.7	0.40	$3.1x10^{-6}$
	Analogue	0.90	-	17.9	15.4	0.41	$5.4x10^{-6}$
	Analogue	1.10	-	16.2	15.9	0.39	$3.1x10^{-6}$

Note: Hyphen indicates data not available or undefined.

Table 3-3 Ranges of Index Properties of Radon Barriers and Analogues at Each Site

Site	Area	Gravel (%)	Sand (%)	Fines (%)	Clay (%)	Liquid Limit	Plasticity Index
Falls City	Facility	0-2	9-20	80-91	42-51	79	41
	Analogue	0	9	91	51	69	46
Bluewater	Facility	<1	32-72	30-68	11-38	28-33	10-17
	Analogue	<1	51-68	40-49	25	22-35	NP-17
Shirley Basin	Facility	0-5	6-33	65-93	34-66	67	38-39
	Analogue	0	4-44	56-96	41-72	-	-
Lakeview	Facility	1-4	24-37	61-74	6-13	45-47	14-15
	Analogue	-	-	-	-	-	-

Notes: Gravel > 4.9 mm, 4.9 mm > sand > 0.075 mm, clay < 2 μm, NP = non plastic, hyphen indicates data not available.

Table 3-4 Ranges of Primary Minerals in Radon Barriers and Analogues at Each Site

Site	Area	Quartz (%)	Montmorillonite (%)	Illite & Mixed Layer (%)	Kaolinite (%)
Falls City	Facility	14-17	59-58	0.5-1.0	<0.5
	Analogue	17	58	0.5	0.5
Bluewater	Facility	27-49	38-39	40-45	1.5-2.0
	Analogue	21-29	1	18-57	0.5
Shirley Basin	Facility	8-12	66-75	1-2	8-13
	Analogue	9-20	55	2-3	6-12
Lakeview	Facility	2	0	65-69	<0.5
	Analogue	4-5	0	54-56	1-3

Table 3-5 Summary of van Genuchten Parameters for SWCCs

Site and Area	Sampling Location	Depth Below Ground Surface (m)	θ_r	θ_s	α (kPa^{-1})	n
Bluewater	TP-3	0.21	0.00	0.29	0.0531	1.25
	TP-7	0.27	0.00	0.28	0.1952	1.14
	TP-7	0.60	0.00	0.32	0.1387	1.19
Bluewater	Analogue	0.28	0.00	0.42	0.3034	1.20
Shirley Basin	DC-4	1.22	0.00	0.40	0.0049	1.20
	DC-5	1.09	0.00	0.50	0.0018	1.36

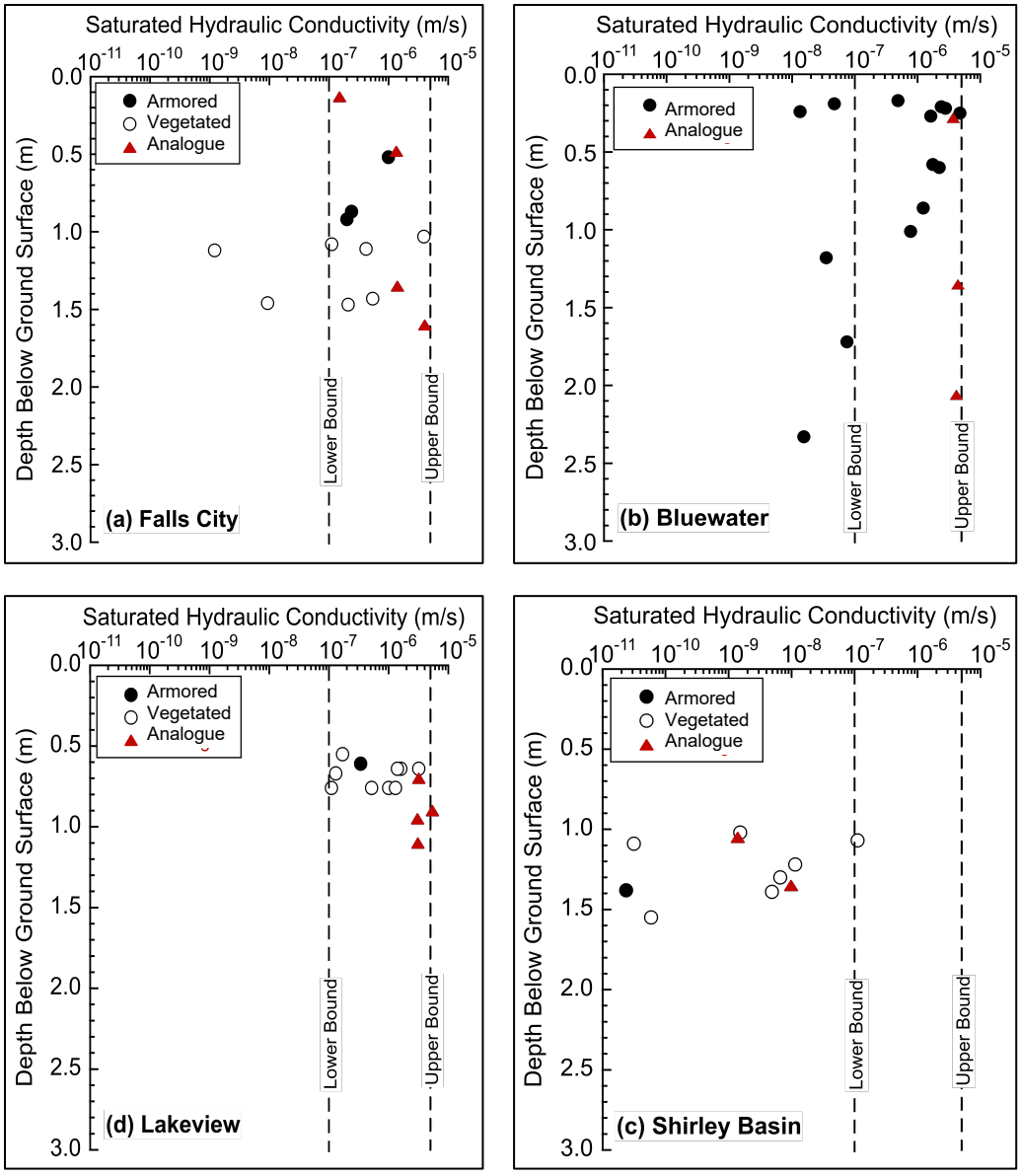

Figure 3-5 Saturated Hydraulic Conductivity of Block Samples Removed from Radon Barriers and Analogue Sites: (a) Falls City, Texas; (b) Bluewater, New Mexico; (c) Shirley Basin, Wyoming; and (d) Lakeview, Oregon. Upper and Lower Bounds from Recommendations in NUREG CR-7028.

root water uptake. The clays in south Texas also have greater propensity for being calcic, limiting their ability to swell and close structural features that contribute to higher hydraulic conductivity.

3.3.2 Soil Water Characteristic Curve

Saturated water content and van Genuchten's α and n parameters are shown as a function of depth below ground surface in Figure 3-6 for the Bluewater and Shirley Basin sites. SWCC tests were not conducted on block samples from the Falls City and Lakeview sites. Residual water content is not shown in Figure 3-6 because all of the residual water contents were determined to be zero (Table 3-5). As with saturated hydraulic conductivity, data are reported for samples from the radon barrier and a block sample from an analogue site.

The α parameter, which is inversely related to the air entry suction (suction beyond which the soil will desaturate), generally falls in the range recommended in NUREG/CR-7028 for the Bluewater site (Figure 3-6a). The α parameter for the Bluewater analogue site also falls in the recommended range, and near the upper bound. In contrast, α for the Shirley Basin samples is 50-100 times lower than the range recommended in NUREG/CR-7028.

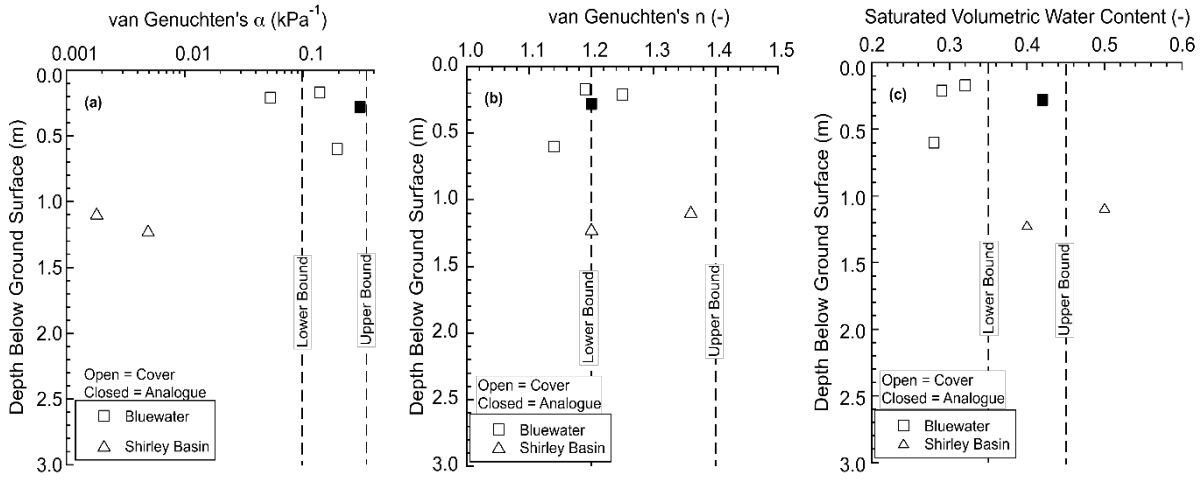

Figure 3-6 Soil Water Characteristic Curve Parameters for Block Samples Removed from the Bluewater and Shirley Basin Sites: (a) α, (b) n, and (c) θ_s. Upper and Lower Bounds from Recommendations in NUREG/CR-7028.

The n parameter, which describes the rate of variation of water content with suction beyond the air entry suction, generally falls within the range recommended in NUREG/CR-7028, with one exception. The sample from the Bluewater analogue also had n in the recommended range (Figure 3-6b). Most of the n parameter data fall towards the lower end of the range, with the outlier from the Bluewater site below the lower bound of the recommended range.

The saturated volumetric water content spans a broader range than recommended in NUREG/CR-7028, but on average (0.37) is within the recommended range (Figure 3-6c). Saturated water content for the Bluewater analogue is within the recommended range, whereas all of the

saturated water contents for the Bluewater radon barrier fall below the recommended range. The saturated water contents for the Shirley Basin site fall within or modestly above the range recommended in NUREG/CR-7028.

The α and n parameters are consistent with each other, and with the saturated hydraulic conductivity as shown in Figure 3-7. Larger pores form as structure develops, causing an increase in the saturated hydraulic conductivity and decrease in the suction required for the soil to desaturate (larger α) (Figure 3-7a). Formation of larger pores also increases the breadth of pore sizes in the radon barrier, which is deliberately compacted during construction to achieve low saturated hydraulic conductivity by eliminating large pores (Benson and Daniel 1990). Creating a broader range of pores by adding large pores associated with structure yields both lower n and larger α, resulting in the correspondence between n and α shown in Figure 3-7b (Benson and Gurdal 2013).

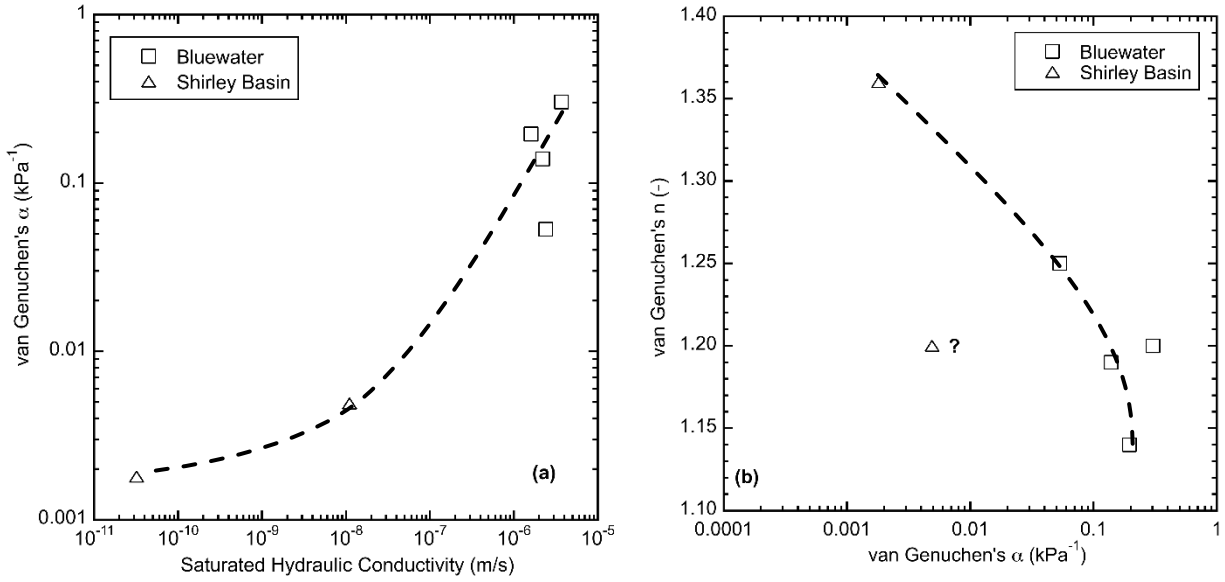

Figure 3-7 Relationships Between (a) Parameter and Saturated Hydraulic Conductivity and (b) n and Parameter for Block Samples Removed from the Bluewater and Shirley Basin Sites

3.4 Summary

Hydraulic properties were measured on block samples collected from the radon barriers and analogue profiles at the four sites described in Section 2. These hydraulic properties are generally consistent with the recommendations in NUREG CR-7028 for parameter ranges representative of naturalized conditions for use in performance assessments. The findings also indicate the following:

- No systematic relationship exists between the hydraulic properties and depth of sampling or type of surface cover (vegetated vs. armored) for the locations evaluated at these sites. Additional discussion of factors contributing to differences in hydraulic conductivity between sites and between sampling locations on each site are in Section 7.

- Saturated hydraulic conductivities of samples collected from all but one of the analogue sites were near the upper bound recommended in NUREG/CR-7028, suggesting that the upper bound may be a realistic condition for simulating fully naturalized conditions in performance assessments.

- The van Genuchten parameters for the SWCC generally were within the bounds recommended in NUREG/CR-7028, but the data varied over a broader range than identified by the bounds. However, the data set for van Genuchten parameters is small, limiting the inferences that can be made from the data.

- Strong correspondence exists between the saturated hydraulic conductivity and the van Genuchten parameters α and n that is consistent with the impact of structural development on hydraulic properties during naturalization.

3.5 References

Albrecht, B. and Benson, C. (2001), Effect of Desiccation on Compacted Natural Clays, *J. Geotech. Geoenvironmental Eng.,* 127(1), 67-76.

Albright, W., Benson, C., Gee, G., Roesler, A., Abichou, T., Apiwantragoon, P., Lyles, B., and Rock, S. (2004), Field Water Balance of Landfill Final Covers, *J. Environ. Quality*, 33(6), 2317-2332.

Benson, C. and Daniel, D. (1990), Influence of Clods on Hydraulic Conductivity of Compacted Clay, *J. Geotech. Eng.*, 116(8), 1231-1248.

Benson, C. and Gurdal, T. (2013), Hydrologic Properties of Final Cover Soils, Foundation Engineering in the Face of Uncertainty, *GSP No. 229*, J. Withiam et al., Eds., ASCE, Reston VA, 283-297.

Benson, C., Sawangsuriya, A., Trzebiatowski, B., and Albright, W. (2007), Post-Construction Changes in the Hydraulic Properties of Water Balance Cover Soils, *J. Geotech. Geoenvironmental Eng.,* 133(4), 349-359.

Benson, C., Albright, W., Fratta, D., Tinjum, J., Kucukkirca, E., Lee, S., Scalia, J., Schlicht, P., Wang, X. (2011), Engineered Covers for Waste Containment: Changes in Engineering Properties & Implications for Long-Term Performance Assessment, NUREG/CR-7028, Office of Research, U.S. Nuclear Regulatory Commission, Washington.

Chamberlain, E., Erickson, A. and Benson, C. (1994), Effects of Frost Action on Compacted Clay Barriers, *Geoenvironment 2000*, ASCE, GSP No. 46, 702-717.

Jo, H., Katsumi, T., Benson, C., and Edil, T. (2001), Hydraulic Conductivity and Swelling of Non-Prehydrated GCLs Permeated with Single Species Salt Solutions, *J. Geotech. Geoenvironmental Eng.,* 127(7), 557-567.

Lin, L. and C. Benson (2000), Effect of Wet-Dry Cycling on Swelling and Hydraulic Conductivity of Geosynthetic Clay Liners, *J. Geotech. Geoenvironmental Eng.,* 126(1), 40-49.

Meer, S. and Benson, C. (2007), Hydraulic Conductivity of Geosynthetic Clay Liners Exhumed from Landfill Final Covers, *J. Geotech. Geoenvironmental Eng.,* 133(5), 550-563.

Moore, D. and Reynolds, R. (1989). *X-ray Diffraction and the Identification of Clay Minerals*. Oxford University Press, New York, 332 p.

Othman, M., Benson, C., Chamberlain, E., and Zimmie, T. (1994), Laboratory Testing to Evaluate Changes in Hydraulic Conductivity Caused by Freeze-Thaw: State-of-the-Art, *Hydraulic Conductivity and Waste Containment Transport in Soils, STP 1142*, ASTM International, S. Trautwein and D. Daniel, eds., 227-254.

Scalia, J. and Benson, C. (2011), Hydraulic Conductivity of Geosynthetic Clay Liners Exhumed from Landfill Final Covers with Composite Barriers, *J. Geotech. Geoenvironmental Eng.,* 137(1), 1-13.

Scalia, J., Benson, C., Albright, W., Smith, B., and Wang, X. (2017), Properties of Barrier Components in a Composite Cover after 14 Years of Service and Differential Settlement, *J. Geotech. Geoenvironmental Eng.,* 04017055.

Scalia, J., Benson, C., Bohnhoff, G., Edil, T., and Shackelford, C. (2014). Long-Term Hydraulic Conductivity of a Bentonite-Polymer Composite Permeated with Aggressive Inorganic solutions. *J. Geotech. and Geoenvironmental Eng.,* 140(3), 10.1061/(ASCE)GT.1943-5606.0001040, 04013025.

4 RADON FLUX

4.1 Introduction

Radon flux is a measure of the quantity of Rn moving through a porous medium, specifically in this case, through the radon barrier. It is measured as a quantity of the gas as it passes a surface of the barrier in terms of surface area (m^2) and per unit time (s), in terms of $Bq/m^2/s$. This is of interest because it is one pathway by which radioactive material can be transported from a disposal facility and because of the potential dose that may be incurred from Rn-222 and its' progeny.

Section 1.2 of this report provides background on uranium mill tailings sites, defines Title I and Title II sites and the regulatory requirements for them. Title 40 CFR 192.02 sets limits for Rn releases from Title I sites by requiring that the design of the facility shall provide reasonable assurance that releases of radon-222 from residual radioactive material to the atmosphere will not: (1) exceed an average release rate of 20 picocuries per square meter per second ($pCi/m^2/s$), or (2) Increase the annual average concentration of radon-222 in air at or above any location outside the disposal site by more than one-half picocurie per liter. Because the standard applies to design, monitoring after disposal is not required to demonstrate compliance with respect to 40 CFR 192.02(a) and (b). This average applies over the entire surface of the disposal site and over at least a 1-year period. Requirements for Title II sites in 10 CFR Part 40, Appendix A, state that radon-222 release is limited to the 20 $pCi/m^2/s$ but with no criterion for off-site concentration increase. The 20 $pCi/m^2/s$ (0.74$Bq/m^2/s$) regulatory requirement does not apply to individual measurements but is used in this report as a convenient benchmark.

The design of radon barriers was based on the assumption that simple diffusion theory adequately describes long-term radon transport through the earthen cover (Rogers et al., 1984). This was based on substantial testing and modeling (e.g., Kalkwarf and Mayer, 1983; Rogers et al., 1989; Rogers et al., 1983; and Rogers et al., 1980). As a result, a diffusion model was used to calculate the thickness needed for radon barriers to achieve the 20 $pCi/m^2/s$ (0.74 $Bq/m^2/s$) regulatory requirement based on estimates of waste emanation and long-term moisture content and porosity of the barrier (U.S. NRC, 1989). Section 5 of this report discussed the use of Pb-210 profiles within Rn barriers to examine Rn transport over long times and to test the assumption of diffusion on barriers that have aged about 20 years.

This chapter reports Rn flux results as measured at the top of the radon barrier (after any protective layer was removed) and flux from the waste under the radon barrier. Discussion includes comparisons of fluxes from locations impacted by surface features, and calculation of diffusion coefficients and Rn travel times. Material from this section has been published in a peer reviewed journal paper reporting flux results (Fuhrmann et al., 2021).

4.2 Methods

Methods for site selection and field work are described in this section. For details about the accumulation chambers, analytical methods related to Rn-222 flux measurements, flux computation, and related laboratory measurements, see Appendix F. Data presented in this section does not differentiate among the various size flux chambers. Analysis of our flux results showed there was essentially no systematic difference when fluxes were examined on a project wide basis and little if any effect was observed for site specific data. The data for this conclusion are examined in Appendix G.

Fieldwork was performed in 2016 at the Falls City, TX and Bluewater, NM sites (Stefani, 2016) and in 2017 at the Shirley Basin South, WY and Lakeview, OR sites (Michaud, 2018). At each site radon flux measurements were obtained at several test pit locations from the top surface of the exposed Rn barrier (i.e., after protective layers were removed by excavation) and from the surface (or near the surface) of the underlying waste at each site (i.e., after excavation through the Rn barrier layer). Measurements were obtained using accumulation chambers containing activated carbon (AC) canisters and connections to continuously monitoring RAD7 alpha detectors. Test pits were excavated at selected locations (sometimes paired with near-by control test pits) so that the effects of surface features including vegetation, seasonal ponding, animal burrowing, cover protection type/thickness, and Rn barrier thickness on Rn flux could be isolated. Many of these parameters are discussed in Chapters 6 and 7. For details of soil properties such as moisture and density profiles see Stefani (2016) and Michaud (2018), and for pedogenic properties see Williams (2019).

4.2.1 Site Selection and Survey Design

Our sampling design was meant to seek impacts related to in service conditions on the covers. In that sense it is deliberately biased. It did not attempt to perform a systematic survey to determine a site-wide average Rn flux for comparison to the closure flux surveys, rather, it quantified Rn flux in areas of the cover that have been impacted by various processes such as large plant growth. In some cases, pairs of nearby test pits were excavated to compare impacted and unimpacted (control) areas. Chapter 2.4 provides details on test pit selection criteria and conditions tested. Locations were often chosen where as-built Rn fluxes and/or Ra-226 levels in tailings were highest, as indicated by measurements during cell construction and closure. See Tables 2-10 through 2-13 for as-built fluxes at test pit locations. Our sampling took place at the historically driest time of the year when we would expect the seasonally driest soil and greatest flux (see Figure 2-3).

Because of the differences in survey objectives and design, no site-wide comparison should be made between averages of in-service measurements and the as-built Rn flux surveys that were conducted at the time of site closure. As-built surveys were conducted on a site-wide grid pattern and generally consisted of at least 100 measurements. These flux measurements were often made soon after emplacement of the radon barrier when they were still conditioned to the moisture content required for construction. As a result, any comparisons of fluxes must recognize these differences. While we have not compared site-wide averages of our flux measurements to those of the as-built surveys, we have compared:

- frequency distributions of our in-service measurements to those of the as-built surveys
- in-service measurements from individual test pits to the as-built average, and
- in service measurements from individual pits to nearby as-built fluxes.

4.2.2 Field Test Pits

Field test pits were excavated through the protection (rooting/bedding layers and/or rip rap) layers using small excavators at each site so that Rn flux could be measured directly from the Rn barrier surface. Test pit dimensions varied at each excavation but were approximately 4 m x 5 m. Materials from the protective layers were stockpiled and later replaced and compacted to as-built conditions after flux measurements were taken.

4.2.3 Surface Radon Flux Measurements ("Top" Flux)

Radon flux measurements were taken from the upper surface of the exposed Rn barrier (after excavation through the overlying protective layers), using accumulation chambers. These measurements are termed "Top Fluxes". In most cases, four sizes of flux chambers (Appendix F and G) were used at each test pit. Prior to beginning each flux measurement, moistened bentonite paste was placed by hand around the edges of the flux chambers to create a seal. This was done to minimize the effects of Rn gas leakage during each flux measurement.

Each accumulation chamber was connected to a RAD7 instrument (Durridge Company, Inc. Billerica, MA) for near real-time Rn measurements (Appendix F). This is a continuous monitoring instrument containing a solid-state alpha detector to measure disintegrations of Rn alpha progeny over a designated time period. The RAD7 has been used extensively in Rn emanation rate studies for building materials (Chao et al. 1997, Tuccimei et al. 2006, Vargas and Ortega 2007, Ujic et al. 2008). A pump in the instrument continually cycles air from the sampling environment through the detector. The RAD7 distinguishes between different energy levels so that only Rn is accounted for in the alpha particle monitoring. A flow rate of 800 mL/min and a sampling frequency (cycle time) of 15 min to 1 h were used for most tests.

Each accumulation chamber also contained a canister of activated carbon (AC) from Radon Testing Corporation of America (RTCA, Elmsford, NY). These canisters, which are analogous to canisters used in residential Rn sensing applications, were 100-mm-diameter open-faced canisters containing 90 g of AC (National Radon Safety Board device code = 10331). Canisters exposed in the flux chambers were sealed and shipped to RTCA for analysis of adsorbed Rn concentration. A discussion of the results from the two methods is given in Appendix F. Only results from the RAD7 instruments are used in this report.

When schedule and test pit size allowed, duplicate flux measurements were taken from the Rn barrier surface to increase the size of the dataset. Typically, these duplicate measurements were taken immediately adjacent to the initial set of flux measurements to minimize any potential differences in tailings activity, Rn barrier thickness, and barrier conditions. Radon measurements were essentially simultaneous in each pit. Fluxes were calculated following the procedures described in Appendix F. Figure 4-1 shows two sets of four different sizes of flux chambers as they are deployed in the field connected to the RAD7 instruments. Figure 4-2 is a cross-section of an accumulation chamber.

Figure 4-1 Field Installation of Eight Flux Chambers of Four Sizes on the Top of the Radon Barrier at Shirley Basin South
The black cases are RAD7 instruments, some of which are in plastic bags for protection for overnight deployment. They are being charged with a portable generator. At top of the photograph a test is being conducted of a portable hydraulic conductivity instrument.

4.2.4 Radon Flux Measurements from the Waste ("Bottom" Flux)

After measurements were obtained from the surface of the Rn barrier (i.e., the "top" flux measurements), the barrier layer was hand excavated to obtain flux measurements directly from the underlying tailings, or as close as possible to the top of the waste. During this process samples were taken for hydraulic conductivity and Pb-210 measurements, and observations of the soil properties were made. Figure 4-2 is a cross-section schematic of a bottom flux being taken and Figure 4-3 is a photograph showing the "small" flux chamber and Rad7 instrument. These measurements are referred to as the "bottom" flux measurements. Only a limited number of these measurements were made due to excavation size limitations and health physics concerns, and only small flux chambers were used for these measurements. Bentonite paste was again used to create a seal between the soil and the edges of the chamber to minimize gas leakage from the chamber.

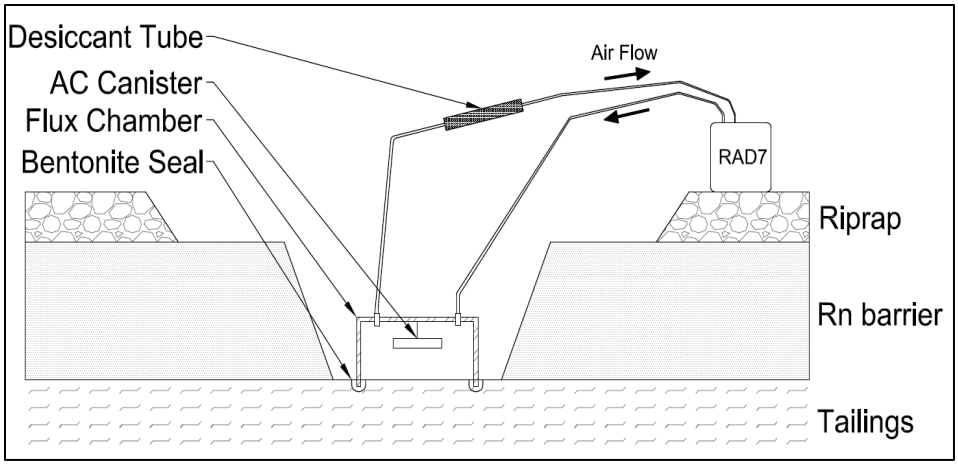

Figure 4-2 Schematic of a "Bottom" Flux Measurement Taken Directly on the Tailings Underlying the Rn Barrier Layer

4.2.5 Flux Measurement and Uncertainty

As mentioned above, RAD7 and AC methods were used to determine Rn-222 concentrations. The RAD7 data were far superior to that from AC, and therefore only RAD7 data were used to determine Rn concentrations and fluxes (see Appendix F). No clear effect of accumulation chamber size was observed (Appendix G) and in most cases this is not considered in results reported here. Chambers were generally left in place for about 20 hours taking RAD7 data every 15 minutes. In the case of bottom fluxes, if the count rate was very high, shorter count cycle times of 5 minutes and total count times of an hour or two were used to reduce the risk of exceeding the instruments counting limits and reduce the need to purge the instrument.

Overall, the uncertainty of radon concentrations varied primarily with the count rate. For low concentrations, those in the range of about 200 Bq/m^3, the 2-sigma uncertainty was about 39%. More typical concentrations of 4000 Bq/m^3 had 2-sigma uncertainty of about 8% while for concentrations of about 25,000 Bq/m^3 the uncertainty was 3.2%. Uncertainties for calculated fluxes are similar.

When possible two methods were used to calculate flux, the initial near linear part of the concentration buildup curve and a best-fit regression to Equation 2 in Appendix F. The time interval used for the initial linear portion of the radon buildup curve varied depending on shape of the curve. Most were four hours, but times varied between 1 and 6 hours. For these initial portions of the buildup curve the average value of R^2 for linear fits of concentration vs time was 0.930, with values ranging from 0.51 to 0.998. Almost all were greater than 0.92. The low R^2 values occurred for low count rate measurements.

Both the linear, initial slope method and Equation 2 with a best-fit regression were generally used to determine flux and the average of the two was used. Both methods usually provided similar values. Plotting fluxes from the two methods gave an R^2 value of 0.994 with a slope of 0.995. showing a close correlation between the two. For most measurements both the early linear and the non-linear best-fit fluxes were averaged. However, in some cases, the early portion of the buildup curves had a reasonable shape but dropped significantly after several

hours. In these cases, only the early linear portion of the Rn buildup curve were used to calculate Rn flux. In other cases, at low concentrations, the initial linear portion was not well defined or consisted of only a few measurements, but the non-linear best-fit was reasonable (although with a high uncertainty as would be expected for the low count rate). Given the correlation between the two methods discussed above, this was considered an acceptable approach.

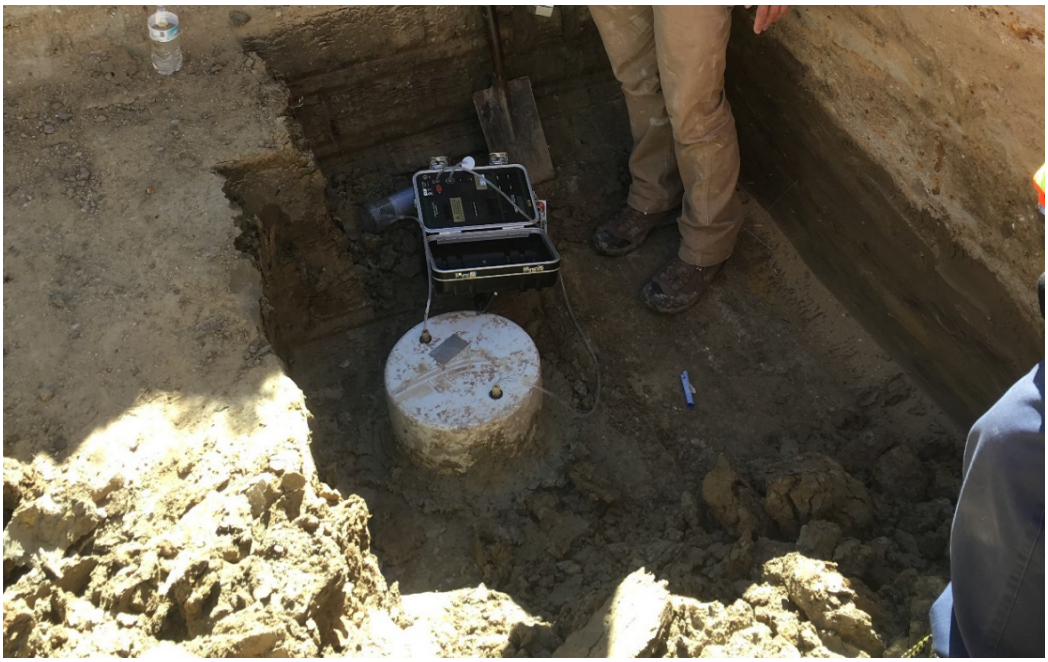

Figure 4-3 A Small Flux Chamber Installed Directly on the Tailings with a Rad7 Instrument to Obtain a "Bottom Flux" Measurement

4.3 Background Fluxes

While the mill tailings and other waste buried at these sites will generate most of the Rn-222, a small flux can be expected to originate from the barrier material itself depending on the Ra-226 content of the material used for the barrier. It is important to quantify background fluxes when evaluating sites with low top fluxes to differentiate between natural Rn fluxes and fluxes from the waste. These background Rn fluxes were calculated with RAECOM (U.S. NRC, 1989) by using the Ra-226 concentrations of the barrier material (taken from the measurements reported in the closure plans or from our measurements), the barrier thickness, and diffusion coefficients calculated from the top and bottom fluxes (see section 4-7). In addition, some completion reports included flux measurements of the barrier material.

4.3.1 Falls City

To estimate the "background flux" derived from the Falls City barrier material itself, RAECOM was used to estimate fluxes from 0.91-meter thickness of barrier material. They were calculated using the average (0.148 Bq/g) and maximum (0.35 Bq/g) Ra-226 concentrations given in the

Completion Report (MK-Ferguson Company, 1996; and U.S. Department of Energy 2017a), the measured emanation factor (0.19) from the completion report, and average values measured for porosity and moisture from the 6 test pits. These estimates likely better represent background fluxes on the top deck rather than on the side slope. The background surface flux was calculated to be 0.028 Bq/m^2/s for the average Falls City Ra-226 concentration. Using the highest observed Ra-226 concentration the flux is calculated to be 0.066 Bq/m^2/s. The average as-built flux of 0.018 Bq/m^2/s is very similar to the calculated background from the average Ra-226 concentration.

4.3.2 Bluewater

Information on the Bluewater site was accessed at U.S. Department of Energy, Legacy Management website (2017b). Test and model results for the Bluewater borrow soil were found in Report RAE-8721-1 (Rogers and Associates, 1987; Atlantic Richfield, 1996). This included estimates of design diffusion coefficients based on properties of the borrow material, specific gravities, moisture content, and radium-226 concentrations. Average Ra-226 concentration in the Bluewater barrier material is 0.022 Bq/g with the highest measured at 0.037. The modeled background Rn fluxes were based on these Ra-226 concentrations, a 0.7 m thick cover, and using RAECOM with the averaged diffusion coefficient determined for measurements from the site (2.6 x 10^{-7} Bq/m^2). The fluxes were calculated to be 0.004 Bq/m^2/s for the average Ra-226 content and 0.005 Bq/m^2/s for the maximum Ra-226 content. In contrast, during pre-construction planning the background Rn flux in the borrow area was measured as 0.033 ± 0.022 Bq/m^2/s (n=5). The difference in background fluxes could be due to the difference in Ra-226 concentration in the barrier material. However, differences in porosity and moisture content are important as well. The higher Rn flux in the borrow area could also indicate the presence of a natural Rn source below the surface material.

4.3.3 Shirley Basin South

The Shirley Basin South background flux of 0.010 Bq/m^2/s was calculated with RAECOM based on Ra-226 values for 4 samples of barrier material from the site, as analyzed by Eberline Labs (Table 4-2). One sample (Clay-1) was from the old storage mound where clay for the barrier was piled during construction. The other samples are from the top of the clay barrier at several of the Shirley Basin South test pits. Parameters used to calculate Rn flux were the measured Ra-226 concentration (mean = 0.162 Bq/g), the barrier thickness in meters, porosity of 0.48, gravimetric moisture content of 24%, fraction passing the 200 Sieve of 0.76, and the emanation factor of 0.35 (default given in NRC Regulatory Guide 3.64). Ra-226 in three samples of the clay used at the Pathfinder site (which is adjacent to the Petrotomics, Shirley Basin South, site) average 0.090 Bq/g (Pathfinder Mines, 1993). Information was obtained from the Petrotomics Company closure reports and flux measurements (2001a, 2001b) and from the U.S. DOE website (2017c).

4.3.4 Lakeview

The mean background radon flux from the barrier material at Lakeview was calculated with RAECOM to be 0.003 ± 0.001 Bq/m^2/s. The average Ra-226 content of the barrier material is reported to be 0.037 Bq/g and the emanation coefficient is 0.4 (MK-Ferguson Company, 1991). Porosity and moisture content from this project were used with a mean diffusion coefficient of 2 x10^{-8} m^2/s as calculated from fluxes measured in this work. Other information was obtained at the U.S. DOE Legacy Management website (2017d).

Table 4-2 Ra-226 Concentration in Barrier Material and fluxes Calculated from Ra-226 for Shirley Basin South

	Ra-226 (Bq/g)	2 Sigma error (Bq/g)	Calculated Background Rn Flux ($Bq/m^2 \cdot s$)
Slope A	0.173	0.049	0.011
Slope A (duplicate)	0.178	0.050	-
DC-2 A	0.163	0.046	0.010
DC-2 A (duplicate)	0.189	0.056	-
DC-3 A	0.155	0.046	0.010
Clay-1	0.155	0.044	0.010

4.4 Measured Radon Fluxes

4.4.1 Falls City, TX

Background information on the Falls City site can be found in Section 2.4.4, including climate (Fig. 2-3), plant ecology (Table 2-6), cover soil classification (Table 2-3) and cover design (Fig. 2-2). The site contains 4.72×10^{13} Bq of Ra-226 (1277 Curies). Six test pits were excavated at the site. An aerial view of the site with pit locations is shown in Figure 2-5. Four test pits were located on the vegetated top deck of the cover (used to grow hay), one was located on the rip-rap covered edge of the top deck (the apron) and the sixth was on the rip-rap covered side slope descending from the top deck. A total of 22 flux measurements were made on the top of the radon barrier (Table 4-3) and 6 were made at the bottom of the barrier (one at each test pit). Test pits were located as near as could be estimated to positions with high flux rates during the as-built survey (Table 2-11).

Table 4-3 Summary of Test Pit Characteristics at Falls City, TX Field Site

Test Pit #	Description	Number of Top Flux Measurements
TP-1	Top-deck, 91 cm rooting medium, mesquite	3
TP-2	Top-deck, 91 cm rooting medium, grasses, near TP 1	3
TP-3	Top-deck, 91 cm rooting medium, mesquite	4
TP-4	Top-deck, 91 cm rooting medium, grasses, near TP 3	4
TP-5	Apron, Rip-rap cover,	4
TP-6	Slope, Rip-rap cover, thinner barrier	4

Radon fluxes as measured in the field at Falls City are shown in Figure 4-4. The geometric mean flux is calculated at each test pit. “Bottom” flux measurements taken from the surface or near the surface of the underlying waste are included on the figure for comparison and are labeled “waste” in the legend.

Mean “top” fluxes from all the pits at the Falls City site were below the benchmark of 0.74 Bq/m^2/s. However, two of the four chambers at TP-3 measured fluxes slightly greater than the limit. This pit was located at a mesquite tree that had been cut down just prior to excavation. Pit 1 was also located at a mesquite tree. On the upper deck, top fluxes ranged from 0.005 to 1.28 Bq/m^2/s, with a geometric mean of 0.254. This contrasts with the two pits at the rip-rap covered apron and side slope (TP- 5 and TP-6), which have a geometric mean of 0.011 Bq/m^2/s, or 23 times lower that the upper deck. The material in these two pits was moist and plastic and fluxes were slightly less than the calculated background. On the top deck the barrier material was dry and brick-like. Three of the four pits on the top deck of the cover had top fluxes greater than the calculated background; with average fluxes that were 11.3, 10.2, and 23.4-times average background for TP-1, TP-2, and TP-3 respectively. The mean of the as-built measurements is 0.024 Bq/m^2/s, similar to the background flux, with fluxes ranging from 0.003 to 0.157 Bq/m^2/s (Fig. 4-4). Fluxes from TP 1, 2, and 3 were more than an order of magnitude higher than the as-built average.

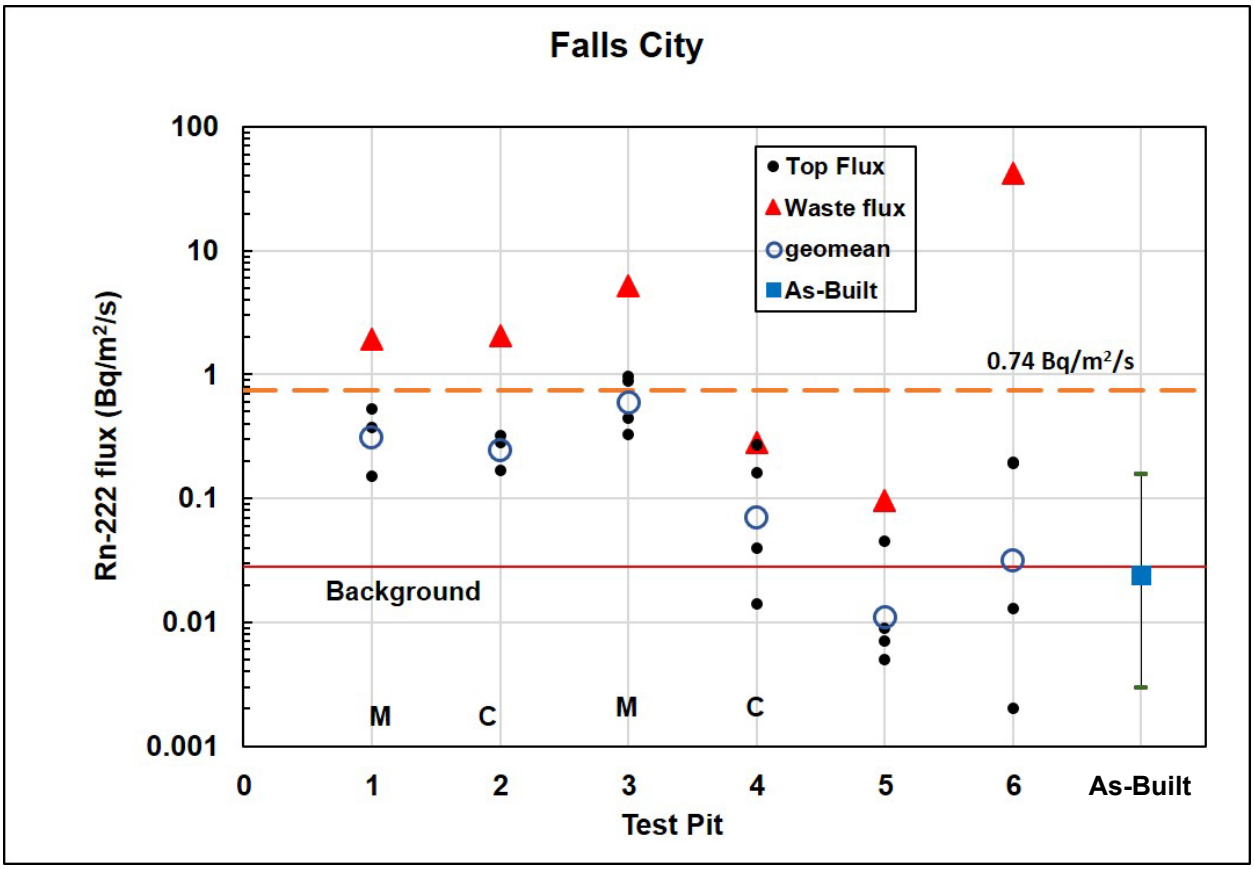

Figure 4-4 Radon Fluxes Measured at the Falls City Site
Note that the bottom fluxes are labeled “waste”. The As-Built values are the mean and the range of 100 measurements. M denotes pit placement on a mesquite bush while C denotes a control pit. Error bars on the as-built data set denote the range of the 100 measurements.

4.4.2 Bluewater, NM

Background information on the Bluewater site can be found in Section 2.4.3, including climate (Fig. 2-3), plant ecology (Table 2-6), cover soil classification (Table 2-3) and cover design (Fig. 2-2). The site contains 4.14 x 10^{14} Bq of Ra-226 (11,200 Ci). Fifteen (15) pits were excavated at the site and 43 top flux measurements were made at 9 of those pits. See Section 2.4.3.1 and Table 2-10 for descriptions of the pits and near-by as-built fluxes. Figure 2-4 shows an aerial photograph with test pit locations. Locations of test pits 3, 4 and 5A/B on the main waste pile were selected for high as-built Rn fluxes, as was test pit 9 on the Acid Pile. Many test pits were positioned in pairs to assess the impact of certain features (Table 4-4). For example, Pit 5 was positioned at a mature saltbush that was removed prior to placing the flux chambers. The large chamber was placed directly over the cut saltbush, while small chambers were placed nearby, on areas containing saltbush roots. Pit 4 was near Pit 5 but with no saltbush present. These comparisons are discussed later (Table 4-8).

Figure 4-5 shows fluxes measured at the Bluewater site. Top fluxes ranged from 0.002 to 1.26 Bq/m^2/s with a geometric mean of 0.044 Bq/m^2/s. Pit 1 was located at an ephemeral pond that forms in a low spot on the cover that has developed from subsidence; the higher moisture content and accumulation of fines resulted in very low top and bottom fluxes. Pits 5, 6, and 9 had high average surface fluxes (0.482, 0.245, 0.272 Bq/m^2/s, respectively) which are substantially above the measured and calculated background fluxes. Pit 5 was located at a saltbush plant with roots observed to penetrate the barrier. Pit 6 was deliberately located on an ant mound to assess impact of bioturbation on Rn flux and on hydraulic conductivity. Pit 9 was on a separate cover for acid waste material. The 25-cm thick radon barrier at that location was very hard, brittle, and dry, leading to high fluxes of Rn. The main tailings pile had a mean as-built flux of 0.079 Bq/m^2/s for 125 measurements with a range of more than two orders of magnitude. Although some test pits had high fluxes, the geometric mean fluxes for most pits were below the as-built geometric mean.

Table 4-4 Summary of Test Pit Characteristics at Bluewater Field Site

	Description	Number of Top Flux Measurements
Test Pit 1	Slimes Tailings/Seasonal Ponding/Thin Rn Barrier	4
Test Pit 2	Slimes Tailings/No Ponding/Thin Rn Barrier	7
Test Pit 3	Sands Tailings/High Ra Activity	6
Test Pit 4	Sands Tailings/No Saltbush	8
Test Pit 5	Sands Tailings/Mature Saltbush	6
Test Pit 6	Sands Tailings/Ant Mound	1
Test Pit 7	Carbonate Cell/Thick Rn Barrier/Saltbush	2
Test Pit 8	Carbonate Cell/Thick Rn Barrier/No Saltbush	2
Test Pit 9	Acid Pile/Vegetated Cover	7

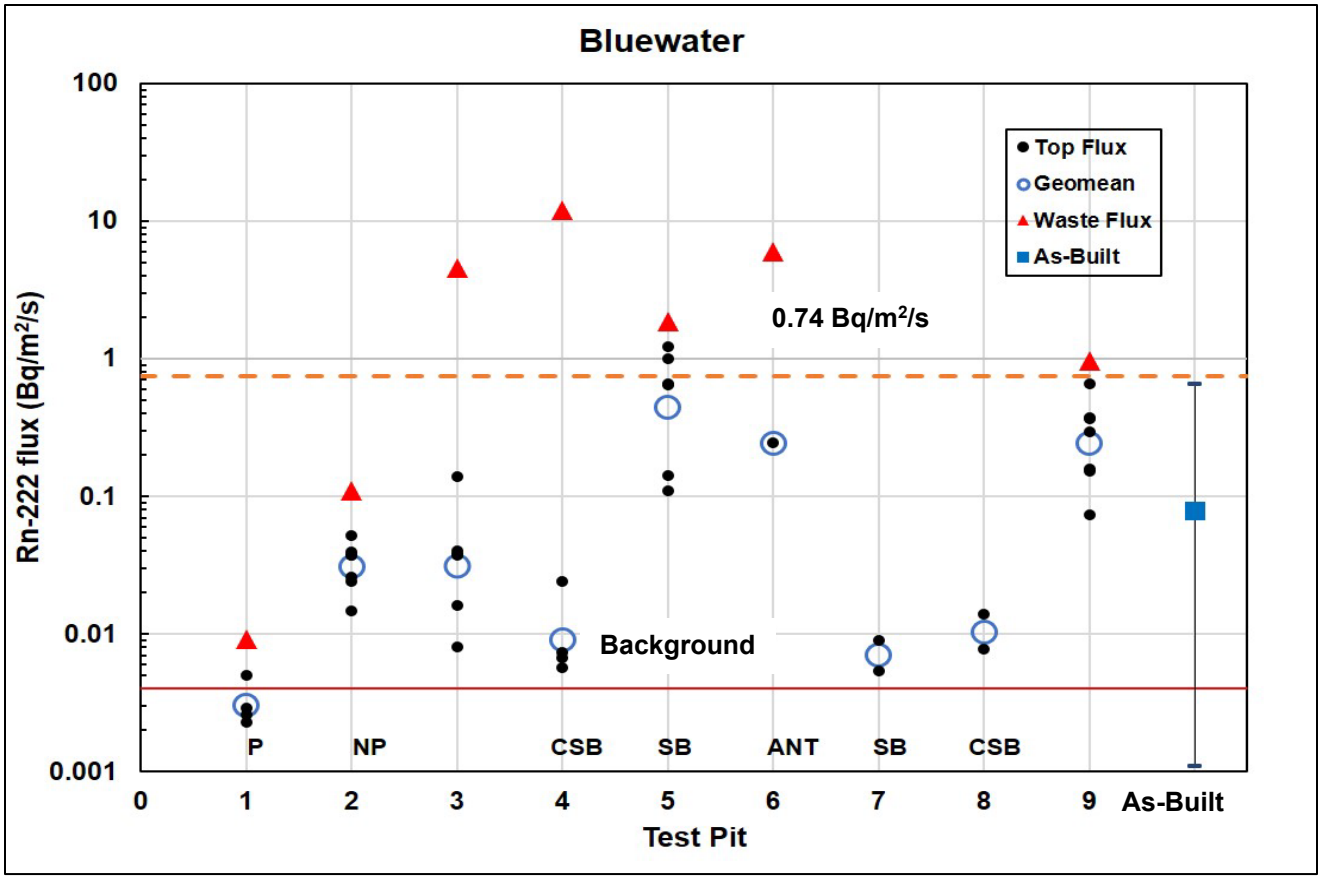

Figure 4-5 Radon Fluxes Measured at the Bluewater Site
Note that the bottom fluxes are labeled "waste". The As-Built values are the mean and the range of 125 measurements on the main tailings pile. P denotes a seasonal pond, NP is no ponding, SB is saltbush, CSB is control for the nearby saltbush pit, and ANT is the ant mound.

4.4.3 Shirley Basin South, WY (Petrotomics)

Background information on the Shirley Basin South (SBS) site can be found in Section 2.4.5, including climate (Fig. 2-3), plant ecology (Table 2-6), cover soil classification (Table 2-3) and cover design (Fig. 2-2). The site contains 3.6 x 10^{13} Bq of Ra-226 (974 Ci). At this site 27 fluxes were measured on the surface of the radon barrier (Table 4-5), while "bottom" fluxes were measured in 5 pits. See Section 2.4.3.1 and Table 2-10 for descriptions of the pits and near-by as-built fluxes. Figure 2-4 shows an aerial photograph with test pit locations. Fluxes are shown in Figure 4-6. The range was 0.004 to 0.226, and all measurements were substantially below the flux benchmark. The top fluxes measured in pits DC-2 and DC-4 range over a factor of about 15, but pit DC-3 had much more consistent and lower fluxes even though the bottom flux at this location was extremely high. No tailings were observed below pit DC-4 to a depth of 2.8 m, although hand auguring very near the pit did show tailings. It is suspected that the edge of a berm between ponds was located at this position.

Table 4-5 Summary of Test Pit Characteristics at Shirley Basin South Field Site

Test Pit	Location	Surface Feature Description	Number of Top Flux Measurements
DC-2	Lower Deck	High As-Built Rn Flux	8
DC-3	Upper Deck	High As-Built Rn Flux	6
DC-4	Lower Deck	High As-Built Rn Flux	7
DC-5	Lower Deck	High As-Built Rn Flux	4
DC-6	Side Slope	Vegetated Riprap Cover	2

Bottom fluxes at some locations were very high. The radon barrier here was placed directly over tailing ponds. For some locations this allowed visual observation of the waste (light gray coarse sand size particles) and confidence that the bottom fluxes at those positions were unattenuated. For example, at DC-3 replicate bottom fluxes were 334 and 457 Bq/m^2/s, the highest measured in this project.

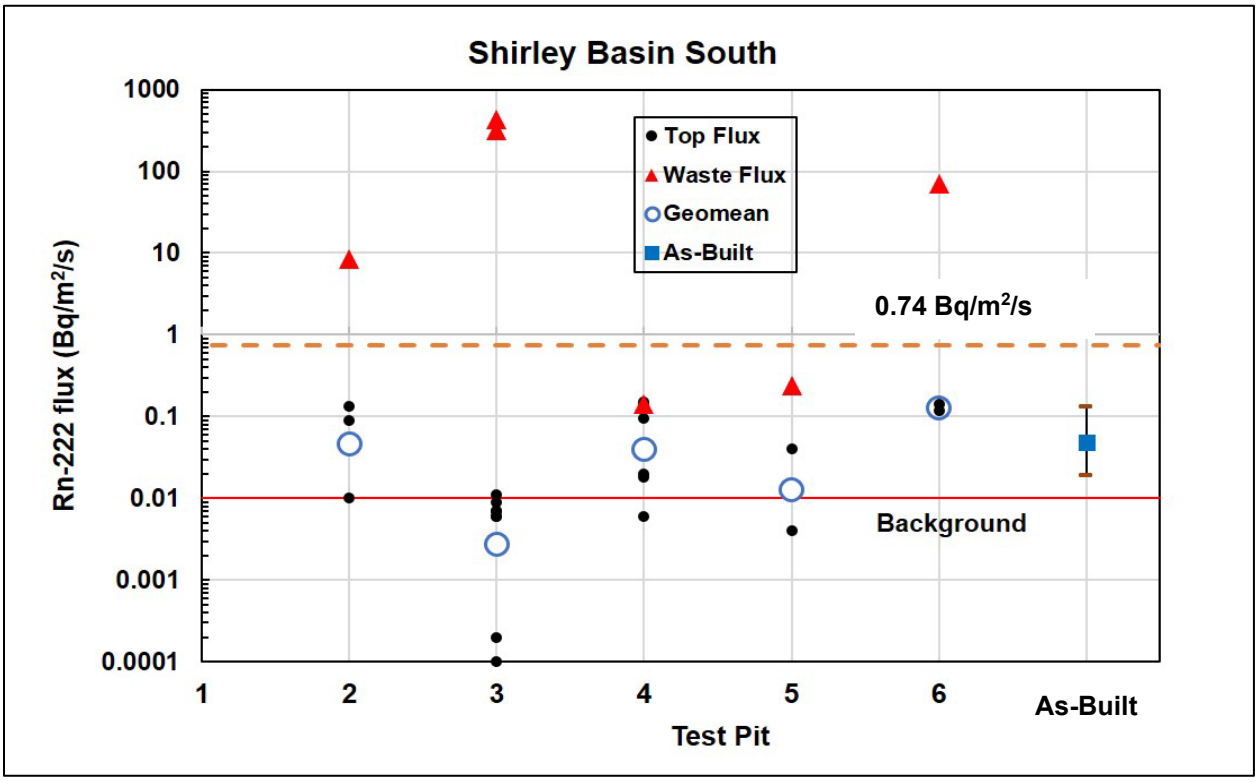

Figure 4-6 Radon Fluxes Measured at the Shirley Basin South Site
Note that the bottom fluxes are labeled "waste". The As-Built values are the mean and the range of 101 measurements. Note that one very high as-built flux has been deleted. That location of the barrier was rebuilt after the high flux was found.

4.4.4 Lakeview, OR

Background information on the Lakeview site can be found in Section 2.4.4, including climate (Fig. 2-3), plant ecology (Table 2-6), cover soil classification (Table 2-3) and cover design (Fig. 2-2). Pit locations are given on an aerial photograph in Figure 2-7. The site contains 42 Ci (1.55×10^{12} Bq) of Ra-226. A total of 26 successful flux measurements were made: 22 top fluxes and 4 bottom fluxes. Several flux measurements, including 4 bottom fluxes failed apparently from leaks in the system. Because of the small Ra-226 inventory at the site and the fact that the material had been moved from the original mill site and low activity waste placed near the top, this site had very low fluxes. Table 4-6 gives pit descriptions and the number of flux measurements. Fluxes are shown in Figure 4-7. All are far below the benchmark, even the bottom fluxes.

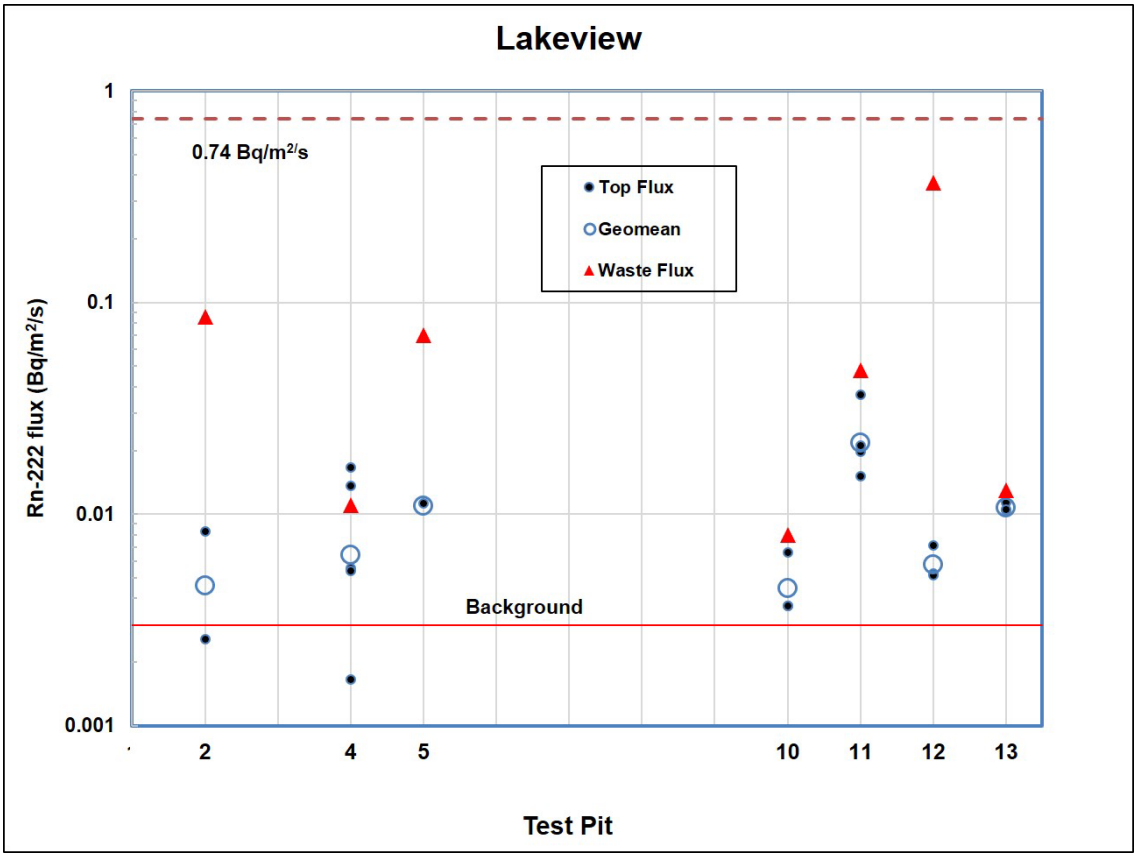

Figure 4-7 Radon Fluxes Measured at the Lakeview Site
Note that the bottom fluxes are labeled "waste". No As-Built survey was found for this site. Radon flux was not measured at all test pits.

Table 4-6 Summary of Test Pit Characteristics at the Lakeview Field Site

Test Pit	Location	Surface Feature Description	Number of Flux Measurements
2	Upper Deck	Bitterbrush/Grass gradient	2
4A	Side Slope	Grass	3
4B	Side Slope	Bare, Control for pit 4A	2
5	Upper Deck	Rabbitbrush and animal burrow	1
10	Upper Deck	Sparse grass, Control for pit 11	4
11	Upper Deck	Mature Bitterbrush	4
12	Upper Deck	Bitterbrush	3
13	Upper Deck	Control for pit 12	3

4.5 Radon Flux Discussion

4.5.1 Radon Flux Overview

Over the two field seasons of this project 114 successful measurements were made of radon fluxes at the tops of the radon barriers. Figure 4-8 provides an overview of all Rn fluxes measured at the tops of radon barriers at each of the four sites. The Y-axes are the same for all plots providing perspective on the relative fluxes. Four flux measurement results exceeded the benchmark of 20 pCi/m^2/s (0.74 Bq/m^2/s); two at Falls City and two at Bluewater. All were associated with larger deep-rooted plants that had become established on the covers. The regulatory limit applies to an average flux over the entire site for one year and none of the sites that were visited came close to that limit.

Bluewater had the highest flux measurements followed closely by Falls City. In contrast Shirley Basin South (SBS) and Lakeview had very low fluxes. The Lakeview site contains very little Ra-226 so low Rn fluxes are expected. The SBS site has much higher Ra-226 content and the Rn barrier sits directly on relatively high activity tailings. Nevertheless, Rn fluxes were very low. Falls City is the wettest and warmest of the sites (Figure 2-3) while SBS is the coolest and is quite dry. Both have similar cover designs (Figure 2-2). The top deck of Falls City and Bluewater both had test pits that showed high fluxes, but their cover designs are entirely different; Falls City has a thick, fine grained vegetated protection layer above the radon barrier while Bluewater has a relatively thin riprap layer directly over the radon barrier. The common feature leading to high fluxes is the presence of deep-rooted plants that dry the underlying radon barrier and create preferential pathways for gas and water transport.

Even sites with high fluxes were found to have areas with very low, sometimes background level, fluxes. At some test pits fluxes varied substantially. The measurements were conducted essentially simultaneously, and the chambers were all located within a meter or so of each other. Even so, as in the extreme case of Bluewater pit 5, fluxes ranged from 0.111 to 1.258 Bq/m^2/s. This behavior indicates high localized small-scale zones of preferential Rn transport. In the case of pit 5, high fluxes were associated with the presence of large deep-rooted plants.

4.5.2 Current Fluxes vs. As-built Radon Fluxes

Comparison between as-built and in-service (2016/2017) Rn flux measurements are presented below for Falls City, Bluewater, and Shirley Basin; no data were found for a closure Rn flux

survey at Lakeview. It is believed that the low Ra-226 content and the fact that the tailings and other debris had been moved from its' original disposal location, precluded a survey. The as-built, closure surveys were done soon after construction and before any protective layers (rip-rap or soil) were put in place on the barrier. In contrast, the flux measurements obtained for this project were conducted on barriers that had been covered and aged for about 20 years. It is of considerable interest to compare results of the two surveys. However, only with great caution can results from the in-service Rn flux measurements be compared to as-built measurements from site closure surveys. Sample location approaches developed for this project and those used for the closure surveys were very different.

As-built surveys were done on a systematic grid with at least 100 measurements. In contrast, in our work many in-service measurements sought areas of potentially high flux. Some areas were selected because the location had relatively high fluxes during the as-built survey. Most locations were selected to quantify radon barrier properties (including flux) that may have been affected by impacts such as large plants and ant mounds. In many cases pairs of measurement locations were defined to allow comparison of impacted areas to near-by unimpacted controls. Also, there were fewer in-service measurements than as-built measurements, and as-built measurements were made using the AC method.

To emphasize; the 2016/2017 in-service sampling was *purposefully* biased to test areas where we anticipated higher than average flux (i.e., high as-built Rn flux, driest season, areas with deep-rooted, late-successional vegetation [most like analogues], areas with burrows and ant mounds); whereas the as-built values are the average for the entire site based on a systematic grid sampling of a newly constructed radon barrier. As a result, it is not appropriate to compare averages of all in-service measurements to the average site-wide as-built measurements. However, as discussed above, comparing fluxes from individual test pits to the site-wide as-built average is reasonable. Similarly comparing individual test pit fluxes to averages of several as-built fluxes from locations near the in-service test pits is appropriate. Histograms are also used to present the distribution of frequency of flux values from the as-built and in-service measurements.

4.5.2.1 Falls City, TX

As-built radon flux data from the Falls City site were obtained from the Completion Report (M-K Ferguson Company, 1996). These data were obtained on a systematic grid of 100 flux chambers. Figure 4-9 is a histogram showing the frequency of occurrence of flux values measured during the in-service fieldwork compared to that of the as-built measurements. Most as-built fluxes are very low, but the distribution does have a tail extending toward the higher fluxes. A very large proportion (77%) of as-built flux values are less than 0.03 Bq/m^2/s. In contrast, the in-service values are bimodal with 27 % being less than 0.03 and about half less than 0.1 Bq/m^2/s. Only two of the as-built fluxes were greater than 0.1 Bq/m^2/s, while nine of 22 from this work were greater than 0.1 Bq/m^2/s. Seven in-service fluxes were higher than any observed in the as-built survey. As noted above, the as-built survey was generated by grid-type sampling which approximates random sampling, while for this work sampling was oriented toward areas with high as-built fluxes and likely alteration. Thus, it is expected that there is a high-side bias in the distribution from this work. Nevertheless, some fluxes from this work fall substantially outside the high side of the range of the as-built survey results, indicating that on aging some areas of the cover have developed higher fluxes.

The fluxes measured from the upper deck area of the disposal cell in 2016 are the main contributor to the higher fluxes relative to as-built. Geometric mean fluxes from three of the four

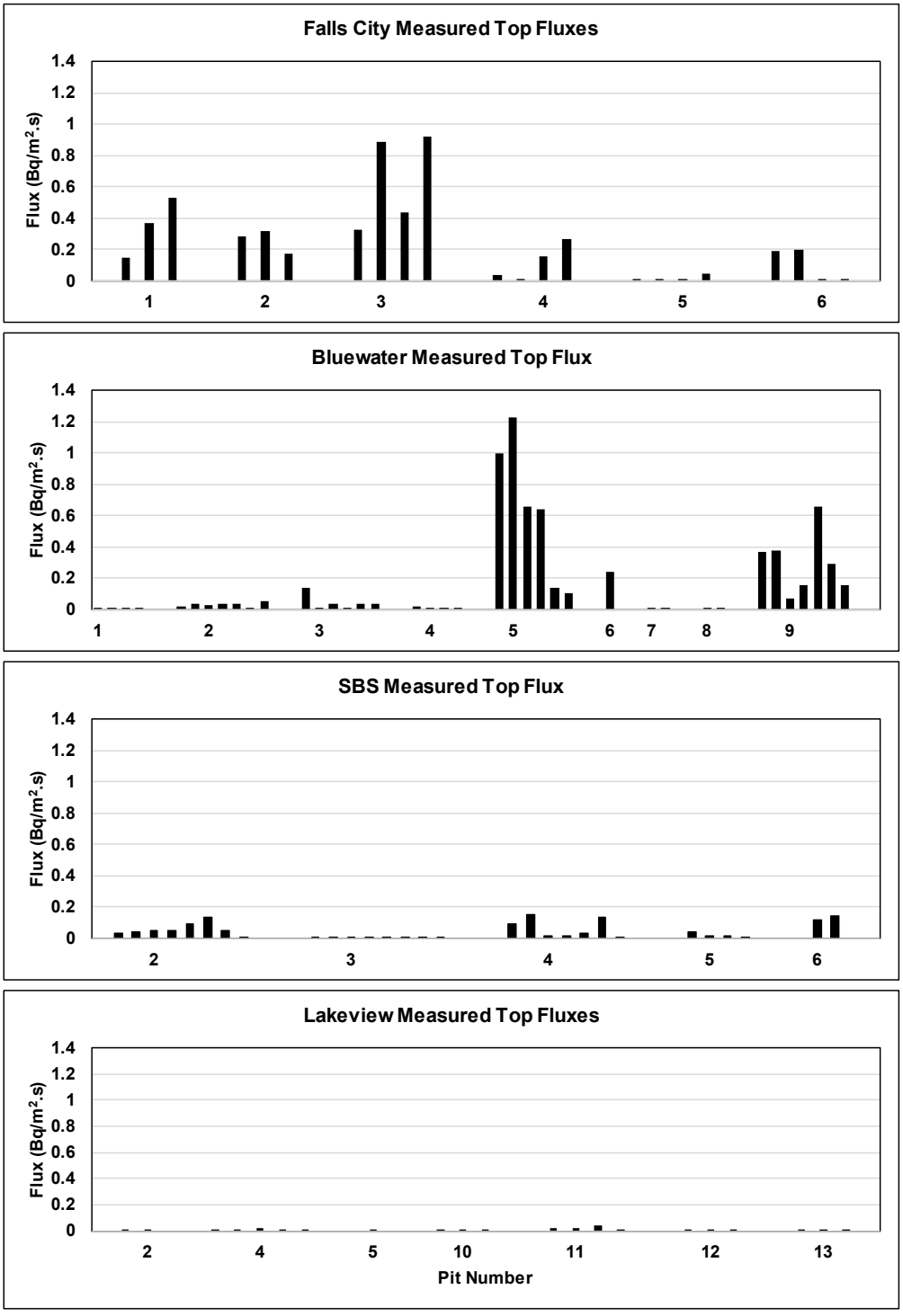

Figure 4-8 All Rn Flux Measurements from the Tops of Rn Barriers at the Four Sites
Scale of the Y-axes are kept the same to better compare fluxes among the sites.

test pits (Fig. 4-4) on the upper deck are 0.317, 0.285, 0.656 Bq/m^2/s, all substantially greater than the 0.024 Bq/m^2/s average of the as-built. Alternatively, the geometric mean flux from the rip-rap covered slope in 2016 was only about 60% of the as-built mean.

In some cases, fluxes from in-service pits can be compared to fluxes from as-built measurements from locations very close to the test pit. For Falls City the average of the four closest as-built flux measurement locations are given on Table 2-11 for each in-service test pit. These values are plotted in Figure 4-10 against the in-service average fluxes from each pit. All top deck flux averages are greater than as-built, but the two rip-rap covered areas are substantially lower. These areas retained moisture due to the lack of plants and to the crested shape of the cover which sheds water to the sides. These findings suggest that the main contributing factors to the elevated flux measurements from the top deck in 2016 are likely the dryer Rn barrier relative to the as-built values, the effect of mesquite roots, and retained soil structure (see Chapter 7).

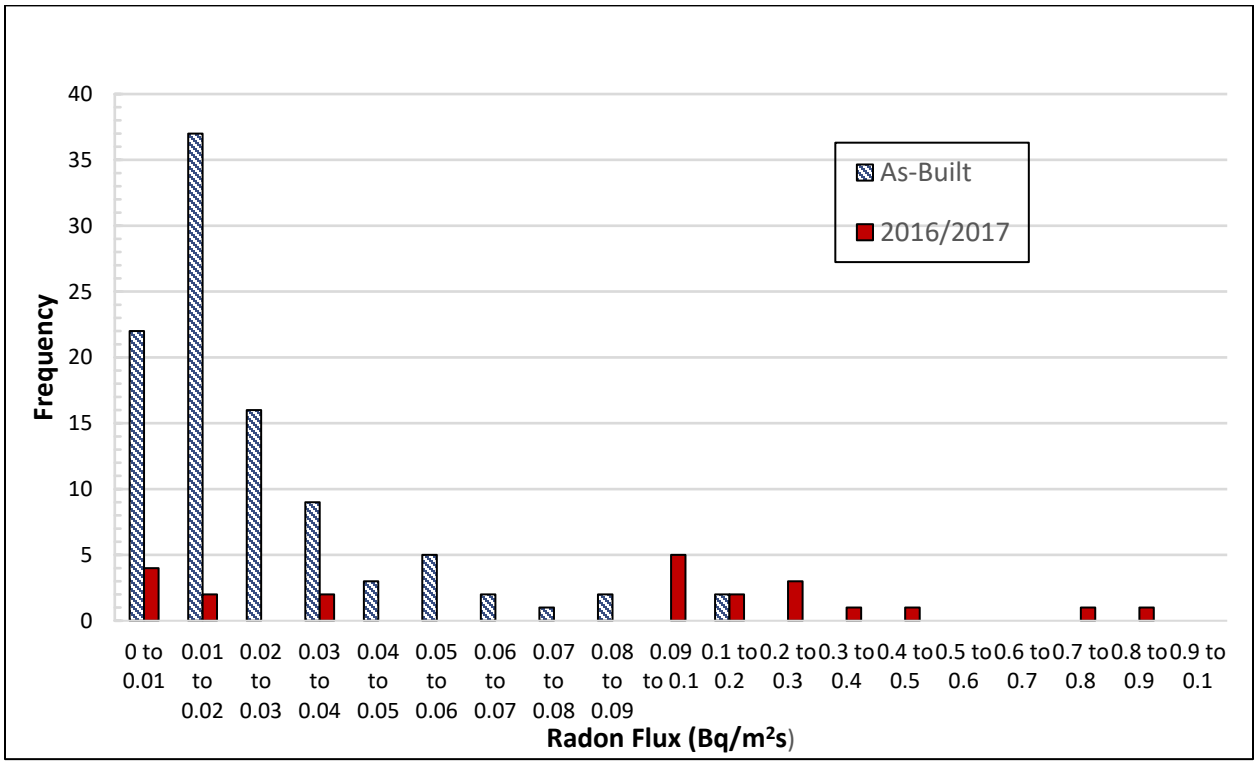

Figure 4-9 Frequency of Falls City Radon Fluxes for As-Built and In-Service Conditions Compares the as-built flux measurements made at the time of closure and then 22 years later, in this work. Note the bin change at 0.1 flux.

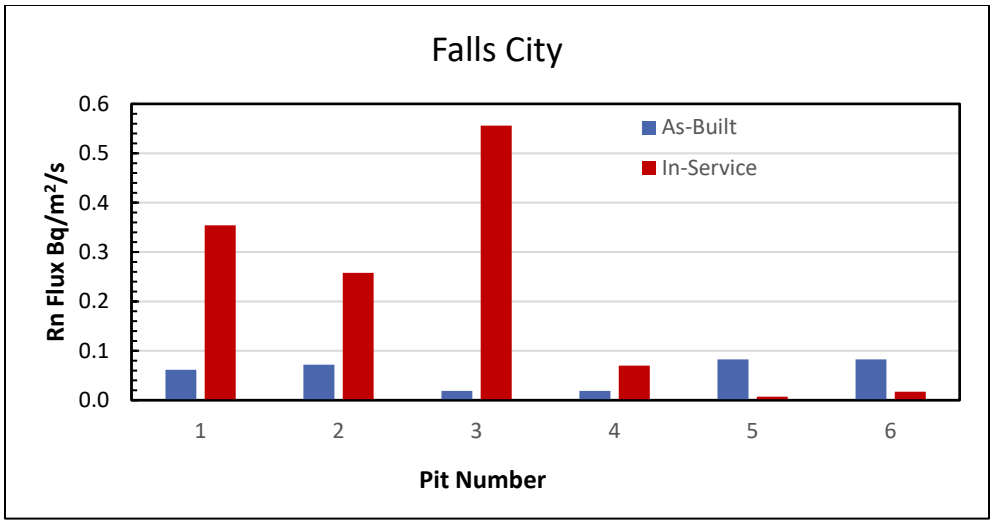

Figure 4-10 Comparison of In-Service Fluxes to As-Built Fluxes from Near-by Measurement Locations

4.5.2.2 Bluewater, NM

As-built radon flux data from the Bluewater site were taken from the closure report (Atlantic Richfield Co., 1996). For the main pile, 125 as-built flux measurements were made, and the geometric mean as-built flux was 0.032 Bq/m^2/s. Figure 4-5 shows the range of as-built fluxes along with individual in-service measurements. As-built values extend over a wide range that encompasses all but a few of the in-service measurements. The highest in-service values were from test pit 5 which was impacted by a saltbush, and which had an unusually broad range of fluxes.

Figure 4-11 is a histogram comparing the as-built and in-service 2016/2017 fluxes. Both data sets have a similar distribution. There are three in-service measurements that are equivalent to the highest single as-built flux and two in-service measurements that exceed any measured during the as-built survey. Figure 4-12 compares fluxes at in-service pits to near-by as-built measurements. Pit 5 in-service flux is notably elevated; it was located on a large saltbush. Several of the in-service measurements are lower than as-built. In one case (pit 1) this is caused by high moisture conditions due to seasonal pond formation. But for pits 3 and 4 as-built fluxes were substantially higher than in-service; this may reflect some aging process but may also be caused by spatial variation in fluxes and inevitable differences in measurement locations. Fluxes at pits 7 and 8 were low with no difference between as-built and in-service values, likely because of the very thick (>2.5 m) radon barrier. Pit 9 was on a thin (25 cm) section of radon barrier that was vegetated, dry and brittle.

The water content profiles measured at Bluewater in 2016 (see Table 4-8) also suggest that the Rn barrier soil (except for the area with the seasonal pond) was significantly drier than when as-built flux measurements were obtained. The main tailings pile and carbonate tailings piles were found to have water contents lower than as-built measurements by 22% and 14%, respectively.

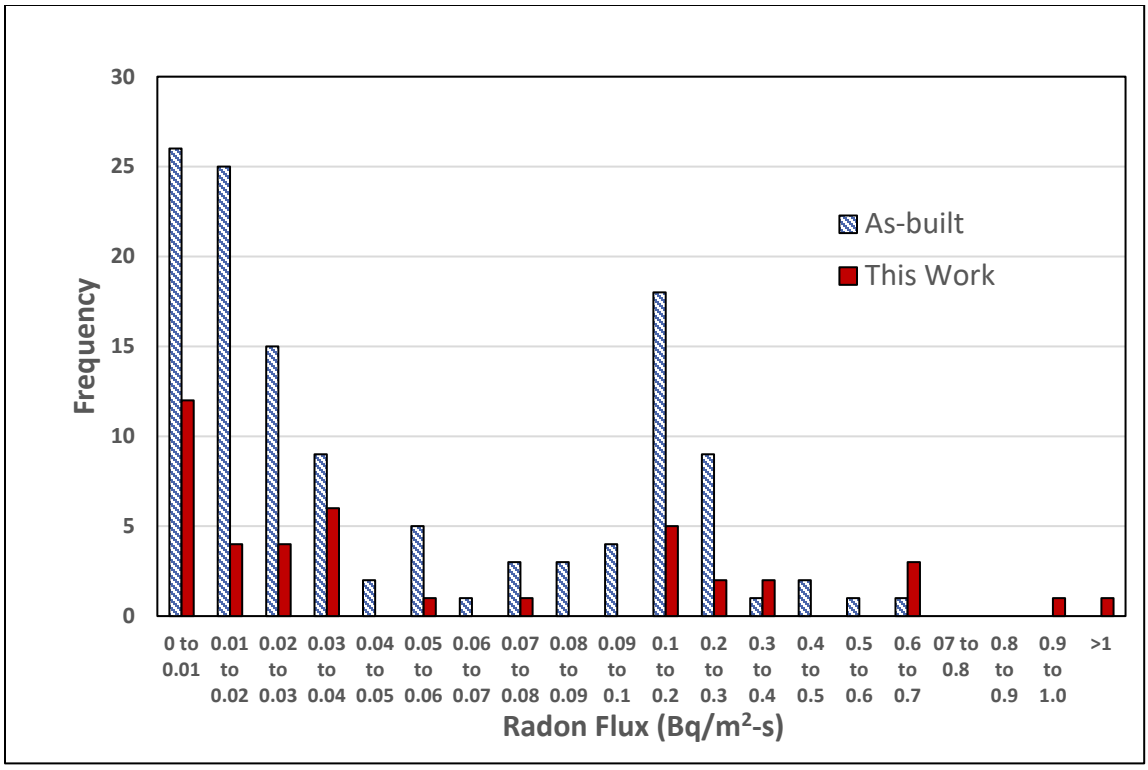

Figure 4-11 Frequency of Bluewater Main Tailings Pile Radon Fluxes for As-built and In-service Conditions Compares the as-built flux measurements made at the time of closure and then 22 years later, in this work. Note the bin change at 0.1 flux.

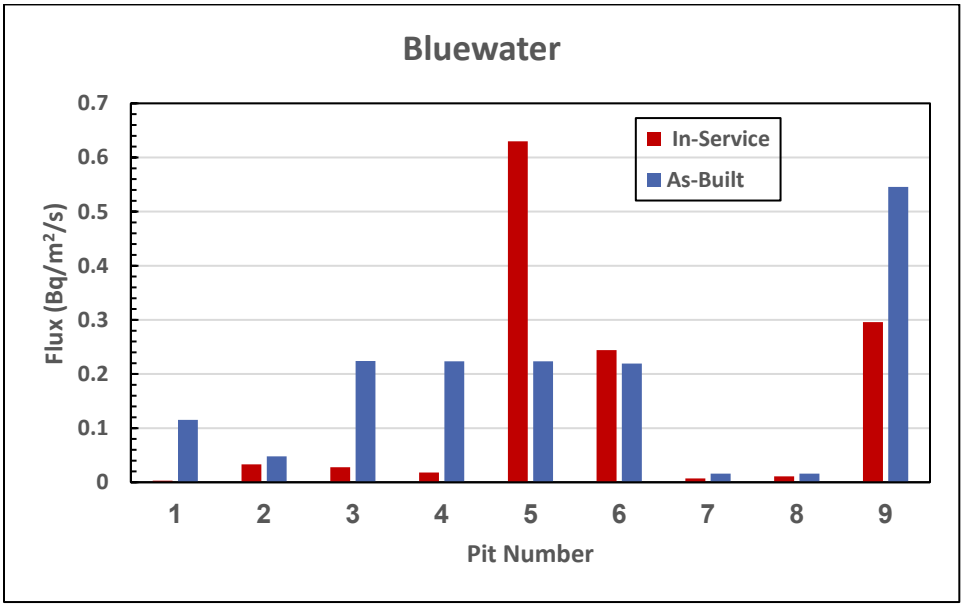

Figure 4-12 Comparison of Bluewater In-service Fluxes to As-built Fluxes from Near-by Measurement Locations The in-service flux for pit 1 is 0.003 Bq/m^2/s, low enough that it does not appear on the plot.

4.5.2.3 Shirley Basin South, WY

Data from the as-built flux measurement campaigns for the Shirley Basin South site were obtained from a letter report to NRC (Petrotomics, 2001b) which summarizes flux measurements made between 1997 and 2000. Flux measurements were made at 130 locations in a grid pattern. Fluxes ranged from detection limits of about 0.05 Bq/m^2/s to 1.20 Bq/m^2/s. This high flux area was recompacted to meet construction requirements and therefore has been left off the comparison plots.

Figure 4- 6 shows in-service fluxes compared to the range of as-built fluxes. That range is remarkably compact and similar to distributions of the highest in-service fluxes. The median as-built value was 0.026 Bq/m^2/s, while the geometric mean was 0.027 Bq/m^2/s. Nine of the 27 in-service measurements were lower than the as-built range and even as low as (or lower) than the background flux. Figure 4-8 shows that SBS fluxes are lower than Falls City and Bluewater even though its bottom fluxes are similar to, or in two pits, substantially higher, because the Rn barrier is placed directly on the tailings, as opposed to lower activity waste.

Figure 4-13 plots the frequency of flux values at Shirley Basin South compared to the as-built survey. There is little change in fluxes over the 18-20 years between surveys. This site was relatively free of surface features that were expected to cause increases in Rn fluxes. Rather, test pit locations were chosen to be in the vicinity of locations where high as-built fluxes were measured. Comparing in-service to as-built fluxes in Figure 4-14 shows most in-service fluxes were lower than as-built; remarkably so for pit 2. This may be related to the observation that the water content measured in 2017, was found to have increased slightly relative to as-built measurements (Table 4-8); this may be due to the smectite rich barrier material. It appears that, if anything, there may be a slight decrease in fluxes over time.

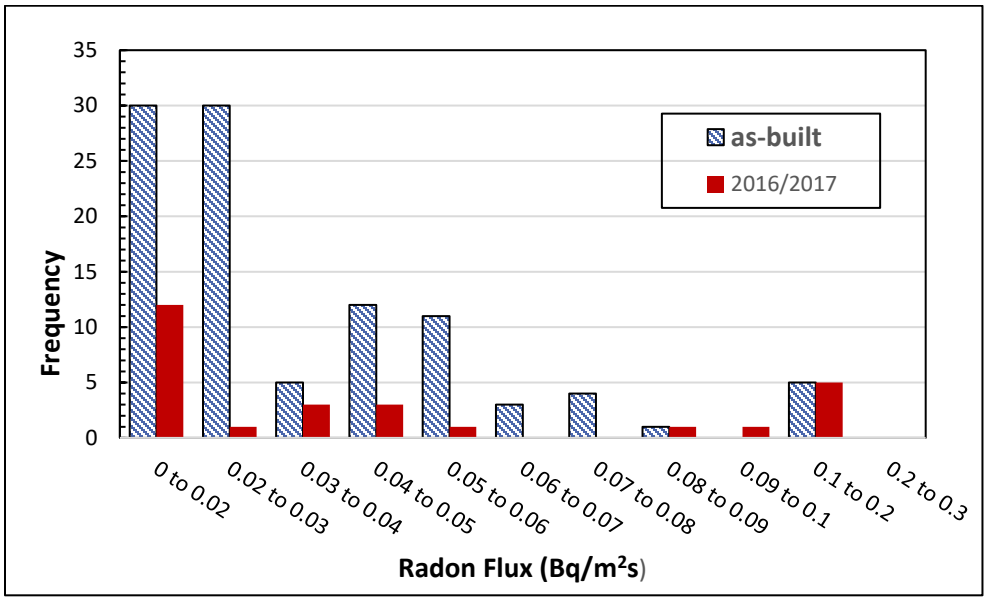

Figure 4-13 Frequency of Flux Values at Shirley Basin South (Petrotomics) Comparing As-built to 2016/2017 In-service Data Note the bin change at 0.1.

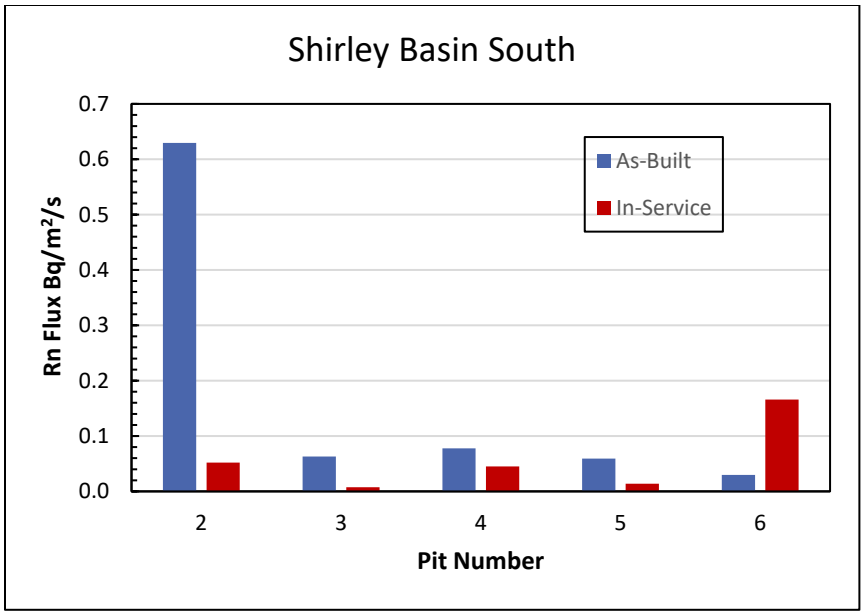

Figure 4-14 Comparison of In-Service Fluxes to As-Built Fluxes from Near-by Measurement Locations

4.5.3 Effects of Surface Features

Test pits in many cases were excavated as pairs so that the fluxes measured from beneath a surface feature thought to affect the performance of the barrier could be compared to a control location that lacked that surface feature. Each paired test pit was chosen to be close to the other so that variability in Rn barrier thickness and tailings activity would be minimized and only the effects of the surface feature would be measured. A total of eight test pit pairs, detailed in Table 4-7, were compared at three of the four sites visited in 2016 and 2017.

4.5.3.1 Effects of Woody Vegetation

The potential impact of plant roots on compacted clay radon barriers was pointed out by Rogers et al, (1984), as one of the mechanisms that could disrupt a barrier. Mechanisms that lead to failure of compacted soil barriers include impacts by roots (Suter et al., 1993) not only of vegetation deliberately planted on a site but those which subsequently establish themselves by ecological succession. While compacted clay inhibits root penetration, small areas of poor compaction are often present, and these are sought by roots that spread out into them. Some roots will grow into compacted clays and can penetrate a 0.6 m layer in three years (Reynolds, 1990). Transpiration would remove moisture from the layer leading to more gas filled porosity and therefore more Rn transport. Also, death or dormancy of roots would lead to shrinkage and macropore formation, a potentially seasonal effect. To determine how roots interact with the compacted clay, roots of 5 mature shrubs (sagebrush, rabbitbrush, and bitterbrush) were excavated at the Lakeview site (Waugh et al, 2007). Tap roots all extended to the radon barrier where they branched and spread across the barriers surface. Smaller roots penetrated the barrier and formed root mats in cracks and structural planes within the barrier. This type of growth would lead to barrier desiccation as well as transport of dissolved Rn, through the plant for release at the leaves (Morris and Fraley, 1989).

Table 4-7 Description of Test Pit Pairs

Site	Test Pit ID	Description
Falls City	TP-2	Control
	TP-1	Mesquite Tree
	TP-4	Control
	TP-3	Mesquite Tree
Bluewater	TP-1	Seasonal Ponding
	TP-2	No Ponding, Grass
	TP-4	Control
	TP-5	Saltbush
	TP-6	Ant Mound
	TP-8	Control
	TP-7	Saltbush
Lakeview	DC-4A	Control
	DC-4B	Grass
	DC-10	Control
	DC-11	Bitterbrush
	DC-13	Control
	DC-12	Bitterbrush

Table 4-8 summarizes the Rn fluxes measured in this project as well as the "bottom" flux, barrier thickness, average water content and average saturation measured at each of the pits. The table allows comparison of the paired pits and Figure 4-15 also summarizes the fluxes measured from each pair of pits, with the surface feature pit and its' control plotted on the same vertical line. In general, Rn fluxes measured at test pits that contained woody vegetation (mesquite, salt bush, and bitterbrush) were greater compared to fluxes measured from control pits, indicating that the vegetation may have affected the performance of the barrier in these locations.

At the Falls City site, two pairs of test pits focused on the effects of mesquite tree(s) roots on Rn flux (Table 4-8 and Figure 4-15). The mean flux measured from TP-3 (mesquite) was 0.656 $Bq/m^2/s$, about five times greater than the adjacent TP-4 (control with mean flux of 0.120) and was very close to the benchmark of 0.74 $Bq/m^2/s$. However, the "bottom" flux measured from the tailings beneath TP-3 was about 5.53 $Bq/m^2/s$, compared to 1.65 $Bq/m^2/s$ for TP-4, about 3.4 times greater than that measured beneath the control pit, contributing to the elevated fluxes measured from the mesquite pit. Because of the log scale on Figure 4-15 these sets of data appear quite close but statistically the means of the two pits are different at the 2-sigma level. The thickness of the Rn barrier at the two pits was comparable. The issue of different bottom fluxes is normalized by calculating the diffusion coefficient as discussed in Section 4-6. In the case of these two test pits the mean diffusion coefficients and Rn travel times are very similar. As discussed in Chapter 6, thin cracks (structure) along the clay clods from construction provide transport routes; Figure 4-16 shows roots growing along one of these fractures in TP-4 (the control), indicating pathways for water and gases.

Table 4-8 Summary of Test Pit Data

Site	Test Pit ID	Surface Feature/Condition	Feature or Control	Geometric Mean Surface Flux ($Bq/m^2/s$)	% Difference from Control Pit Flux	Rn Barrier Thickness (m)	Bottom Flux ($Bq/m^2/s$)	Mean Water Content*	Mean % Saturation
Falls City, TX	TP-2	Mesquite Tree	Control	0.284	-	0.91	2.208	0.38	93
	TP-1		Mesquite Tree	0.317	12	0.91	2.068	0.34	79
	TP-4	Mesquite Tree	Control	0.077	-	0.91	1.648	0.32	91
	TP-3		Mesquite Tree	0.656	750	0.91	5.525	0.37	nm
	TP-6	5:1 Rock Slope	Top of Slope	0.011	-	0.56	45.57	0.41	88
	TP-5		Middle of Slope	0.012	-	0.91	0.104	0.38	94
Bluewater, NM	TP-1	Seasonal Pond	Pond	0.003	-	0.67	0.010	0.12	86
	TP-2		No Pond	0.033	1000	0.63	0.117	0.11	60
	TP-4	Saltbush/Ant Mound	Control	0.015	-	0.71	12.86	0.09	69
	TP-5		Saltbush	0.482	3110	0.64	1.989	0.06	nm
	TP-6		Ant Mound	0.245	1530	0.66	6.387	0.07	41
	TP-8	Saltbush	Control	0.011	-	1.06	nm	0.11	65
	TP-7		Small Saltbush	0.007	-36	2.35	nm	0.09	59
	TP-3	Vegetation	Sparse	0.037	-	0.65	4.836	0.08	77
	TP-9		Plentiful	0.272	-	0.43	1.100	nm	nm
Shirley Basin South, WY	DC-2	Top Deck	Higher As-Built Flux	0.052	-	0.68	8.989	0.25	88
	DC-3	Lower Deck		0.008	-	0.65	397.2	0.24	92
	DC-4			0.045	-	nm	nm	0.23	90
	DC-5			0.014	-	0.56	0.257	0.32	97
	DC-6	5:1 Rock Slope	Wind-Blown Fines	0.166	-	0.38	75.01	0.26	97
Lakeview, OR	DC-4A	5:1 Rock Slope w/Vegetation	Control	0.006	-	0.38	nm	0.42	92
	DC-4B		Grass	0.009	50	0.38	nm	0.42	92
	DC-10	Bitterbrush	Control	0.005	-	0.41	nm	0.38	87
	DC-11		Bitterbrush	0.024	380	0.43	0.051	0.33	nm
	DC-13	Rabbitbrush	Control	0.011	-	0.66	nm	0.26	nm
	DC-12		Rabbitbrush	0.006	-45	0.61	0.395	0.36	nm
	DC-2	Bitterbrush	Bitterbrush	0.005	-	0.43	0.092	0.30	84
	DC-5	Animal Burrow	Animal Burrow	0.011	-	0.46	0.075	0.29	81

nm = not measured or calculated * Gravimetric water content and % saturation determined from Shelby Tube samples.

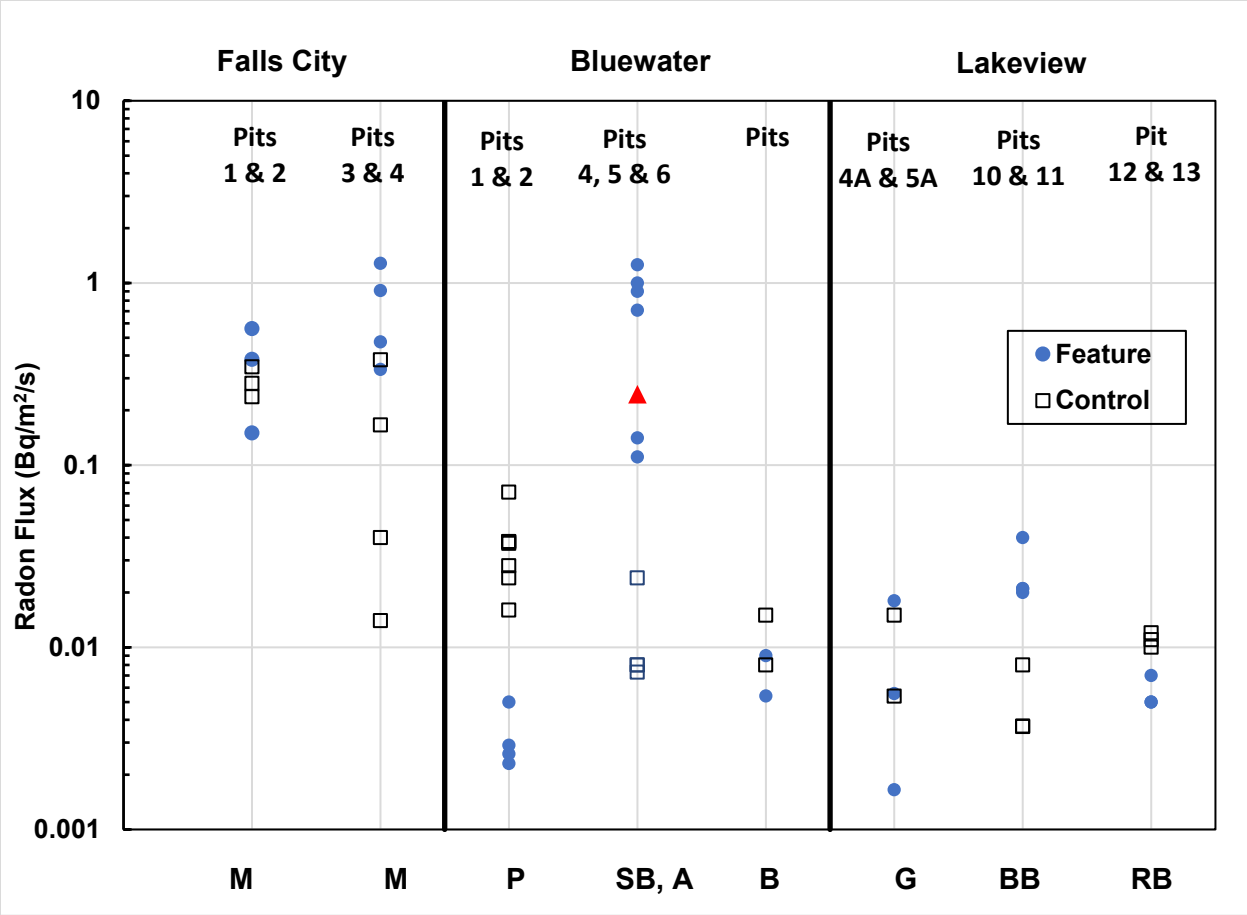

Figure 4-15 Fluxes Measured from Test Pit Pairs Showing Results from Pits Containing Features (Numbered) that May Influence Flux and Their Controls M = mesquite bush, P = seasonal ponding, SB = saltbush, A = ant colony (red triangle), G = grass on Rip-rap, BB = bitterbrush, and RB = rabbitbrush

Also at Falls City, top and bottom fluxes from TP-1 (mesquite) and TP-2 (control) were both essentially the same, with the fluxes from the control pit being relatively high. Root morphology analysis by Williams (2019) (see Chapter 6 of this report) of these two pits shows that fine and very fine roots are common in the rooting material above the radon barrier but there were some (categorized as "few") that extended through the radon barrier at both TP-1 (mesquite) and TP-2 (control). TP-1 did have more and courser roots, but these were confined to the rooting material layer; only very fine roots extended through the barrier, suggesting that these few very thin roots can impact Rn flux.

At the Bluewater site, two pairs of test pits were excavated to study the effects of saltbush colonies on Rn flux. The average flux measured from TP-5 (saltbush colony) was greater than 30 times the average flux measured from TP-4 (control). The thickness of the barrier at each of the test pits was comparable. The average water content in TP-5 was approximately 33% lower than the control test pit. Furthermore, the bottom flux from the tailings beneath TP-5 (saltbush colony) was much less than the bottom flux at TP-4 (control), strengthening the view that the saltbush colony was the main cause of the elevated flux measurements.

Figure 4-16 Small Roots Grow in Thin Structural Cracks in the Radon Barrier at Falls City TP-4 These cracks are common along the edges of clay clods that remain from construction. TP-4 was a control, located many meters from a mesquite bush.

The much greater effect of saltbush on Rn flux at Bluewater compared to the effect of mesquite on Rn flux at Falls City may be attributable in part to the thinner cover and a protection layer at Bluewater that allowed direct rooting into the barrier (compared to the meter of rooting zone at Falls City). The saltbushes reduce the moisture content of the barrier, creating structure (cracking) and pathways leading to increased surface Rn flux. On Figure 4-15, fluxes from the saltbush location (TP-5) and its' control (TP-4) are statistically different at the 2-sigma level. The average water content in all pits at Bluewater was very low. Multiple roots were observed in the Shelby tube samples obtained from TP-5 (Figures 4-16 and 4-17). Both of these characteristics are why elevated fluxes were measured, see Chapter 6.3.2. An additional pair of test pits was excavated at a saltbush colony on the carbonate tailings pile at the Bluewater site. The average flux measured from TP-7 (a small saltbush) was essentially the same as that measured at TP-8 (control). The radon barrier here was very thick and both sets of fluxes were very low, about 0.011 Bq/m^2/s, and represent background.

At Lakeview, fluxes were very low, making comparisons difficult. The average top flux measured from DC-11 (bitterbrush) was greater than four times the average flux measured from DC-10 (control), which was about background. The two data sets are statistically different at the 2-sigma level. The thicknesses of the Rn barrier at both test pit locations were within 2 cm of each other. The average water content of the Rn barrier beneath the bitterbrush was approximately 13% lower than the soil in the control test pit, but even the bottom flux at the control was background. At the other pair of pits, the top flux at DC-12 (rabbitbrush) was 0.006 Bq/m^2/s, less than the 0.011 measured at DC-13 the control location, although top fluxes from both pits were only slightly above background. In fact, the bottom flux at DC-12 was relatively high for Lakeview, about 0.395 Bq/m^2/s, so the barrier performed well even in the presence of

the rabbitbrush. Pit 5 contained a small animal burrow and the flux from that location also was low, 0.011 Bq/m^2/s.

While flux measurements were not conducted in transects away from these bushes, examination of the root morphology was. For a saltbush at Bluewater, for example, medium and course size roots were found up to 2 meters away at the surface and smaller roots extended to about 50 cm depth. At Lakeview a transect of bitterbrush root morphology showed that at the plant a range of root sizes were present and extended to more than 1.1 m depth. Lateral spread extended out to 2.5 m where some very fine sized roots extended to about 1 m depth (Williams, 2019, Fuhrmann et al., 2019, and Chapter 6 of this report). It is likely that Rn fluxes are influenced to some extent within the entire circle through which roots radiate.

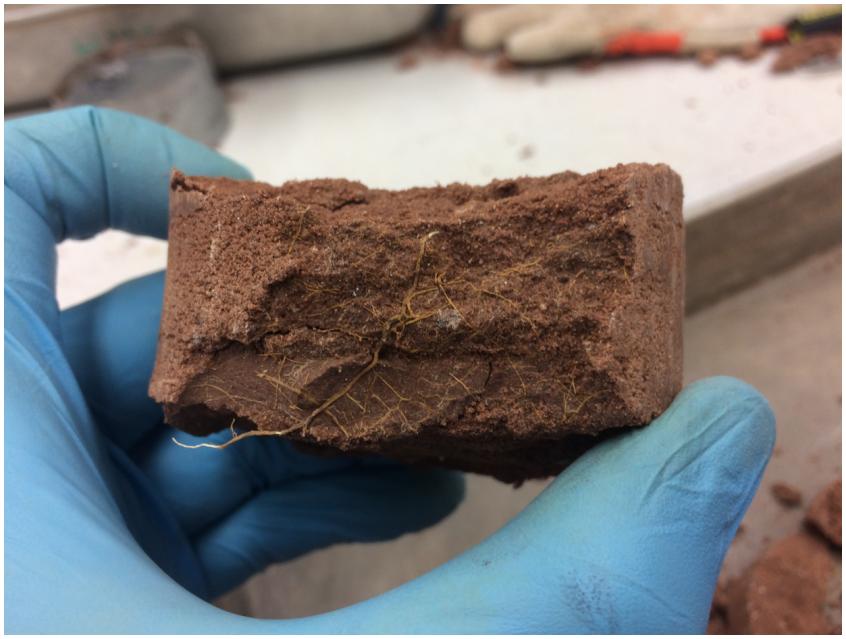

Figure 4-17 Root Structure in 70 mm Diameter Shelby Tube Sample from Bluewater Test Pit 5

Figure 4-18 Large Root in the Radon Barrier in a Shelby Tube Sample from Bluewater Test Pit 5 here Fluxes ere High and Exhibited a Wide Range

4.5.3.2 Effects of Seasonal Ponding

At Bluewater, TP-1 was positioned on an area of seasonal ponding, which was dry at the time of sampling. A control test pit (TP-2) was located nearby. This area is visible on Figure 2-4 which shows white salt deposits. The Rn barrier at the pond location had average water contents and saturations 9% and 43% greater than the location without ponding, respectively. As a result, the average Rn flux measured from the location without ponding was approximately 9.3 times larger than the location with ponding. The thickness of the Rn Barrier at each of the test pits was comparable, however, the bottom fluxes measured at the pond area were approximately 12 times lower than the bottom fluxes at the location without ponding. This undoubtedly contributed to the difference in surface flux measurements and may be the result of moisture from the pond inhibiting emanation of Rn from the waste. Other properties, such as hydraulic conductivity and other soil properties were also impacted by ponding (see Chapter 6).

4.5.3.3 Effects of Animal Burrowing

At the Bluewater site, TP-6 was excavated at a large harvester ant mound and was compared to the control TP-4. The flux measured from TP-6 (a single measurement) was 0.245 Bq/m^2/s, 16 times greater than the control flux of 0.015 Bq/m^2/s, even though the bottom flux at the control was higher. As with the ponded area, other soil properties were also impacted as discussed in Chapter 6. The thickness of the barrier at each location was very similar but the ant colony extended to about 75 cm below the top of the rock layer. A small animal burrow (Chapter 6) was observed at Pit 5 at Lakeview; the flux from that location also was low, 0.011 Bq/m^2/s.

4.5.3.4 Effects of Grass Growth in Rip-Rap

Lakeview TP-4A (bare rip-rap) and 4B (rip-rap with grass) were chosen to evaluate the effects of grass growth within the rip-rap covered slope, with the thought that the grass would dry the barrier and increase Rn flux. The range of fluxes from beneath the grass overlapped the range measured beneath the pit with bare rip-rap (Figure 4-15, Labeled G); indicating there is no observed difference in top fluxes from these two locations. Additionally, no significant differences in water content were observed between the two pits. The roots of the grass may not have penetrated into (or deeply into) the Rn barrier and thus did not affect the engineering properties of the barrier.

4.6 Diffusion Modeling

4.6.1 RAECOM 2-Flux Calculations

Several approaches were used to estimate the effective Rn diffusion coefficient (D) based on site-specific data. Our primary approach, and that used to determine diffusion coefficients presented below for each site, are based on the RAECOM code (Radiation Attenuation Effectiveness and Cover Optimization with Moisture Effects) (Rogers et al., 1984, Nielson and Rogers, 1982, and U.S.NRC, 1989). The RAECOM code is available at the Wise Uranium Project website (http://www.wise-uranium.org). Its' calculations of radon flux were checked against calculations given in Regulatory Guide 3.64 (NRC, 1989). The code performs one-dimensional, steady-state radon diffusion calculations for a multi-layered system of porous media (e.g., soil), giving D as the effective diffusion coefficient for Rn in the total pore space. Diffusion coefficients can be determined based on a pair of known fluxes at the top and bottom of the barrier, such as the "top flux" and "bottom flux" measurements described above (the 2-flux method). This is the approach used to generate values of D in this work and is described below. RAECOM also calculates Rn fluxes and steady state concentrations at user defined locations within the barrier profile. Background Rn fluxes from the barrier material itself can be calculated from an entered diffusion coefficient and a Ra-226 concentration; this approach was used to estimate background fluxes discussed earlier.

Calculations of Rn diffusion coefficients using the 2-flux method were based on the measured inlet flux at the bottom of the radon barrier and the exit flux measured at the top of the barrier (see Figure 4-19). The measured inlet (bottom) flux from the waste and the barrier thickness were entered into the RAECOM code and the diffusion coefficient was iterated until an exit (top) flux was obtained that was generally within 1% of that observed by our flux measurements at the site. In some cases, results were calculated in terms of a flux profile through the thickness of barrier, giving fluxes and steady state concentrations at select depths. These fluxes, along with the measured fluxes at the bottom of the barrier (top of the waste) and the top of the barrier were plotted against depth in the barrier and were used to model Pb-210 concentrations in the barriers (see Chapter 5).

4.6.2 Empirical Correlations to Estimate D

Moisture Saturation. Another approach to estimate the radon diffusion coefficient in RAECOM is to use the thickness of the soil layer (or radon barrier), moisture content and porosity data. From this information moisture saturation (m) is calculated and Rn D is estimated from an empirical relationship from Rogers and Nielson (1991) based on a plot of D against moisture

saturation containing 1073 measurements with a one sigma geometric standard deviation (for m greater than 0.5) of 2.85. This correlation function (Eq. 6) is used in the code:

$$D = D_{ra}\, N \exp\,[-6Nm - 6\, m^{14N}] \qquad (6)$$

where D_{ra} is the radon diffusion coefficient in air (1 x 10^{-5} m^2/s), N is total porosity, and m is the moisture saturation fraction as defined in Regulatory Guide 3.64. For some of the results reported herein, three different sources of moisture measurements were used to determine m; 1) those determined from the field samples measured in the lab (Shelby tube samples), 2) in-situ measurements with a dielectric soil moisture sensor (GS3 with ProCheck data logger manufactured by Decagon Devices, Pullman, Washington), and 3) those obtained in-situ from Troxler gauge measurements during pit reconstruction.

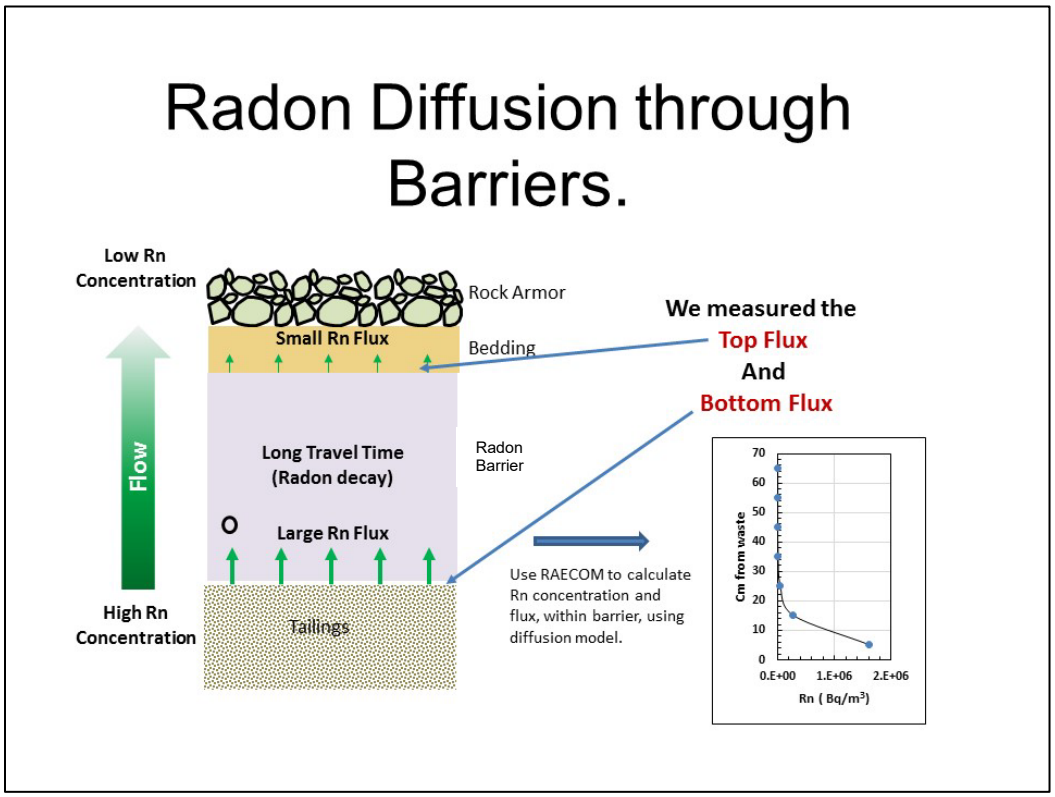

Figure 4-19 Schematic Showing the Approach to Determining Rn Diffusion Coefficients in Rn Barriers

IAEA Technical Report Equations. In addition to the RAECOM calculations, diffusion coefficients were estimated using equation 26 in IAEA Technical Report 474 (Ishimori et al., 2013), which also uses a 2-flux method. Measured "top flux" and the "bottom flux" from the field-testing program were used in these calculations. Corresponding equations are:

$$f_b \approx f_t \exp\,[-z/L_c] \qquad (7)$$

where f_b is measured top flux (top of the radon barrier), f_t is the measured bottom flux (top of the tailings), z is the barrier thickness, and L_c is the diffusion length:

$$L_c = [D_b/\lambda]^{½} \quad (8)$$

where D_b is the diffusion coefficient of Rn in the barrier, and λ is the radon-222 decay constant (2.0984×10^{-6}/s).

Finally, diffusion coefficients were estimated using barrier thickness, moisture content, porosity, and equation 14 in IAEA Technical Report 474 (Ishimori et al, 2013; Rogers and Nielson, 1991).

4.6.3 Comparison of Diffusion Coefficients by Several Methods

While diffusion coefficients presented elsewhere in this report are calculated with the RAECOM 2-flux method, it is useful to compare calculations at the same site using several different approaches. Figure 4-20, for example, is a summary of diffusion coefficients calculated in several ways for six test pits from the Falls City site. Calculation methods include:

- 2-flux method using RAECOM (using measured top and bottom fluxes),
- 2-flux method using equations 7 and 8 (equation 26 from IAEA report 474),
- Moisture and porosity method (Eq. 6) using lab analysis of samples,
- Moisture and porosity method (Eq. 6) using Troxler gauge measurements from the field.
- Moisture and porosity method (Eq. 6) using in-situ probe measurements.

While the first method is a modeled calculation, all other methods are estimates of the diffusion coefficients based on different correlations. Diffusion coefficients by these various approaches vary substantially, ranging generally from about 2×10^{-6} m^2/s to about 1×10^{-8} m^2/s, and averaging about 4×10^{-7} m^2/s. The lowest values at the Falls City site were for pit 6 for both 2-flux methods. Here the diffusion coefficients were 1×10^{-8} m^2/s to 2×10^{-8} m^2/s, much lower than those estimated by the moisture methods. This location was moister than the others and had a very low surface flux even though the bottom flux was quite high (Figure 4-4). The barrier at this location was damp and plastic, in contrast to the very hard and brittle texture of the same material on the top deck, indicating long-term retention of moisture.

The 2-flux RAECOM method results always provided the lowest value of D, whereas D estimated from moisture measured with the Troxler gauge consistently were the highest. This is not surprising since these moisture values were the lowest (these measurements were made during reconstruction of the test pits). In general, values for D spanned about an order of magnitude. Results in Figure 4-20 show that only the two 2-flux methods reflect the reality that top fluxes in Pit 6 are very low even though the flux measured at the bottom of the pit was quite high and the radon barrier was relatively thin. The moisture saturation for Pit 6 was high which provided effective attenuation of Rn. This was well reflected by the 2-flux methods but not at all by the moisture/porosity methods. For this reason, the Rn D values reported for our measurements below are based on the 2-flux method.

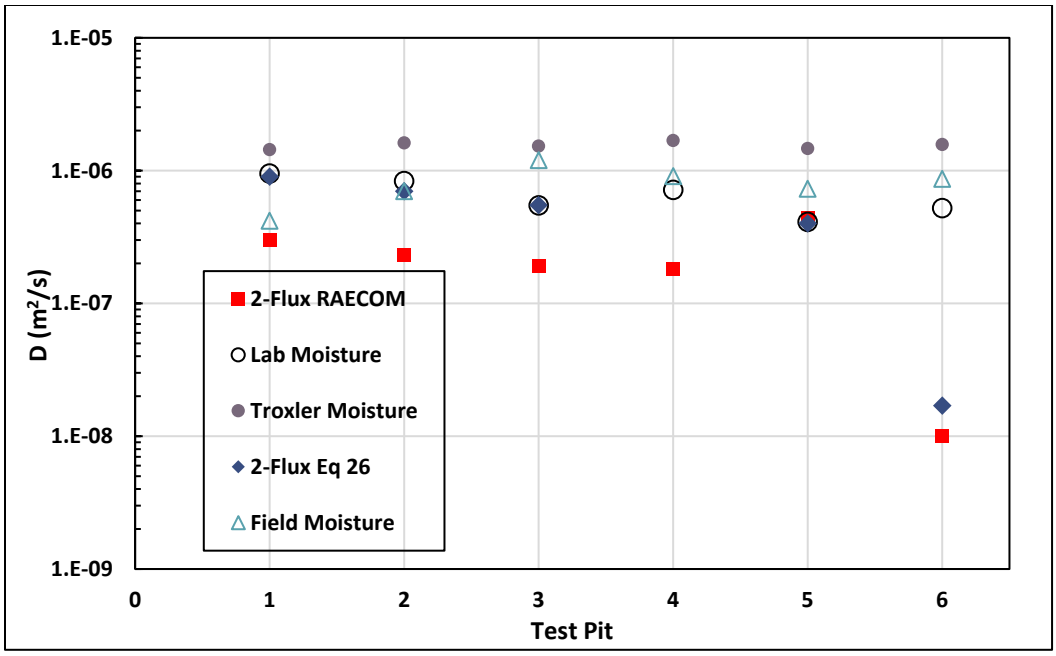

Figure 4-20 Diffusion Coefficients Calculated in Several Ways for Test Pits at the Falls City Site

4.6.4 Site Specific Diffusion Coefficients and Rn Travel Times

Tables 4-9 through 4-12 present the measured top and bottom fluxes and barrier thickness for each test pit at each site. Some fluxes are not shown if the bottom flux was not successfully measured, and D could not be computed. From these, 2-flux diffusion coefficients were calculated using RAECOM. Radon transport times through the barrier material were calculated based on:

$$t = h^2/2D \qquad (9)$$

where h is the thickness of the barrier in meters and D is the diffusion coefficient in m^2/s. This calculation was then converted to time in days as well as dividing days by 3.82 to obtain the number of Rn-222 half-lives required to move through the barrier to better indicate the impact of travel time on Rn concentration. A small number of half-lives indicates that Rn is moving quickly enough that little decay takes place and an observable flux at the surface could be present. However, if the number of half-lives is larger, more Rn will decay within the barrier and there will be less emanating from the top of the barrier. Defining a number of half-lives at which no Rn would be released from the top of the barrier is arbitrary, but a generally used figure of merit is 10 half-lives because with this amount of decay very little activity remains (less than 0.01%).

4.6.4.1 Falls City

Diffusion coefficients at Falls City (Table 4-9) range from 1.1×10^{-8} m^2/s to 4.4×10^{-7} m^2/s. On the top deck, which is vegetated, the number of half-lives needed to traverse the barrier is about 6. This suggests that about 2% of Rn generated from the waste reaches the top of the barrier before it decays. The lowest diffusion coefficients are found at Pit 6 on the side slope, where Rn would need about 63 half-lives to cross the barrier. Both pits 5 and 6 are rip-rap covered

and have moisture contents that are close to the as-built averages of 42.0%, higher than on the vegetated top deck. However, the diffusion coefficient for test pit 5 was much higher than pit 6 because the bottom flux from pit 5 was very low, impacting the diffusion calculation. Overall, at Falls City the radon barrier at the top deck retains about 98% of Rn from the waste, while on the side slope all Rn is retained.

4.6.4.2 Bluewater

Diffusion coefficients at the Bluewater site (Table 4-10) range from 1.6×10^{-8} m^2/s to 7.4×10^{-7} m^2/s. Of the eight test pits with adequate data to calculate diffusion coefficients (pit 8 had no usable bottom flux measurement), calculated Rn travel times had a wide range among pits but was generally consistent within a single pit. Four pits had travel times greater than 10 half-lives. This essentially precludes Rn generated by the waste from reaching the top of the barrier. Pit 1 had a very low bottom flux (and its' top fluxes were background) which resulted in particularly long travel times of about 48 half-lives, but this is essentially a detection limit for this site. This location is the site of a seasonal pond that has formed due to subsidence of the waste; as a result both the Rn barrier and presumably the underlying tailings have high moisture contents. Pit 5 had high top and bottom fluxes, thus providing better resolution of the diffusion coefficient calculation. Travel time at pit 5 was only about 1.5 half-lives, suggesting that about a third of the Rn from the waste reaches the top of the barrier before it decays. Pits 2 and 9 had estimated transport times of about 3 half-lives, which would allow about 10 % of the radon from the waste to reach the surface. In summary, at Bluewater there are some locations that provide good retention of Rn while others have limited capacity to inhibit its' transport.

4.6.4.3 Shirley Basin South

Diffusion coefficients at the Shirley Basin South site (Table 4-11) range from 1.0×10^{-7} m^2/s to 6.0×10^{-9} m^2/s. No usable flux data were measured for pit DC-4. This location appears to have been on a berm between two tailings ponds (where no tailings were found by excavation to a depth of 2.82 m). Six flux measurements were background with the resulting D around 7×10^{-9} Bq/m^2 and travel times of 89 half-lives, which is a minimum time. For the other test pits, transport time, expressed as the number of Rn half-lives, indicates that at least 10 half-lives are needed to traverse the barrier. The barrier is very effective and retains radon well. Most pits had high bottom fluxes (pit 3 was very high) which allows good confidence in the calculation of D.

4.6.4.4 Lakeview

Results for the Lakeview site are shown in Table 4-12. In general, the top fluxes are very low, with many at or close to background of 0.003 $Bq/m^2/s$. The highest was only 0.040 $Bq/m^2/s$. However, bottom fluxes are also very low. This makes it difficult to determine diffusion coefficients. The average value of D based on measurable fluxes above background is 7.4×10^{-7} m^2/s. Pit 12 had lower D values and a slightly higher bottom flux (only 0.395 Bq.m2/s), as a result it had an average transport time of 17.3 half-lives. There is very little Rn being released from the waste as indicated by the low bottom fluxes.

Table 4-9 Falls City: Rn Diffusion Coefficients and Transport Times

Top Flux ($Bq/m^2/s$) [barrier thickness, m]	Bottom Flux ($Bq/m^2/s$)	Chamber Size	Diffusion Coefficient (m^2/s)	Transport Time (days)	Number of Rn Half-lives	Mean Number of Half-lives
Pit 1 [0.91]						
0.152	2.07	L	1.6×10^{-7}	30.0	7.8	4.9
0.380		M	3.1×10^{-7}	15.5	4.1	
0.561		S	4.4×10^{-7}	10.9	2.9	
Pit 2 [0.91]						
0.281	2.21	L	2.3×10^{-7}	20.8	5.5	5.5
0.346		S	2.7×10^{-7}	17.8	4.7	
0.237		ES	2.0×10^{-7}	24.0	6.3	
Pit 3 [0.91]						
0.335	5.53	L	1.4×10^{-7}	34.2	9.0	6.1
0.908		M	2.8×10^{-7}	30.0	4.5	
0.475		S	1.8×10^{-7}	26.6	7.0	
1.281		ES	3.3×10^{-7}	14.5	3.8	
Pit 4 [0.91]						
0.040	1.65	L	9.0×10^{-8}	23.9	6.3	4.3
0.014		M	6.0×10^{-8}	35.9	9.4	
0.166		S	1.9×10^{-7}	11.3	3.0	
0.378		ES	3.8×10^{-7}	5.7	1.5	
Pit 5 [0.91]						
0.005	0.104	L	1.3×10^{-7} B*	36.9	9.7	6.4
0.007		M	1.6×10^{-7} B*	30.0	7.8	
0.010		S	1.8×10^{-7} B*	26.6	7.0	
0.063		ES	1.3×10^{-6}	3.7	1.0	
Pit 6 [0.61]						
0.019	42.57	L	1.1×10^{-8}	196	51	63
0.020		M	1.1×10^{-8}	196	51	
0.011		S	1.0×10^{-8} B*	215	56	
0.003		ES	6.0×10^{-9} B*	359	94	

Background Flux is 0.028 $Bq/m^2/s$, *B top flux is background or less, D is a maximum value.
Chamber sizes: L = large, M= medium, S = small, ES = very small.

Table 4-10 Bluewater: Rn Diffusion Coefficients and Transport Times

Top Flux ($Bq/m^2/s$) [Barrier thickness, m]	Bottom Flux ($Bq/m^2/s$)	Chamber Size	Diffusion Coefficient (m^2/s)	Transport Time (days)	Number of Rn Half-lives	Mean Number of Half-lives
Pit-1 A [0.67]						
0.003	0.01	L	1.4×10^{-8} B*	185.6	48.6	48.6
0.005		M	1.4×10^{-8} B*	185.6	48.6	
0.002		S	1.4×10^{-8} B*	185.6	48.6	
Pit 1B [0.67]						
0.003	0.01	L	1.4×10^{-8} B*	185.6	48.6	48.6
Pit 2A [0.63]						
0.024	0.117	L	2.0×10^{-7}	12.2	3.2	2.8
0.038		M	3.0×10^{-7}	8.2	2.1	
0.028		S	2.0×10^{-7}	12.2	3.2	
Pit-2B [0.63]						
0.040	0.117	L	2.8×10^{-7}	8.7	2.3	2.7
0.038		M	2.6×10^{-7}	8.7	2.3	
0.016		S	1.2×10^{-7}	20.4	5.3	
0.071		ES	6.8×10^{-7}	3.6	0.9	
Pit-3A [0.65]						
0.138	4.84	L	4.9×10^{-8}	49.9	13.1	24.1
0.016		M	2.2×10^{-8}	111	29.1	
0.043		S	3.1×10^{-8}	78.9	20.6	
0.011		ES	1.9×10^{-8}	129	33.7	
Pit-3B [0.65]						
0.041	4.84	S	3.1×10^{-8}	78.9	20.6	20.0
0.056		ES	3.3×10^{-8}	74.1	19.4	
Pit-4A [0.71]						
0.024	12.86	L	2.2×10^{-8}	133	34.7	45.3
0.007		M	1.5×10^{-8}	195	50.9	
0.008		S	1.6×10^{-8}	182	47.7	
0.008		ES	1.6×10^{-8}	182	47.7	

Background Flux is 0.004 $Bq/m^2/s$, *B top flux is background or less, D is a maximum value.

Table 4-10 Bluewater: Rn Diffusion Coefficients and Transport Times (Continued)

Top Flux ($Bq/m^2/s$) [Barrier thickness, m]	Bottom Flux ($Bq/m^2/s$)	Chamber Size	Diffusion Coefficient (m^2/s)	Transport Time (days)	Number of Rn Half-lives	Mean Number of Half-lives
Pit-4B [0.71]						
0.009	12.86	L	1.6×10^{-8}	182	47.7	37.0
0.021		M	2.1×10^{-8}	139	36.4	
0.065		S	3.0×10^{-8}	97.2	25.5	
0.018		ES	2.0×10^{-8}	146	38.2	
Pit-5A [0.64]						
0.999	1.99	L	5.0×10^{-7}	4.7	1.2	1.4
1.258		M	7.4×10^{-7}	3.2	0.8	
0.708		S	3.0×10^{-7}	7.9	2.1	
0.899		ES	4.1×10^{-7}	5.8	1.5	
Pit-5B [0.64]						
0.141	1.99	L	7.7×10^{-8}	30.8	8.1	8.7
0.111		M	6.7×10^{-8}	135.4	9.3	
Pit-6A [0.66]						
0.245	6.39	L	5.9×10^{-8}	42.7	11.2	11.2
Pit-9A [0.43]						
0.374	1.10	M	1.3×10^{-7}	8.2	2.2	3.6
0.400		S	1.4×10^{-7}	7.6	2.0	
0.104		ES	4.2×10^{-8}	25.5	6.7	
Pit-9B [0.43]						
0.152	1.10	L	5.6×10^{-8}	19.1	5.0	3.1
0.672		M	3.3×10^{-7}	3.2	0.8	
0.314		S	1.0×10^{-7}	10.7	2.8	
0.220		ES	7.4×10^{-8}	14.5	3.8	

Background Flux is 0.004 $Bq/m^2/s$, *B top flux is background or less, D is a maximum value.
No successful bottom flux measurements were made at Pits 7 and 8.

Table 4-11 Shirley Basin South: Rn Diffusion Coefficients and Transport Times

Top Flux (Bq/m2/s) [Barrier thickness, m]	Bottom Flux (Bq/m^2/s)	Chamber Size	Diffusion Coefficient (m^2/s)	Transport Time (days)	Number of Rn Half-lives	Mean Number of Half-lives
DC-2 A [0.68]						
0.036	8.99	L	2.5×10^{-8}	107	28.0	25.0
0.046		M	2.8×10^{-8}	96	25.0	
0.051		S	2.8×10^{-8}	96	25.0	
0.071		ES	3.2×10^{-8}	84	21.9	
DC-2 B [0.68]						
0.089	8.99	L	3.5×10^{-8}	76	20.0	25.3
0.135		M	4.1×10^{-8}	65	17.1	
0.051		S	2.8×10^{-8}	96	25.0	
0.014		ES	1.8×10^{-8} B*	149	38.9	
DC-3 A [0.65]						
0.011	397	L	7.7×10^{-9}	318	83.1	87.0
0.007		M	7.2×10^{-9} B*	340	88.9	
0.006		S	7.2×10^{-9} B*	340	88.9	
0.009 possible leak		ES	--- B*			
DC-3 B [0.65]						
0.009	397	L	7.7×10^{-9} B*	318	83.1	87.0
0.006		M	7.2×10^{-9} B*	340	88.9	
0.007		S	7.2×10^{-9} B*	340	88.9	
0.0001 possible leak		ES	--- B*			
DC-5 [0.56]						
0.040	0.257	L	1.0×10^{-7}	18	4.3	10.1
0.013		M	5.0×10^{-8}	36	9.5	
0.013		S	5.0×10^{-8}	36	9.5	
0.004		ES	2.8×10^{-8} B*	65	16.9	
Rock Slope [0.38]						
0.122	75.0	M	6.0×10^{-9}	140	36.7	33.6
0.226		S	7.2×10^{-9}	117	30.5	

Background Flux is 0.010 Bq/m^2/s, *B top flux is background or less, D is a maximum value.
No successful bottom flux measurement was made at Pit 4.

Table 4-12 Lakeview: Rn Diffusion Coefficients and Transport Times

Top Flux ($Bq/m^2/s$) [Barrier thickness, m]	Bottom Flux ($Bq/m^2/s$)	Chamber Size	Diffusion Coefficient (m^2/s)	Transport Time (days)	Number of Rn Half-lives	Mean Number of Half-lives
DC-2 [0.43]						
0.003	0.092	M	3.0×10^{-8} B*	35.7	9.3	
0.008		M	4.0×10^{-8}	26.8	7.0	8.2
DC-4 Grass [0.38]						
0.006	N/A	M	---	---		
0.002		M	---	---		
0.018		S	---	---		
DC-4 No plants [0.38]						
0.005	N/A	M	---	---		
0.015		S	---	---		
DC-5 [0.46]						
0.011	0.075	M	6.5×10^{-8}	18.8	4.9	4.9
DC-10 [0.41]						
0.004		L				
0.004		M				
0.008	N/A Poor statistics	S				
0.006		ES				
DC-11 [0.43]						
0.020		L	1.8×10^{-7}	5.9	1.6	
0.021		M	1.8×10^{-7}	5.9	1.6	
0.040	0.051	S	6.5×10^{-7}	1.7	0.4	1.3
0.021		ES	1.8×10^{-7}	5.9	1.6	
DC-12 [0.60]						
0.007		L	3.5×10^{-8}	59.5	15.6	
0.005	0.395	M	3.0×10^{-8}	69.4	18.2	17.3
0.005		S	3.0×10^{-8}	69.4	18.2	
DC-13 [0.66]						
0.010		L	---	---		
0.011	N/A	M	---	---		
0.012		S	---	---		

Background Flux is 0.003 $Bq/m^2/s$, *B top flux is background or less, D is a maximum value.

4.6.5 Laboratory Diffusion Coefficients and Comparison to Field D

Shelby tube samples from the field sites were used for laboratory measurements of D for comparison to field measurements. Only samples from the Shirley Basin South site remained intact enough to use for these tests. Permeameters typically used for hydraulic conductivity were adapted for Rn diffusion measurements (Figure 4-21). Chambers below and above the barrier material allowed near real-time measurement of Rn on the inlet side and after having passed through the barrier material. The Rn source was a mass of Wisconsin Red Granite gravel. The entire column of the barrier material and the two Rn chambers were surrounded with a flexible wall membrane and O-rings so that the column could be sealed by external water pressure (2.5 kPa) to ensure that Rn diffused only through the barrier material.

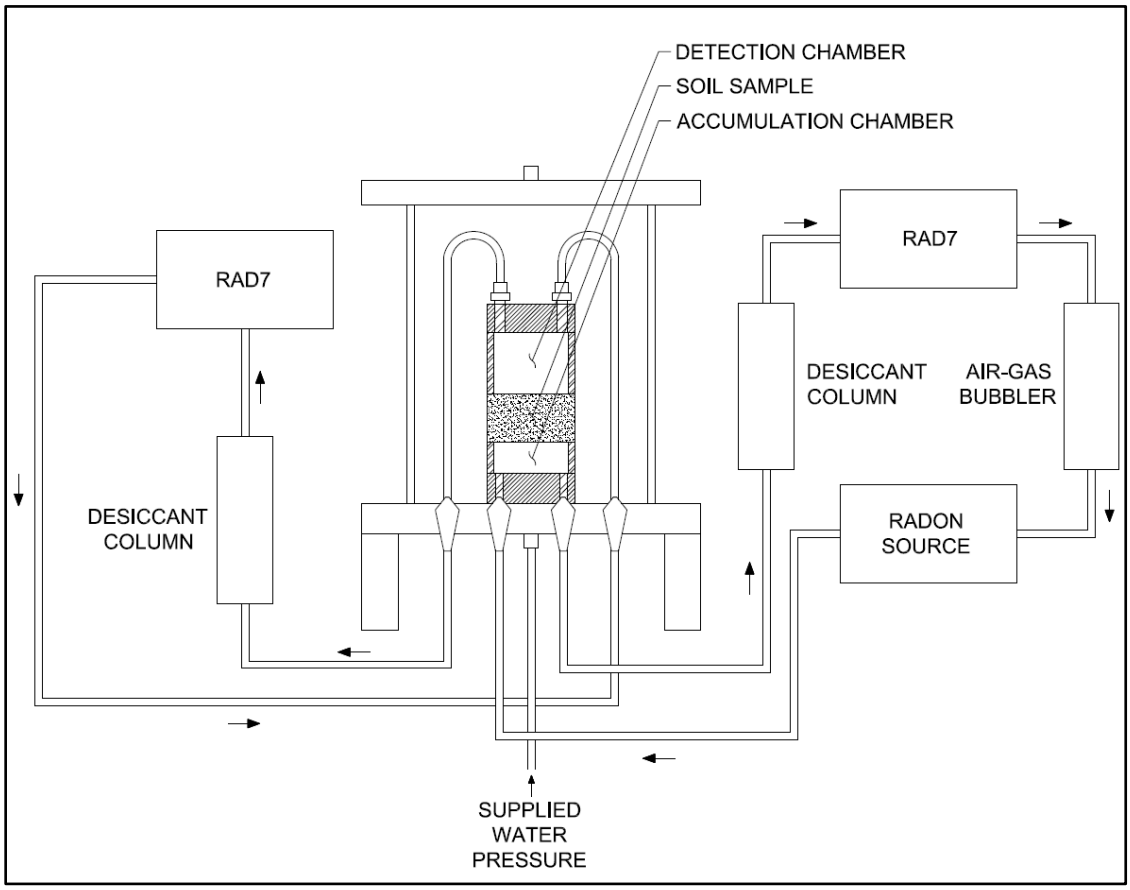

Figure 4-21 Schematic of Apparatus for Lab Measurements of Rn Diffusion Coefficients of Samples Taken from Shelby Tubes

Table 4-13 compares values of D for lab and field measurements as well as those calculated from the Equation 6 relationship (Rogers and Nielson, 1991). Moisture saturation was determined at the start and end of the lab tests. Some drying occurred during testing and the value reported is the average of the two. Values of D were calculated from field Rn flux measurements are taken from Table 4-11 using the 2-flux method. Results show a relatively small range of D for the lab samples, from 5.4 to 9.8 x 10^{-8} m^2/s.

Table 4-13 Comparison of D for Samples from the Shirley Basin South Site

Test Pit	Sample ID	Depth from Barrier Top (cm)	Porosity %	Moisture Saturation %	Rn D (m^2/s) Lab	Rn D (m^2/s) Eq. 6	Rn D (m^2/s) Field
DC-2	A	45	45	91	8.7×10^{-8}	3.2×10^{-8}	2.5×10^{-8} to 4.1×10^{-8}
	B	46	44	92	6.0×10^{-8}	1.1×10^{-8}	
	C	53	41	86	6.8×10^{-8}	3.9×10^{-8}	
DC-5	A	14	49	92	5.4×10^{-8}	1.2×10^{-8}	5.0×10^{-8} to 1.0×10^{-7}
DC-6	A	4	46	80	8.3×10^{-8}	1.3×10^{-7}	6.0×10^{-9} to 7.2×10^{-9}
	B	8	46	79	9.8×10^{-8}	1.5×10^{-7}	

For DC-2 the Eq. 6 and field values are similar while lab measurements are a factor of 2 to 3 higher. For DC-5 the lab and field values are about 5 to 10 times greater than the Eq 6 value. These are all within the range expected when determining D with a variety of methods (Figure 4-20). Values calculated with Eq 6 for DC-6 are higher than all others with the lab measurements being slightly lower. However, the field values of D are substantially lower, by over a factor of 20. This is likely the impact of the field measurements being integrated over the entire thickness of the barrier while the lab and Eq 6 values are based on measurements of small samples, only a few cm thick, taken from the top of the radon barrier that are typically drier than the lower parts of the barrier. The Rn barrier material at SBS on average has a high fines content but there are areas within the barrier that tend to have more sand (see Chapter 6, Figure 6-14), as a result small lab samples may reflect some of that inhomogeneity.

To evaluate D determined for field and lab samples, relative to the empirical Eq.6 calculation, Figure 4-22 presents the Eq 6 curve based on porosity (N) = 0.41 which was typical of the measured SBS porosity. D estimated with Eq. 6 using measured moisture saturation of small samples for the lab tests, plot along the curve, as expected. D from the lab diffusion measurements are plotted against those same saturation values and show as much as an order of magnitude difference in D. The 2-flux field data are plotted using average moisture saturation through the barrier (Mean) and with maximum moisture saturation at any location within the barrier (Max). It is important to note that the 2-flux method is independent of moisture content, it only uses the top and bottom Rn fluxes and the thickness of the barrier (D is determined by iteration to obtain a match to the top flux). Two of the field measurements using the mean saturation values fall on the calculated line but all others are above the line, some by as much as two orders of magnitude. Field determinations of D at high saturation are generally substantially higher than predicted by Eq. 6. The 1-sigma standard deviation of the Eq. 6 curve at 95% saturation is about an order of magnitude (Rogers and Nielson, 1991). Seven of the nine field D measurements plotted against the maximum moisture saturation measured are above the 1-sigma distribution of Eq. 6. This equation was developed from a large number of laboratory measurements of materials prepared specifically for the tests (Rogers and Nielson, 1991); thus, they appear to represent an ideal condition. In contrast, the field measurements reflect D as it develops after aging in service for about 20 years. It is likely that small

preferential pathways and inhomogeneities have developed that do not much impact moisture content (especially in smectite rich material) but have important implications for Rn transport.

The Shirley Basin site is unique, having barrier material with up to 60% smectite, high moisture saturation, and measured hydraulic conductivities that are extremely low (see Chapters 3 and 6). The 2-flux measurements are integrated over the entire thickness of the barrier and represent material that has been in service for 20 years, without disruption by sampling. Allowing for the difference in saturation, the difference between the field measurements and those from the lab and Eq. 6 suggest that the larger area of the Rn flux chambers captures Rn releases from zones of rapid transport that are often missed in small lab samples. This has been observed for hydraulic conductivity measurements, where it was found that 30 cm diameter samples are needed to provide reasonably representative measurements (Benson et al., 1994).

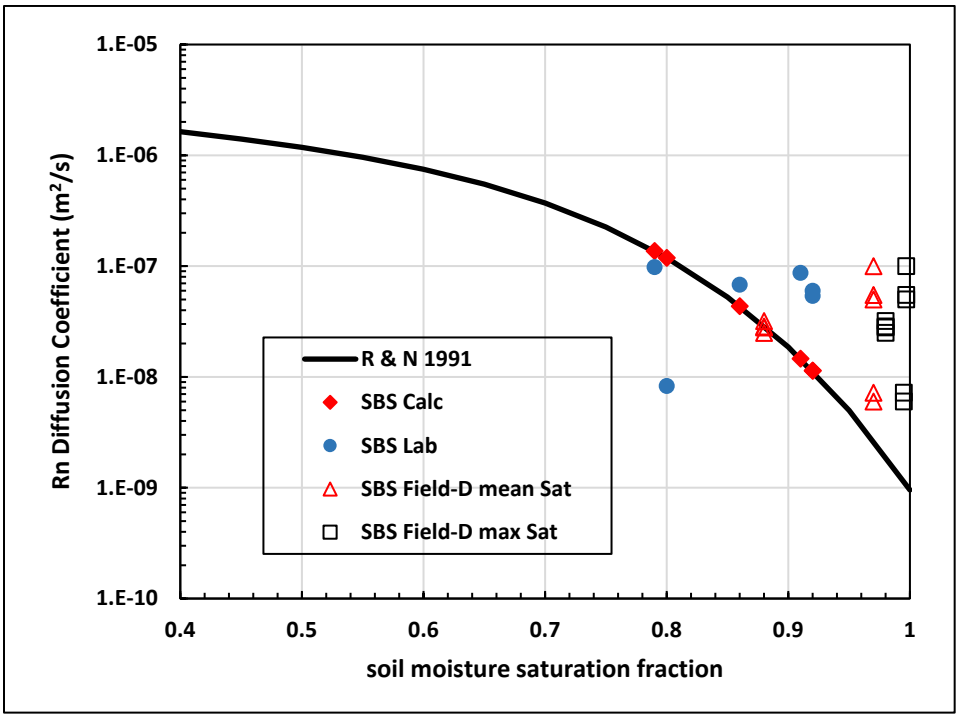

Figure 4-22 Comparison of a Curve Calculated from Eq. 6 with Samples Taken from the Shirley Basin South Site
D from laboratory tests scatter around the line while D from 2-flux field measurements (plotted against mean saturation and maximum saturation, open triangles and open squares) are as much as two orders of magnitude above the curve suggesting the presence of areas of preferential Rn transport and therefore greater values of D.

4.6.6 Comparison of Moisture Saturation Flux Correlation to Field Measurements of D

In Figure 4-23 all values of D from field measurements (2-flux method) at the four sites are plotted against mean moisture saturation measured from Shelby tube samples at each

respective pit. These data are compared to the Eq. 6 line (indicated in the figure as R & N, 1991), recognizing that this should be represented as a band as indicated by the gray vertical lines which are redrawn from Rogers and Nielson (1991) who noted that this band was generated from 1073 laboratory diffusion measurements. The relationship of our field measurements to the Eq. 6 band is instructive. Differences in methodology and sampling scale (presumably small lab samples versus the large scale 2-flux field method) must account for some of the difference.

Some data sets, especially from the Bluewater site, have diffusion coefficients equal to or notably lower than the Eq. 6 band. For example, the Bluewater (pit 1) point at 0.7 moisture saturation is actually four measurements of D with similar values. This test pit is located on an area of the cover that has subsided and a seasonal pond forms. Tests were done during the dry season when the Rn barrier itself had dried but moisture must have been retained in the fine-grained (slimes) waste such that the Rn flux measured from the waste was very low. This resulted in fluxes at the top of the Rn barrier that were very low, essentially background. The low bottom fluxes cause substantial uncertainty in the calculation of D, but clearly Rn releases were at background values. In contrast, the data set at 0.67 moisture saturation (Bluewater pit 4) had very low top fluxes but had a high (11.99 $Bq/m^2/s$) bottom flux, making the calculation of D more robust.

The single Bluewater point at 0.41 moisture saturation (pit 6) was located on an ant mound. This location had high flux from the waste and the flux at the top of the barrier was 0.244 $Bq/m^2/s$. Venting from the ant tunnels would be expected and there is a moderate Rn flux, nevertheless D was anomalously low compared to the Eq. 6 line considering the conditions of low moisture saturation and open structure. It is unclear if there is something about the ant colony structure, or perhaps moisture behavior under it, that inhibits Rn transport.

The diffusion coefficients for the data set from Falls City at moisture saturation of 0.88 is quite low. This is from pit 6 which is on the rock covered slope and the barrier material was damp and pliable at this location. The low moisture content is thought to be the result of a problem with sealing and storing Shelby tubes and that the actual saturation value should be higher, moving these points to the right on the plot, closer to the Eq. 6 line. In general diffusion coefficients from in-service radon barriers with high moisture saturation values are greater than expected. This appears to be the case for Falls City and some samples from Shirley Basin. Interestingly, samples from Bluewater tend to fall under the Eq. 6 line. However, in this case the moisture saturation is always below 0.8.

Many diffusion coefficients for higher moisture saturations are above the Eq. 6 band, suggesting a trend toward higher than expected fluxes at moisture saturation above about 0.8. The Log regression of the data points ($y = -3E\text{-}7Lnx + 6E\text{-}8$) has a very shallow slope and implies that over-all an averaging of flux has taken place that is independent of moisture saturation. This trend seems to indicate the deleterious influence of weathering or the incursion of vegetation over the 20 years or so of the covers lifetimes. These data suggest that even when moisture is retained in the barrier, Rn flows along a few preferential pathways that have developed, perhaps due to the formation of soil structure in the evolving barrier. As a result, values of D, especially when moisture saturation is above about 80%, often are higher than would be expected based on moisture saturation.

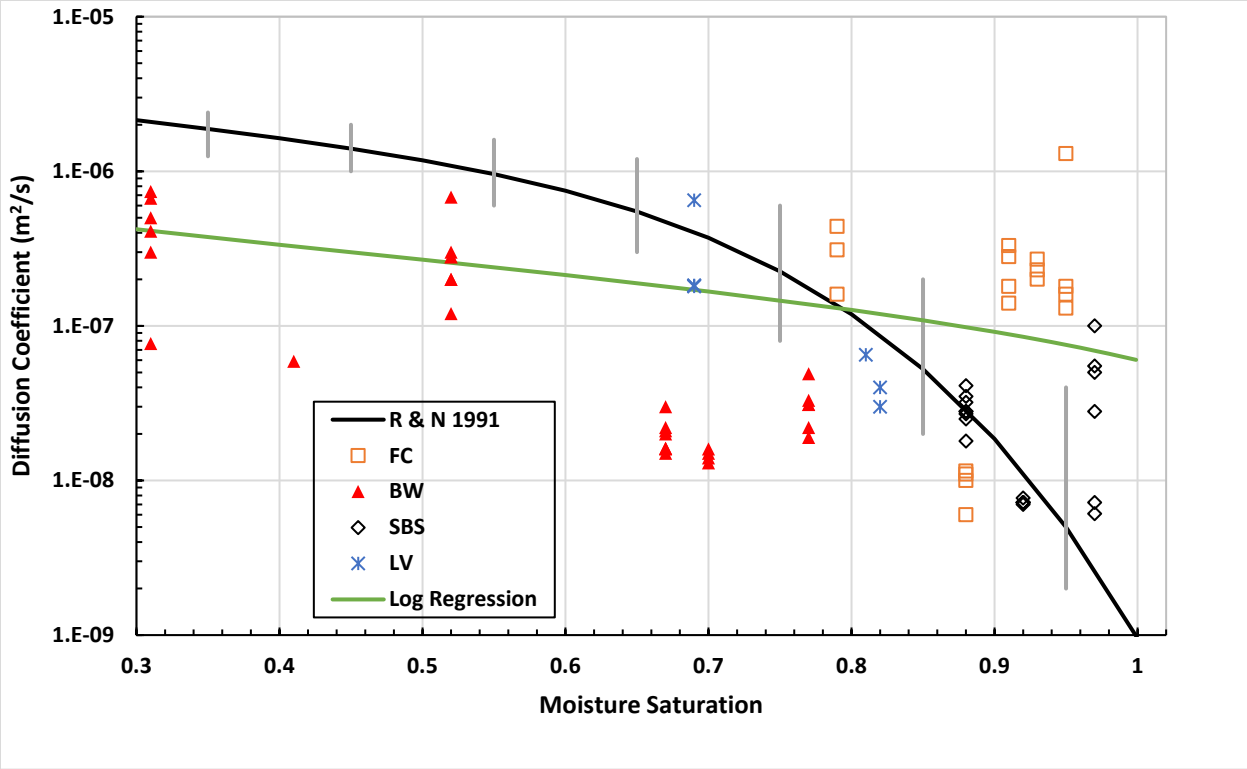

Figure 4-23 Rn Diffusion Coefficients Determined from Field Flux Measurements at All Four Sites Compared to an Empirical Relationship Between Moisture Saturation and Flux from Rogers and Nielson, 1991
The green line is the Log Regression of the data points. The gray vertical bars are redrawn from that paper and are the 1-sigma distribution of the data used to generate the curve.

4.7 Summary and Conclusions

Over the two field seasons of this project over 100 successful measurements were made of radon fluxes at the tops of the radon barriers at four sites, as well as “bottom” fluxes, at the top of the waste under the radon barrier, at 20 test pits. These measurements provided Rn concentration and flux data which, along with the thickness of the barrier, was used to model Rn transport with a diffusion-based code. The difference in objectives and design of the in-service (2016/2017) and the as-built surveys preclude the direct comparison of overall averages of fluxes. However, it is appropriate to examine is-service fluxes from individual test pits with respect to overall as-built averages or distributions.

The distribution of in-service fluxes at the Falls City site, which was closed in 1994, has shifted slightly toward higher fluxes, as shown in Figure 4-9. This took place on the top deck where the radon barrier was protected by topsoil and a rooting zone that was in combination about 1 m thick. Figure 4-4 shows fluxes from this area are above the range of all as-built measurements. In contrast low fluxes were measured at the rock covered edge and slope of the cover. Here the radon barrier was damp and plastic, suggesting long-term moisture retention.

Bluewater was closed in 1995 and over the course of 21 years the distribution of fluxes (Figure 4-11) show a modest trend toward higher fluxes, although the two distributions are quite similar.

Some locations on the main deck were impacted by ponding which resulted in essentially no Rn flux while others exhibited high fluxes due to the impact of deep-rooted plants. The broad range of as-built fluxes, shown in Figure 4-5, encompass all but a few in-service measurements. In this cover the radon barrier is protected by a relatively thin rip-rap layer; an entirely different design than Falls City.

The Shirley Basin South site was closed in 2000. Figure 4-13 shows the in-service and as-built flux distributions are very similar. As-built fluxes have a small range (Figure 4-6) and it is remarkable that about half of in-service fluxes are outside of that range, on the low side. No as-built radon flux measurements were found for Lakeview. Overall, fluxes were low, but this is not surprising since the Ra-226 content of the site is very low as were the bottom flux measurements.

Studies of paired test pits (an impacted pit and a nearby control shown in Figure 4-15) were used to examine effects of features such as a large deep-rooted plant. The geometric means of the control and the impacted pits were compared and in several cases fluxes were greater by factors from 4 to over 30 over the control. The features causing differences in fluxes were mesquite trees, saltbush colonies, bitterbrush, and an ant mound. In other cases, a small saltbush, grass, and rabbitbrush, little if any differences in flux were measured. Differences in surface flux may also be attributable to difference in bottom flux and barrier thickness. This is normalized by using the diffusion coefficient.

Modeling using RAECOM provided diffusion coefficients from which travel times were calculated for Rn moving through the barrier (Tables 4-9 through 4-12). These were expressed in terms of diffusion length and number of Rn-222 half-lives needed to move through the barrier. For SBS travel times were generally long, with the minimum being 10 half-lives; essentially no Rn from the waste should arrive at the top of the barrier. At Falls City generally 5-6 half-life travel times were determined indicating about 2% of Rn from the waste moves through the barrier. The exception is a location where radon barrier material was moist and plastic (compared to hard brick-like material on the top deck) and the travel time was 63 half-lives. At Bluewater results are very mixed; one pit had an average travel time of 48.6 half-lives while several pits were found with travel-times of less than three half-lives showing that retention of Rn was limited. Generally, both the top and bottom fluxes at Lakeview were very low making evaluation of transport difficult.

Radon diffusion coefficients were plotted against measured moisture saturation. These were compared to an empirical plot from an equation by Rogers and Nielson, 1991, based on a large number of laboratory measurements. At higher saturation levels, our field values of D were generally substantially greater than the lab-based equation, sometimes several orders of magnitude higher. This suggests that aging in the field for several decades results in higher Rn fluxes than is expected based on the degree of moisture saturation of the barrier. From this it appears that small preferential pathways have formed that allow Rn transport even though the moisture saturation is high enough that it should inhibit transport. The difference between the field measurements and those from the lab that generated Eq. 6 (Rogers and Nielson, 1991b) suggest that the larger area of the Rn flux chambers captures Rn releases from zones of rapid transport that are often missed in small lab samples. These age-related differences in Rn transport should be considered in models to design new radon barrier systems.

4.8 References

ARCO Coal Co Bluewater Mill Reclamation Plan, Volumes 1-3, 1990, 1099 pages, ADAMS Accession Number 9004050501, U.S. Nuclear Regulatory Commission, Washington DC.

Atlantic Richfield Co., 1996, Completion Report for Reclamation of the Bluewater Mill Site, Vol. 1-4. ADAMS Accession Number ML16047A198, U.S. Nuclear Regulatory Commission, Washington DC.

Benson, C., Hardianto, F., and Motan, E. (1994), Representative Specimen Size for Hydraulic Conductivity of Compacted Soil Liners, *Hydraulic Conductivity and Waste Contaminant Transport in Soils, STP 1142*, ASTM, S. Trautwein and D. Daniel, eds., 3-29.

Fuhrmann, M., C. H. Benson, W. J. Likos, N. Stefani, A. Michaud, W. J. Waugh, and M. M. Williams, 2021, Radon Fluxes at Four Uranium Mill Tailings Disposal Sites after About 20 Years of Service, *Journal of Environmental Radioactivity (in press)*.

Ishimori, Y., K. Lange, P. Martin, Y.S. Mayya, M. Phaneuf, (2013), Measurement and Calculation of Radon Releases from NORM Residues, International Atomic Energy Agency Technical Report 474.

Kalkwarf, D.R. and D.W. Mayer, (1983) Influence of Cover Defects on the Attenuation of Radon with Earthen Covers, NUREG/CR-3395, U.S. Nuclear Regulatory Commission, Washington, DC.

Michaud, A.M., (2018) Long-Term Performance of Radon Barriers in Limiting Radon Flux from Four Uranium Mill tailings Containment Facilities, http://digital.library.wisc.edu/1793/78602, Thesis for Master of Science, University of Wisconsin-Madison.

MK-Ferguson Company, (1991) Lakeview Oregon Final Completion Report, Volumes 1-6, Department of Energy Contract No. DE-AC04-83AL18796.

MK-Ferguson Company, (1996) Falls City Texas Final Completion Report, Volumes 1-5, Department of Energy Contract No. DE-AC04-83AL18796.

Morris, R.C. and L. Fraley Jr, 1989, Effects of Vegetation, a Clay cap, and Environmental Variables on Rn-222 Fluence Rate from Reclaimed U Mill tailings, Health Physics, Vol. 56 pp. 431-440.

Nielson, K.K. and V.C. Rogers, (1982) A Mathematical Model for Radon Diffusion in Earthen Materials, NUREG/CR-2765, U.S. Nuclear Regulatory Commission, Washington DC.

Pathfinder Mines (1993), Pathfinder Mines Tailings Reclamation Plan, ADAMS Accession Number ML081570290, U.S. Nuclear Regulatory Commission, Washington DC.

Petrotomics Company (2001a), Tailings Reclamation Construction Completion Report, Volumes 1-3. USNRC ADAMS Accession Number ML020040278, U.S. Nuclear Regulatory Commission, Washington DC.

Petrotomics Company (2001b), Shirley Basin South letter report to NRC from Petrotomics dated January 16, 2001, ADAMS Accession Number ML003774667, U.S. Nuclear Regulatory Commission, Washington DC.

RAECOM code (Accessed 2016) (Radiation Attenuation Effectiveness and Cover Optimization with Moisture Effects) available at the Wise Uranium Project (http://www.wise-uranium.org/ctch.html.)

Reynolds, T.D., 1990, Effectiveness of Three Natural Biobarriers in Reducing Root Intrusion by Four Semi-arid Plant Species, Health Physics, 59, pp. 849-852.

Rogers and Associates Engineering Corporation, (1987) Characterization of Borrow Soil at the Bluewater Uranium Mill Site, RAE-8721-1.

Rogers, V. C. & Nielson, K. K. (1991b). Multiphase Radon Generation and Transport in Porous Materials. Health Physics, 60(6), 807-815.

Rogers, V. C., K. K. Nielson, and G. B. Merrell, (1989) Radon Generation, Adsorption, Absorption, and Transport in Porous Media, DOE/ER/60664-1, U.S. Department of Energy, Washington, D. C.

Rogers, V. C., K. K. Nielson, G. B. Merrell, and D.R. Kalkwarf, (1983), The effects of advection on radon transport through earthen materials, NUREG/CR-3409, U.S. Nuclear Regulatory Commission, Washington DC.

Rogers, V. C., Overmyer, R. F., Putzig, K. M., Jensen, C. M., Nielson, K. K., & Sermon, B. W. (1980). Characterization of Uranium Tailings Cover Materials for Radon Flux Reduction. NUREG/CR-1081. U.S. Nuclear Regulatory Commission, Washington DC.

Rogers, V.C. and K.K. Nielson, (1991a) Correlations for Predicting air Permeabilities and ^{222}Rn Diffusion Coefficients of Soil, Health Physics, vol. 61, #2, pp. 225-230.

Rogers, V.C., K.K. Nielson and D.R. Kalkwarf, (1984) Radon Attenuation Handbook for Uranium Mill Tailing Cover Design, NUREG/CR-3533, U.S. Nuclear Regulatory Commission, Washington DC.

Stefani, N., (2016) Field and Laboratory Measurement of Radon Flux and Diffusion for Uranium Mill Tailings Cover Systems, Thesis for Master of Science, University of Wisconsin-Madison. https://minds.wisconsin.edu/handle/1793/75426

Suter, G.W., R.J. Luxmoore, and E.D. Smith, 1993, Compacted Soil Barriers at Abandoned Landfill Sites are Likely to Fail in the Long term, Journal of Environmental Quality, Vol. 22 pp. 217-226.

U.S. Department of Energy, Legacy Management (accessed 2017a). Falls City, Texas, Disposal Site. Fact Sheet and other documents at https://www.lm.doe.gov/falls/Sites.aspx.

U.S. Department of Energy, Legacy Management (accessed 2017b). Bluewater, New Mexico, Disposal Site. Fact Sheet and other documents at https://www.lm.doe.gov/bluewater/Sites.aspx

U.S. Department of Energy, Legacy Management (accessed 2017c). Shirley Basin South, Wyoming, Disposal Site. Fact Sheet and other documents at https://www.lm.doe.gov/shirley_basin/Sites.aspx

U.S. Department of Energy, Legacy Management (accessed 2017d). Lakeview, Oregon, Disposal Site. Fact Sheet and other documents at https://www.lm.doe.gov/Lakeview/Disposal/Sites.aspx

U.S. NRC, (1989) Regulatory Guide 3.64, Calculation of Radon Flux Attenuation by Earthen Uranium Mill Tailings Covers. U.S. Nuclear Regulatory Commission, Washington DC.

Waugh, J., G. Smith, B. Danforth, G. Gee, V. Kothari, and T. Pauling, 2007, Performance Evaluation of the Engineered Cover at the Lakeview, Oregon, Uranium Mill Tailing Site, Waste Management 2007, Tucson AZ. https://www.wmsym.org/archives/2007/pdfs/7499.pdf

5 LEAD-210 PROFILES IN RADON BARRIERS, INDICATORS OF LONG-TERM RADON-222 TRANSPORT

5.1 Introduction

To design engineered earthen covers for Uranium Mill Tailings Radioactive Control Act (UMTRCA) disposal sites, radon transport was modeled under the assumption that the primary transport mechanism was diffusion and that the barrier material was a homogeneous medium with averaged porosity and moisture content [Rogers et al. 1984]. Radon barriers were built with a corresponding thickness determined by modeling radon diffusion based on measurements of optimum density and moisture content or, in some cases, from lab measurements of diffusion coefficients in column tests. Modeled transport rates through this design thickness were meant to ensure that radon-222 (3.8-day half-life) would decay within the barrier instead of being released to the atmosphere at the barrier surface. There is uncertainty, however, whether or not this assumption still applies after the barriers have aged for decades (if it ever did)?

Releases of Rn-222 from uranium mill tailing sites in the United States are regulated by 40 CFR Part 192.02, which states that control of residual radioactive materials and their listed constituents shall be designed to be effective for at least 200 years, and shall provide reasonable assurance that releases of Rn-222 are limited to certain criteria (for some sites an average site-wide flux of 20 $pCi/m^2.s$ (0.74 $Bq/m^2.s$) is stipulated). These criteria apply only to the design specifications of the cover such that Rn flux measurements are typically done only at site closure (i.e., immediately following construction). While monitoring of atmospheric Rn at the periphery of many sites is conducted, long-term surveys of Rn flux from the barrier surface years after the post-construction survey are rarely, if ever, done.

Field research of earthen covers at disposal facilities for various types of waste has demonstrated that increases in hydraulic conductivity and changes in water retention behavior (reflecting formation of larger pores) can occur with time, regardless of climate, cover design or service time [Benson et al. 2007, Benson et al. 2011]. Soil processes including root intrusion, insect and animal intrusion, wet-dry cycling, and freeze-thaw cycling result in volume change, cracking, translocation of materials, and the formation of soil aggregates. These processes, which are inevitable and ubiquitous at the near surface, can create macro-structure in the cover material, and are expected to cause the hydraulic conductivity and gas diffusivity to increase. Such changes in cover properties at UMTRCA sites can potentially result in greater Rn emissions and seepage of contaminants to groundwater [Suter et al.1993, Albright et al. 2006, Kelln et al. 2009]. Soil drying caused by evapotranspiration may also reduce the water saturation of the Rn barrier, resulting in a higher gaseous Rn diffusion coefficient and higher fluxes. Understanding relationships among these processes, the development of soil structure, and corresponding changes in the engineering properties of the cover system is an important component of assessing long-term cover performance.

Rn fluxes through earthen covers are subject to short-term variables such as changes in barometric pressure [Singh et al. 1988, Ferry et al. 2002, Asher-Bolinder et al. 1991] as well as seasonal and much longer-term changes in moisture content and porosity of the barrier material [Asher-Bolinder et al. 1990, Prasad et al. 2012]. Conventional radon flux measurements using surface accumulation chambers are short-duration (24 hour) and are difficult to perform on completed site covers since the Rn barriers are buried under layers of protective material. These factors make radon flux measurements very difficult to use for confirming that the design

performance requirement is actually being met over the long term. Furthermore, understanding how soil change affects Rn transport within the barriers and ultimately Rn emissions to the atmosphere is critical for designing and predicting the performance of Rn barriers.
This scoping study was initiated to determine if Pb-210 profiles in UMTRCA radon barriers can be adequately measured, and if the data can help evaluate long-term Rn transport within the barriers as they age. The main study question is: Can Pb-210 measurements provide a simple monitoring approach for long-term radon fluxes in order to evaluate long-term radon barrier performance?

5.2 Radon Decay and Progeny

Radon-222 (half-life = 3.8 days) is generated by alpha decay of Ra-226 (half-life = 1622 years). This radionuclide is typically left in uranium mill tailings after processing and is discarded with the tailings. As a result, Rn-222 is constantly generated at the disposal site. Rn-222 is a gas but its' progeny are not; they rapidly become associated with solids in the local (within

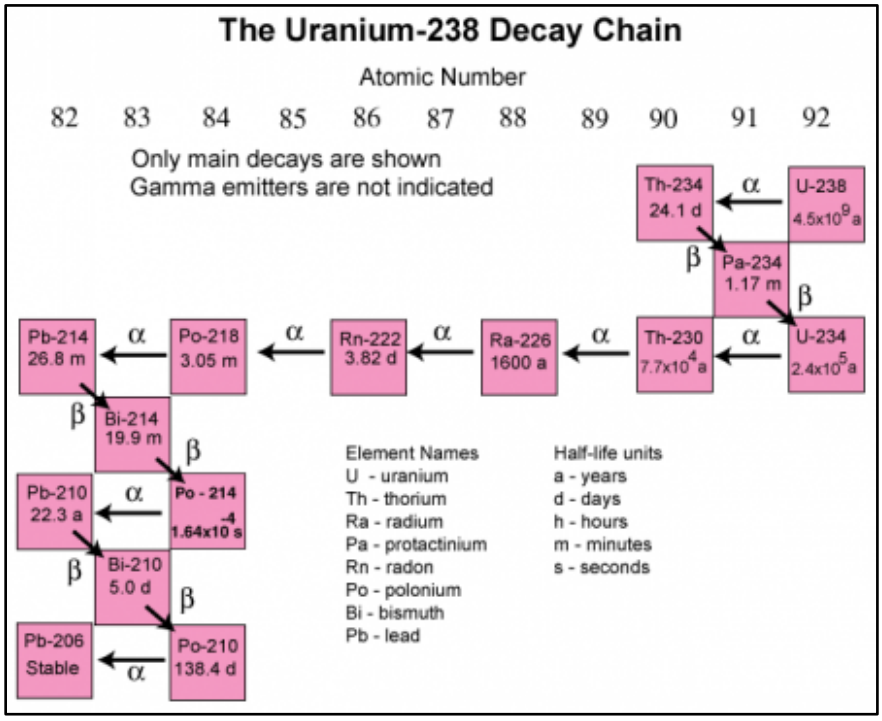

Figure 5-1 Decay chain for U-238 (U.S. EPA)

micrometers) environment and are expected to be relatively immobile. Rn-222 decays through a chain (Figure 5-1) of four short-lived radionuclides (Po-218, Pb-214, Bi-214 and Po-214) before Pb-210 is generated by alpha decay of Po-214, within several hours of the original Rn-222 decay. The beta decaying Pb-210 (half-life = 22.2 years) accumulates as Rn-222 decays, providing a long-term indication of where in the radon barrier Rn-222 decayed and quantifies the activity of Rn-222 that decayed over many years at various depths within the barrier. With steady state Rn-222 fluxes from the tailings, as assumed here, Pb-210 activity within the barrier will increase until it is in equilibrium with Rn-222 activity after about 250 years (about 11 half-lives of Pb-210) [Friedlander et al. 1981].

5.3 Methods

Field measurements and sampling were conducted at four uranium mill tailings disposal sites: Falls City in Texas, Bluewater in New Mexico, Shirley Basin South in Wyoming, and Lakeview in Oregon. Each of these covers has been in service for about 20 years. Descriptions of the sites, their cover designs, climate, and test pit locations are provided in Chapter 2. Between 5 and 9 test pits were excavated at each site. As discussed in Chapter 4, test pit locations were deliberately biased by selecting locations or conditions likely to result in higher Rn fluxes, including areas of higher as- built Rn fluxes, higher Ra-226 content of the underlying waste, and areas with notable intrusion of large plants. Overburden and protective layers above the Rn barrier were removed by backhoe and a set of Rn flux measurements (as many as 8 at each pit) were taken from the barrier surface using accumulation chambers and a Rad7 (Durridge Company, Billerica MA) radon detector [Stefani 2016, Michaud 2018]. Measurement of Rn-222 fluxes and concentrations are described in Chapter 4 of this report. Samples of barrier material were taken at discrete depths within the barrier as it was excavated down to near the tailings. Barrier material was then removed by hand to expose the tailings where possible and a Rn flux measurement was made at the top of the waste.

For Pb-210 analysis, samples of barrier material were taken at the top of the Rn barrier, near the bottom of the barrier (as close as practical to the tailings), and then at a number of points in between at depths measured from the waste surface. In some cases, samples were also obtained from Shelby tube cores pushed from the barrier surface, but they did not always reach the bottom of the barrier. Each sample represents a thickness of 2-3 cm. In-situ measurements and a variety of samples were taken for an array of analysis, including moisture content, bulk density, saturated hydraulic conductivity, and root intrusion. Site descriptions and photographs can be found in Chapter 2 of this report and in Fuhrmann et al. 2019. Chapter 6 provides analysis of soil properties with detailed descriptions of cover cross-sections.

Samples of the barrier material for analysis of Pb-210 were sent to Eberline Services, Oak Ridge Tennessee. For samples reported here, Pb-210 was analyzed using an organic extraction technique for bismuth which was then precipitated with a selective buffered water pH adjustment, filtered, dried, and weighed. Samples were held for 10 hours to allow for decay of Bi-214, Bi-212, and Bi-211. They were then beta counted for Bi-210 on gas proportional detectors using a Tennelec LB-4100 system. Count times were two hours providing a Minimum Detectable Activity (MDA) of about 0.023 Bq/g. Ra-226 was analyzed using a modified EPA 903.0 method with an MDA of about 0.009 Bq/g. This radionuclide, the parent of Rn-222, was measured in some samples to estimate background Rn-222 fluxes from the barrier material itself. To obtain background concentrations, measurements of Pb-210 were also made on samples of barrier material taken away from the disposal area.

Modeling of Rn transport was done with RAECOM [Rogers et al. 1984, U.S. NRC 1989]. This is a 1-D model that calculates the Rn flux based on diffusive transport in the porous barrier medium based on a model by Nielson and Rogers, 1981. RAECOM can calculate Rn flux and concentration from the waste, as well as the Rn flux and steady state concentration within specified depths in the barrier and at its top surface. The diffusion coefficient is estimated by RAECOM based on bulk dry density and moisture content of the barrier using a correlation function derived from laboratory studies [Rogers and Nielson 1991], or can be calculated with measured Rn fluxes from the top and bottom of the barrier. This is the method used in this work and is discussed in detail in section 4.6. Partitioning of Rn between the aqueous and gaseous phases in the pore space is accounted for and it is assumed that Rn transport is by gaseous diffusion and that rates are steady state.

Based on measured Rn fluxes and calculations with RAECOM, the Pb-210 content at different locations within the barrier were calculated with a spreadsheet model that converts Rn flux to Pb-210 concentration. This model accounts for build-up of Pb-210 according to the age of the barrier. Ideally the concentration of Pb-210 measured in the barrier is proportional to the quantity of Rn-222 that decayed in that location over the age of the barrier.

Sorption studies indicate that the Pb is well retained on soil grains [U.S. EPA 1999]. Pb is highly particle reactive; the distribution coefficient (K_d) for Pb on a variety of earth materials typically is in the thousands (see for example [Sheppard et al. 2009]). Polonium too sorbs well [Vandenhove et a. 2009, Maity et al. 2011]. Lead's predecessors, Po-218, Pb-214, Bi-214, and possibly even the very short-lived Po-214 associate with solids when they are formed. This discussion ignores effects of alpha recoil but overall, any transport of Pb-210 in radon barriers is expected to be minimal on the scale of interest in this project.

5.4 Results

Schematics, showing cover construction and location of samples for Pb-210, and photographs of cross-sections of the covers are shown for each pit. Depth profiles of Pb-210 concentrations and moisture saturation are shown for each pit within the radon barrier itself, not the entire cover. Depths are measured from the bottom of the barrier (top of the waste). Also shown are the Minimum Detected Activity (MDA) and concentration of background Pb-210. The error bar on each Pb-210 data point is the 2-sigma Combined Standard Uncertainty as reported by the laboratory. The background Pb-210 activities were determined directly from samples of barrier material from either the borrow area from which the cover material was originally obtained or from storage yards located away from the disposal cell. Both methods give very similar results. Under each Pb-210 graph is the average of the Rn fluxes measured at the top of the barrier and the flux measured at the bottom of the radon barrier. The attenuation factor is the bottom flux divided by the top flux and provides an indication of how effectively the barrier is functioning at that location. Higher attenuation factors mean that more Rn is retained in the barrier. For each site a bar graph provides Rn fluxes from the top of the Rn barrier for the pits at which Pb-210 measurements were made. These figures also show background Rn flux as well as the average of the flux measurements made at the time of cell closure; the as-built values. Tables for each test site provide depths, concentrations of Pb-210 and background subtracted Pb-210 along with the 2-sigma Combined Standard Uncertainty as reported by the laboratory. Measured Rn-222 fluxes from the top surface and the bottom of the Rn barrier (the top of the waste) are also provided.

5.4.1 Falls City

Figures 5-2 and 5-3 show the top deck of the disposal cell consists of about 20 cm of topsoil, approximately 80 cm of rooting medium, and then about 91 cm of radon barrier. This site contains 4.72×10^{13} Bq (1277 Ci) of Ra-226. The top deck is vegetated and is planted with a cultivar of yellow bluestem (*Bothriochloa ischaemum var. songarica*) which is harvested and used as animal feed. Many other species of plants are present, notably Honey Mesquite. The rooting medium and the Rn barrier are the same material taken from a local borrow area, but the Rn barrier was compacted to meet requirements. This is apparent by the different textures visible in the photos in Figures 5-2 and 5-3. On the rock covered side slope of the cell (Pit 6), Figure 5-4, the uppermost material was about 60 cm of rip-rap underlain by 15 cm of sandy

bedding material. Below that was about 61 cm of radon barrier. Samples for Pb-210 analysis were taken from several depths in Shelby tubes.

Pb-210 profiles for Pits 2, 3 and 6 are shown in Figures 5-2, 5-3 and 5-4, respectively. Note that the MDA's for Pits 2 and 6 are higher than Pit 3. These were the first samples analyzed and a method with a relatively high MDA was used on samples from those two pits. All subsequent analysis was conducted with the more sensitive protocol given in the Methods section. Data for this site are shown in Table 5-1. Test Pit 2 was located on an area of grass while Pit 3 was nearby but centered on a large mesquite plant. Both test Pits 2 and 3 had Pb-210 concentrations that were relatively high at the top of the barrier indicating that over long times Rn had been present at elevated concentrations in the upper portion of the barrier. The radon attenuation factors for these locations are about 7 and 9, low numbers that indicate transport of Rn. Similarly, Figure 5-5 shows that Rn fluxes measured at the top of the radon barrier at these two pits are well above background. In contrast, top fluxes from Pit 6 are very low, essentially background, agreeing well with the low concentrations of Pb-210 in Figure 5-4. The top two samples are indistinguishable from the MDA but because of the high MDA it is not certain if they are greater than background. The attenuation factor for the side slope location was greater than 3000 showing that the barrier here was quite effective. The bottom flux at this location was 42.5 $Bq/m^2/s$ which was higher than anywhere else at this site. In addition, the thickness of the barrier on the side slope location was less than on the top deck. Nevertheless, Rn was well retained by the barrier in Pit 6.

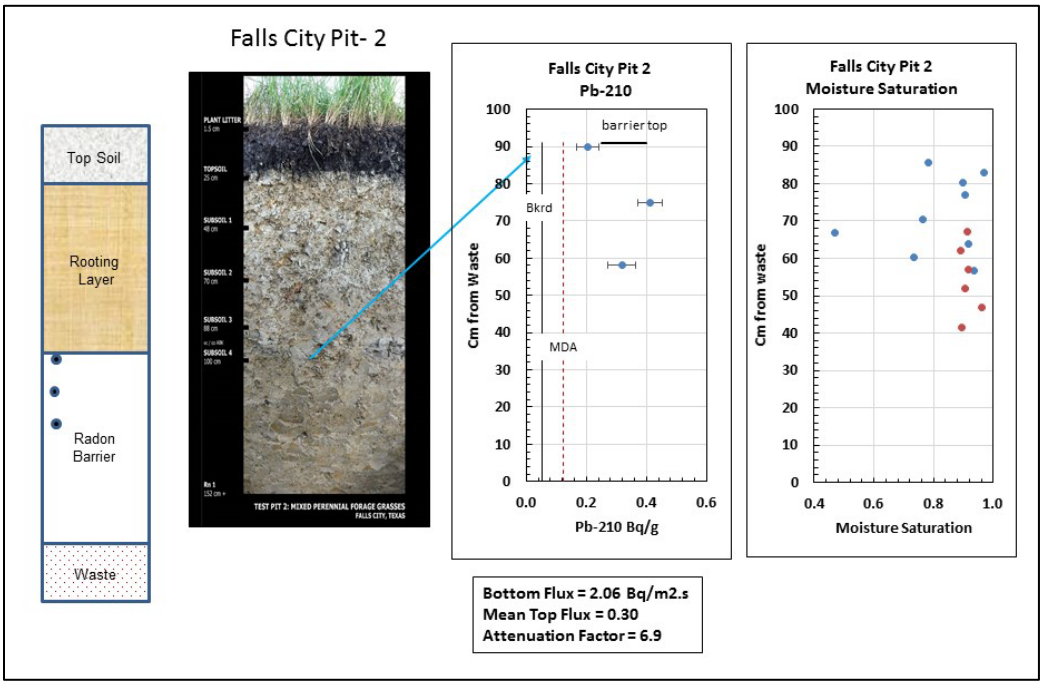

Figure 5-2 Pb-210 Sample Locations (Circles) and Concentrations within the Rn Barrier at Pit 2 at Falls City This location was grass covered. Moisture saturation data are taken from two Shelby tubes (the blue and red circles) within 20 cm of each other. The MDA (dotted) and background Pb-210 (solid line) are shown.

Table 5-1 Falls City Samples

Sample ID	Distance from Tailings	Measured Pb-210	2 Sigma error	Background Subtracted Pb-210	Measured Rn Flux Barrier Top	Note
	cm	Bq/g	Bq/g	Bq/g	Bq/m^2/s	
Pit 2A a	90	0.205	0.074	0.151	0.30	Barrier Top
Pit 2A f	75	0.411	0.084	0.357		Pb-210 MDA=0.123
Pit 2A k	58	0.317	0.092	0.263		
Pit 3A 1	84	0.148	0.028	0.094	0.60	Near Barrier Top
Pit 3A 5	69	0.121	0.032	0.067		Pb-210 MDA=0.028
Pit 3A 9	56	0.084	0.024	0.030		
Pit 6A a	59	0.107*	0.106	0.053	0.013	Barrier Top
Pit 6A f	43	0.138	0.092	0.084		Pb-210 MDA=0.123
Pit 6A g	40	0.173	0.080	0.119		Max Bkrd = 0.054 calculated from Ra-226 activity

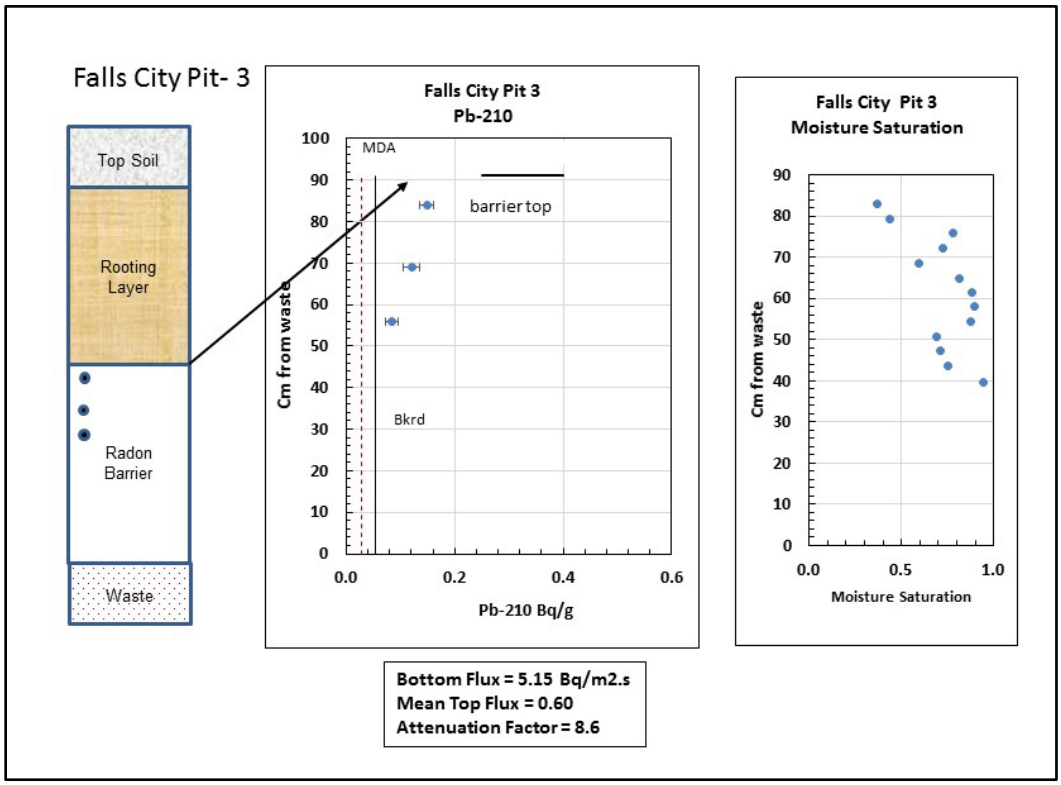

Figure 5-3 Pb-210 Sample Locations (Circles) and Concentrations Within the Rn Barrier at Pit 3 at Falls City This pit was centered on a large mesquite plant. The MDA (dotted) and background Pb-210 (solid line) are shown. No Photo of the Pit 3 profile is available, but it closely resembled pit 2.

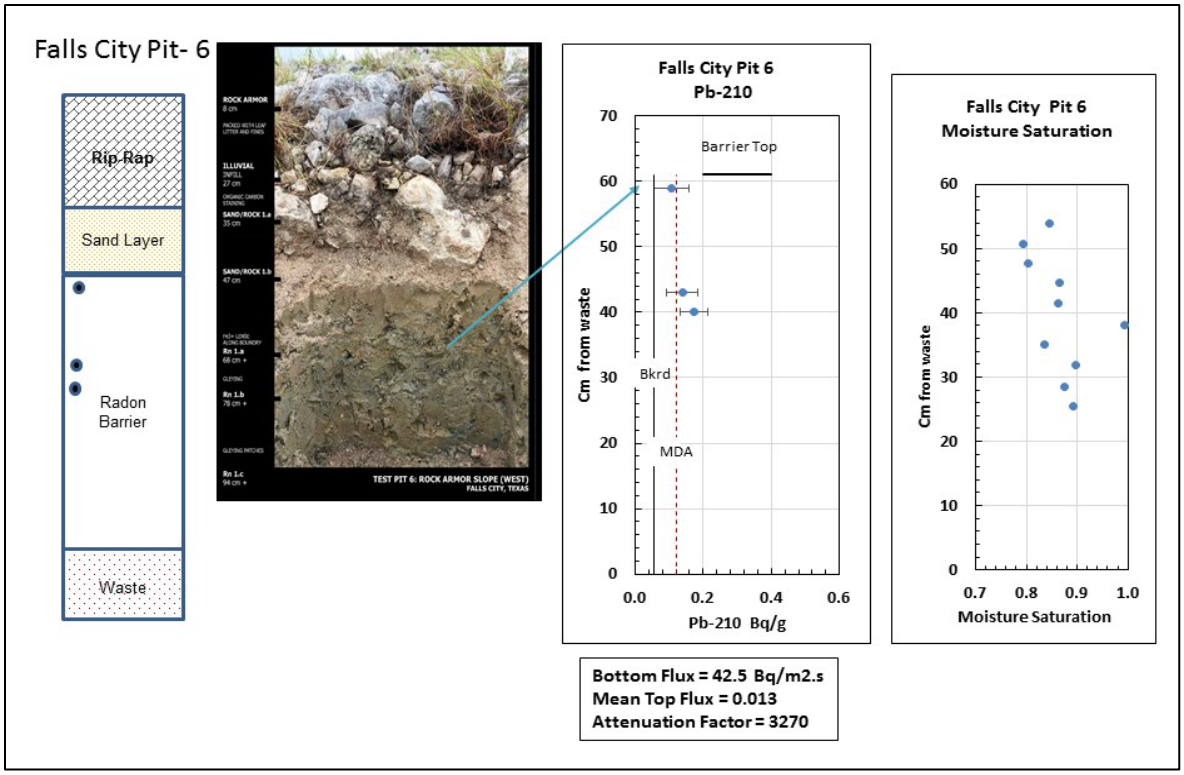

Figure 5-4 Pb-210 Sample Locations (Circles) and Concentrations Within the Rn Barrier at Pit 6 at Falls City The MDA (dotted) and background Pb-210 (solid line) are shown.

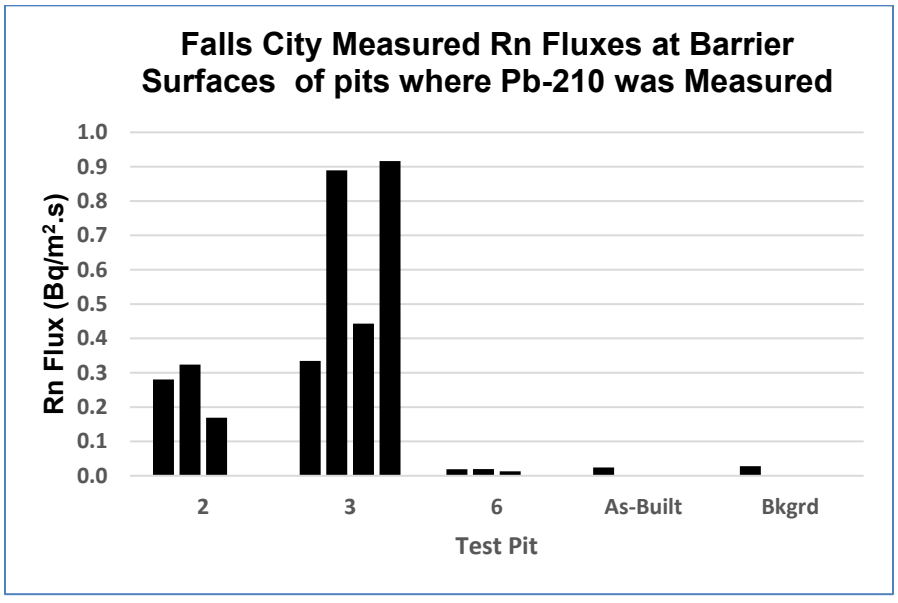

Figure 5-5 Rn Fluxes Measured on the Top of the Rn Barrier at Falls City, for Pits Where Pb-210 Samples Were Taken

5.4.2 Bluewater

The cover design at the Bluewater site varied depending on the type of waste buried. There are several disposal cells. The Pb-210 analysis was conducted on material from two locations on the main disposal cell, test Pits 4 and 5, where the cover consisted of a rip-rap upper layer that was 6-14 cm thick. Beneath that the Rn barrier was 64-71 cm thick. This disposal cell contains 4.14×10^{14} Bq (11,200 Ci) of Ra-226. While this site is covered with rock there are many areas that have become vegetated. Background Pb-210 was 0.030 ± 0.012 Bq/g which was determined from two samples from the source area of the cover material. Profiles of Pb-210 are shown in Figures 5-6 and 5-7, Rn fluxes are provided in Figure 5-8, and the data are presented in Table 5-2.

Profiles of both pits are similar; they show no Pb-210 above the background of 0.042 Bq/g except for the lowermost sample at each pit (9 and 12 cm above the bottom of the barrier) which are significantly greater than background. The similarity of Pb-210 profiles in these two locations is surprising because Pit 5, which was located at a large fourwing saltbush (*Atriplex canecens*), has low moisture saturation, a high top flux, and low attenuation factor indicating that Rn moved readily through the barrier at this spot. In contrast, Pit 4 was an unvegetated "control" with high moisture saturation in the lower part of the barrier, very low top flux, a high bottom flux and therefore a high attenuation factor indicating the barrier here is quite effective. The contrast in moisture content, as a result of the saltbush, is dramatic. The fraction of moisture saturation for both pits shows that Pit 5 has a consistently low fraction of saturation while the lower part of Pit 4 is very close to saturated. The Rn fluxes in Figure 5-4 reflect the difference in moisture saturation but the Pb-210 profiles of the two pits are very similar and do not conform to the moisture profiles. These profiles are considered further in the Section 5.5.2.

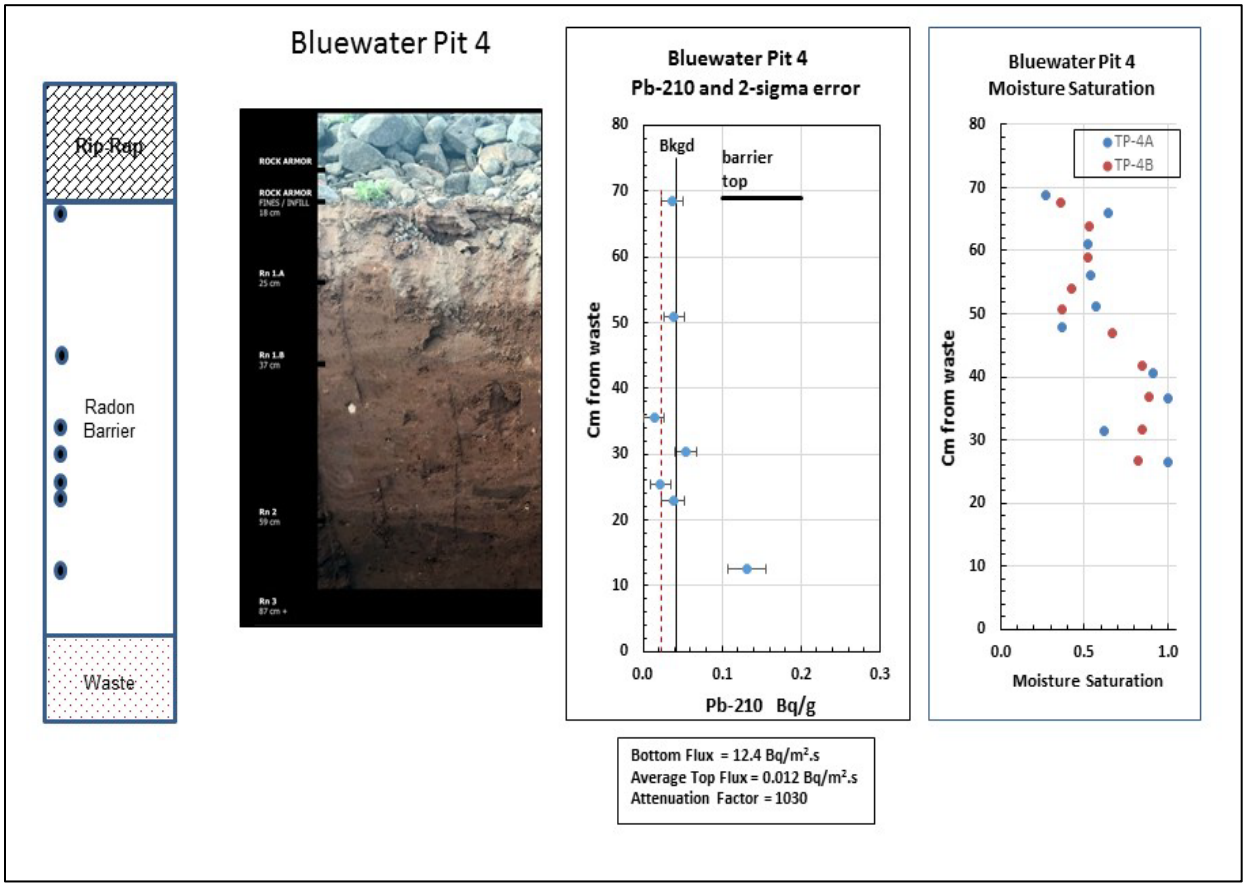

Figure 5-6 Pb-210 Sample Locations (Circles) and Concentrations ithin the Rn Barrier at Pit 4 at Bluewater
The MDA (dotted) and background Pb-210 (solid line) are shown. Moisture saturation data are taken from two Shelby tubes (the red and blue circles).

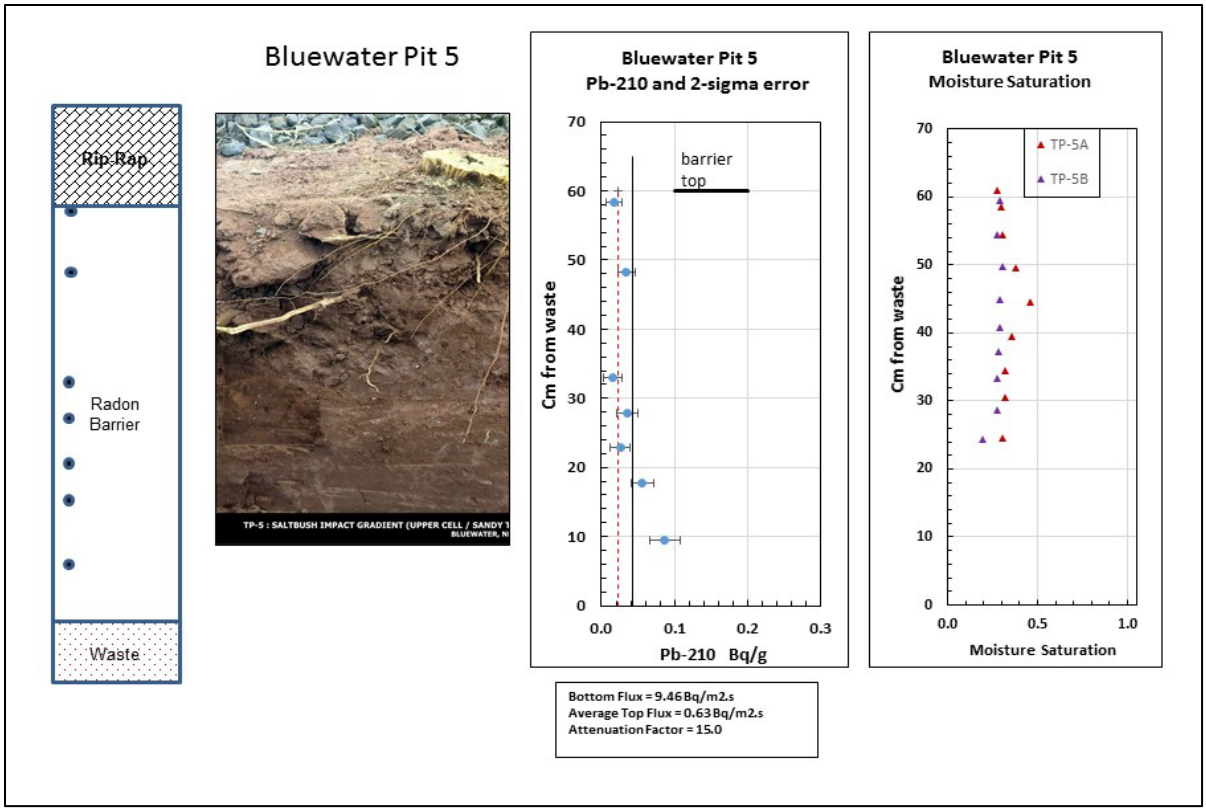

Figure 5-7 Pb-210 Sample Locations (Circles) and Concentrations Within the Rn Barrier at Pit 5 at Bluewater This pit was centered on a large fourwing saltbush (note the stump in the top right of the photograph). The MDA (dotted) and background Pb-210 (solid line) are shown. Moisture saturation data are taken from two Shelby tubes (the red and blue circles).

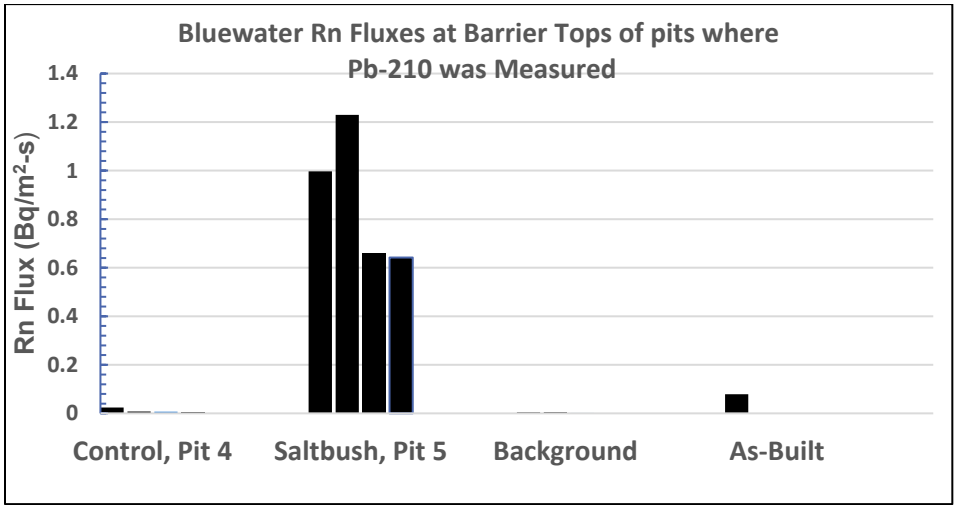

Figure 5-8 Rn Fluxes from the Top of the Rn Barrier at Bluewater The 3 Background Fluxes Are All Below 0.005 Bq/m^2/s

Table 5-2 Bluewater Samples

Sample ID	Distance from Tailings	Measured Pb-210	2 Sigma error	Background subtracted Pb-210	Measured Rn Flux Barrier Top	Note
	Cm	Bq/g	Bq/g	Bq/g	Bq/m^2/s	Pb-210 MDA = 0.024
Pit 4 A	69	0.037	0.014	-0.005	0.012	Barrier Top
Pit 4 B	51	0.039	0.013	-0.003		
Pit 4 C	36	0.014	0.013	-0.028		
Pit 4 D	31	0.054	0.014	0.012		
Pit 4 E	25	0.022	0.012	-0.022		
Pit 4 F	23	0.038	0.015	-0.004		
Pit 4 G	13	0.131	0.024	0.089	12.4	Near tailings
Pit 5 A	58	0.017	0.012	-0.025	0.63	Barrier Top
Pit 5 B	48	0.034	0.013	-0.008		
Pit 5 C	33	0.015	0.013	-0.027		
Pit 5 D	28	0.036	0.015	-0.006		
Pit 5 E	23	0.025	0.014	-0.017		
Pit 5 F	18	0.056	0.015	0.014		
Pit 5 G	9	0.087	0.020	0.045	9.46	Near Tailings
Analogue A		0.007	0.026	---		15 cm depth
Analogue B		0.030	0.024	---		Bkrd = 0.030 ± 0.012 122 cm depth

5.4.3 Shirley Basin South

The Shirley Basin South (SBS) cover is comprised of a vegetated upper soil layer approximately 20 cm thick, a rooting soil about 70 – 80 cm thick, and then a clay radon barrier 56 – 69 cm thick at our test pits. In some areas the cover is sloped and has a top layer of rip-rap underlain by about 46 cm of Rn barrier. The cover was built over a series of tailings ponds and the bottom of the radon barrier layer is in contact with relatively high activity sand size light gray tailings, allowing visual identification of the waste.

Results of Pb-210 analysis for SBS samples are given in Table 5-3. In all cases at SBS, including background samples, Pb-210 measurements were substantially above the MDA. Pb-210 was measured in the Clay-1 sample taken from an old storage area for the barrier clay and was found to be 0.129 ± 0.012 Bq/g. Concentrations of Pb-210 at the surface of the radon barrier (the A samples in Table 5-3) consistently had similar or slightly lower concentrations than the Clay-1 background sample and can be taken as background as well. We have defined background as the average of these 5 samples at 0.123 ±0.012 Bq/g.

Figures 5-9 through 5-12 show Pb-210 values ranged from 0.11 to 0.46 Bq/g with highest concentrations at deepest parts of the barrier and lower concentrations with increasing distance above the waste. Background is shown as a line at 0.123 Bq/g and MDA is also indicated. Figure 5-13 gives radon fluxes measured at the top of each pit.

In Figure 5-9, the Pb-210 concentration in Pit-2 increased from 0.23 Bq/g at the lowermost sample to 0.285 at 14 cm from the bottom. This is the highest concentration in this profile and corresponds the beginning of an area of high moisture content. Pb-210 then decreased to 0.17 Bq/g at 19 cm. The concentrations at 19 cm and 43 cm are slightly above background. This suggests that while much of the Rn-222 is retained below about 20 cm from the bottom of the barrier, some is transported higher (to at least 43 cm from the bottom). Eight flux measurements were made at the top of the barrier, averaging 0.057 Bq/m^2/s. All but one measurement was substantially above the background flux of 0.01 Bq/m^2/s. Pb-210 is at background at the top surface of the barrier.

Figure 5-10 shows the Pb-210 profile in Pit-3. The bottom-most sample is the highest concentration and Pb-210 decreases to background at 25 cm from the bottom. The samples at 25, 38 and 64 cm (the top) are essentially the same concentration and indistinguishable from background. At this location Rn-222 is effectively retained in the barrier below 25 cm from the bottom. Eight top flux measurements were made at this cell, and all were at (or below) background, while the two Rn flux measurements at the bottom of the pit were very high at 312 and 428 Bq/m^2/s.

The Pb-210 profile for Pit 5 (Figure 5-11) shows elevated Pb-210 values in the two lowermost samples. Concentrations become background at 15 cm from the bottom of the excavation. The tailings were not reached at this location (this location may have been a berm between tailings ponds) so the measured bottom flux of 0.244 Bq/m^2/s is quite low, showing that Pb-210 profiles can be discerned even when fluxes are low. The average top flux is essentially background. Figure 5-12 shows the Pb-210 profile for Pit 6 which was on a rock covered side slope. Pb-210 increases to a maximum activity at 5 cm above the tailings, it then decreases at 10 cm, remaining constant at about 0.2 Bq/g to 28 cm above the tailings. These three samples are higher than the average background of 0.123 Bq/g (or the 0.117 Bq/g that was measured at the surface of the Rn barrier at this cell). The two top flux measurements at this location were both high, averaging 0.13 Bq/m^2/s, while the bottom flux was relatively high at 69.9 Bq/m^2/s.

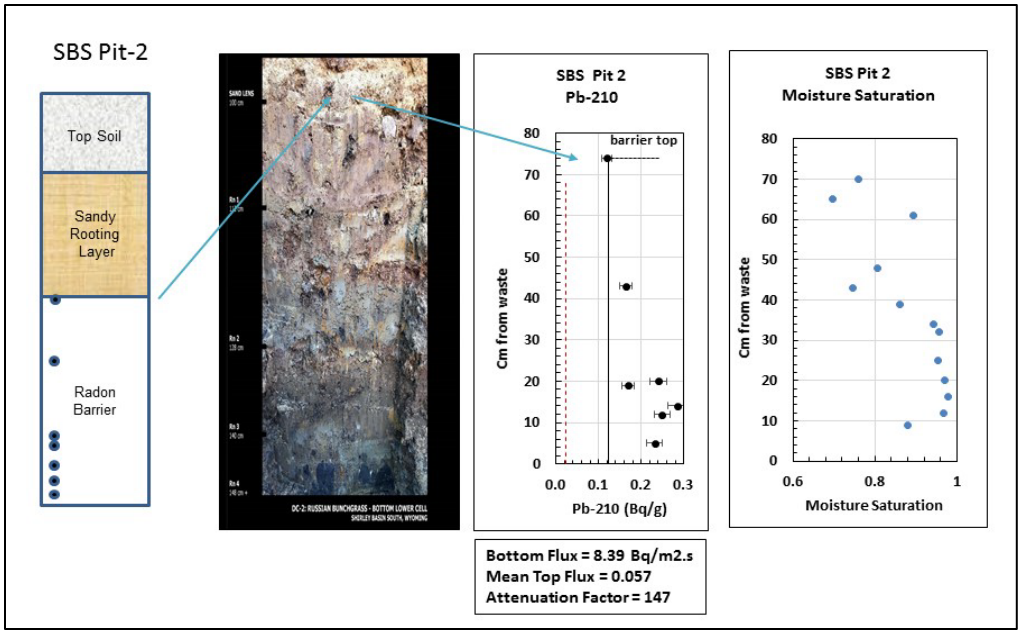

Figure 5-9 Pb-210 Sample Locations (Circles) and Concentrations Within the Rn Barrier at Pit 2 at Shirley Basin South The MDA (dotted) and background Pb-210 (solid line) are shown.

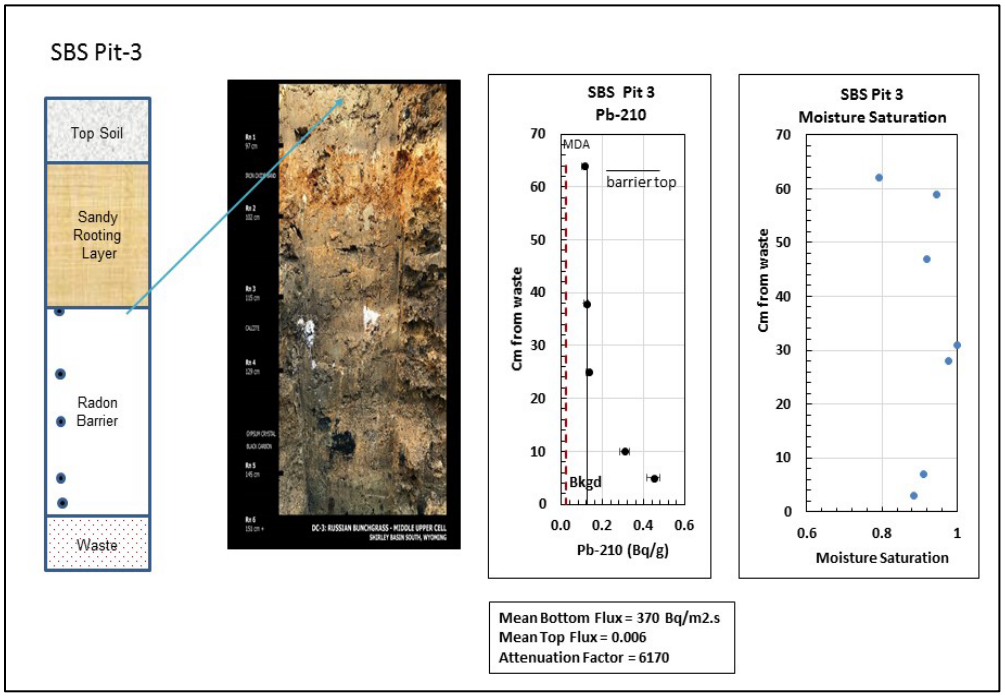

Figure 5-10 Pb-210 Sample Locations (Circles) and Concentrations Within the Rn Barrier at Pit 3 at Shirley Basin South The MDA (dotted) and background Pb-210 (solid line) are shown.

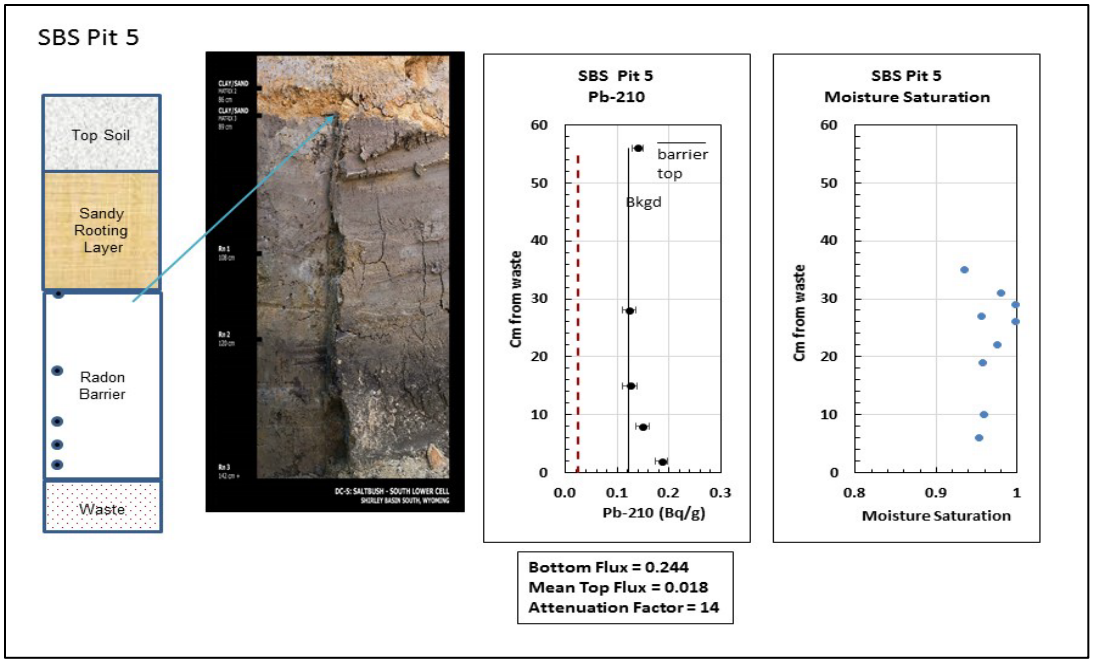

Figure 5-11 Pb-210 Sample Locations (Circles) and Concentrations Within the Rn Barrier at Pit 5 at Shirley Basin South The MDA (dotted) and background Pb-210 (solid line) are shown.

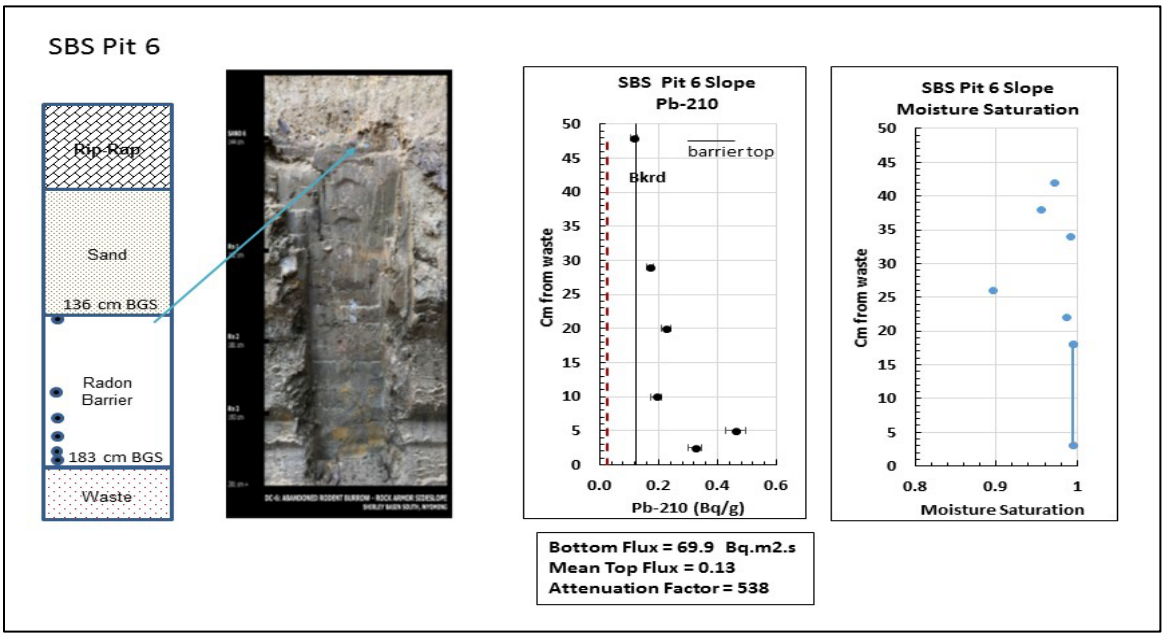

Figure 5-12 Pb-210 Sample Locations (Circles) and Concentrations Within the Rn Barrier at Pit 6 at a Rip-Rap Covered Slope at Shirley Basin South The MDA (dotted) and background Pb-210 (solid line) are shown. The lowest moisture saturation point was taken from a large block sample.

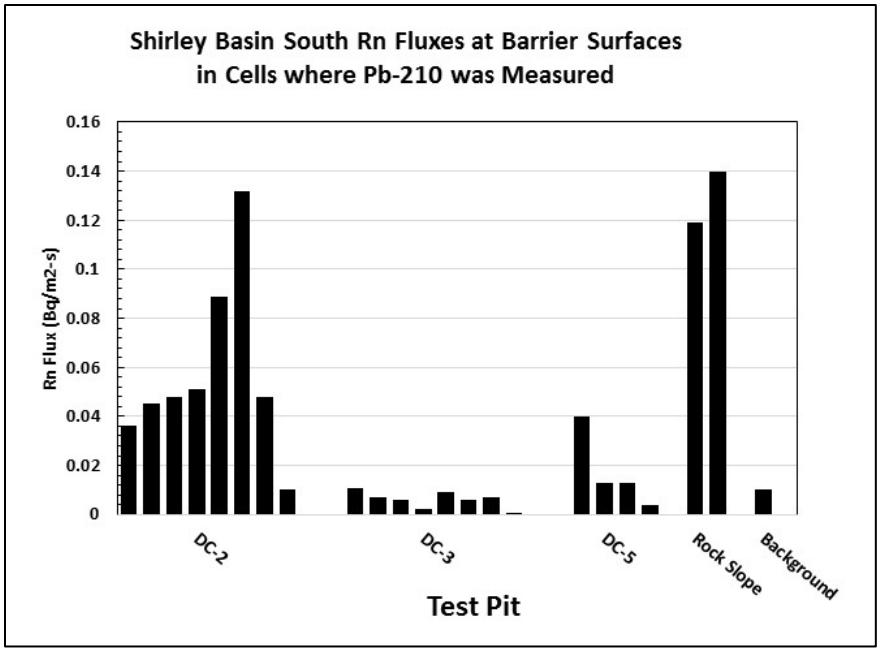

Figure 5-13 Radon Fluxes Measured at the Top of the Radon Barrier at Pits Where Pb-210 Was Measured

5.4.4 Lakeview

According to construction plans, the cover at Lakeview is composed of a 45 cm thick radon barrier, a 15 cm thick sand layer and, on the top deck, a 45 cm rock/soil layer. On the steeper side slope the top layer is a 30 cm rip-rap layer. The radionuclide content of this site is especially low, about 1.6 x 10^{12} Bq (42 Ci) of Ra-226, and radon fluxes are correspondingly low. Pb-210 analysis was done on samples from Pit 12 which has the highest radon fluxes from the bottom of the barrier. At this location the radon barrier was found to be a little thicker than plans indicate. It was also the location of a large rubber rabbitbrush (*Ericameria nauseosa*).
The Pb-210 profile for Pit 12 at Lakeview is shown in Figure 5-14. Background Pb-210 was 0.029 Bq/g. The lowermost sample has the highest Pb-210 activity while the other three samples within 20 cm from the bottom of the barrier are slightly above background. The two samples at 30 and 52 cm above the waste are at background for Pb-210; no excess Pb-210 is present in the upper portion of the barrier. This indicates that no Rn reached the upper parts of the barrier. Therefore Rn-222 fluxes from the top of the barrier should be very low. Data in Table 5-4 confirm that the top Rn fluxes from this pit are essentially background. Even with the low bottom flux of 0.37 Bq/m^2/s, a clear signal of excess Pb-210 at the lower portion of the barrier was observed.

Table 5-3 Shirley Basin South Samples

Sample ID	Distance from Tailings	Measured Pb-210	2 Sigma error	Background subtracted Pb-210	Measured Rn Flux	Note
	Cm	Bq/g	Bq/g	Bq/g	$Bq/m^2/s$	
Pit 2 A	69	0.119	0.023	-0.004	0.010 – 0.132	Barrier Top
2 B	38	0.164	0.028	0.041		
2 C	15	0.170	0.030	0.047		
2 D	14	0.240	0.037	0.117		
2 E	9	0.285	0.043	0.162		
2 F	6	0.249	0.038	0.126		
2 G	3	0.231	0.036	0.108	8.39	Just above tailings
3 A	64	0.110	0.023	-0.013	0.0001 – 0.011	Barrier Top
3 B	38	0.121	0.022	-0.002		
3 C	25	0.131	0.023	0.008		
3 D	10	0.309	0.046	0.186		
3 E	5	0.448	0.063	0.325	312, 428	Just above tailings
5 A	56	0.139	0.020	0.016	0.004 – 0.04	Barrier Top
5 B	28	0.123	0.023	0.000		
5 C	15	0.125	0.028	0.002		
5 D	8	0.149	0.025	0.026		
5 E	2	0.186	0.023	0.063	0.244	No tailing observed
6 A	48	0.117	0.021	-0.006	0.119 – 0.140	Barrier Top
6 B	29	0.172	0.024	0.049		
6 C	20	0.225	0.029	0.102		
6 D	10	0.192	0.036	0.069		
6 E	5	0.460	0.067	0.337		
6 F	2.5	0.323	0.048	0.200	69.9	Just above tailings
Clay 1		0.129	0.025		---	Old Clay Storage Pile

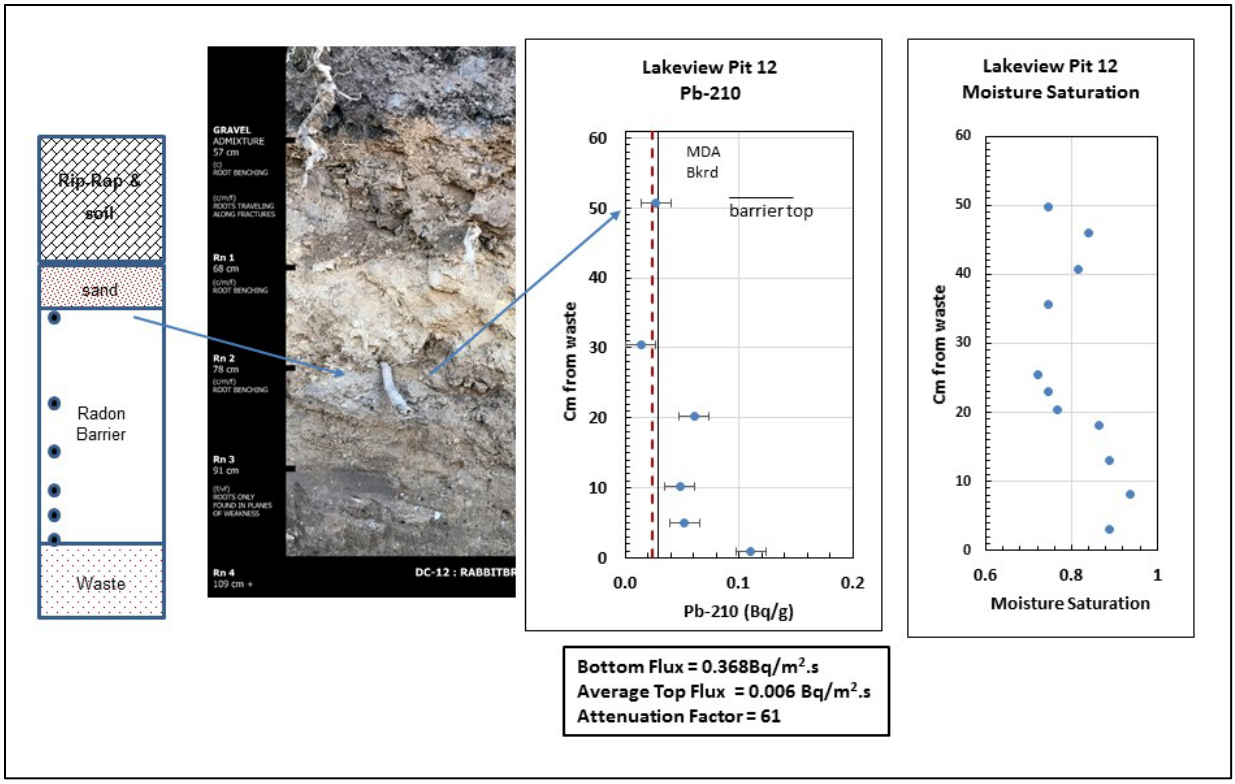

Figure 5-14 Pb-210 Sample Locations (Circles) and Concentrations Within the Rn Barrier at Pit 12 at Lakeview The MDA (dotted) and background Pb-210 (solid line) are shown.

Table 5-4 Lakeview Samples

Sample ID	Distance from Tailings	Measured Pb-210	2 Sigma error	Background subtracted Pb-210	Measured Rn Flux Barrier Top	Note
	Cm	Bq/g	Bq/g	Bq/g	Bq/m^2/s	Pb-210 MDA = 0.024
Pit 12 F	51	0.027	0.026	-0.002	0.006	Barrier Top
Pit 12 E	30	0.014	0.024	-0.015		
Pit 12 D	20	0.060	0.032	0.031		
Pit 12 C	10	0.048	0.028	0.019		
Pit 12 B	5	0.052	0.034	0.023		
Pit 12 A	0	0.110	0.044	0.081	0.368	Just above tailings
Analogue A		0.012	0.026	---		61 cm depth
Analogue B		0.046	0.028	---		mean Bkrd = 0.029 91 cm depth

5.5 Discussion

Designs of radon barriers were based on models of diffusion through a porous medium that is regulated by moisture content [Rogers et al. 1984]. However, long-term data were not available to provide any insight on how the properties of those barriers may change over time. In this project, we have examined radon fluxes from the surfaces of radon barriers of sites that have been in service for about 20 years. Our measurements indicate that all sites we visited meet the regulatory requirement for radon flux. However, at some sites, a few fluxes were measured that substantially exceed any measured during the radon surveys performed directly after completion of the radon barriers. As discussed in Chapter 4 of this report, the locations of these higher fluxes are generally associated with impacts such as the presence of large plants, ant colonies, and emergent soil structure. How extensively and at what rate these local impacts can expand to the whole site is poorly understood, but likely is site and species specific. At some sites, more general processes such as freeze thaw and desiccation cracking will slowly impact the site as a whole. As a result, there is interest in better defining radon transport in these barriers, so that long-term trends can be determined. While diffusion will generally be the dominant transport process, changes in porosity and moisture saturation will impact the diffusion coefficient and this may be depth and location specific. Superimposed on that variability is the likely seasonal and annual variability of moisture content. Development of preferential pathways must be considered as well.

Initially it was not clear if Pb-210 could be measured in the radon barriers and if the data would provide useful profiles. Results from Falls City, the first site, showed that Pb-210 could be measured and was elevated above background in the upper portions of the barrier. The samples for Pb-210 were obtained from Shelby tubes that did not extend to lower portions of the barrier. As a result, detailed profiles for this site were not obtained. Nevertheless, results in Figure 5-2 shows that measurements can be obtained with standard commercial methods for Pb-210 analysis. With more detailed sampling, in many cases the profiles contain systematic trends in Pb-210 values that are above background (see the profiles in Figure 5-5 for example). Once background Pb-210 is established, any measurements of Pb-210 within the barrier in excess of that background can be taken to have been generated by Rn-222 coming from the tailings at the bottom of the barrier. The Pb-210 profile develops as Rn-222 decays at that depth. Because the half-life of Rn-222 is only 3.8 days, there should be a profile with a general trend of higher Pb-210 at depth. The shape of the profile indicates transport rates and possibly materials properties that alter the rate or process. If the original assumptions about simple diffusive transport within the barrier are true, the Pb-210 profile should correspond to radon fluxes (or steady state concentrations), and this can be tested against diffusion models of radon. This being the case, there should be a systematic curve decreasing toward background as the surface of the barrier is approached.

Activities of Pb-210 were measurable in all sampled pits, including one where the bottom flux was quite low (Shirley Basin South, Pit 5 at 0.244 $Bq/m^2/s$) and in another where the bottom flux was extremely high (Shirley Basin South, Pit 3, average of 370 $Bq/m^2/s$). In locations where samples were obtained near the bottom of the radon barrier, all showed higher Pb-210 activities near the bottom and then activities decreased toward the top of the barrier. In many cases (e.g., SBS Pits 3 and 5, and Bluewater Pits 4 and 5) a number of Pb-210 concentrations fall within the 2-sigma analytical error of background, confirming that background tends to be quite consistent at these sites.

5.5.1 Modeling

Figure 5-15 shows the measured Pb-210 profile for Pit 3 at the Shirley Basin South site (refer also to Figure 5-10) as well as Pb-210 calculated from a modeled diffusion curve based on measured radon fluxes and concentrations at that pit. The radon diffusion model was run as a two-layer model in RAECOM, with a source layer and a barrier layer. The barrier layer itself had 6 layers which were set closer together at the bottom of the barrier to better define Pb-210 concentrations where they change most rapidly. Inputs to RAECOM included the measured Rn concentration at the top of the waste as 3.71×10^{6} Bq/m^3 which was adjusted to allow for Rn partitioning between the gas and water phases. The diffusion coefficient was calculated to be 1×10^{-8} m^2/s with a barrier thickness of 0.65 m. This diffusion coefficient was determined by iteration to give a Rn flux at the top of the barrier that matched the flux measured in the field (which in this case was background). The model provided Rn fluxes and steady state Rn concentrations for each of the 6 layers. These were then converted to Pb-210 concentrations and corrected for radioactive ingrowth of Pb-210 from the modeled Rn concentration which was assumed to be steady state over the 17-year life of the barrier. A similar approach was taken for data from other locations.

There is good agreement, shown in Figure 5-15, between the model and measured Pb-210 concentrations, supporting the assumption used in the barrier design of diffusive transport. Both the measured and modeled Pb-210 show that all Rn from the waste decays away by the time it reaches 40 cm above the waste. This is also confirmed by measured Rn flux at the top of the barrier, which is essentially background. Incorporating the age of the barrier in the conversion of Rn flux to Pb-210 concentration is important as the Pb-210 activity will increase for several hundred years. Using barrier ages that are incorrect by even ten years makes a noticeable difference in the calculated Pb-210 profile.

This pit (SBS, Pit 3) had a very high Rn flux from the waste (370 Bq/m^2/s) and all of it was retained in the barrier, giving an attenuation factor greater than 6100. Profiles of Pb-210 at several other locations, such as Pit 5 at Shirley Basin South and Pit 12 at Lakeview also fit the diffusive transport model. These two locations are notable because the bottom flux at each site was very low but excess Pb-210 could be observed. Figure 5-16 shows measured Pb-210 from Lakeview with a diffusion model based on measured top and bottom fluxes providing a diffusion coefficient of 6.5×10^{-8} m^2/s. Several others, such as the two pits at Bluewater Fig. 5-6 and 5-7, are inconclusive as they each have one point with excess Pb-210 at the bottom of the profile. These are discussed later in Section 5.5.1.

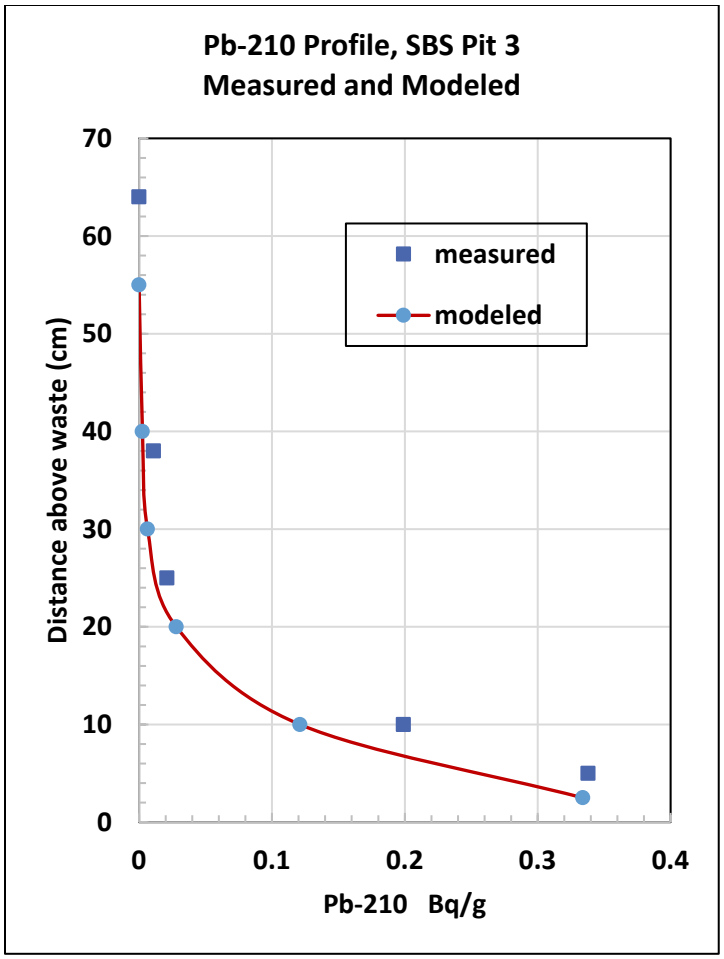

Figure 5-15 Measured and Modeled Pb-210 Profiles from Pit 3 at the Shirley Basin South Site Modeled Rn concentrations within the barrier are based on site-specific Rn flux measurements.

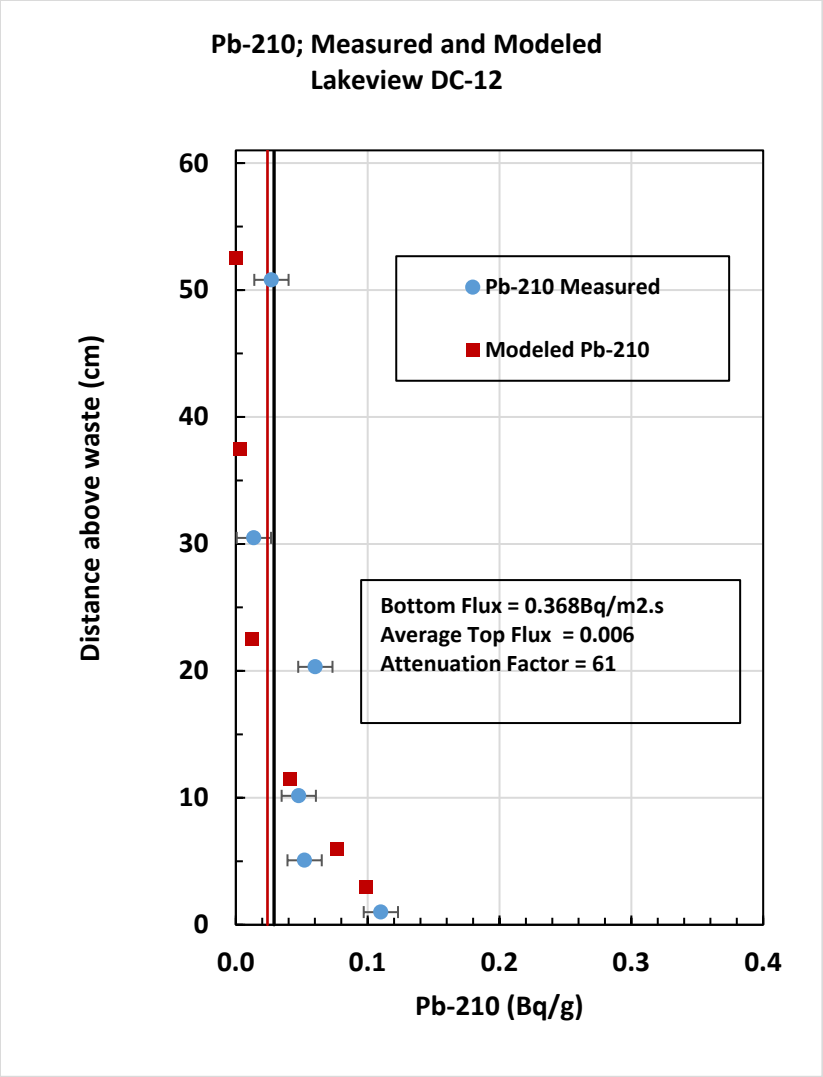

Figure 5-16 Pb-210 Measured at Lakeview and a Diffusion Model Using D = 6.5 x 10^{-8} m^2/s Which Was Calculated from Measured Fluxes at Pit 12

5.5.2 Complexities in Radon Transport

In two cases, SBS Pits 2 and 6 (the Rock Slope) (Figures 5-9 and 5-12), Pb-210 profiles were quite different than expected for simple diffusive transport. The highest Pb-210 values were found at 14 and 5 cm above the waste respectively, with values decreasing both closer to the waste and further up the profile. In these profiles, excess Pb-210 was observed at 29 and 38 cm above the tailings, showing that Rn had moved further up through the barrier. Moreover, at these two pits elevated radon fluxes were measured at the top of the barrier, as given in the boxes under the Pb-210 graphs in Figures 5-9 and 5-12. This is in contrast to Pits 3 and 5 at SBS where the Pb-210 concentrations decline to background, indicating that Rn was not transported above 25 cm and 15 cm from the tailings, respectively. In these two pits, Rn fluxes measured at the top of the barrier were very low (see Figure 5-13). Thus, excess Pb-210 above about 30 cm from the tailings seems to indicate higher top Rn fluxes. While Pb-210 at

background concentrations in the upper portions of the Rn barrier indicates little Rn flux at the top of the barrier.

Moisture content and porosity are major controls on Rn transport; diffusion of Rn in the pore structure of Rn barrier material is essentially all in the gas phase. For SBS Pit 2 (Figure 5-9), the high Pb-210 values correspond well to the highest moisture saturation values. The lower moisture content at the bottom of the profile may be the result of moisture draining to the tailings which are much coarser grained than the barrier material. Radon is able to diffuse up from the waste because of the lower moisture content in the few cm above the tailings, but when the area of saturated porosity is reached Rn is inhibited from moving up through the barrier sufficiently that much of it decays in place, leaving a Pb-210 maximum at 12-14 cm.

The Pb-210 profile in SBS Pit 2 shows that about 54% of Pb-210 is found below 15 cm where moisture measurements indicate water saturation or close to it (Fig. 5-9). However about 46 % is found above the saturated zone. At this pit plant rooting is absent from the zone below 15cm, and higher than site average above the saturated zone. Moreover, some of that radon escapes from the top of the radon barrier where we measured an average flux of 0.057 $Bq/m^2/s$ (Figure 5-9).

A similar relationship is found at the Rock Slope Pit 6 at Shirley Basin. As shown in Figure 5-17, 57% of Pb-210 resides below 10 cm and 43% is in the upper 38 cm. The average Rn flux at the top of the barrier was relatively high for this site at 0.13 $Bq/m^2/s$. Percent moisture saturation could not be calculated for the lower portion of the Shelby Tube samples at this location, but it was determined for a large block sample taken nearby (Fig. 5-12) which indicated near saturated conditions. In SBS Pit 6, plant rooting occurs through the depth of the barrier. At Pits 2 and 6 Rn transport is complex and results in emissions from the surface, corresponds well with the Pb-210 profiles that show low but measurably elevated concentrations approaching the top of the Rn barrier. In these cases, a substantial fraction of Rn must be escaping the high moisture content areas of the barrier and moving to the surface.

There are several possible mechanisms by which radon could move past the saturated area of the profile. First, while measurements indicate that the porosity is saturated at some depths there is likely sufficient error in the measurements that a small percentage of porosity may not be observed which is open enough to allow flow of gas, this is especially the case for a few macropores that may drain readily. Second, the saturated area may not be continuous but very localized so Rn from nearby areas could move up the profile. Third, water saturation may not be constant in time; at some times over the last 20 years less water may be present, allowing more Rn transport. Fourth, Rn may be emitted from the aqueous phase back to the gas phase at the top of the saturated area and be available for transport. In addition, very fine roots could contribute to Rn transport, perhaps by transporting Rn dissolved in the porewater [Lewis and MacDonell 1986]; some were observed in the barrier just above the saturated area, but none within it.

At Pits 4 and 5 at the Bluewater site (Figures 5-6 and 5-7) the Pb-210 profiles were similar to each other, excess Pb-210 was observed only in the bottom-most sample, each about 10 cm above the waste. As shown in Figure 5-6 the mean top flux at Pit 4 was background, 0.012 $Bq/m^2/s$, while at Pit 5 the top flux was 50 times higher with a mean of 0.63 $Bq/m^2/s$. As a result, the attenuation factor for Pit 4 was greater than 1000, meaning that little if any Rn moved through the barrier while for Pit 5 it was only 15, showing substantial loss of Rn. The disconnect between the similar Pb-210 profiles and the discordant Rn fluxes presents an interesting problem.

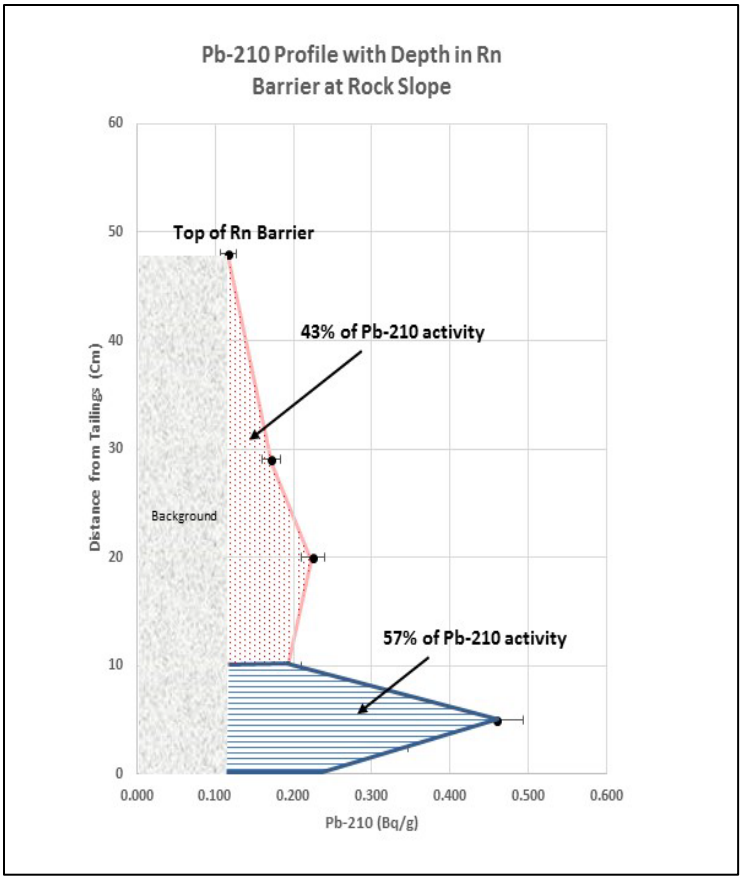

Figure 5-17 Pb-210 Profile at the Rock Slope Pit 6 at Shirley Basin South Showing Zones Discussed in Text

For Bluewater, moisture content and density were measured from the same and duplicate Shelby tubes from which Pb-210 samples were obtained. Moisture saturation values calculated from these measurements are shown in Figures 5-6 and 5-7. These pits were excavated close to each other as a pair of test pits; Pit 5 on a large saltbush while Pit 4 was nearby but on unvegetated cover material. Pit 5 had high Rn flux at the top of the barrier, very low saturation, and the material was described as being hard with many small diameter roots, and numerous root lined vertical cracks that span from the top of the barrier to the bottom. Pit 4 was essentially a control; it had low Rn flux, was saturated (or close to it) at several depths and was described as very homogenous sandy soil with no visible cracks, roots, or planes of weakness. Data from Pit 5 shows that the saltbush dried its local area of barrier while the control area retained substantial moisture. The controls of moisture saturation on Rn transport are strong and are illustrated well here.

Transport times were calculated from diffusion coefficients for these two Bluewater test pits as described above using the two-flux method (see Chapter 4.6). The average D for Pit 4 is 5.4 x 10^{-8} m^2/s giving an average transport time through the 71 cm thick barrier of 58 days or 15 half-lives. For Pit 5 the average D is 1.48 x 10^{-6} m^2/s giving an average transport time through the 64 cm thick barrier of 1.7 days or 0.45 half-lives. These vastly different transport times may explain the apparent contradiction between the low top flux and low Pb-210 at Pit 4 and the high-top flux and low Pb-210 at Pit 5. It seems likely that both Pb-210 profiles were similar over much of the life of the barrier, with no Rn reaching the top of the barrier. The recent

development of the saltbush at Pit 5 has dried the barrier so that Rn moves through the barrier very quickly; so quickly in fact there is little time for decay and deposition of Pb-210. This high rate suggests that Rn transport is preferential through interconnected macropores. Careful examination of the barrier at Pit 5 showed that it had, by far, the most interconnected macropores/fractures from depth to surface at Bluewater. It is likely that the plant was only a few years old which would not be time enough to alter the Pb-210 profile. As a result of the growth of the saltbush, the Pb-210 profiles of the two locations look similar even though the top fluxes are markedly different.

5.5.3 Relationship Between Rn flux at the Barrier Top and Excess Pb-210

Plotting the measured mean Rn flux from the top of the radon barrier against the excess Pb-210 concentration measured in the first sample taken below the top of the barrier (Figure 5-18A) suggests a linear relationship between the concentration of Pb-210 and Rn flux measured at the top of the barrier when fluxes are below about 0.4 Bq/m^2/s. The coefficient of determination (R^2) for the seven lower flux samples is 0.99. These same data are plotted in a semi-log graph (Figure 5-18B) to better show the relationship of the low flux data points. These samples were taken at various depths below the top of the barrier, from 7 to 31 cm and are on locations with little if any plant growth. When fluxes are greater than 0.4 Bq/m^2/s, Pb-210 concentrations are lower than expected. This is shown by the two red squares in Figure 5-18 which are locations with the highest Rn fluxes (Falls City Pit 3 and Bluewater Pit 5) but with low Pb-210 concentrations; both are impacted by the presence of large deep-rooted plants. The areas of low moisture content or pathways of preferential flow created by these plants appear to allow Rn to move quickly enough that deposition of Pb-210 is very low. The uppermost samples from the top surface of the Rn barrier were not used for this assessment as most of these showed no excess Pb-210, with the Rn gas apparently moving quickly from these surfaces into less porous material. It was expected that the difference in sampling depth for the low flux locations would lead to considerable variability, but this does not appear to be the case; it is unclear why. Sampling at a constant depth would be more appropriate for a standardized method to define the relationship between surficial Rn flux and Pb-210 concentration.

Table 5-5 provides a view of the ability of Pb-210 profiles to indicate if radon fluxes at the top of barriers will be observed. The Rn flux attenuation factor indicates how much the barrier inhibits transport of Rn from the waste to the surface of the barrier. The Top Flux to Background Flux Ratio is calculated by dividing the mean Top Flux by the measured or calculated background Rn Flux. A value of one or less shows that the Top Fluxes are similar to or less than the background flux. However, some of these values are low and there is at least a 20% uncertainty associated with the background determinations. Because of this we take a ratio value below 3 to indicate that measured surface fluxes are essentially equivalent to background. These are marked with a “B”. The last column is based on the measured Pb-210 profiles shown in the figures and refers to whether or not the Pb-210 activities reduce to background values as the top of the barrier is approached. In most cases when there are elevated Rn fluxes at the top of the barrier, then Pb-210 concentrations are elevated in the upper portions of the profile. Only in the case of Pit 5 at Bluewater does this relationship fail due to extremely fast Rn transport rates.

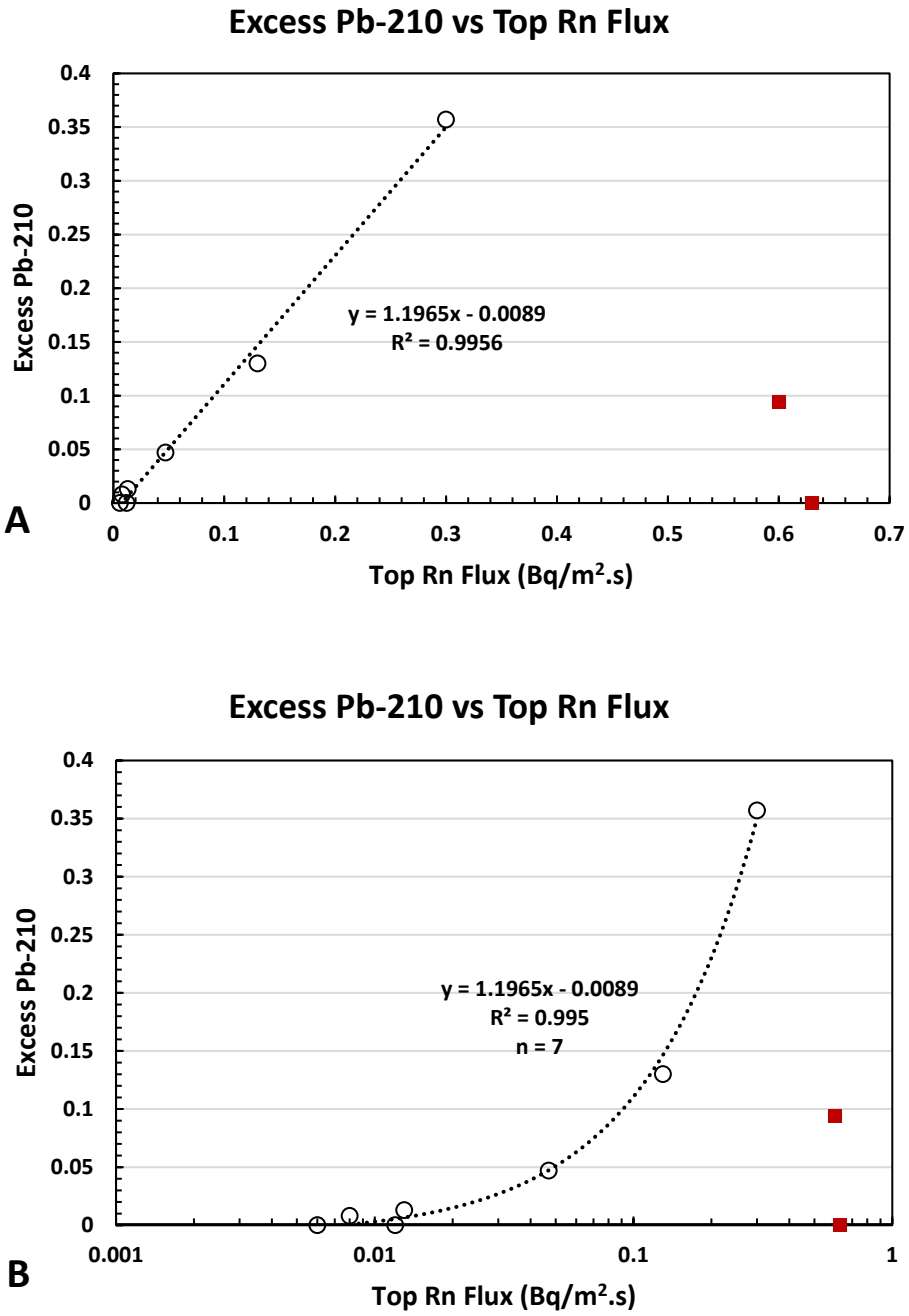

Figure 5-18 Relationship Between Excess Measured Pb-210 Concentrations in the Upper Part of the Barrier vs Rn Fluxes Measured at the Top of the Barrier. This relationship is generally linear except in areas of very high flux impacted by large deep-rooted plants (the two red square data points). A is a linear plot, B is a semi-log plot to better show the low flux data points.

Table 5-5 Pb-210 as an Indicator of Top Flux

Site	Pit #	Rn Flux Attenuation Factor	Top Rn Flux to Background Flux Ratio	Pb-210 Profile goes to Background
FC	2	6.9	7.1	No
FC	3	8.6	21	No
BW	4	1030	B 2.8	Yes
BW	5	15	220	Yes *
SBS	2	147	5.7	No
SBS	3	6170	B 0.6	Yes
SBS	5	14	B 1.8	Yes
SBS	Slope	538	13	No
LV	12	61	B 1.0	Yes

5.6 Summary and Application

Analysis of material from nine locations at four in-use radon barriers shows that Pb-210 at background levels is measurable and that in many cases Pb-210 in excess of background is present. Systematic depth profiles of Pb-210 within those barriers present information on long-term deposition of Pb-210 due to the in-place decay of Rn-222. From this very limited sampling we observed two types of Pb-210 profiles; those that describe simple diffusive transport of Rn-222 through the barrier and those that describe complex transport. Profiles that show a monotonically decreasing trend of Pb-210 activity with distance from the bottom of the barrier can be simulated with a diffusion-based model using diffusion coefficients determined from site specific measured Rn fluxes from the bottom and top of the radon barrier as well as the thickness of the barrier. The age of the barrier needs to be used in decay calculations to accurately convert the modeled Rn flux to Pb-210 concentrations, indicating that profiles reflect long-term processes. Generally, this type of diffusion-based profile results in little if any Rn flux at the top of the barrier, confirming calculations done to design the barriers.

The more complex Pb-210 profiles are the result of zones of saturated porosity within the barrier, but it is not clear in what way some Rn is transported past the saturated zones. It is unknown if these profiles represent areas of the barrier that have changed since they were built. However, root counts at SBS suggest that depth of plant rooting corresponds to elevated Pb-210 at locations higher in the barrier. Sorption of Rn onto organic matter in marine sediments has been observed [Wong et al. 1992]. Retention of Rn in zones of higher organic matter, either originally present in the barrier material or developed in-situ from plant growth could result in areas of elevated Pb-210. This complex profile of Pb-210 is associated with elevated Rn fluxes at the top of the barrier and does not conform to the assumed transport mechanism (simple diffusion) used to design the covers.

The linear relationship between Rn flux and excess Pb-210 near the top of the Rn barrier, as shown in Figure 5-18, suggests the use of Pb-210 concentrations for monitoring long-term radon fluxes at UMTRCA sites. A simple monitoring method could be developed by measuring Pb-210 in the top 10 - 20 cm of the Rn barrier; this appears to be able to provide a useful means of estimating long-term Rn flux based on Pb-210 concentrations. Samples could be obtained by geoprobe or in some cases manually. This approach may be sufficiently easy and unobtrusive that it could be done periodically (perhaps on ten-year intervals) on a grid pattern that can be

replicated. The exceptions are Pit 5 at Bluewater and Pit 3 at Falls City which are impacted by large deep-rooted plants, causing poor retention of Rn. For some locations, such as near large plants, it may be advisable to perform a quick measurement of Rn-222 in the sampling hole simply to ascertain high or low activities of Rn.

In addition to the potential for a relatively simple monitoring approach, Pb-210 provides the means of assessing mechanisms of long-term transport of Rn-222 through barriers. This is important to confirm or deny the assumption of simple diffusive transport used to design the barriers and to more effectively model Rn behavior as barriers age. For this type of transport analysis, detailed sampling for Pb-210, moisture and density measurements are needed throughout the thickness of the barrier, especially in the 20 cm or so closest to the interface with the tailings. Material from this section has been published in a peer reviewed journal (Fuhrmann et al., 2019b).

5.7 References

Albright, W., C. Benson, G. Gee, T. Abichou, E McDonald, S. Tyler, and S. Rock, 2006, Field Performance of a Compacted Clay Landfill Final Cover at a Humid Site. Journal of Geotechnical and Geoenvironmental Engineering, 132(11), 1393-1403.

Asher-Bolinder, S., D. E. Owen, R. R. Schumann, 1990, Pedologic and climatic controls on Rn-222 concentrations in soil gas, Denver, Colorado, Geophysical Research Letters, 17:6**,** 825-828, https://doi.org/10.1029/GL017i006p00825

Asher-Bolinder, S., D. E. Owen, R. R. Schumann, 1991, A preliminary evaluation of environmental factors influencing day-to-day and seasonal soil-gas radon concentrations, in; Field Studies of Radon in Rocks, Soils, and Water, L.C.S. Gundersen and R. B. Wanty, Editors U.S. Geological Survey Bulletin # 1971.

Benson, C., A. Sawangsuriya, B. Trzebiatowski, and W. Albright., 2007, Post-Construction Changes in the Hydraulic Properties of Water Balance Cover Soils. Journal of Geotechnical and Geoenvironmental Engineering, 133(4), 349-359.

Benson, C., C. Enson, W. Albright, D. Fratta, J. Tinjum, E. Kucukkirca, S. Lee, J. Scalia, P. Schlicht, and X. Wang, 2011, Engineered Covers for Waste Containment: Changes in Engineering Properties & Implications for Long-Term Performance Assessment, NUREG/CR-7028, U.S. Nuclear Regulatory Commission, Washington DC.

Ferry, C., P. Richon, A. Beneito, M-C Robé, 2002, Evaluation of the effect of a cover layer on radon exhalation from uranium mill tailings: transient radon flux analysis, Journal of Environmental Radioactivity, 63:1, 49-64, doi.org/10.1016/S0265-931X(02)00015-2

Friedlander, G., J. W. Kennedy, E. S. Macias, and J. M. Miller, 1981, Nuclear and Radiochemistry, John Wiley and Sons, NY, 684 pages.

Fuhrmann, M., C. Benson, J. Waugh, M. Williams, and H. Arlt, 2019, Proceedings of the Radon Barriers Workshop, NUREG/CP-0312, https://www.nrc.gov/reading-rm/doc-collections/nuregs/conference/cp0312/ , U.S. Nuclear Regulatory Commission, Washington, DC.

Fuhrmann, M., A. Michaud, M. Salay, C. H. Benson, W. J. Likos, N. Stefani, W. J. Waugh, and M. Williams, 2019b, Lead-210 profiles in Radon Barriers, Indicators of Long-term Radon-222 Transport, Applied Geochemistry, Volume 110, 104434, ISSN 0883-2927.

Kelln, C., L. Barbour, and C. Qualizza, 2009. Fracture-Dominated Subsurface Flow and Transport in a Sloping Reclamation Cover. Vadose Zone Journal, 8, 96-107.

Lewis, B.G., and M.M. MacDonell. 1986, Radon transport through a cool-season grass, Journal of Environmental Radioactivity, 4:2, 123-132.

Maity, S., S. Mishra, S. Bhalke, G. Pandit, V. Puranik, and H. Kushwaha, 2011, Estimation of distribution coefficient of polonium in geological matrices around uranium mining site, Journal of Radioanalytical and Nuclear Chemistry, 290:1, 75-79.

Michaud, A.M., 2018, Long-Term Performance of Radon Barriers in Limiting Radon Flux from Four Uranium Mill tailings Containment Facilities, https://minds.wisconsin.edu/handle/1793/78602, Thesis for Master of Science, University of Wisconsin-Madison.

Nielson, K.K. and V.C. Rogers, 1982, A Mathematical Model for Radon Diffusion in Earthen Materials, NUREG/CR-2765, U.S. Nuclear Regulatory Commission, Washington DC.

Prasad G., T. Ishikawa, M. Hosoda, A. Sorimachi, S.K. Sahoo, N. Kavasi, S. Tokonami, M. Sugino, and S. Uchida, 2012, Seasonal and diurnal variations of radon/thoron exhalation rate in Kanto-loam area in Japan, Journal of Radioanalytical and Nuclear Chemistry, 292, 1385-1390, doi: 10.1007/s10967-012-1620-6

Rogers, V.C. and K.K. Nielson, 1991, Correlations for Predicting air Permeabilities and ^{222}Rn Diffusion Coefficients of Soil, Health Physics, vol. 61, #2, pp. 225-230.

Rogers, V.C., K.K. Nielson and D.R. Kalkwarf, 1984, Radon Attenuation Handbook for Uranium Mill Tailing Cover Design, NUREG/CR-3533, U.S. Nuclear Regulatory Commission, Washington DC.

Sheppard S., J. Long, B. Sanipelli, and G. Solenius, 2009, Solid/liquid partition coefficients (Kd) for selected soils and sediments at Forsmark and Laxemar-Simpevarp, SKB Report R-09-27, Swedish Nuclear Fuel and Waste Management Co, Stockholm, Sweden.

Singh, M., Ramola, R. C., Singh, S., and Virk, H. S., 1988, Influence of meteorological parameters on soil gas radon, Journal of the Association of Exploration Geophysics, IX:2, 85-90.

Stefani, N., 2016, Field and Laboratory Measurement of Radon Flux and Diffusion for Uranium Mill Tailings Cover Systems, https://minds.wisconsin.edu/handle/1793/75426, Thesis for Master of Science, University of Wisconsin-Madison.

Suter, G., R. Luxmoore and E. Smith, 1993, Compacted Soil Barriers at Abandoned Landfill Sites are Likely to Fail in the Long Term. Journal of Environmental Quality, 22(2), 217-226.

U.S. EPA, 1999, EPA402-R-99-04B, Understanding Variations in Partition Coefficients, Kd, Values Vol. II. Review of Geochemistry and Available K_d Values for Cadmium, Cesium, Chromium, Lead, Plutonium, Radon, Strontium, Thorium, Tritium (3H), and Uranium. USEPA, Washington, DC

U.S. NRC, 1989, Regulatory Guide 3.64, Calculation of Radon Flux Attenuation by Earthen Uranium Mill Tailings Covers. U.S. Nuclear Regulatory Commission, Washington DC.

Vandenhove, H., C. Gil-Garcia, A. Rigol, and M. Vidal, 2009, New best estimates for radionuclide solid-liquid distribution coefficients in soils. Part 2. Naturally occurring radionuclides, Journal of Environmental Radioactivity, 100, 697-703.

Wong, C.S., Y-P Chin, and P.M. Gschwend, 1992, Sorption of radon-222 to natural sediments, Geochimica et Cosmochimica Acta, 56, 3923-393

6 SOIL MORPHOLOGY OF FOUR IN-SERVICE UMTRCA WASTE COVERS AND CORRESPONDING NATURAL ANALOGUES

6.1 Introduction

Soils are open and dynamic systems that are subject to recurring fluxes of energy and mass with impacts to both short-term function and long-term evolution. Historically, the dynamic properties of soil development, and the emergence of novel soil morphology, have been underemphasized in the planning of engineered cover systems intended for the long-term containment of wastes. Conventional cover systems that use compacted mineral barriers (CMBs) to isolate wastes have largely been designed to resist natural processes, as opposed to working with them. The term “radon barrier” is used when explicitly referring to CMBs used in Uranium Mill Tailings Radiation Control Act (UMTRCA) covers. In the first several years postconstruction, soil processes including bioturbation by plants and animals can result in significant and irreversible changes to as-built CMB morphology with impacts to performance.

Given the uncertainty associated with long-term soil change in waste cover systems and service lives in hundreds to thousands of years, studies of natural analogue environments can provide an understanding of future soil conditions. The characterization of soil morphology in natural analogue environments, with well-defined soil-forming factors, may be used to forecast the long-term equilibrium condition of an engineered cover.

This section presents results from field investigations at four UMTRCA sites: the Falls City, Texas, Disposal Site; the Bluewater, New Mexico, Disposal Site; the Shirley Basin South, Wyoming, Disposal Site; and the Lakeview, Oregon, Disposal Site. Special emphasis is placed on documenting the soil morphology *within* the radon barrier and at corresponding depths of adjacent natural analogues.

At cover and analogue locations representative of soil-forming factors of interest, profiles were excavated for morphological investigation and sample collection. Comparisons between individual profiles on single sites were used to investigate how vegetation establishment, slope and drainage, and design/material composition correspond to the development of soil morphology in cover profiles. Comparisons between sites were used to explore the impact of climate on soil morphology. At each site, natural analogue environments were studied to understand the impact of time on the development of soil morphology and to forecast the long-term equilibrium condition of radon barriers given natural processes.

6.2 Soil-Forming Factors and Pedogenic Process in Waste Covers

This brief summary is condensed from Appendix H based on primary work from Williams (2019). For a detailed discussion of pedogenic processes and how they relate to properties of earthen covers over waste, one is encouraged to read that heavily referenced appendix. It reviews factors of soil development and the qualities and rates of pedogenic processes. A framework of soil development is proposed that incorporates soil-forming factors relevant to UMTRCA covers, and it presents a conceptual model that describes the coevolution of soil processes and morphology.

As discussed in detail in Appendix H, engineering design is influenced by a combination of site factors, natural material properties, and human cultural factors. Site factors include climate and

terrain features that influence overall disposal cell design and geometry, including aspect and slope. Natural material properties include properties of the waste, cover stratigraphy, material texture, material mineralogy, construction heterogeneities, and soil edaphic suitability for plant growth. Human cultural factors influencing site development include construction practices, stakeholder engagement, political processes, regulations, and cost. Ongoing active cover management can be considered a recurring flux factor along with climate and intrusion of organisms. Overlain on these are risks associated with groundwater contamination, ownership disputes or bankruptcies and episodic natural events such as fires, floods, or earthquakes.

Figure 6-1 illustrates the interrelationship among site factors, soil processes, and soil morphological development. It also illustrates the idea of evolution of the cover through changes in soil morphology that are induced by many processes ranging from very short term physically dominated alterations to very long-term impacts that include geochemical processes. This figure is explained more fully in Appendix H, but here it illustrates the factors and time scales that result in the ultimate properties of earthen covers.

In as few as 5 years after construction, soil processes including bioturbation by plants and animals (Arthur and Markham 1983; Burt and Cox 1993; Link et al. 1995; Waugh et al. 1999), freeze-thaw cycling (Kim and Daniel 1992; Benson et al. 1995), and desiccation cracking (Montgomery and Parsons 1989; Melchior 1997) have led to the emergence of soil morphology and subsequent alterations to as-built hydraulic properties of CMBs that can lead to increased water percolation. These short-term changes are part of a longer-term evolution of the system.

Medium-term processes take place on annual and decadal scales (Burt and Cox 1993; Link et al. 1995) and are dominated by bioturbation by plants and animals, with establishment of larger woody plants if maintenance is not provided. Long-term and very long-term processes emphasize the accumulation and redistribution of materials (e.g., reaggregation and stabilization of soil structure, pore clogging, and horizon development) and can be understood through the study of natural analogues.

For those waste covers that cannot support vegetation (i.e., because of climate, cover design, or aggressive vegetation management) and surfaces that are covered with rock riprap for erosion control, short-term soil processes may dominate indefinitely. Very hot and very dry sites may fit in this category. The formation of soil morphology in arid environments is generally a very slow process occurring over hundreds of thousands of years (Wells et al. 1985), and episodic events (such as large rainstorms) play a significant role in the development of soil morphology, specifically through erosion (Cable and Huxman 2004; Schwinning et al. 2004). Over sufficiently long time scales, the accumulation and redistribution of mobile elements (including dust and carbonate from rainfall) may eventually lead to the formation of desert pavements in arid and semiarid environments.

In the following sections, observations are presented from fieldwork at the four sites. These observations illustrate a single moment in what is likely a slow evolution of these covers. That evolution may result in a steady-state condition (at least on the regulatory time scale) similar to the natural analogue areas for each site. In the figures that follow, the analogues can be readily compared to the covers, for example in terms of soil and root structure. Also emphasized is the small-scale horizontal variability of structural changes in cross sections across features on the covers such as large plants, rodent burrows, and an ant mound. These can be closely related to the increases in hydraulic conductivity and radon flux described in Sections 3 and 4, respectively.

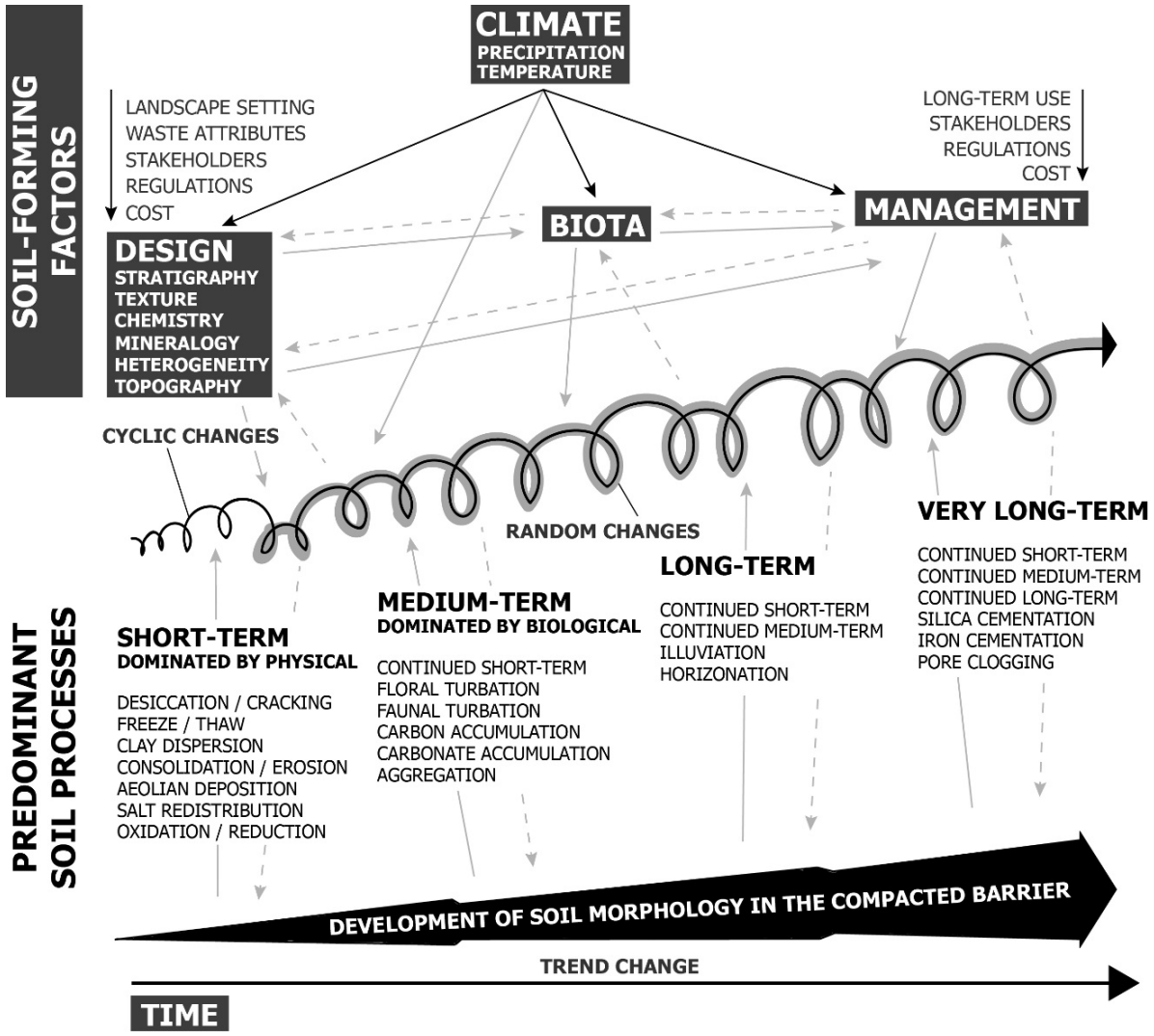

Figure 6-1 Site Factors, Soil Process, and Morphological Development in Compacted Mineral Barriers[1]

[1] Conceptual model of the coevolution of soil process and morphology in CMBs for waste containment is based on Lin (2010). Solid black arrows represent the dominant direction of influence. Solid gray arrows represent interactions. Dashed arrows represent a feedback between factors, change, soil processes, and morphology. Time frames for the incremental evolution of soil processes are based on Targulian and Krasilnikov (2007) and the field investigation presented in this section.

6.3 Methods

Field work was performed in 2016 at the Falls City site and the Bluewater site; and in 2017 at the Shirley Basin South site and the Lakeview site. At each site, representative test pit locations were identified (e.g., DC, TP, AN designation; see Section 2) and radon flux measurements performed (Section 4). After instrumentation was removed, the morphology of cover soils was characterized. Additionally, large diameter block samples were collected for laboratory characterization of soil hydraulic properties (Section 3). The morphology of block samples was

derived from observations of the excavated profile at shared depths. Soil observations and block sampling were also performed for a series of natural analogue locations adjacent to each disposal cell. In total, 32 soil profiles were studied. A detailed discussion of site selection, vegetation survey methods, analogue conditions, and surface characteristics are in Section 2. Full site reports are included in a series of soil and vegetation surveys reported elsewhere (DOE 2021a – d), and a preliminary reporting is in Fuhrmann et al (2019a).

6.3.1 Soil Morphological Characterization

A backhoe was used to excavate trenches to allow for the collection of samples and the morphological description of cover profiles, with emphasis on the radon barrier section, and when possible to within 50 millimeters (mm) of the depth of wastes. Excavations were closely monitored with radiation survey meters. Depth to the waste was generally determined with a hand auger. Trenches were not less than 1.5 meters (m) in width and in some instances reached depths in excess of 3 m. OSHA requirements for benching were met for all excavations. The same methods were used to excavate natural analogue profiles. The locations of the excavations, at each site, are presented in full in Section 2. Care was taken to protect the surface of the profile face from being disturbed during excavation, and trench walls were excavated to within 150 mm from the intended plane of observation to protect in-field morphology from disruption caused from the excavator bucket and to preserve the profile face from drying during radon flux measurements (Section 4) and block sample excavation (Section 3). After all instrumentation was removed, the trenches were thoroughly cleaned of debris and the intended plane of observation cut back 10–100 mm with a spade to remove excavator smear marks or dried materials. Photographs were taken to provide pictorial representation of layer thickness, soil structure, root patterning, macropores, and other anomalous emergent or as-built features. The bottom of the radon barrier was differentiated from underlying wastes through observed color, textural shifts, or a substantial increase in ionizing radiation (over background) with a Ludlum Model 12/44-9 radiation survey meter.

For each soil horizon, records were made for morphological properties including: profile thickness, horizon/material thickness, boundary, Munsell color system, pedality/structure (size, shape and grade, consistence), root morphology per unit area (abundance, diameter, class), the shape and size of void structures or animal excavations, rupture resistance, descriptions of inclusions, and other anomalous morphology in accordance with the U.S. Department of Agriculture (USDA) Natural Resource Conservation Service *Field Book for Describing and Sampling Soils*, version 3.0 (USDA 2012). Soil structure (Table 6-1), soil grade (Table 6-2), root size (Table 6-3), root quantity (Table 6-4), and rupture resistance (Table 6-5) descriptions from USDA (2012) are provided to aid in figure and data interpretation. Soil moisture was determined gravimetrically (gravimetric water content percentage [GWC%]) by Stefani (2016) and Michaud (2018), and a model that relates GWC% to suction was used to group soils by water class state (USDA 2012) in the following classes: saturated (>30%), wet (20–30%), moist (10–20%), dry (7–10%), and very dry (<7%).

The detailed characterization of (visible) interpedal, intrapedal, transpedal macropore space (size, type, and quantity) was adapted from Lin et al. (1999). Pore size was based on radius (for cylindrical pores) or width (for planar pores) in six classes: very fine (<0.5 mm), fine (0.5–1 mm), medium (1–2.5 mm), coarse (2.5–5 mm), very coarse (5–10 mm), and extremely coarse (>10 mm). Pore type corresponds to the general shape, continuity, and connectivity of pores across three classes: vughs (small spherical or elliptical cavities), channels (cylindrical and elongated), or planar fractures. Quantity of pores was visually recorded across the soil surface

to charts of pore areal percentages as modified from USDA (2012) across five classes: very few (<0.25%), few (0.25–0.5%), common (0.5–2%), many (2–5%), and very many (>5%).

Table 6-1 Soil Structure and Size Classifications

Size Class	Code	Criteria for Structural Unit Size (mm)		
		Granular (gr), platy (pl)	Columnar (cpr), prismatic (pr), wedge (wg)	Angular blocky (abk), subangular blocky (sbk), lenticular (lp)
Very fine	vf	<1	<10	<5
Fine	f	1 to <2	10 to <20	5 to <10
Medium	m	2 to <5	20 to <50	10 to <20
Coarse	co	5 to <10	50 to <100	20 to <50
Very coarse	vc	≥10	100 to <500	≥50
Extremely coarse	ec		≥500	

Table 6-2 Soil Grade Classifications

Grade	Code	Criteria
Structureless	0	No discrete units observable in place or in hand samples
Weak	1	Units are barely observable in place or in a hand sample
Moderate	2	Units well-formed and evident in place or in a hand sample
Strong	3	Units are distinct in place (undisturbed soil) and separate cleanly when disturbed

Table 6-3 Root Size

Size class	Code	Root Diameter	Soil Area Assessed
Very fine	vf	<1 mm	1 cm^2
Fine	f	1 to <2 mm	1 cm^2
Medium	m	2 to <5 mm	10 cm^2
Coarse	co	5 to <10 mm	10 cm^2
Very coarse	vc	≥10 mm	1 m^2

Table 6-4 Root Quantity

Grade	Code	Criteria
Few	1	<1 per area of soil assessed 0.2 to <1 per area of soil assessed <0.2 per area of soil assessed
Common	2	1 to <5 per area of soil assessed
Many	3	≥5 per area of soil assessed

Table 6-5 Rupture Resistance

Measured At Field Moist Soil Water State		Specimen Fails Under
Class	**Code**	
Very friable/friable	VFR/FR	Very slight to slight force with fingers, <20 N
Firm/very firm	FI/VFI	Moderate to strong force with fingers, 20–80 N
Extremely firm/slightly rigid	EF/SR	Hand or foot pressure with body weight, 80–800 N
Rigid/very rigid	R/VR	Blow by hammer, 800 N $\leq$ 3 J

Abbreviations: cm^2 = square centimeters, m^2 = square meters, N = newtons, J = joules

6.3.2 Laboratory Analysis

Soil samples were collected from each horizon from no fewer than five locations across the observed face of each profile. Soil samples were air dried, crushed, and passed through a 2 mm sieve prior to analysis. Samples were submitted to the Cornell Nutrient Analysis Laboratory (Ithaca, New York) for measurement of soil organic matter, total carbon, nitrogen, and hydrogen, macro- and micronutrients, nitrogen speciation, calcium carbonate, electrical conductivity (EC), pH, and grain size analysis. Soil organic matter (SOM) was derived by wet oxidation method (CNAL 2011a). Total carbon, nitrogen, and hydrogen were measured by a Vario El Cube CHNOS Elemental Analyzer (Foster City, California) method (CNAL 2017). Macro- and micronutrients were measured using inductively coupled argon plasma spectrophotometry after extraction in Morgan's solution (CNAL 2013). Nitrate, nitrite, and ammonia were measured by potassium chloride extraction and analysis by a Bran+Luebbe automated injection ion analyzer (Germany) (CNAL 2011b; CNAL 2011c). Calcium carbonate percentage was measured by titration (CNAL 2011d). EC was measured by a VWR Symphony SB70C conductivity meter (Radnor, Pennsylvania) in a 2:1 soil-to-water suspension (CNAL 2016a). Soil pH was measured using a LIGNIN Robotic pH meter (Albuquerque, New Mexico) and Thermo Scientific Ross combination pH electrode (Waltham, Massachusetts) in a 2:1 soil-to-water suspension (CNAL 2019). Grain size analysis was determined by mechanical sieving and hydrometer (CNAL 2016b). GWC% was derived by dry mass (ASTM D2216) and performed by Stefani (2016) and Michaud (2018) methods. The determination of clay mineralogy was performed through X-ray diffraction by Mineralogy Inc. (Tulsa, Oklahoma) on dried soils sieved to less than 0.075 mm. Corresponding data are reported in full elsewhere (DOE 2021a – d).

6.4 Field Observations and Results

Summary figures of soil structuring and root morphology are presented in Figure 6-2 and Figure 6-3. Hypothetical as-built conditions are based on design specifications and are included to represent what the cover system looked like at the time of construction. Profiles are generally organized from lowest to highest morphological development (left to right) across variable surface and vegetation condition. Down/side slope conditions are grouped separately as these profiles receive water drainage from the cell and presumably maintain higher soil water content throughout the year. Analogue soils are presented to compare on-cell soil condition against natural soils that may represent a long-term steady-state soil condition given shared soil-forming factors. A discussion of soil-forming factors is presented in Appendix H. Descriptions from individual sites follow.

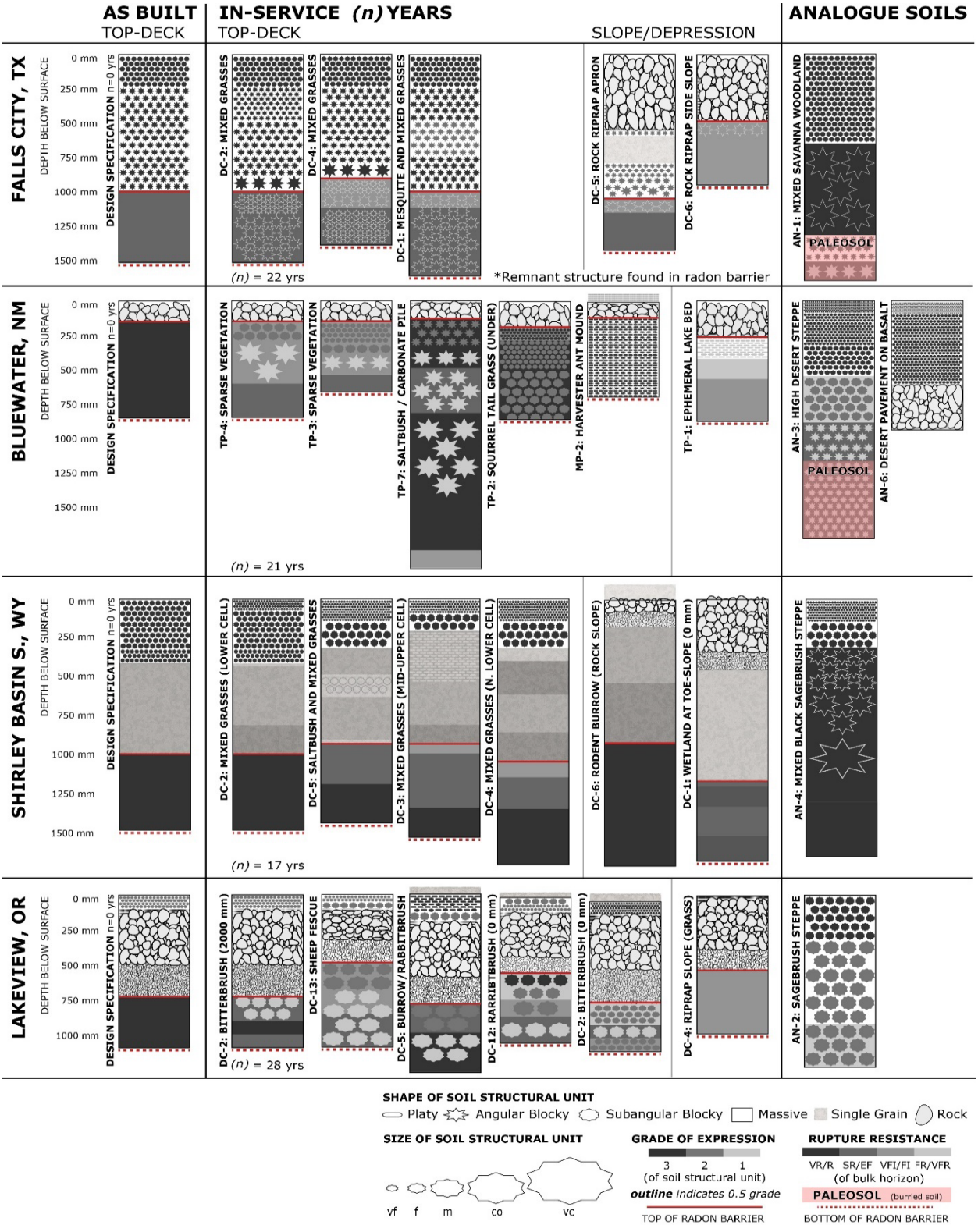

Figure 6-2 Soil Structure of UMTRCA Covers and Natural Analogues Under Variable Surface Conditions

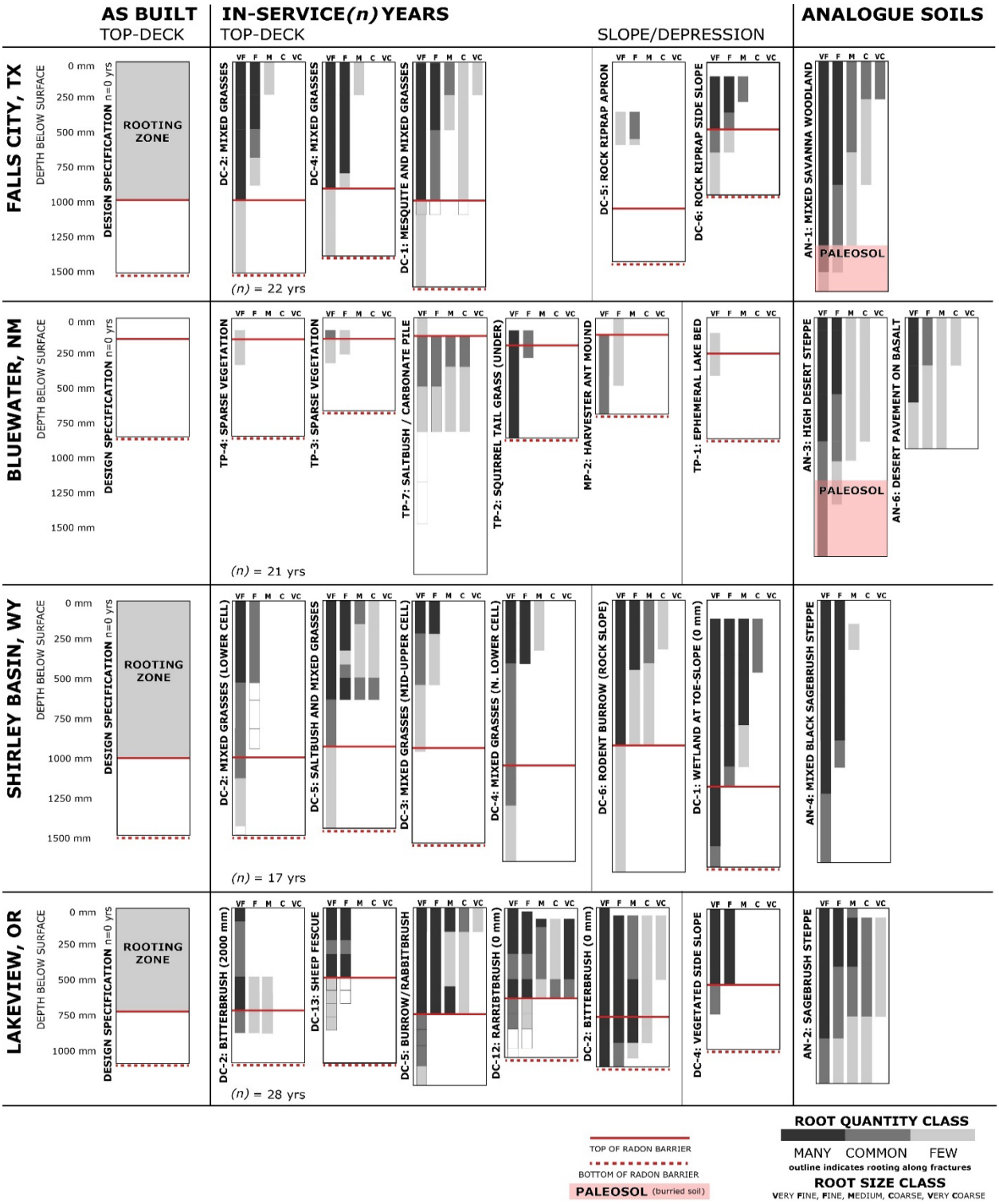

Figure 6-3 Root Structure of UMTRCA Covers and Natural Analogues Under Variable Surface Conditions

6.4.1 Falls City, Texas

Six on-cell profiles and two analogue profiles were excavated at the Falls City site in May 2016. After 22 years of service, the main deck of the disposal cell was characterized by a uniform stand of perennial forage grasses dominated by yellow bluestem (*Bothriochloa ischaemum* var. *songarica*) interspersed with honey mesquite (*Prosopis glandulosa*) (Figure 6-4). The rock riprap side slope was characterized by patchy areas of mixed vegetation, with deep-rooted vegetation managed by cutting and spot spraying with herbicide. The top of the disposal cell is mowed up to three times per year with hay being used by nearby cattle ranchers. Management is intended to reduce fire risk and the deep rooting of mesquite into the radon barrier. The mowed mesquite likely has a larger and deeper root system than similarly sized plants that are not mowed. The full survey is reported elsewhere (DOE 2021a).

Figure 6-4 Representative Surface and Vegetation Condition on the Disposal Cell at Falls City, Texas

The top deck of the disposal cell at the Falls City site is a vegetated topsoil cover, while the side slope is made of riprap with bedding cover. On the top deck of the disposal cell, measured topsoil thickness ranged from 240–250 mm while the thickness of the overburden layer ranged from 680–750 mm. The depth from ground surface to the top of the radon barrier ranged from 930 mm–1000 mm. Radon barrier thickness ranged from 460–920 mm. Individual lift-and-compaction events were largely indiscernible in the radon barrier.

The profile observed on the side slope (DC-6, see Fig. 2-5) had a 270 mm rock riprap cover, with 70% of the rock interstices containing mixed illuvial infill. Rock riprap was placed on top of a 200 mm sandy gravel drainage layer, with the top of the radon barrier observed at 470 mm below ground surface. The radon barrier was found in a saturated state with active water flow observed in the drainage layer.

6.4.1.1 Structuring in the Radon Barrier and Cover Materials

The radon barrier at the Falls City site was composed of remnant soil structure from the borrow area of mixed sizes from fine to coarse, delineated by hairline fractures that served as preferred sites for root matting and iron precipitation (Figure 6-5). The observance of remnant soil structure increased as the face of the profile was exposed to drying in ambient air during morphological characterization. Given the high smectite percentage of the radon barrier (Section 6.4.5.2) and the sensitivity to shrink-swell, changes to soil moisture play a significant role in regulating radon barrier morphology at this site.

Figure 6-5 Remnant Soil Structure in the Radon Barrier at Falls City, Texas

Soil structuring in the topsoil and overburden layers was composed of blocky structures of mixed sizes (fine to medium) that generally increased in size with depth, and of mixed grades that generally remained consistent with depth (Figure 6-6). Variation in soil structuring in the topsoil and overburden layers of the cover generally resemble the natural analogue (AN-1).

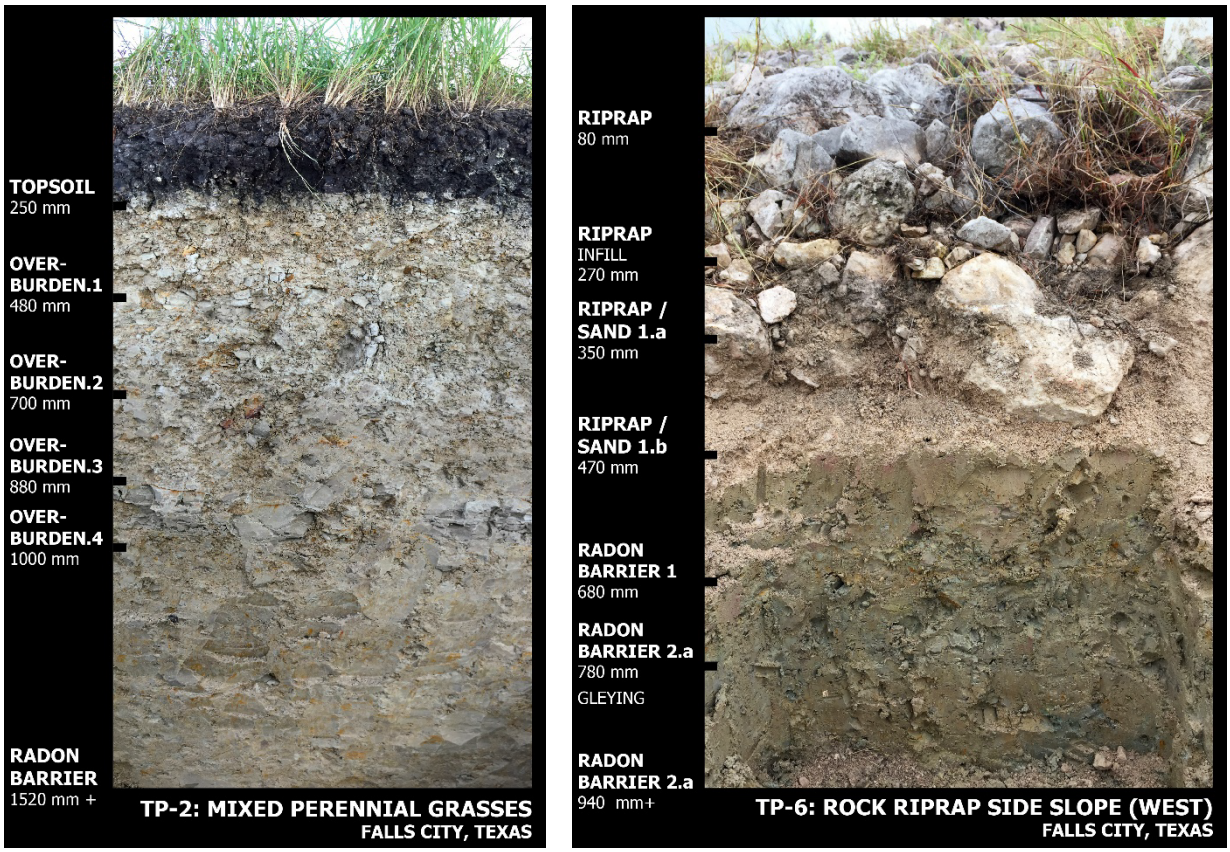

Figure 6-6 Soil Profile Sections on the Disposal Cell at Falls City, Texas

6.4.1.2 Plant Rooting in the Radon Barrier and Cover Materials

Root size, quantity, and depth correspond to vegetation type, with the honey mesquite profile (DC-1) having the greatest variation in root size (very fine to coarse) and quantity, within the radon barrier. Fine and coarse roots were infrequently observed along fracture planes of remnant soil structure in the top 80 mm of the radon barrier in DC-1 but the majority of the fine and coarse root mass remained benched along the top boundary of the radon barrier (Figure 6-7). Root benching corresponded to the observation of gleying in the top 80 mm of the radon barrier, suggesting that moisture may perch in the top section of the radon barrier serving as a reservoir for mesquite roots. With exception to the profile associated with the rock riprap top apron (DC-5), very fine roots traveled through the depth of the radon barrier on all profiles on the top deck (1380 mm–1610 mm). No roots were observed in the radon barrier of DC-5 as vegetation was very limited at this location. Fine roots were observed liberally in the top section of the radon barrier in the rock riprap side slope profile (DC-6), with very fine roots traveling through the depth of the radon barrier (940 mm), representing the highest root mass in any profile observed at the Falls City disposal cell. Transect excavations away from the mesquite taproot found that root benching, within fracture planes in the top section of the radon barrier, extends to distances in excess of 2500 mm away from central taproot (Figure 6-8). Along this transect, rooting and structuring, within the radon barrier, remain consistent with distance away from taproot.

Figure 6-7 Honey Mesquite Root Benching and Gleying Along the Top Boundary of the Radon Barrier at Falls City, Texas

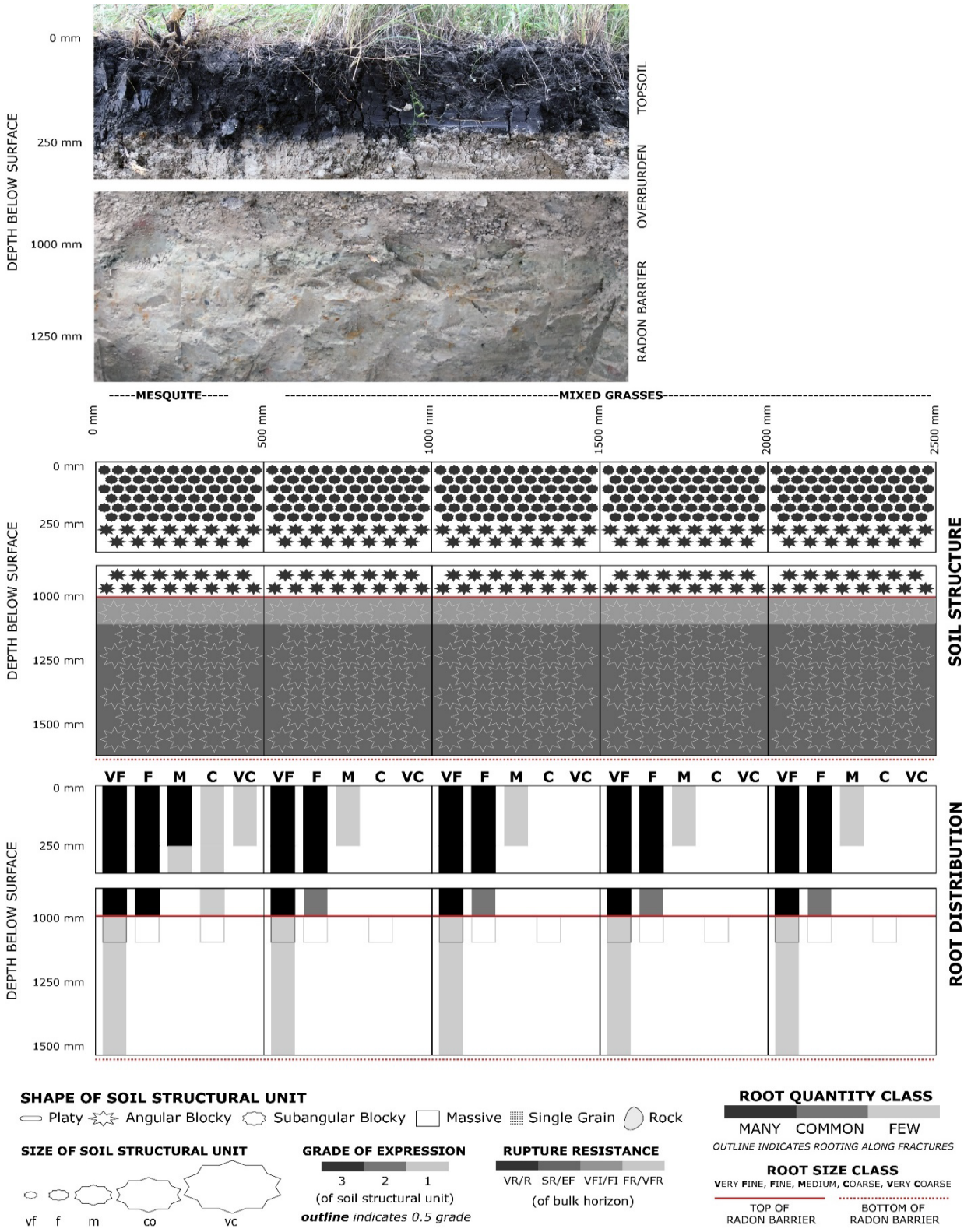

Figure 6-8 Honey Mesquite Soil Morphology Impact Gradient (TP-1), Falls City, Texas

6.4.1.3 Natural Analogue Soil Morphology

The natural analogue soil profile is presented in Figure 6-9. The soil structure in the analogue is comprised of blocky structures of mixed sizes (fine to very coarse) that generally increase in size with depth (to 1260 mm) and of mixed grades that generally decrease with depth (to 1260 mm). At a depth of 610 mm, an argillic (zone of clay accumulation) horizon has formed. The material is very hard (more so than the radon barrier), and soil structure is weak—blocky-to-prismatic. Below 1260 mm a paleosol (buried soil horizon) is encountered.

Root size, quantity, and class generally decreased with depth, with medium root benching occurring at the horizon boundary at 1260 mm. Medium, fine, and very fine roots were observed to a depth of 1260 mm. Coarse roots were observed to a depth of 900 mm. Very fine roots were observed through the depth of the profile (more than 1650 mm).

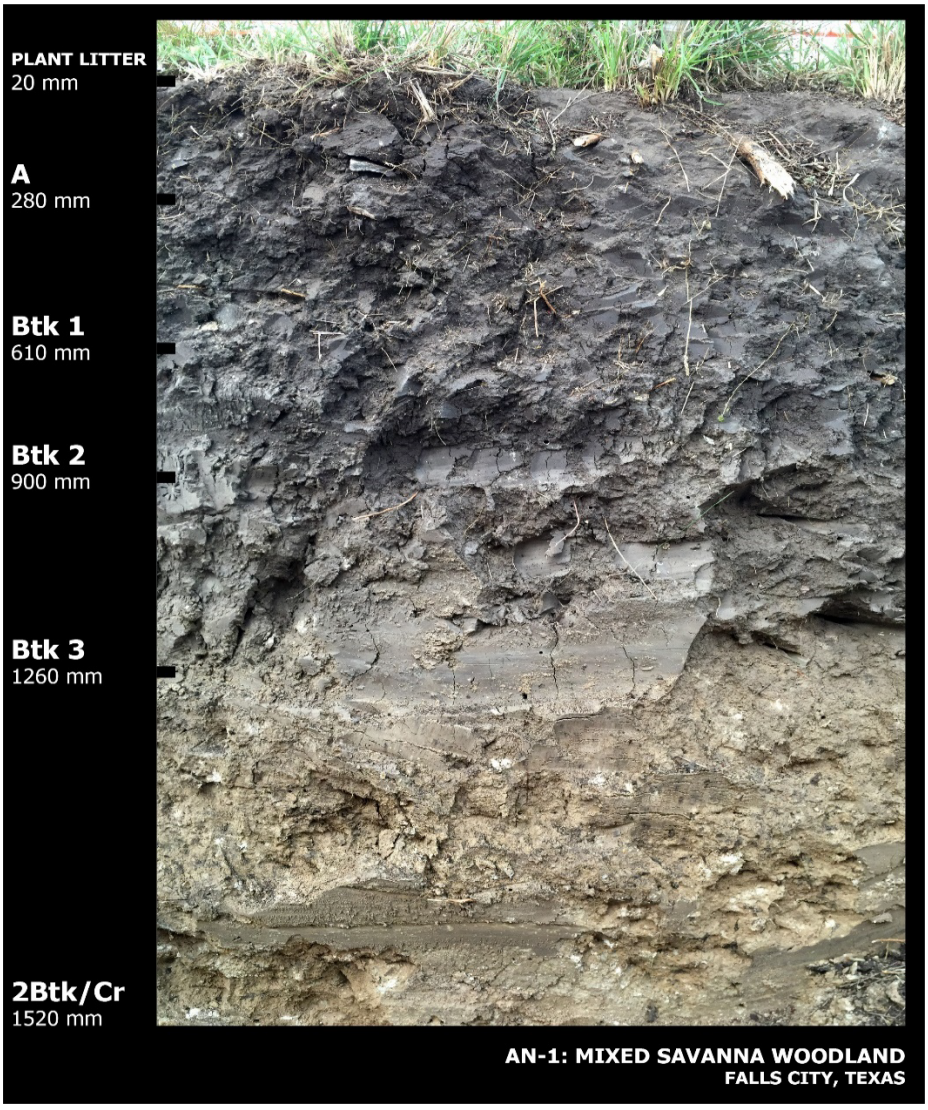

Figure 6-9 Natural Analogue Soil Profile at the Falls City Site

6.4.1.4 Comparison of Soil Morphology in the Radon Barrier to the Natural Analogue

The soil morphology at 1250–1500 mm below ground surface of the radon barrier and natural analogue is summarized in Table 6-6. Rooting is far more developed in the natural analogue than the on-cell profiles, with medium and fine roots observed to depths that would be well into the radon barrier. This corresponds to greater soil structuring in the natural analogue compared to the radon barrier. Such observations are attributed to variations in the soil-forming factors, namely management and time (see Appendix H). Under alternative management conditions (i.e., allowing mesquite to establish on the cover) and additional time, plant rooting and corresponding soil structuring would likely occur with greater intensity (and at greater depths) versus current conditions.

Table 6-6 Summary of Soil Condition at 1250–1500 mm from Ground Surface

	Analogue-1	**TP-1**	**TP-2**	**TP-4**
	Mixed Woodland	**Mesquite**	**Mixed Grasses**	**Mixed Grasses**
Soil structure	2f/m abk	1m sbk	1m sbk	1f sbk
Root morphology	1m 2f 2vf	0.5vf	1vf	1vf
Texture[a]	C	SICL	SICL	SICL
Dry density (g/cm^3)[b]	-	1.16	1.26	1.35
Gravimetric H_2O %[b]	-	34.0%	38.0%	32.0%
SOM %	1.72	2.03	2.05	1.93
pH	8.75	7.13	7.24	7.68
EC	0.49	3.42	3.05	2.47
K_{sat}[c] (m/s)	1.40E-06	2.10E-07	9.37E-09	-

[a] USDA (2012) textural soil classification.
[b] From Stefani (2016) and Michaud (2018).
[c] See Section 3 and Section 7 for full reporting on K_{sat}.

6.4.2 Bluewater, New Mexico

Seven profiles were excavated on the main cell, two profiles on the carbonate cell, one profile on the acid cell, and two profiles under natural analogue conditions at the Bluewater site in June 2016. After 21 years of service, the main disposal cell was characterized by a patchwork of vegetation and surface conditions (Figure 6-10) that correspond to emergent radon barrier morphology (Figure 6-2 and Figure 6-3). Surface conditions include sparsely vegetated rock riprap, ephemeral ponding, mixed perennial grass establishment dominated by squirreltail grass (*Elymus elymoides*), mixed annual weed development dominated by Russian thistle (*Salsola tragus*) and burning brush (*Bassia scoparia*), patches of fourwing saltbush (*Atriplex canescens*), and infrequent harvester ant (*Pogonomyrmex spp.*) mounds. Similar conditions were present on the carbonate cell, while the vegetated acid cell had a relatively uniform stand of mixed grasses. On the main and carbonate cells, management for deep rooting plants, including tamarisk (*Atriplex spp)* and Siberian elm (*Ulmus pumila)*, consists of hand cutting and spot spraying with herbicide. Noxious weeds are also sprayed with herbicide as needed. The full survey is reported elsewhere (DOE 2021b).

Figure 6-10 Surface and Vegetation Condition on the Main Disposal Cell at Bluewater, New Mexico

The main and carbonate disposal cells at the Bluewater site are rock riprap covers. Among the profiles surveyed, rock riprap thickness varied between 80–150 mm. The interstices of the rock riprap were occasionally filled with organic materials from nearby vegetation, blown seeds, animal scat, aeolian dust, rock fines, and anthropogenic debris including blasting caps, ball bearings, scrap metal, tire shards, and survey stakes.

The surface of the radon barrier was in direct contact with overlying rock riprap, and the minimum depth from the top of the rip-rap to the radon barrier was 80 mm. Radon barrier thickness ranged from 540–700 mm, with individual lift-and-compaction events ranging from 80–230 mm. One profile on the carbonate cell (TP-7) had a total depth in excess of 2580 mm, with the radon barrier accounting for 2420 mm (the total depth to waste was not determined). With exception to the downslope ephemeral lake profile on the main cell (TP-1), radon barrier materials were dry and very hard below 250 mm from ground surface. Variation in as-built condition was evident in rock riprap thickness, rock fines thickness, radon barrier horizon thickness, color of radon barrier lift events, and slight variation in the gravel content and remnant soil structure from borrow sources in the radon barrier.

6.4.2.1 Structuring in the Radon Barrier

A diversity of soil structuring was found within the radon barrier as a function of surface condition and depth (Figure 6-11). Single grain, granular, platy, blocky, and massive structures were present with decreased structuring observed with increased depth (e.g., Bluewater TP-7 in Figure 6-2). The profile associated with the ephemeral lake (TP-1) had the least structural development (corresponding to higher moisture content) and was characterized by weak platy structure, constrained to the first lift-and-compaction horizon (460 mm). The sparsely vegetated

profiles (TP-3 and TP-4) had blocky structures of mixed sizes (very fine to coarse) that increased in size with depth and of mixed grades decreasing in intensity with depth, to a depth not exceeding 590 mm. Profiles TP-1, TP-3, and TP-4 contained sections of radon barrier that remained massive and did not visually display emergent soil structure.

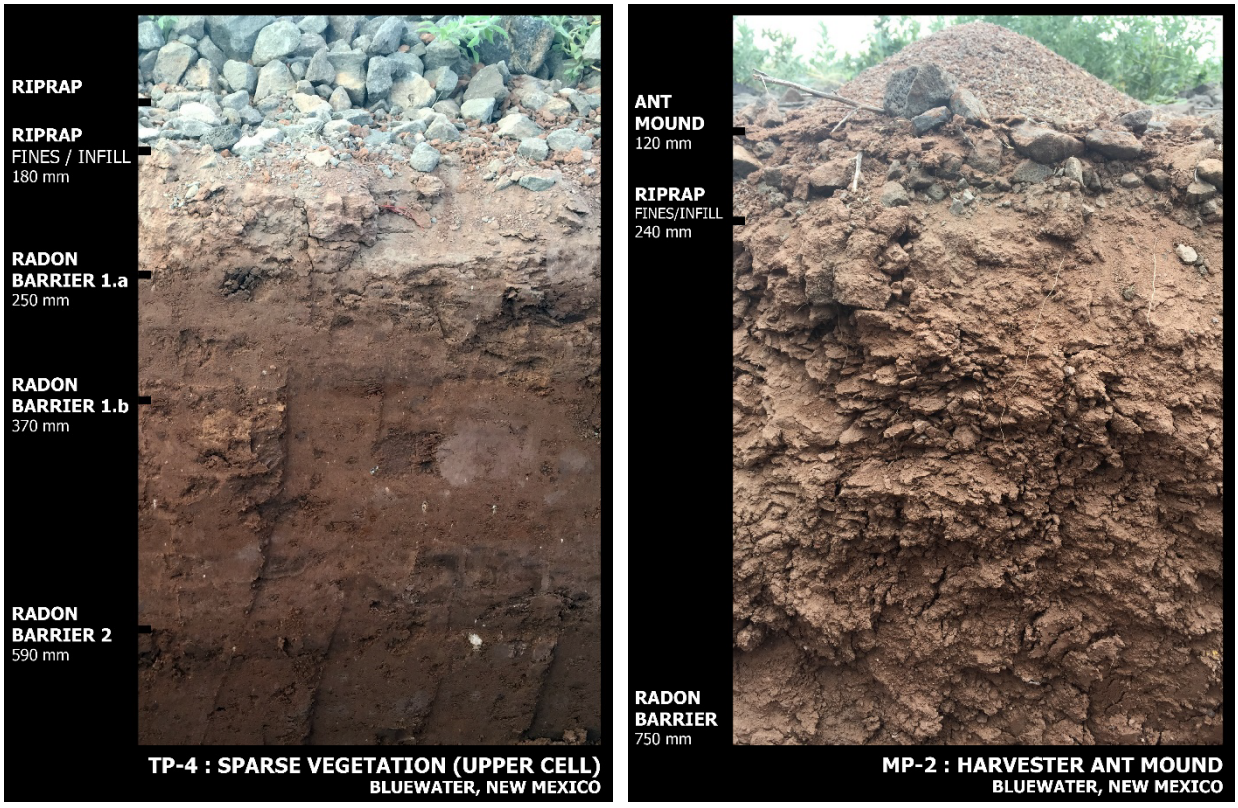

Figure 6-11 Soil Profile Sections on the Main Disposal Cell at Bluewater, New Mexico

The saltbush profiles were characterized by blocky structure of mixed sizes (fine to coarse) that increased in size with depth and of mixed grades decreasing in intensity with depth. Profile TP-5 on the main cell displayed structuring through the depth of the observed radon barrier (740 mm). Profile TP-7 on the carbonate cell displayed structuring to a depth of 1580 mm with the remaining 1000 mm of radon barrier visually devoid of emergent structure.

The profile associated with squirreltail grass (TP-2) was characterized by granular structure in the wind-blown sediment collected in the interstices of the rock riprap. The radon barrier had blocky structure of mixed sizes (very fine to medium) that increased in size with depth, and of mixed grades decreasing in intensity with depth. Structuring was observed through the depth of the observed profile to 880 mm. The soil structuring observed in TP-2 resembled that of the natural analogue profile located in the undisturbed area adjacent to the borrow pit (AN-3).

Excavations of a harvester ant mound (*Pogonomyrmex spp.*) (MP-2, see Fig. 2-4) show structuring 1100 mm away from the center of the mound to a depth of at least 750 mm (Figure 6-12). Under the ant mound, the radon barrier was characterized by intermixed blocky and platy

structures of sizes ranging from very fine to fine, through the depth of the radon barrier. As distance increased away from the mound, soil structure transitioned to larger blocky structures (shared by the squirreltail grass profile TP-2). Due to the invasive sampling methods required to extract block samples for hydrological analysis, detailed morphological characterization of TP-6, also associated with a harvester ant mound, was not possible.

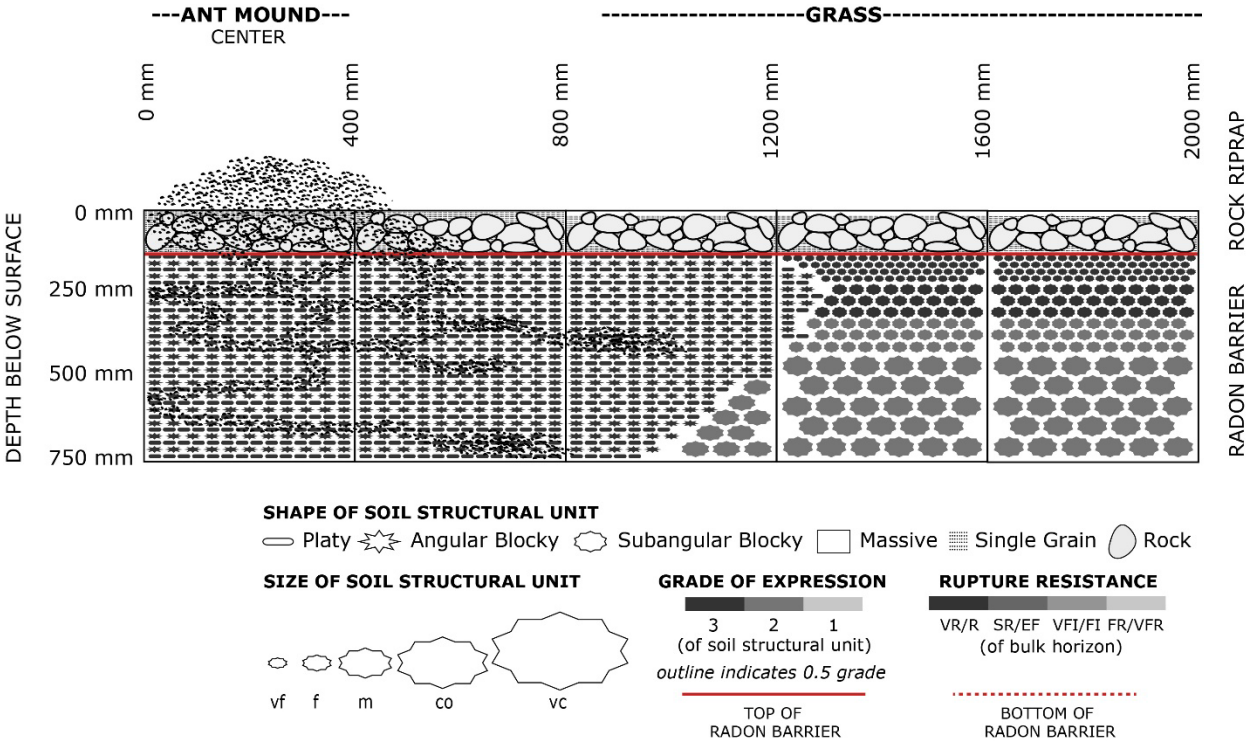

Figure 6-12 Bioturbation by Harvester Ants, Bluewater, New Mexico Main Disposal Cell

6.4.2.2 Plant Rooting in the Radon Barrier

Plant roots were found in the radon barrier of all profiles surveyed, regardless of surface condition (Figure 6-3). Root size, quantity, and depth correspond to vegetation type, with saltbush profiles (TP-5 and TP-7) having the greatest variation in root size and quantity. In the TP-5 saltbush profile on the main cell, coarse, medium, fine, and very fine roots were observed in the bulk soil to a depth of 550 mm, with medium, fine, and very fine roots observed in vertical fractures through the depth of the observed barrier (710 mm). In the TP-7 saltbush profile on the carbonate cell, coarse, medium, fine, and very fine roots were observed in the bulk soil to a depth of 890 mm, with very fine roots observed along vertical fractures to a depth of 1580 mm. The squirreltail grass profile (TP-2) had the greatest overall rooting density, with fine and very fine roots observed in the bulk soil to a depth of 290 mm and very fine roots observed in the bulk soil fraction through the depth of the observed radon barrier (880 mm). Sparsely vegetated profiles (TP-3 and TP-4) and the ephemeral lake bed (TP-1) had the least abundance of roots, with very fine roots terminating at 380 mm, 370 mm, and 460 mm, respectively.

Root benching was commonly observed at radon barrier lift-and-compaction boundaries, particularly in locations where underlying materials had greater consistence/cementation. Such conditions served to restrict rooting in the bulk barrier material, with rooting confined to fracture planes. Dense root mats were commonly observed along vertical fracture planes in desiccated radon barrier materials (Figure 6-13). Several of the root-filled fractures observed in TP-2 and TP-5 traveled through the depth of the radon barrier and into subsurface materials. Considerable organic matter accumulation was observed in the rock riprap underneath shrubs. Dead roots were observed sparingly in the radon barrier and may have been attributed to debris transported from borrow materials.

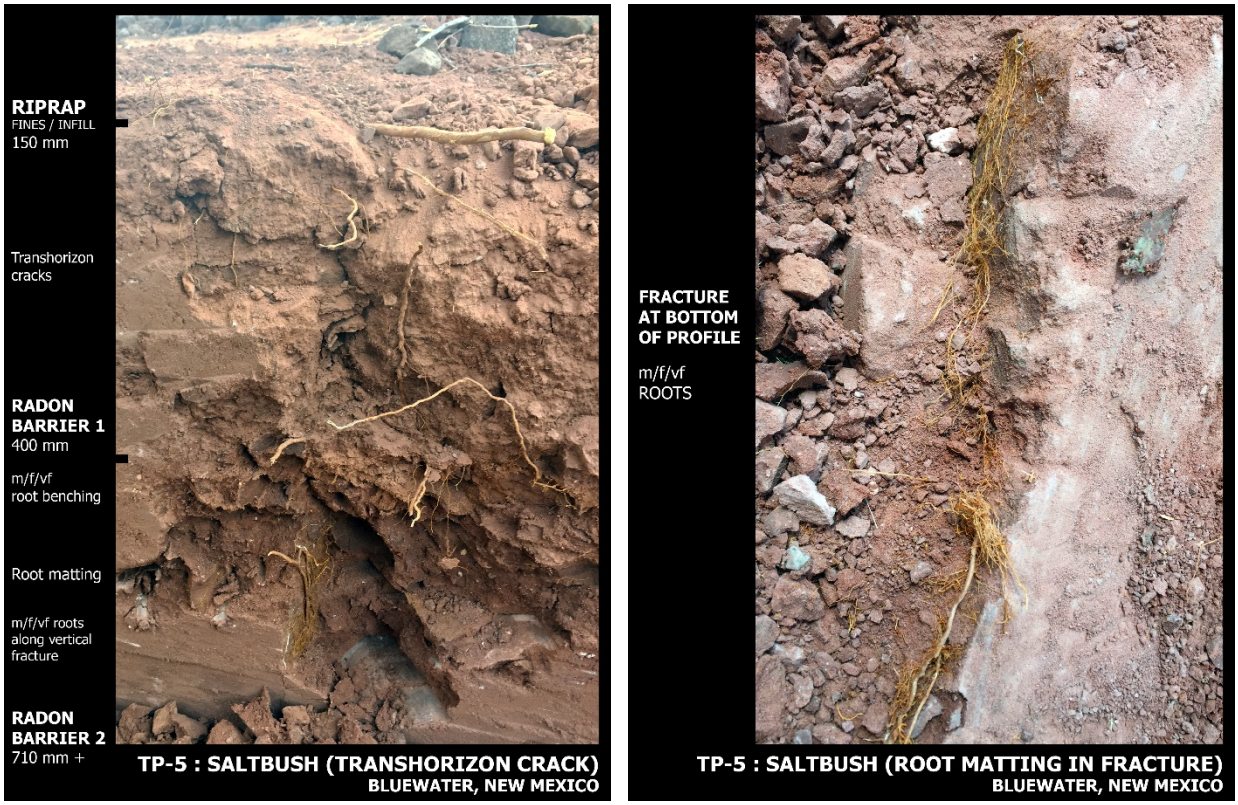

Figure 6-13 Rooting Along Fractures Under Saltbush at the Bluewater, New Mexico, Disposal Cell

Patchy vegetation establishment results in the emergence of gradients of soil morphological impact in the radon barrier. At lateral distances away from the saltbush taproot in TP-5, rooting density decreases with very coarse and coarse roots terminating at 1500 mm away from the plant center. Rock riprap was thinner under the base of the saltbush and increased in thickness with distance from the taproot. Medium, fine, and very fine roots were observed at distances exceeding 2000 mm from the taproot. With exception to greater rupture resistance (cementation) directly underneath the saltbush, soil structuring remains consistent across the 2500 mm horizontal transect (Figure 6-14). Similar patterning was observed in the squirreltail grass gradient (Figure 6-15), with more pronounced variation in soil structuring with distance. At 500 mm away from the edge of the squirreltail grass stand, intermixed platy structures were

observed to a depth of 500 mm, more closely resembling the structure of the less developed ephemeral lake profile (TP-1).

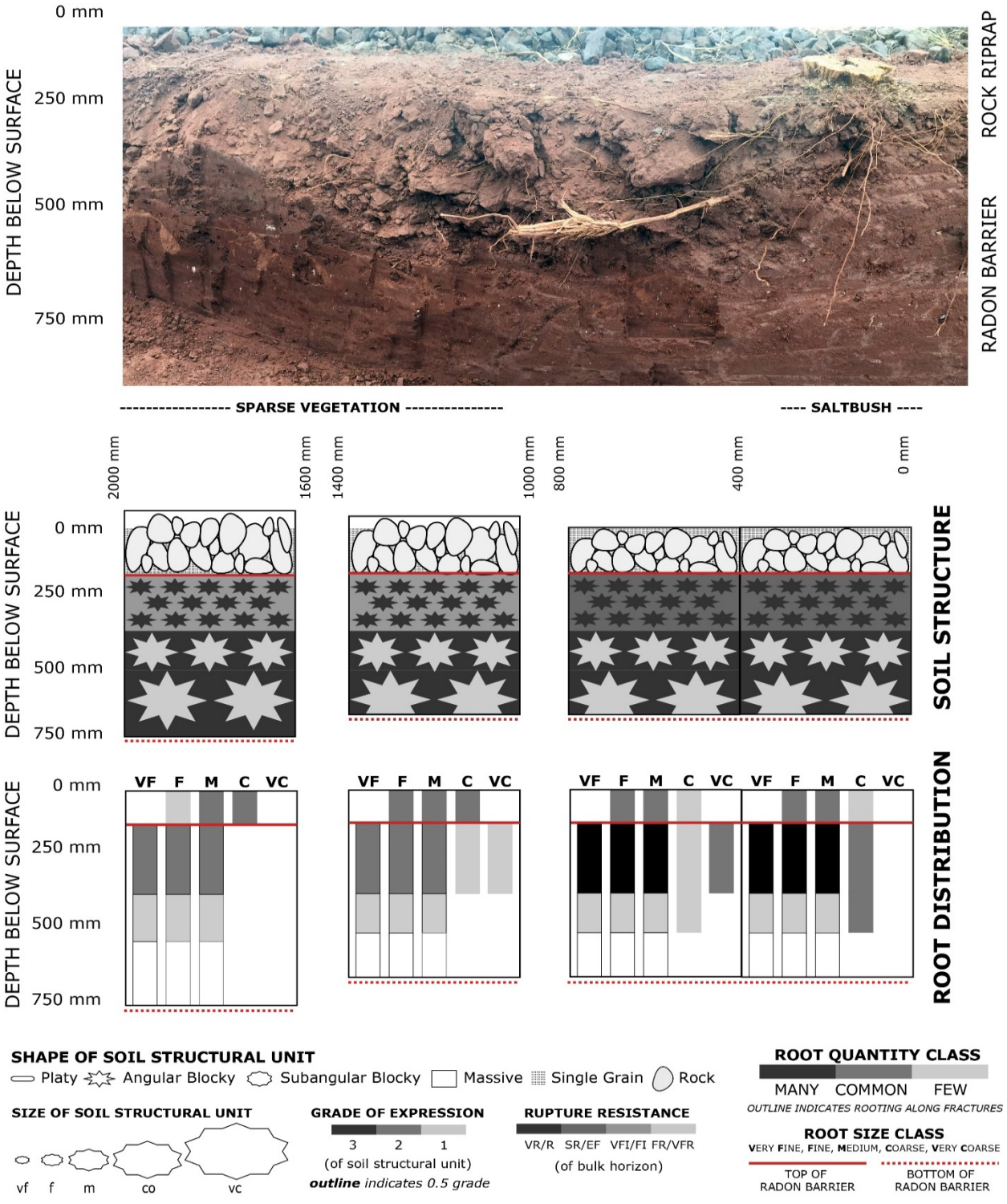

Figure 6-14 Fourwing Saltbush Soil Morphology Impact Gradient (TP-5), Bluewater, New Mexico

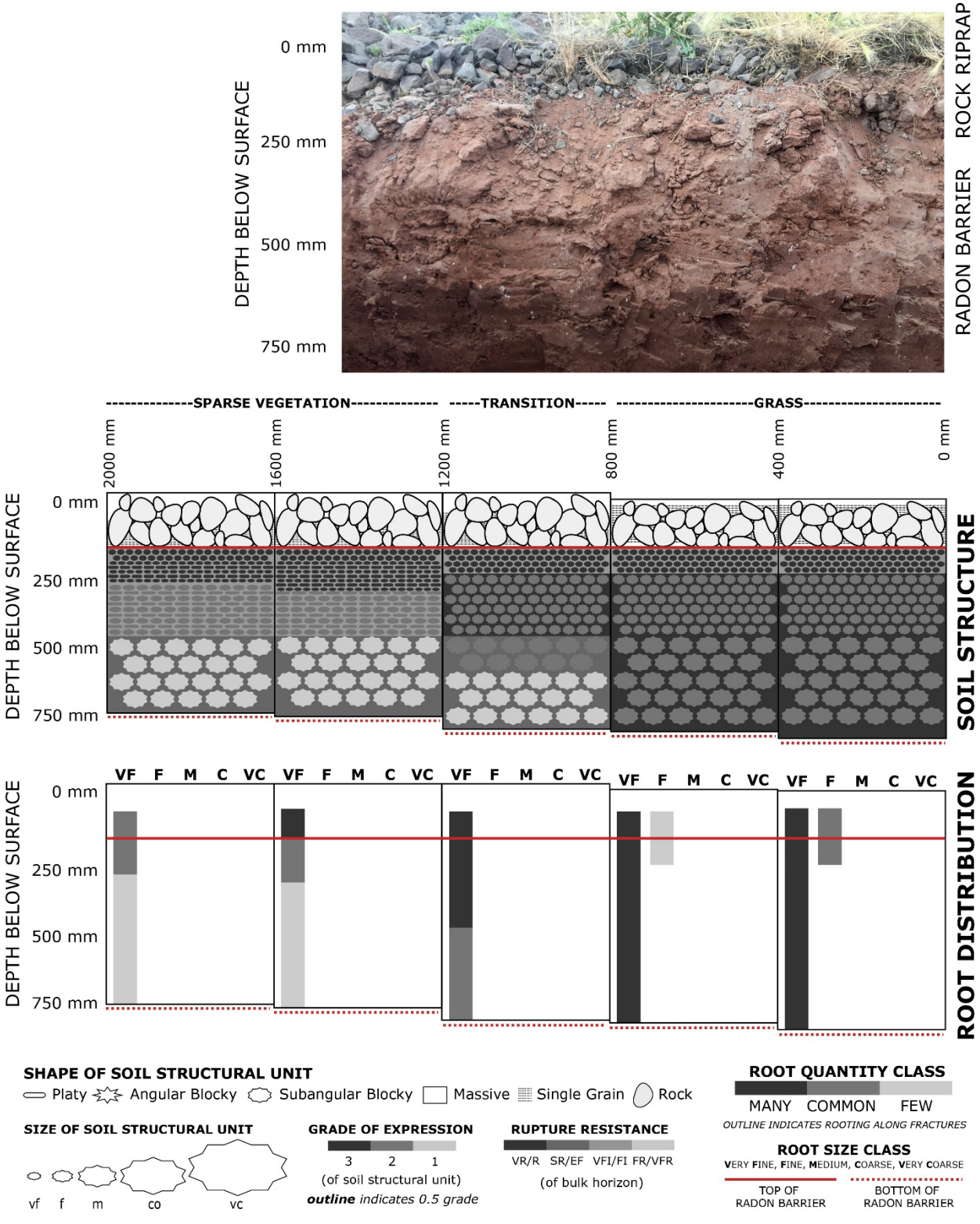

Figure 6-15 Squirreltail Grass Soil Morphology Impact Gradient (TP-2), Bluewater, New Mexico

6.4.2.3 Natural Analogue Soil Morphology

The natural analogue soil profiles are presented in Figure 6-16. Soil structuring in the analogue associated with high desert steppe vegetation on mixed alluvial and aeolian sediments (AN-3) comprises blocky structures of mixed sizes (very fine to medium) and mixed grades that increase in size and decrease in grade with depth (to 1090 mm). A paleosol is encountered from 1090–1780 mm that is characterized by brittle angular structures high in carbonate. Root size, quantity, and class decrease with depth—with coarse rooting occurring to a depth of 970 mm, medium rooting to a depth of 1090 mm, fine rooting to a depth of 1420 mm, and very fine rooting through the depth of the observed profile (1780 mm).

Soil structuring in the desert pavement analogue (AN-6) is composed of very fine blocky structures to the top of fractured basalt (660 mm). Root size, quantity, and class decrease with depth, with medium, fine, and very fine rooting occurring through fractured basalt through the depth of the observed profile (960 mm).

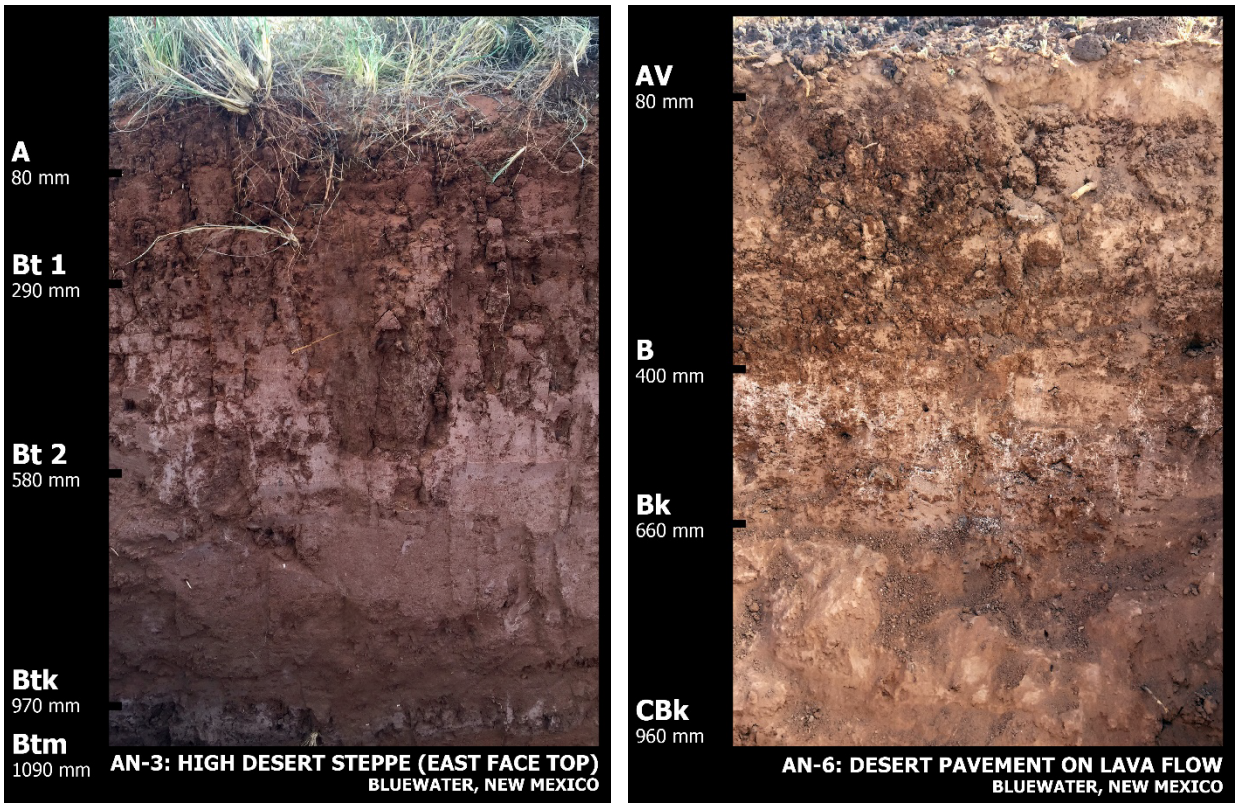

Figure 6-16 Natural Analogue Soil Profiles at the Bluewater Site

6.4.2.4 Comparison of Soil Morphology in the Radon Barrier to the Natural Analogues

The soil morphology at 500–750 mm below ground surface of the radon barrier and natural analogues (AN-3 and AN-6) is summarized in Table 6-7. The ant mound (MP-2), grass (TP-2), and saltbush (TP-5) profiles most resemble the analogues with regards to structuring and rooting (when overlaid). A profile on the cover that had both saltbush and grass would

presumably contain radon barrier morphology that most resembles the high desert steppe analogue (AN-3). The sparse vegetation (TP-4) and the dry ephemeral lakebed (TP-1) are least similar to the analogues and are the least developed profiles on the top-deck of the main cover. As mixed vegetation becomes more developed on the cover, and bioturbation by insects becomes more frequent, average conditions of the radon barrier will begin to resemble that of the analogue. EC is lower in the analogue (AN-3) and most developed radon barriers, and higher in the least developed radon barriers suggesting a connection between profile development and soil hydraulic properties relating to water balance and salt accumulation (AN-6 is excluded as EC values are elevated because the profile sits on top of basalt). This observation is supported by saturated hydraulic conductivity (K_{sat} data), with an inverse relationship between EC and K_{sat}.

Table 6-7 Summary of Soil Condition at 500–750 mm from Ground Surface

	AN-3	AN-6	MP-2	TP-2	TP-5	TP-4	TP-1
	High Desert Steppe	**Desert Pavement**	**Ant Mound**	**Grass**	**Saltbush**	**Sparse Vegetation**	**Dry Lake**
Soil structure	2m sbk	3vf sbk	3f pl; 3vf abk	2m sbk	1vc abk	Massive	Massive
Root morphology	1c 1m 2f 3vf	1m 1f 3vf	1f 2vf	3vf	3m 3f 3vf (in fractures)	No roots	No roots
Texture[a]	SCL	CL	L	C	FSL	SCL	FSL
Dry density (g/cm^3)[b]	-	-	-	1.72	-	1.89	1.95
Gravimetric H_2O %[b]	-	-	-	10.0%	7.0%	9.0%	13.0%
SOM %	1.62%	2.71	1.88%	1.60%	0.74%	0.84%	0.38%
pH	8.71	8.48	8.23	8.16	8.67	8.71	8.58
EC	0.07	4.96[c]	1.10	0.96	5.20	8.20	3.40
K_{sat}[d] (m/s)	4.38E-06	-	4.72E-06[e]	2.77E-06	-	4.70E-08	1.34E-08

[a] USDA (2012) textural soil classification.
[b] From Stefani (2016) and Michaud (2018).
[c] Benched on top of basalt.
[d] See Sections 3 and Section 7 for full reporting on K_{sat}.
[e] Measured in TP-6 ant mound profile at depth of 860 mm.

6.4.3 Shirley Basin South, Wyoming

Seven profiles were excavated on the Shirley Basin South disposal cell cover in September 2017, with one analogue profile excavated in June 2018. After 17 years of service, the disposal cell was characterized by a uniform stand of mixed perennial forage grasses dominated by blue grama (*Bouteloua gracilis),* western wheatgrass *(Pascopyrum smithii),* and needlegrass (*Hesperostipa comate)* interspersed with occasional fourwing saltbush (*Atriplex canescens*) and chickpea milkvetch (*Astragalus cicer*) (Figure 6-17). The rock riprap side slope was characterized by patchy areas of sediment infill interspersed with mixed perennial grasses including blue grama and western wheatgrass. The top of the disposal cell is actively grazed by cattle and pronghorn antelope. Noxious weeds are sprayed with herbicide as needed. The full soil and vegetation survey is reported elsewhere (DOE 2021c).

Figure 6-17 Surface and Vegetation Condition on the Disposal Cell at Shirley Basin South, Wyoming

The top deck of the disposal cell at the Shirley Basin South site is a vegetated topsoil cover while the side slope is a rock riprap with frost protection cover. On the top deck of the disposal cell, topsoil thickness ranged from 230–410 mm while the thickness of the sandy overburden fill layer ranged from 570–680 mm. The depth from ground surface to the top of the radon barrier ranged from 890–1140 mm. Radon barrier thickness ranged from 480–860 mm, with individual lift events ranging from 60–230 mm. The as-built condition of the cell displayed less profile-to-profile variability in material thickness than the Bluewater or Lakeview sites and was slightly more variable than the Falls City site.

6.4.3.1 Structuring in the Radon Barrier and Cover Materials

The radon barrier at the Shirley Basin South site was devoid of visually observable emergent soil structuring. Soil structuring was limited to the topsoil layers and composed of blocky structures of mixed sizes (very fine to medium) that generally increased in size with depth and well-developed grades that remained consistent with depth. The sandy overburden fill layer was single grain/massive and largely structureless apart from occasional vertical fractures. Variation in sandy overburden fill layer materials were commonly observed and characterized by horizontal iron staining along laminar planes of variable grain size (Figure 6-18). Overburden and radon barrier materials were very hard in the mixed grass profile (DC-4), and no structural development was observed below the topsoil layer.

Variations in radon barrier rupture resistance were common between lift-and-compaction events as indicated by the shading in bulk soil horizons presented in Figure 6-2. As with the Falls City site, remnant soil structure from borrow pit materials were observed in the radon barrier as

indicated by variations in color, but the units were structurally indecipherable to the massive bulk soil matrix upon visual inspection.

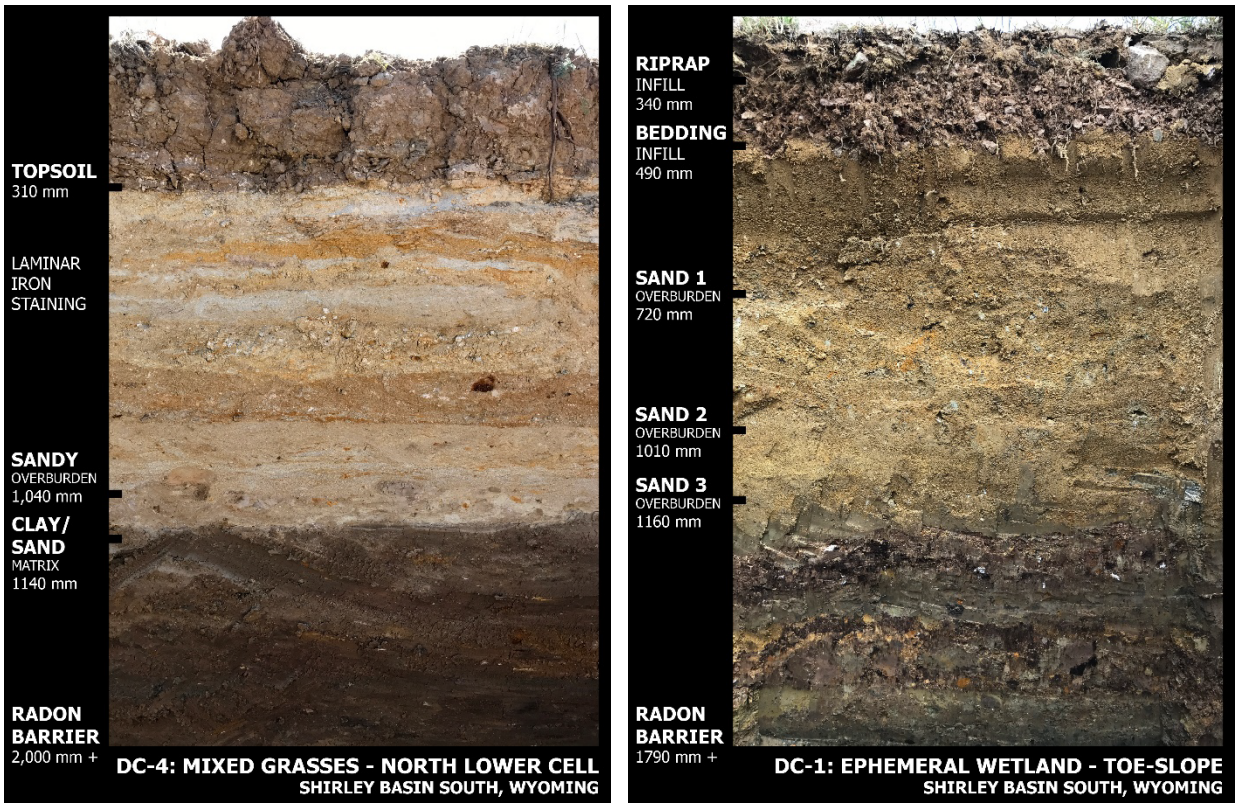

Figure 6-18 Soil Profile Sections on the Disposal Cell at Shirley Basin South, Wyoming

The profile observed on the toe slope associated with ephemeral ponding and wetland plant ecology (DC-1) had a 340 mm rock riprap cover, with 40 mm of rock riprap infill dominated by moderately decomposed plant litter and 170 mm of illuvial fines transported from upslope. Rock riprap was located atop a 150 mm sandy/infilled gravel drainage layer, with a 670 mm sandy overburden fill layer underneath. The top of the radon barrier was observed at 1160 mm below ground surface. The radon barrier was found in a saturated state with no observable structuring.

The profile observed on the rock riprap side slope associated with pocket gopher burrowing (likely *Thomomys clusius*) (DC-6) had an 80 mm rock riprap cover on top of a 160 mm sandy/infilled gravel drainage layer with a 970 mm sandy overburden fill layer underneath. The top of the radon barrier was observed at 1170 mm below ground surface. The radon barrier appeared to be saturated given the presence of flowing water. The observed pocket gopher burrow was confined to a 2000 mm radius on the surface. Burrow tunnels extended underneath the rock riprap and gravel layers to a depth of 330 mm, terminating in the first 80 mm of the sandy overburden fill material, resulting in the intermixing of gravels and fill material. Rodent burrowing had no direct impact on radon barrier morphology (Figure 6-19).

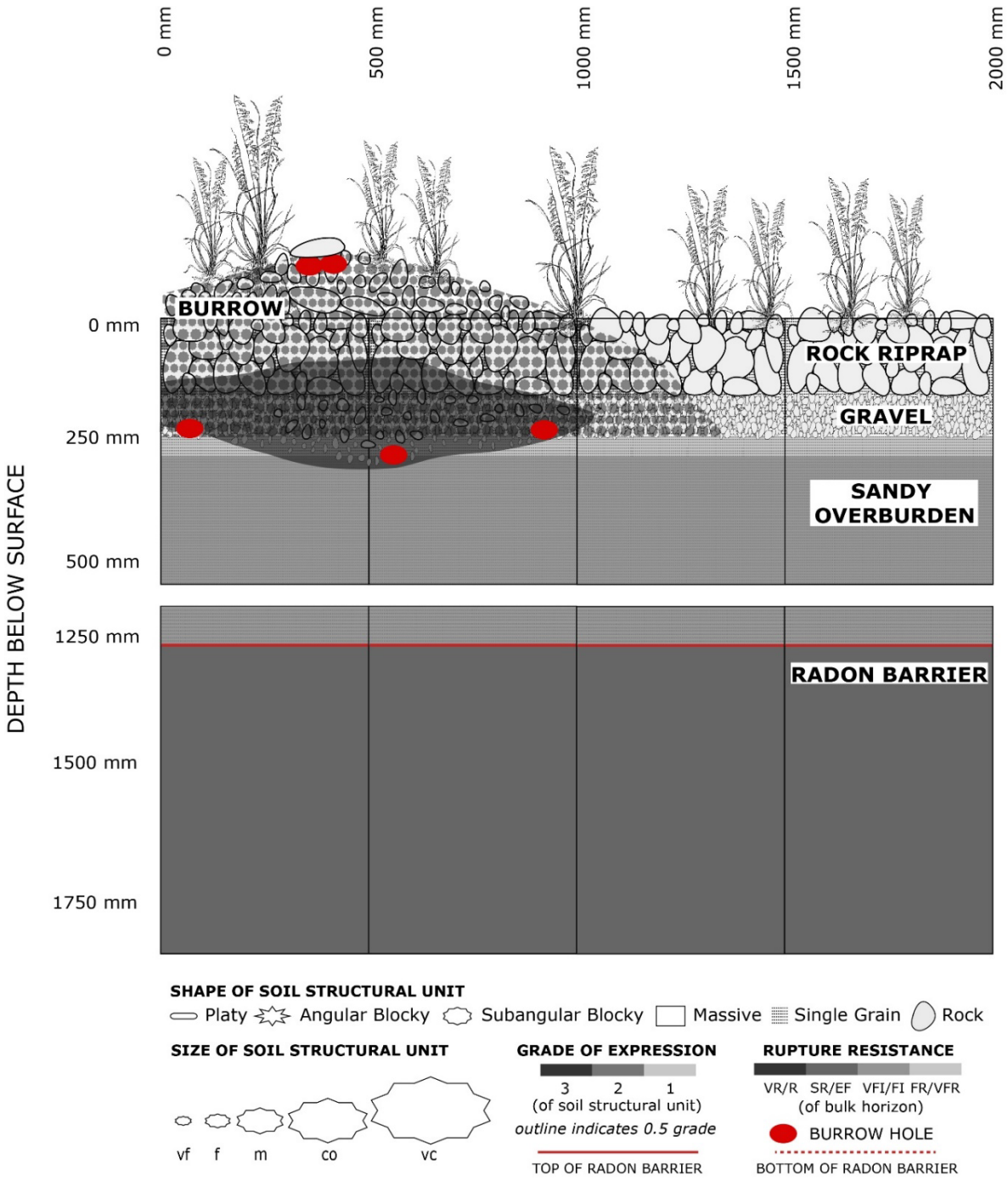

Figure 6-19 Pocket Gopher Mixing of Rock Riprap and Gravel Layers, Shirley Basin South, Wyoming

6.4.3.2 Plant Rooting in the Radon Barrier and Cover Materials

Most roots larger than very fine were constrained to the top 600 mm of the cover profiles and within emergent fractures in the sandy overburden fill layer. Roots larger than medium were associated with chickpea milkvetch (DC-2) and fourwing saltbush (DC-5). Saltbush roots in DC-5 benched atop a compacted clay lens in the sandy overburden fill layer at 560 mm. Across all profiles, no roots larger than very fine were observed in the radon barrier. Sparse amounts of very fine roots traveled through the thickness of the radon barrier (in excess of 2010 mm) in two of the four main deck profiles, and both profiles associated with the side slope. The rock riprap profile associated with the ephemeral wetland at the toe of the side slope (DC-1) had the greatest density of very fine plant rooting in the radon barrier. Up-cell profile DC-3 had the least rooting in the radon barrier, and very fine roots were constrained to the first 60 mm of the radon barrier corresponding to the most acidic conditions observed on the cover (pH 3.48).

6.4.3.3 Natural Analogue Soil Morphology

The natural analogue soil profile is presented in Figure 6-20. The soil structure in the analogue is comprised of blocky to prismatic structures of mixed sizes (very fine to very coarse) and mixed grades that increase in size and decrease in grade with depth (to 1000 mm). At 1000 mm below ground surface, soil structure in the analogue becomes massive, with very infrequent fractures to a depth of 1610 mm. Root size, quantity, and class slightly decrease with depth, with medium rooting occurring to a depth of 310 mm, fine rooting to a depth of 1000 mm, and very fine rooting through the depth of the observed profile (1610 mm). Rooting along fractures is common to a depth of 1000 mm and exclusive to fractures from 1000–1610 mm.

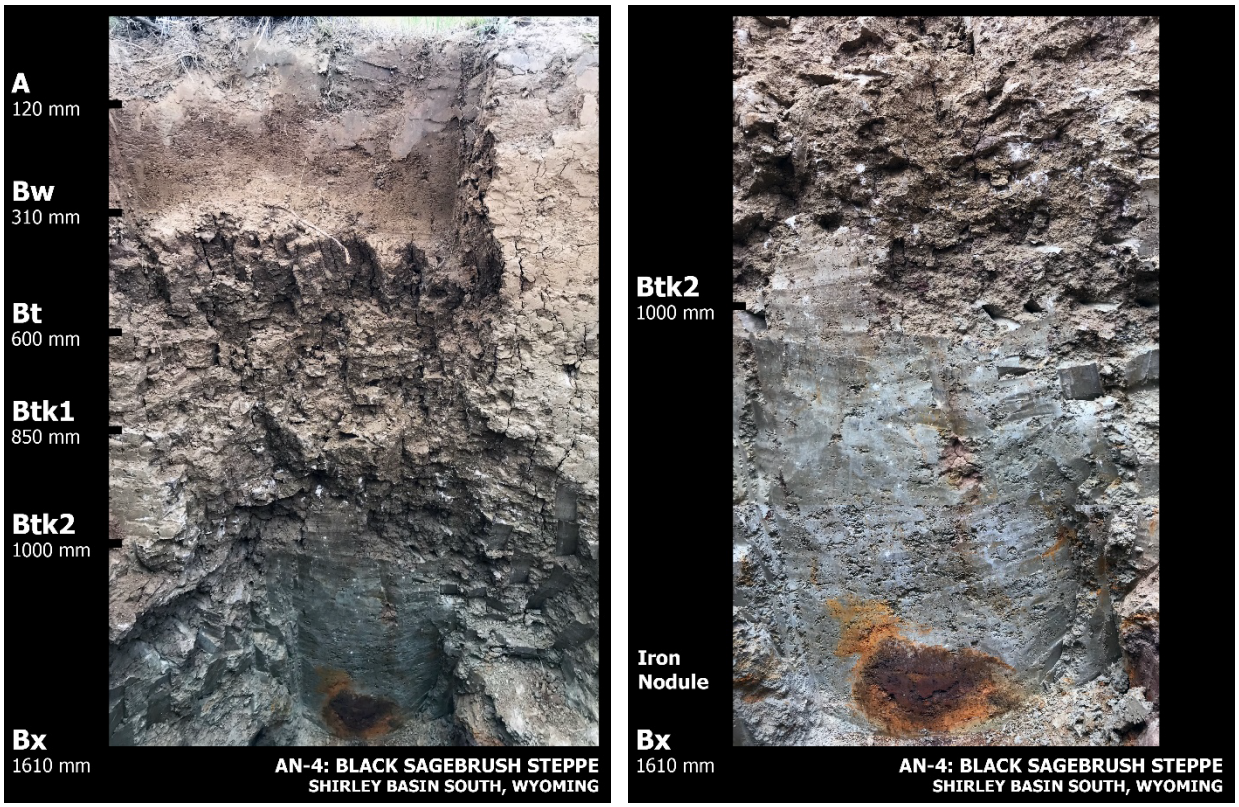

Figure 6-20 Natural Analogue Soil Profile at the Shirley Basin South Site

6.4.3.4 Comparison of Soil Morphology in the Radon Barrier to the Natural Analogue

The soil morphology at 1250–1500 mm below ground surface of the radon barrier and natural analogue is summarized in Table 6-8. The analogue and the cover profiles are all characteristic of very nominal structural development at the depth of the radon barrier. The toe-slope wetland profile (DC-1) had slightly elevated root counts versus other profiles on the cover, likely attributed to greater than cell average soil moisture conditions. Limited structural development is attributed to isolation from surface processes including desiccation cracking and freeze thaw, in addition to the presence of limited roots that would increase desiccation. Low root mass is attributed to acidic soil conditions that presumably limit nutrient uptake. Such conditions naturally protect as-built radon barrier engineering properties including K_{sat}. Given analogue condition, it is likely that the radon barrier will not appreciably change over regulatory time frames if soil-forming factors remain constant (see Appendix H).

Table 6-8 Summary of Soil Condition at 1250–1500 mm from Ground Surface

	AN-4	DC-1	DC-2	DC-5	DC-3
	Sagebrush Steppe	**Wetland**	**Mixed Grasses**	**Saltbush / Mixed Grasses**	**Mixed Grasses**
Soil structure	Massive	Massive	Massive	Massive	Massive
Root morphology	2vf	3vf	1vf	1vf	None
Texture[a]	CL	C	C	C	CL
Dry density (g/cm^3)[b]	-	-	1.52	1.48	1.69
Gravimetric H_2O%[b]	-	-	23.0%	32.0%	25%
SOM %	2.84%	3.98%	4.32%	6.56%	4.03%
pH	5.10	4.95	4.55	3.59	3.48
EC	0.45	0.81	1.26	5.13	2.30
K_{sat}[c] (m/s)	9.81E-09	-	4.90E-09	1.24E-10	6.6E-09

[a] USDA (2012) textural soil classification.
[b] From Stefani (2016) and Michaud (2018).
[c] See Section 3 and Section 7 for full reporting on K_{sat}.

6.4.4 Lakeview, Oregon

Seven profiles were excavated on the disposal cell at the Lakeview site in October 2017, with two analogue profiles excavated in June 2018. After 28 years of service, the disposal cell was characterized by moderate surface condition patchiness, approaching that of the sagebrush steppe environment of the surrounding lowlands (Figure 6-21). Surface conditions include sparsely vegetated interstices between shrubs; zones of mixed native grasses dominated by western wheatgrass (*Pascopyrum smithii*) and sheep fescue (*Festuca ovina*); patches of invasive cheatgrass (*Bromus tectorum*); distributed antelope bitterbrush (*Purshia tridentata*), rubber rabbitbrush (*Ericameria nauseosa*), big sagebrush (*Artemisia tridentata*); and infrequent Great Basin pocket mouse (*Perognathus parvus*) burrows. The rock riprap side slope was largely unvegetated, with infrequent patches of thickspike wheatgrass (*Elymus lanceolatus*) and slender wheatgrass (*Elymus trachycaulus*). Management for deep-rooted plants, including western juniper (*Juniperus occidentalis*), consists of hand cutting and spraying with herbicide. Noxious weeds are also sprayed with herbicide as needed. The full soil and vegetation survey is reported elsewhere (DOE 2021d).

The top deck of the disposal cell at the Lakeview site is a vegetated rock-soil multicomponent cover, while the side slope is a rock riprap with bedding cover. On the top deck of the disposal cell, topsoil thickness ranged from 10–270 mm. Topsoil application, surface erosional scouring, and downward infill of topsoil into the interstices of riprap and gravels was inconsistent across the cell. An organic horizon composed of leaf litter was frequently observed in profiles associated with shrubs and ranged in thickness between 0–70 mm, with decreasing thickness at an increasing distance from the base of the tap root. The depth from ground surface to the top of the radon barrier ranged from 510–780 mm. Radon barrier thickness ranged from 330–650 mm. Variation in the as-built condition was evident in inconsistent lift-and-compaction horizon thickness (70–160 mm), color of radon barrier lift events, radon barrier gravel content, and variation in remnant soil structure within radon barrier lift-and-compaction events.

Figure 6-21 Representative Surface and Vegetation Condition on the Disposal Cell at Lakeview, Oregon

6.4.4.1 Structuring in the Radon Barrier

Blocky and massive structures were present in the radon barrier, with decreased structuring observed with increased depth from ground surface (Figure 6-2). The side slope profiles (DC-4A and DC-4B) were very moist with active downslope water shedding observed and no visible structuring in the radon barrier (Figure 6-22). The profile associated with sheep fescue (DC-13) had blocky structures of mixed sizes (fine to medium) that increased in size with depth and of mixed grades decreasing in intensity with depth to a depth not exceeding 820 mm. Profiles DC-2.2000 mm, DC2.2500 mm, DC-5, DC-13, and DC-4A/DC-4B contained sections of radon barrier that remained massive and did not display visually pronounced soil structuring. The profile associated with sparse vegetation (DC-10) had blocky structures of mixed sizes (medium to very coarse) that increased in size with depth and of mixed grades decreasing in intensity with depth.

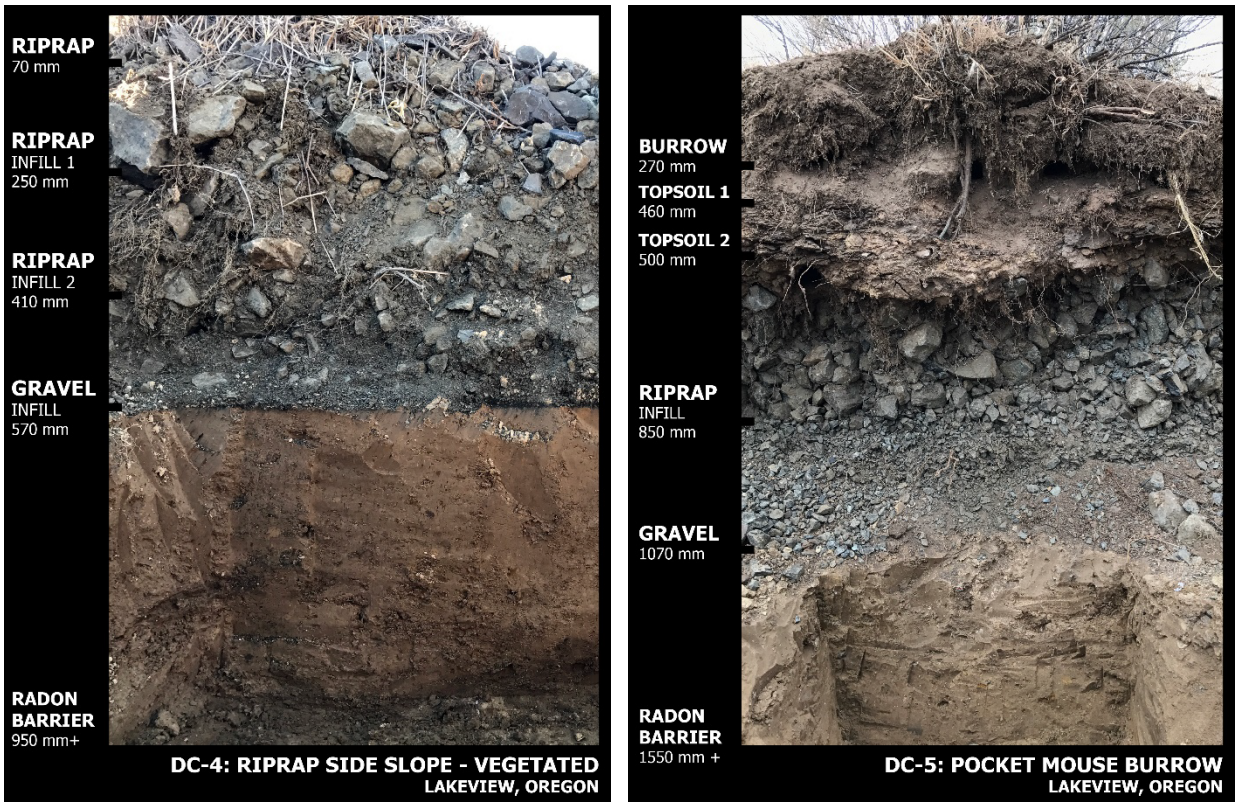

Figure 6-22 Soil Profile Sections on the Disposal Cell at Lakeview, Oregon

Numerous horizontal impact gradients were observed on the disposal cell cover with each having distinct morphological patterning. The profile associated with pocket mouse burrowing (DC-5) had a 270-mm-high mound of transported materials above the rock riprap (Figure 6-23). The center of the mound occurred on top of a 100 mm depression in the rock armor. The depression could be an as-built heterogeneity that created a favorable condition for burrowing or the result of the burrowing process itself. A young rabbitbrush was located on top of the active burrow with an extensive network of tunnels occurring directly beneath the plant to a depth of 360 mm below mound surface. All burrows were confined above the rock admixture boundary. The radon barrier had intermixed blocky structures of mixed sizes (course to medium) to a depth not exceeding 1400 mm across the transect. The pocket mouse burrow at the Lakeview site did not directly displace any of the radon barrier materials.

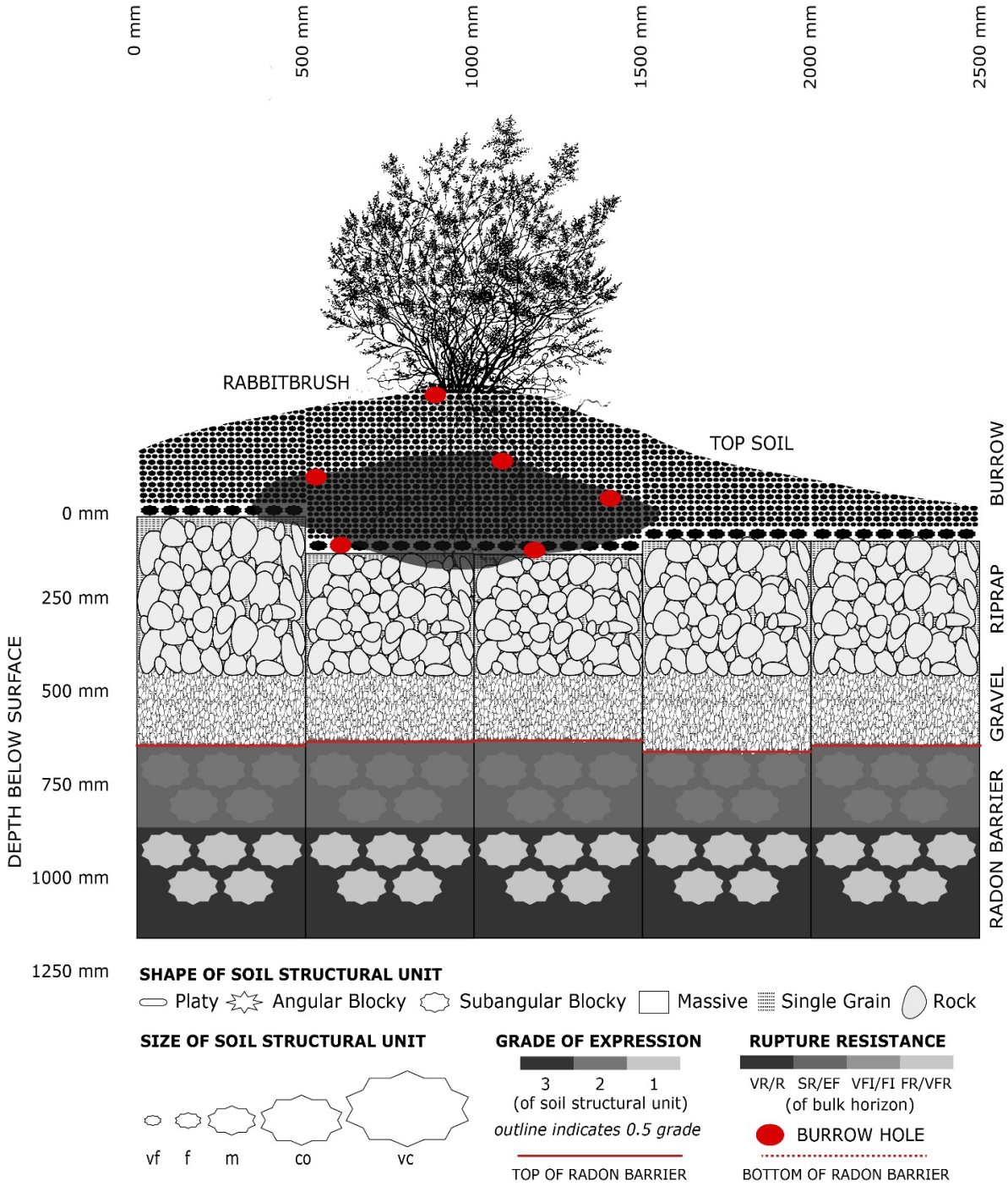

Figure 6-23 Great Basin Pocket Mouse Burrow Perched Above Rock Riprap (DC-5), Lakeview, Oregon

The radon barrier associated with mature rabbitbrush (DC-12) was characterized by blocky structures of mixed sizes (fine to coarse) that increased in size with depth, and of mixed grades decreasing in intensity with depth (Figure 6-24). As distance from plant center increased horizontally, grade decreased across all sizes over a 2000 mm distance. The greatest soil

structuring was observed in the radon barrier directly underneath the rabbitbrush. Structuring was observed through the depth of the profile (more than 1090 mm) across all DC-12 transect locations. Similar radon barrier structuring was observed in the rodent burrow profile with young rabbitbrush (DC-5).

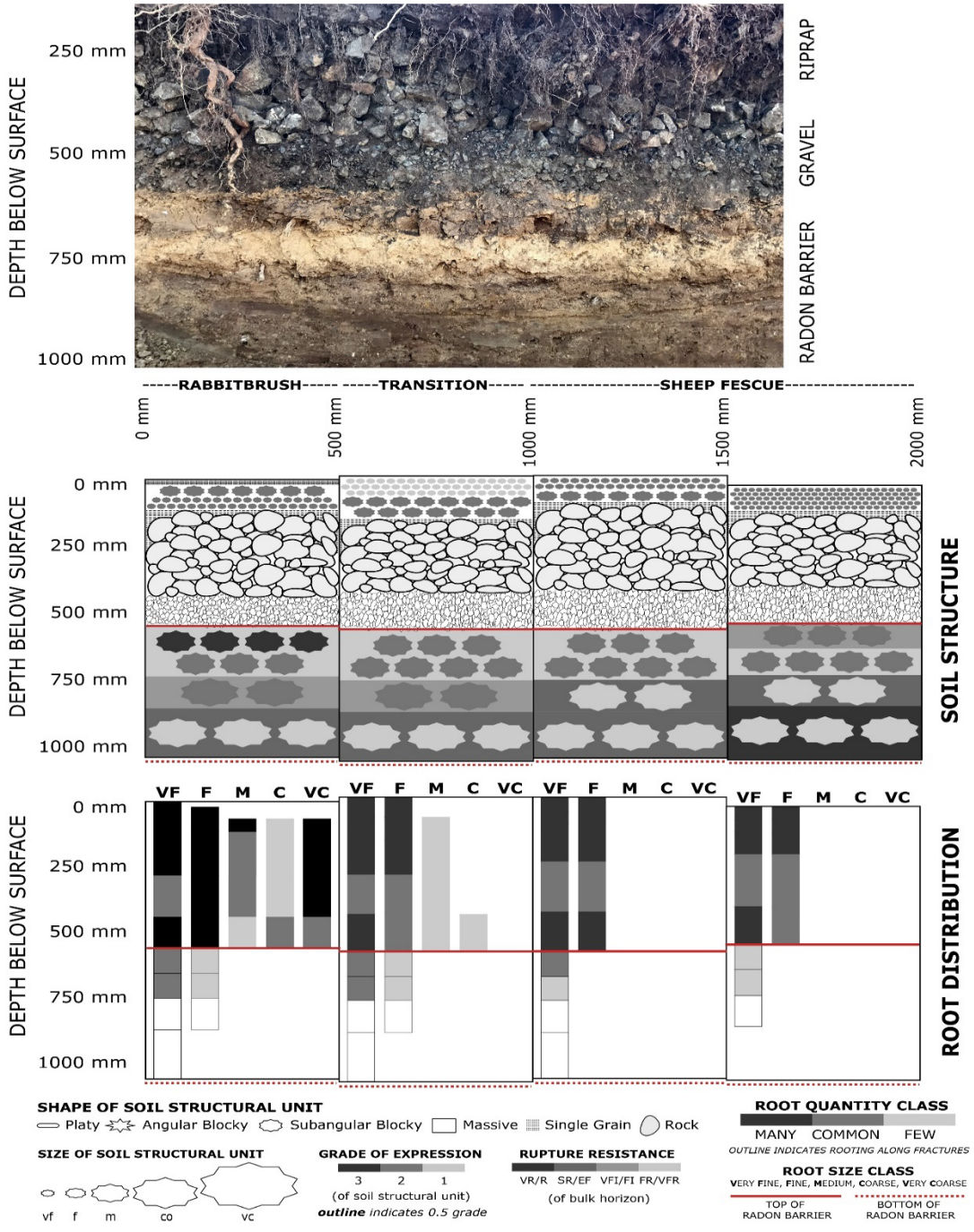

Figure 6-24 Rabbitbrush Soil Morphology Impact Gradient (DC-12), Lakeview, Oregon

The mature bitterbrush profile (DC-2) had blocky structures of mixed sizes (fine to coarse) that generally increased in size with depth and were of mixed grades that generally decreased in intensity with depth (Figure 6-25). Soil structuring was most developed in the radon barrier directly underneath the bitterbrush and decreased in intensity with horizontal distance away from plant center. At 1500 mm from plant center, radon barrier sections below 900 mm displayed no structural development. Such observations suggest that the lateral impact to soil structural development associated with a single bitterbrush of this age is most significant within a 1500-mm radius from plant center.

In addition to correlation with surface condition, depth, and bioturbation, soil structuring at the Lakeview site is influenced by radon barrier lift-and-compaction events. Running counter to observations of depth dependence on soil structuring, bands of larger sized structures were found in between bands of smaller sized structures in profiles DC-5 and DC-2, even under shared rooting condition. Such structure could be attributed to variable soil properties within lift-and-compaction events in addition to the existence of remnant soil structure from borrow materials.

6.4.4.2 Plant Rooting in the Radon Barrier and Cover Materials

Root size, quantity, and depth correspond to vegetation type, with bitterbrush profiles (DC-2 and DC-11) having the greatest variation in root size (very fine to coarse) and quantity. Fine and very fine roots were observed in the bulk soil fraction and throughout the depth of the radon barrier (more than 1100 mm) directly underneath the bitterbrush in DC-2. Coarse roots were observed underneath the bitterbrush in DC-2 to a depth of 910 mm, with medium roots terminating at 970 mm. At horizontal distances away from the plant center, root quantity, class, and depth decrease over distances up to 2000 mm. At horizontal distances of 1000 mm from plant center, the bottom section of the radon barrier was free from plant roots. Medium and coarse roots were observed traveling horizontally (within the radon barrier) along the top interface of a cemented lift-and-compaction event to a distance exceeding 2500 mm from plant center (Figure 6-25).

The rock riprap side slope profile (DC-4), the sheep fescue profile (DC-13), and the transect profile locations at horizontal distances away from the center of shrubs had the least abundance of roots. Roots were not observed through the depth of the radon barrier in DC-4, DC-10, DC-13, or at 2000 mm away from the taproot associated with the bitterbrush at DC-2. Dense root matts were commonly observed along vertical fracture planes in desiccated radon barrier materials. Several of the root filled fractures observed in the rabbitbrush profile (DC-12) traveled through the depth of the radon barrier (more than 1090 mm). Overall, rabbitbrush rooting intensity was less than bitterbrush rooting intensity given the presence of medium and coarse roots in the top section of radon barriers associated with bitterbrush.

Root benching was commonly observed at radon barrier lift-and-compaction event boundaries in locations where underlying materials had greater consistence/cementation. Such lift-and-compaction events served to restrict rooting in the bulk soil, with subsequent rooting confined to fracture planes. The radon barrier generally restricted roots of medium size or larger except profiles directly underneath bitterbrush (DC-2 and DC-11) and within emergent fractures found in rabbitbrush profiles (DC-5 and DC-12). Medium, coarse, and very coarse roots were commonly observed to travel horizontally along the top boundary of the radon barrier, directly underneath the gravel drainage layer. Dead roots of mixed sizes and stages of decomposition were commonly observed in the radon barrier, suggesting that active root turnover is occurring within the barrier at the Lakeview site.

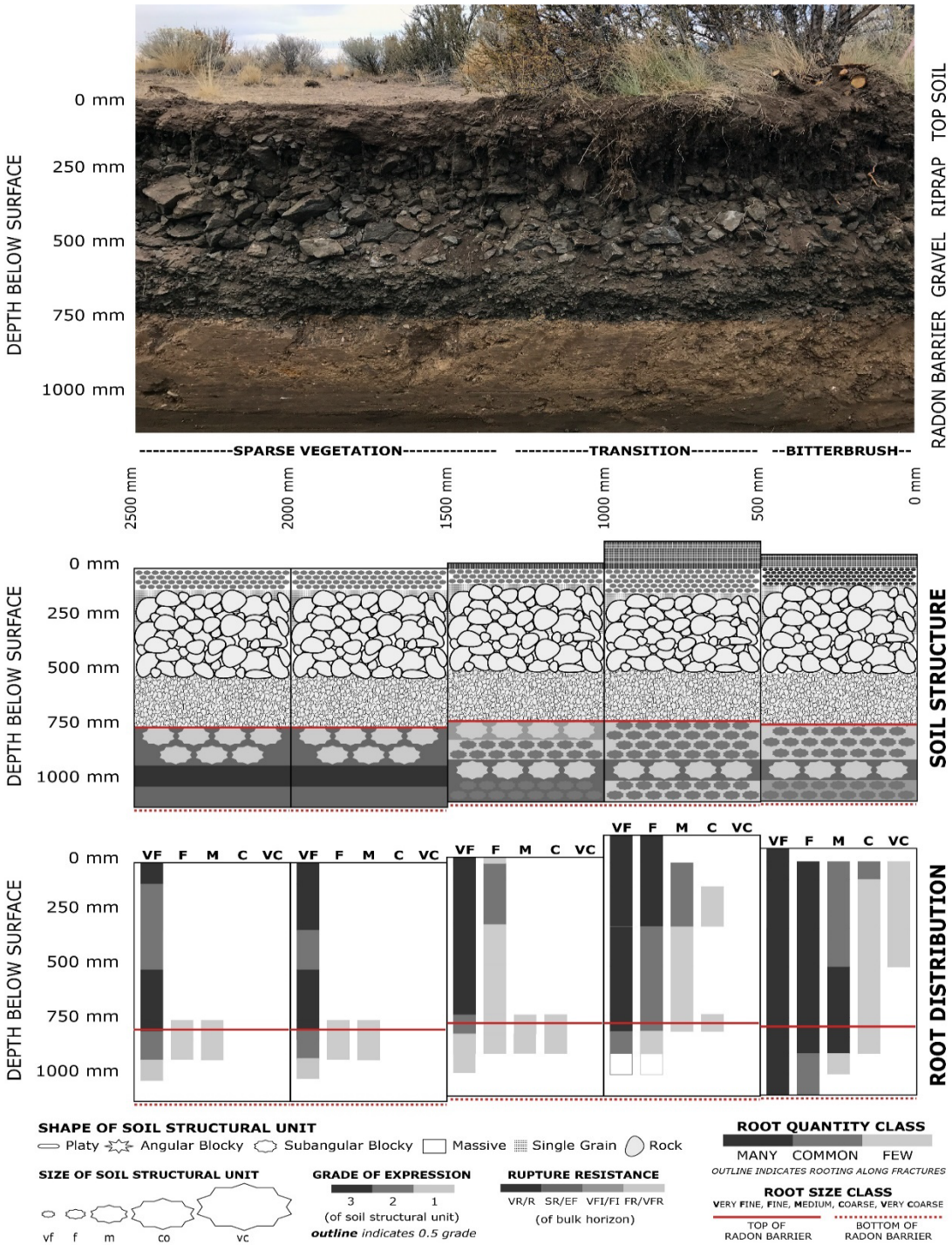

Figure 6-25 Bitterbrush Soil Morphology Impact Gradient (DC-2), Lakeview, Oregon

6.4.4.3 Natural Analogue Soil Morphology

The sagebrush steppe natural analogue soil profile is presented in Figure 6-26. The soil structure in the analogue is composed of blocky structures of mixed sizes (fine to medium) that slightly increase in size and decrease in grade with depth (to 1270 mm). Bioturbation by insect, earthworm, and rodents is very common to a depth of 1020 mm. Root size, quantity, and class slightly decrease with depth, with coarse, medium, fine, and very fine roots occurring through the depth of the observed profile (more than 1270 mm).

Figure 6-26 Natural Analogue Soil Profile at the Lakeview Site

6.4.4.4 Comparison of Soil Morphology in the Radon Barrier to the Natural Analogue

The soil morphology at 750–1000 mm below ground surface of the radon barrier and natural analogue is summarized in Table 6-9. The bitterbrush profile (DC-2) most resembles the analogue with regards to structuring and rooting. The 2000 mm profile away from the bitterbrush and the sheep fescue profile (DC-13) are least similar to the analogue and are the least developed profiles on the top deck of the cover. As deep-rooted vegetation becomes more developed on the cover, average conditions of the radon barrier will begin to resemble that of the analogue. Electrical conductivity (EC) is lower in the analogue and the most developed radon barriers (i.e., DC-2 [0 mm] and DC-12), and higher in the least developed radon barriers (i.e., DC-2 [2000 mm] and DC-13), suggesting a connection between profile development and soil hydraulic properties relating to water balance and salt accumulation. K_{sat} values are within one order of magnitude between profiles, with some radon barriers sharing K_{sat} with the analogue.

Table 6-9 Summary of Soil Condition at 750–1000 mm from Ground Surface

	Analogue	DC-2 (0 mm)	DC-12	DC-2 (2000 mm)	DC-13
	Sagebrush Steppe	**Bitterbrush**	**Rabbitbrush**	**Bitterbrush**	**Sheep Fescue**
Soil structure	2m sbk	2f sbk	2co sbk / 1vc sbk	Massive	Massive
Root morphology	1c 1m 2f 3vf	1c 3m 3f 3vf	2f 3vf (fracture planes)	1vf	None
Texture[a]	SCL	L	L	L	SIL
Dry density (g/cm^3)[b]	-	1.36	1.26	-	1.36
Gravimetric H_2O %[b]	-	30.0%	30.0%	-	36.0%
SOM %	1.91%	2.80%	2.50%	2.72%	2.79%
pH	6.62	6.57	7.01	7.49	7.05
EC	0.03	0.04	0.08	0.20	0.75
K_{sat}[c] (m/s)	3.06E-06	1.10E-07	1.69E-07[d]	-	-

[a] USDA (2012) textural soil classification.
[b] From Stefani (2016) and Michaud (2018).
[c] See Sections 3 and Section 7 for full reporting on K_{sat}.
[d] Measured at ~500 mm away from taproot.

6.4.5 Physical and Chemical Characteristics of UMTRCA Covers and Analogues

Several physical and chemical properties of cover materials, radon barriers, and analogue soils at the depth of the radon barrier, are reported to aid in interpreting processes of soil development.

6.4.5.1 Soil Texture

Across the four sites surveyed, the percentage of clay fraction within the radon barrier ranged from 8–68% and represented nine of the 12 USDA textural soil classifications (Figure 6-27). Radon barrier materials at Falls City, Shirley Basin South, Bluewater, and Lakeview sites were of marine, lacustrine/fluvial, aeolian/fluvial, and lacustrine/fluvial origin, respectively. Textural heterogeneities were observed between radon barrier lift-and-compaction events in the same profile, with coarser textured sand lenses embedded within individual radon barrier lift events, and between remnant soil structure within the same radon barrier lift event. Such variation presumably results from the use of different borrow pit soil horizons that were mixed during material sourcing, transport, and installation.

6.4.5.2 Clay Mineralogy

The variation in radon barrier clay mineralogy within and between the four sites is presented in Figure 6-28. The relative abundance of smectite group minerals ranges from 38–76% across sites. The Bluewater site had the lowest smectite percentage in the radon barrier while the Shirley Basin South site had the highest. In radon barriers with high smectite percentages, changes to soil moisture can play a significant role in regulating radon barrier morphology. The mineralogy within and between sites should be considered when interpreting engineering performance and comparing trends in soil change between sites.

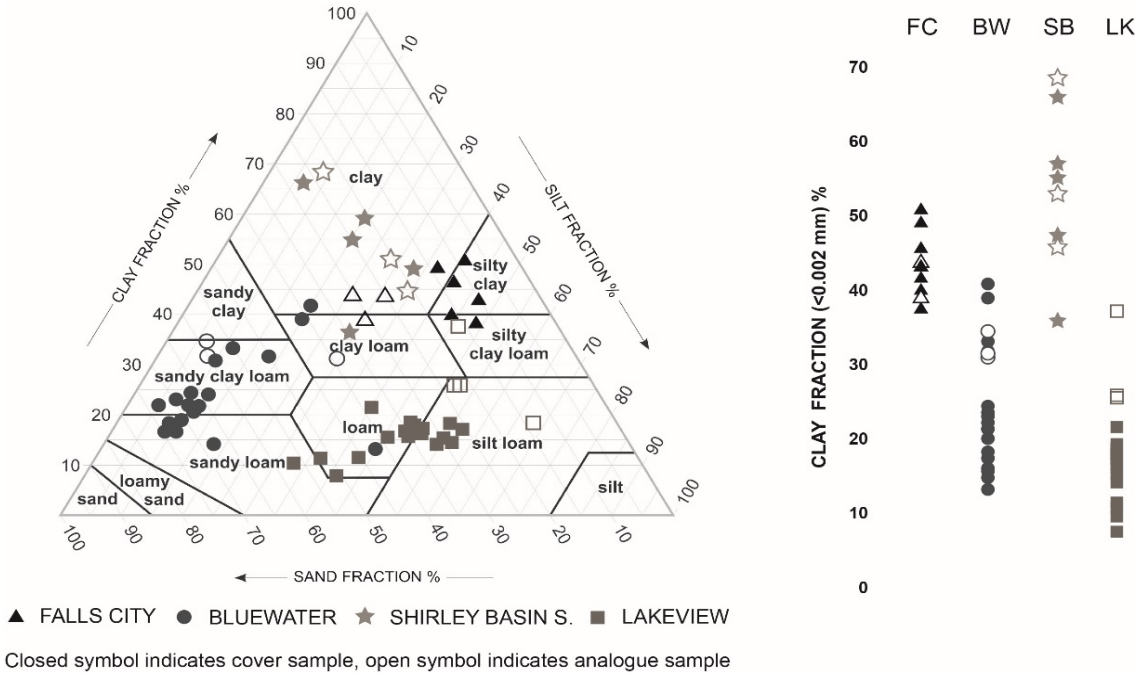

Figure 6-27 Soil Texture Found in Four UMTRCA Radon Barriers and Analogues

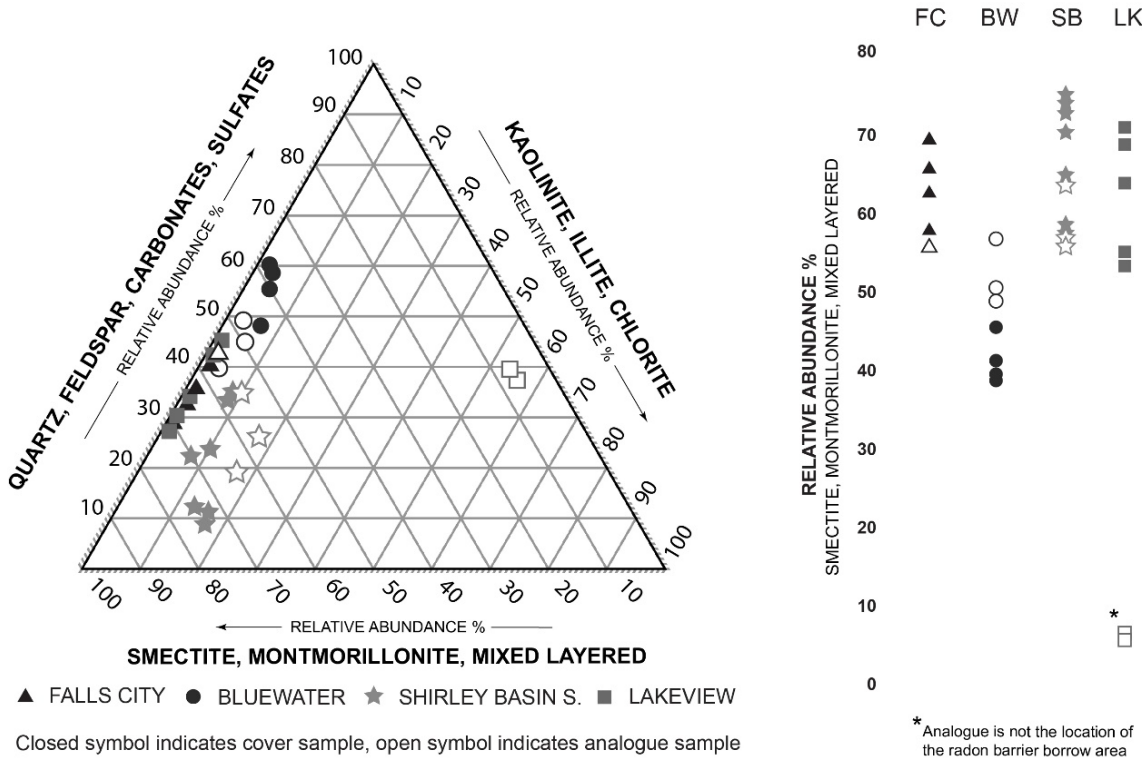

Figure 6-28 Clay Mineralogy Found in Four UMTRCA Radon Barriers and Analogues

6.4.5.3 Soil Organic Matter

With exception to the cover at the Shirley Basin South site, soil organic matter (SOM) percentage generally decreased with depth from ground surface (Figure 6-29). In Figure 6-29, profiles in waste covers are displayed as solid lines, while analogue profiles are displayed as dashed lines. At the Bluewater site, locations associated with perennial grasses and ants had the highest amounts of SOM with depth. At the Lakeview site, SOM was greatest at the surface, dissipating with depth to the top of the radon barrier. Within the radon barrier at the Lakeview site, SOM was highest at the top, decreasing slightly with depth across all surface conditions observed. Such depth trends are common to native steppe and grassland soils as rates of carbon accumulation are primarily concentrated in the active rooting zone (Rumpel and Kögel-Knabner 2011).

At the Falls City and Shirley Basin South sites, the top portion of the overburden layers had a greater amount of SOM than the lower section of the subsoil/rooting layers, indicating that additions of SOM have likely occurred at the surface and decreased with depth, a trend that matches natural analogues in both areas. SOM percentage in the radon barrier at the Shirley Basin South site was the highest of all sites investigated. This could be attributed to the presence of parent materials presumably made from carbonaceous shales (Harshman 1972).

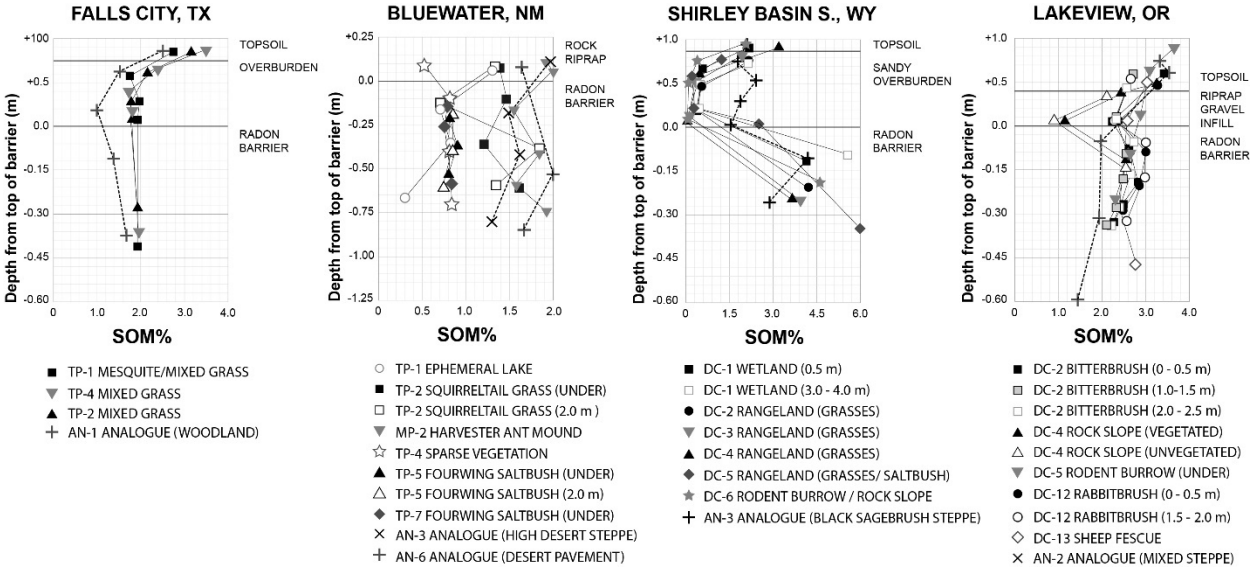

Figure 6-29 Distribution of Soil Organic Matter in Four UMTRCA Covers and Analogues

The relationship between the soil organic matter percent, soil structural unit size, and grade (degree of aggregation) in the radon barriers at the Lakeview and Bluewater sites is presented in Figure 6-30. Considering set averages, as soil organic matter increases, soil structural unit size tends to decrease at Bluewater, while no relationship is evident at the Lakeview site.

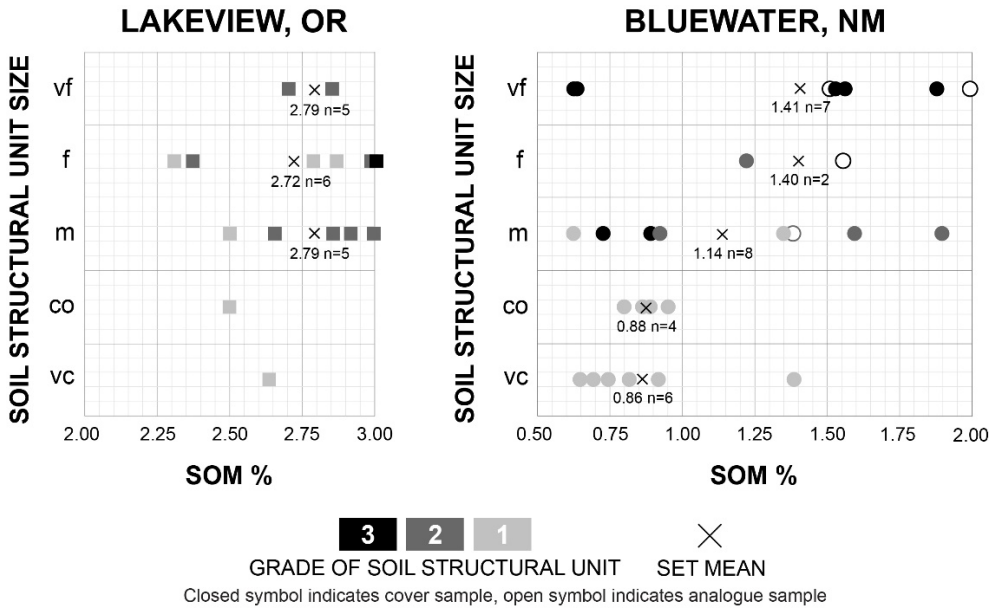

Figure 6-30 Relationship Between Soil Organic Matter Percent and Soil Structural Unit Size

Soil structural unit size contributes to the regulation of hydraulic conductivity (Benson et al. 1994; Lin et al. 1999). As such, feedbacks between vegetation establishment, soil organic matter deposition, and evolved soil ped size in bioturbated radon barriers is of importance. However, given the heterogeneity of radon barrier construction materials from borrow areas, the presence of cofactors that influence soil structuring (i.e., depth to ground surface, surface condition, and construction heterogeneity) in addition to the various co-occurring processes that influence structuring in CMBs (see Appendix H), untangling the factors that contribute to soil structural unit size distribution is complex and beyond the scope of this section. On a highly simplified level, and given the significance of plant-soil feedbacks to near surface soil-carbon dynamics, shallow rock riprap covers with emergent vegetation (such as the Bluewater site) are likely most prone to the emergence of carbon stabilized soil structure over multi-decadal time frames with impacts to hydraulic properties. Other binding agents, such as calcium carbonate ($CaCO_3$), silica, and pedogenic iron, may also stabilize emergent radon barrier structural units over time.

6.4.5.4 Soil pH

Soil pH values are presented in Figure 6-31. Soil pH is generally neutral at the surface across the four sites. With exception to the Shirley Basin South site, pH varies roughly 1.5 units within the radon barrier across cover conditions and depths. At the Lakeview and Shirley Basin South sites, radon barrier pH decreases with depth from ground surface. Soil pH in the radon barrier at the Shirley Basin South site is very low (3.5–6.7) corresponding to minimal soil structuring (Figure 6-2) and rooting density (Figure 6-3). Acidic soils tend to deter root growth due to aluminum toxicity and limitations with nutrient uptake. Acidic clays have been intentionally selected for the construction of compacted mineral barriers to deter root growth and maintain engineered protectiveness (Robinson and Handel 1995). The acidic conditions in the radon barrier at the Shirley Basin South site are presumably less hospitable to root growth, and

therefore make the radon barrier more resistant to degradation by plants. Such conditions may also contribute to the dominance of shallow rooting grasses versus deep rooting shrubs at the Shirley Basin South site.

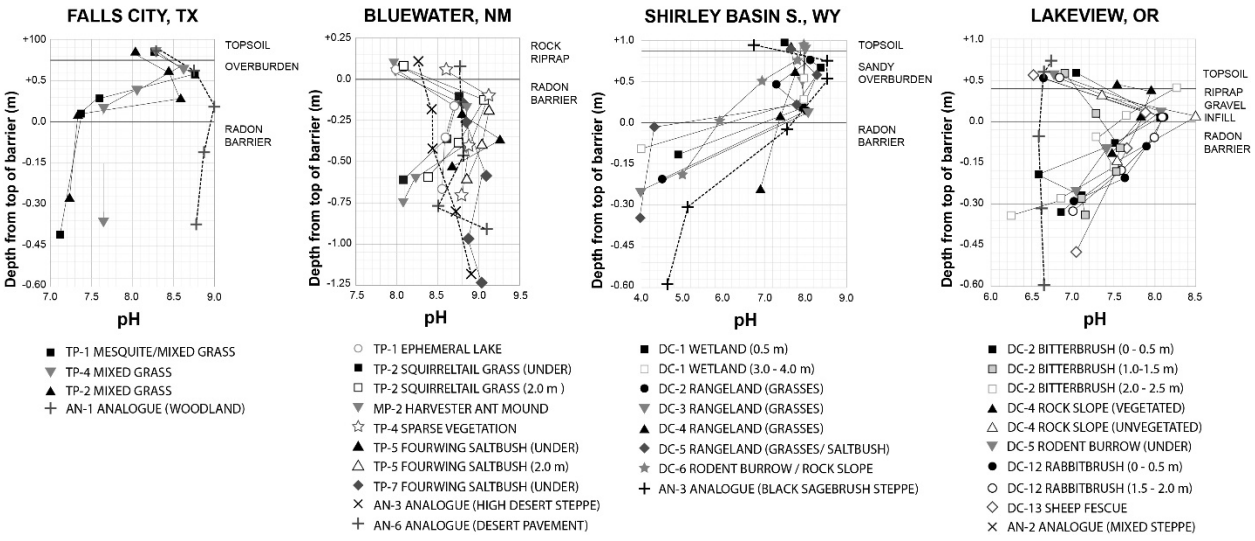

Figure 6-31 Distribution of pH in Four UMTRCA Covers and Analogues

6.4.5.5 Soluble Salts

The distribution of soluble salts across four in-service UMTRCA disposal cells is presented in Figure 6-32. In Figure 6-32, profiles in waste covers are displayed as solid lines while analogue profiles are displayed as dashed lines. A bimodal distribution exists at the Bluewater site with salts accumulating at the top and the bottom of the cover. The Lakeview site has relatively low EC and a trend toward higher EC with greater depth from ground surface in radon barrier profiles.

At the Shirley Basin South site, the general trend across the cell and in natural analogue soils is an increasing amount of soluble salts with depth, indicating one of two scenarios: (1) very slow infiltration is favored over evapotranspiration or (2) given low hydraulic conductivity across the cell (see Section 3), it is possible that radon barrier condition has remained constant through time and that elevated salt concentrations within the barrier match those found in borrow pit materials at the time of construction (i.e., there has not been appreciable salt accumulation). At the Shirley Basin South site, a spike in EC occurs at ~ 0.5 m from ground surface, indicating some preferential salt deposition is occurring above the barrier presumably due to a combination of average depths of wetting fronts and the thermodynamic conditions of soil solution including supersaturation and dissolution kinetics of soluble salts. Additional higher resolution depth sampling would be needed to characterize EC more accurately within the radon barrier section at the Shirley Basin South site.

At the Falls City site, salts are leaching within the subsoil section and collecting along the surface of the low permeability barrier. The same salt distribution pattern is observed in the Falls City analogue profile (AN-1) with salt accumulation occurring on top of the argillic horizon.

The profiles at the Falls City site that are responsible for lateral drainage off of the slope (DS-6 and DS-5) display elevated levels of soluble salts compared to on-cell averages suggesting that salts are being removed from the cell as a function of relief (DOE 2021a).

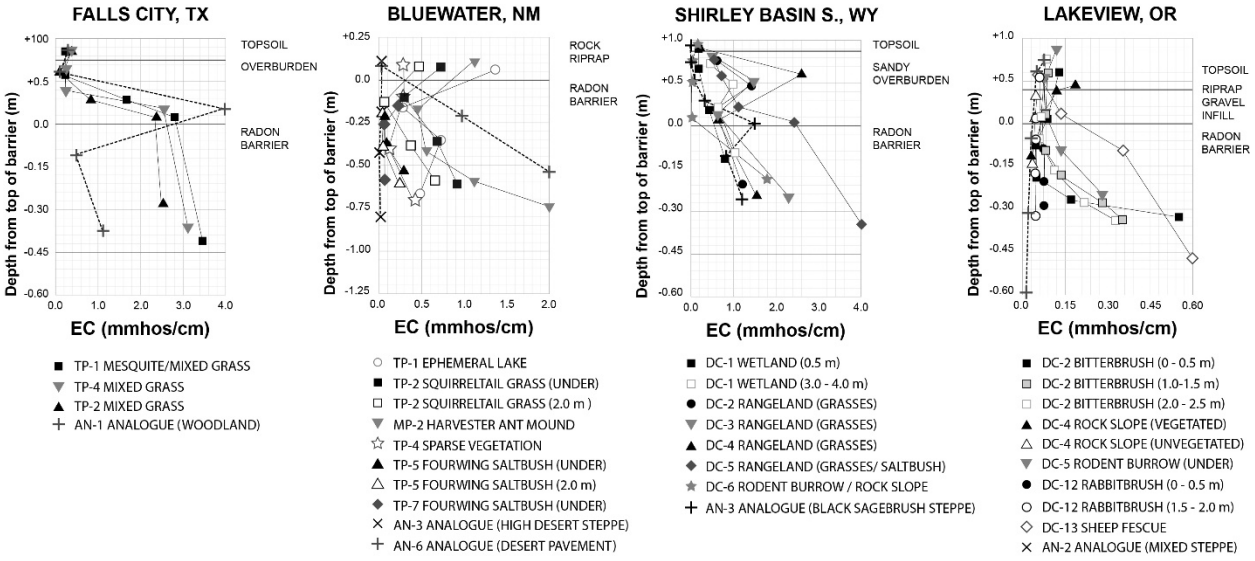

Figure 6-32 Distribution of Soluble Salts (EC) in Four UMTRCA Covers and Analogues

6.4.5.6 Calcium Carbonate

The radon barrier on the main Bluewater disposal cell displays highly variable $CaCO_3$ distribution across surface conditions (Figure 6-33). In Figure 6-33, profiles in waste covers are displayed as solid lines, while analogue profiles are displayed as dashed lines. Patterning is characterized by a bimodal distribution with highest concentrations at the top and at the bottom of the radon barrier, a trend shared in the young desert pavement analogue (AN-6) but not in the steppe analogue (AN-3). Stage I $CaCO_3$ accumulation along former fine root channels was also observed within the radon barrier at the Bluewater site. Stage II $CaCO_3$ accumulation was observed in AN-6.

At the Falls City site, $CaCO_3$ is preferentially accumulating at the top interface of the radon barrier and at lower elevation locations of the disposal cell that were designed to facilitate drainage off the cover. When coupled with lower-than-average hydraulic conductivity in the radon barrier (Section 3), and the gradual slope of the design, it is plausible that lateral drainage is favored over infiltration.

At the Shirley Basin South site, $CaCO_3$ benches were commonly observed directly on top of the radon barrier (DOE 2021c). This observation indicates that $CaCO_3$ was leaching through the more porous topsoil and overburden materials, and that the radon barrier limited further transport. Such a finding serves as a qualitative indicator that the radon barrier at the Shirley Basin South site has been successful at limiting water infiltration, as intended. This observation is supported by the low hydraulic conductivity measurements measured at the Shirley Basin South site (Section 3). Cover design, high clay texture (>60% clay), mineralogy dominated by

smectite in the radon barrier, and acidic soil conditions in the radon barrier are likely contributors to the preservation of limited soil structure and low K_{sat} through time.

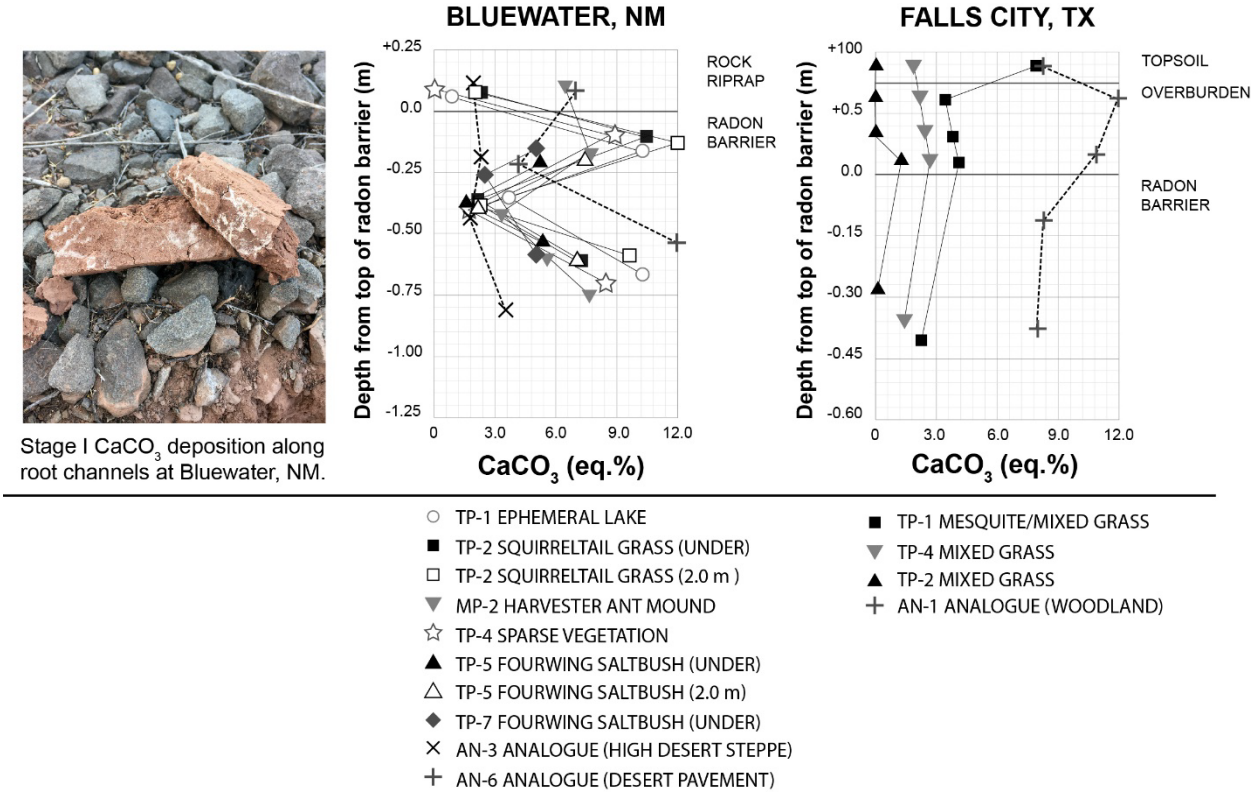

Stage I $CaCO_3$ deposition along root channels at Bluewater, NM.

Figure 6-33 Distribution of Calcium Carbonate (eq.%) in Two UMTRCA Covers and Analogues

6.4.6 Reduction and Oxidation

Strong gleyic features were observed on the side slopes of the Falls City (TP-1 and TP-6) and Shirley Basin South (DC-5 and DC-6) sites (Figure 6-6, Figure 6-7, Figure 6-34). The corresponding radon diffusion coefficients at locations with gleyic features were among the lowest measured (see Section 4). Gleyic features were not observed at the bottom terminus of the radon barrier but were located above non-gleyed radon barrier lift-and-compaction events, suggesting that water in those profiles is perched and infiltration is limited. This observation is supported by the low hydraulic conductivity measurements observed at the Shirley Basin South and Falls City sites (see Section 3). In addition to providing supporting evidence of long-term radon barrier hydraulic condition, the careful observation of gleyic features may serve as a helpful tool when interpreting lead-210 (^{210}Pb) profiles (Fuhrmann et al. 2019b).

Figure 6-34 Gleying in a Clay Lens Located Above the Radon Barrier at Shirley Basin South, Wyoming

6.5 Conceptual Models of Decadal Cover Evolution and Soil Morphology

Engineered covers are open and dynamic systems that are subject to recurring fluxes of energy and mass. Covers change and evolve by taking freely available energy from the environment (in the form of sunlight, water, nutrients, and other materials), transforming it, and moving toward higher order (more complex) systems (Lin 2011). The morphology of a cover system is created, regulated, and maintained by additions, losses, transformations, and transfers (i.e., "fluxes") occurring at the Earth's surface through space and time (Simonson 1959). Variations in soil- forming factors (i.e., design and management) inform how an engineered cover will interact with such fluxes. A summary of soil-forming factors on the four covers and analogues is presented in Table 6-10, and a summary of observed pedogenic processes is presented in Table 6-11.

As summarized in Figure 6-2 and Figure 6-3, the Shirley Basin South site radon barrier displays considerably less soil structuring than the Falls City site radon barrier. Structuring in the Falls City site radon barrier is attributed to shrink-swell occurring along hairline fractures of remnant soil structure as enhanced by the removal of water by roots. Both sites display less emergent structuring and plant rooting than the Bluewater and Lakeview sites. A combination of factors, including cover design, management, climate, vegetation, slope, and depth from ground surface, are believed to contribute to these observations (see Appendix H).

Conceptual site process models are presented to describe cover morphology at construction and at the time of this study in the vegetated topsoil cover at the Shirley Basin South site (Figure 6-35), the vegetated topsoil cover at the Falls City site (Figure 6-36), and at the rock riprap cover at the Bluewater site (Figure 6-37). Additions, transfers, transformations, and losses are indicated by green, blue, purple, and red arrows, respectively.

The Shirley Basin South site largely dissipates environmental fluxes *above* the radon barrier. The majority of soil processes characteristic of energy exchange that would result in soil morphological development occur in topsoil and overburden materials (i.e., shrinking/swelling, desiccation/cracking, organic matter deposition, root growth, and soil structuring). Furthermore, acidic conditions in the radon barrier (Figure 6-31) presumably deter root growth. Given spatial uniformity in surface condition across most of the cell (i.e., grass vegetation that is actively grazed), pedogenic processes in the barrier are similar between profiles or absent all together (see Table 6-11). The combination of soil-forming factors at the Shirley Basin South site has resulted in the resilient physical isolation of wastes.

The design of the Falls City site is similar to the Shirley Basin South site; however, they differ in climate and management. The Falls City site is hotter and wetter, and deep-rooted trees and shrubs (notably honey mesquite) are common. Such conditions require active management on the Falls City cover to limit plant rooting into the radon barrier. If such management were to be discontinued, plant rooting and soil structuring in the radon barrier would likely begin to resemble the natural analogue which is characterized by abundant rooting and structuring at depths shared by the radon barrier (Table 6-6).

The Bluewater site was not designed with an adequate capacity to dissipate environmental fluxes above the radon barrier. Therefore, most soil processes must occur *within* the radon barrier resulting in morphological development in the radon barrier through time. Given the spatial heterogeneity of emergent surface conditions across the cell, pedogenic processes in the barrier are highly variable between profiles after two decades of service (see Table 6-11).

While a similar collection of pedogenic processes occurs at the Bluewater and Shirley Basin South sites, the cumulative impacts of those processes to radon barrier morphology are relatively stable and even at the Shirley Basin South site and variable and uneven at the Bluewater site. These observations demonstrate how soil-forming factors (i.e., design, vegetation, management) contribute to the maintenance or alteration of radon barrier morphology through time, with subsequent impacts to engineered performance as discussed in Section 7.

Table 6-10 Summary of Soil-Forming Factors at Four Engineered Covers for Waste Containment and Natural Analogues

		Cover Design / Material Properties / Setting					Climate		Biota[a]		Management	Time
	Setting	Type	Radon Barrier Depth (*range*)	Texture (clay %) (*range*)	Mineralogy (2:1 clay %) (*range*)	Slope	Soil Moisture Regime	Soil Temperature Regime	Flora	Fauna	Strategy	Years
Falls City	Top deck	Vegetated	0.97-1.54 m	38–51%	57–70%	1–2%	Udic-Ustic	Hyperthermic	Managed grassland	*Limited*	Mowing	22[b]
	Side slope	Rock riprap	0.47-0.94 m	43%	59%	20%			Mixed/sparse	*Limited*	Hand removal of trees/shrubs	
	AN-1	-	-	43% at ~1.0 m	58% at ~1.0 m	1–4%			Mixed woodland	Cattle	Cattle grazing	<30,000[c]
Bluewater	Top deck main cell	Rock riprap	0.14-0.85 m	13–41%	37–45%	2–4%	Aridic-Ustic	Mesic	Kochia, squirreltail grass, fourwing saltbush	Ants, rodents	Hand removal of trees	21[b]
	AN-3	-	-	31% at ~0.5 m	48% at ~0.5 m	1–3%			High altitude steppe	Elk, rodents, ants	Wildlife	<15,000[d]
	AN-6	-	-	29% at ~0.5 m	51% at ~0.5 m	4%			High altitude steppe	Elk, rodents, ants	Wildlife	<15,000[e]
Lakeview	Top deck	Vegetated	0.59-–1.10 m	8-22%	52–71%	2–5%	Xeric	Frigid	Sagebrush, rabbitbrush, bitterbrush, mixed grasses	Ants, rodents	Hand removal of trees	28[b]
	Side slope	Rock riprap	0.5–0.85 m	16%	-	20%			Grasses/sparse	Rodents	Hand removal of trees	
	AN-2	-	-	27% at ~0.8 m	5%[f] at ~0.8 m	2–7%			sagebrush steppe	deer, rodents	Wildlife	<20,000[g]
Shirley Basin S.	Top deck	Vegetated	0.99–1.52 m	37-66%	58–76%	1–3%	Aridic-Ustic	Mesic	Mixed grasses, sparse fourwing saltbush	Rodents, cattle, antelope	Grazing, hand removal of noxious weeds	17[b]
	Side slope	Rock riprap	1.17–1.80 m	55%	-	20%			Mixed grasses/sparse	Rodents	Hand removal of noxious weeds	
	AN-4	-	-	69% at ~1.3 m	55% at ~1.3 m	1–3%			High altitude grassland/steppe	Ants, rodents, badgers	Wildlife	<15,000[h]

[a] See Section 2 for more detailed descriptions of plant ecology.
[b] Time since construction (circa 2017 at time of this study).
[c] Age of soils at the Falls City site. Natural analogue estimated based on paleoenvironmental repots by Bryant and Shafer (1977); formed in Eocene age alluvial sediments.
[d] Age of soils based on estimated late Pleistocene, early Holocene alluvial sediments (Zeigler et al. 2012).
[e] Age of soils based on basalt lava flow age estimations (Dunbar and Phillips 2004) and late sediment ages (Zeigler et al. 2012).
[f] 5% mixed layer illite/smectite; 56% illite/mica.
[g] Age of soils based on estimated late Pleistocene, early Holocene alluvial and lakeshore sediment age from Summer Lake, Oregon (Cohen et al. 2000).
[h] Age of soils based on estimated late Pleistocene, early Holocene alluvial sediments (Harshman 1972).

Table 6-11 Summary of Pedogenic Process in Four Radon Barriers in the UMTRCA Program

	UMTRCA Disposal Sites			
Pedogenic Process	**Falls City, TX**	**Bluewater, NM**	**Shirley Basin S., WY**	**Lakeview, OR**
Visually observed desiccation-cracking in barrier : present / absent	Present (*along remnant soil structure*)	Present	Absent	Present
Freeze-thaw in barrier : probable / unlikely	Unlikely (climate and barrier depth)	Possible (ephemeral lake freezes)	Unlikely (barrier depth)	Unlikely (barrier depth)
Plant rooting is : similar / variable	Variable (slope has more roots)	Highly variable	Relatively similar (slope has more roots)	Highly variable
Soil structuring is : similar / variable	Similar	Variable	Similar	Variable
Bioturbation by animals in barrier : present / absent	Absent	Present	Absent	Absent
Soil organic carbon distribution is : similar / variable	Similar	Variable	Relatively similar / somewhat variable	Relatively similar / somewhat variable
Distribution of soil pH is : similar / variable	Similar	Variable	Relatively similar	Relatively similar / somewhat variable
Distribution of soluble salt is : similar / variable	Relatively similar	Variable	Relatively similar (DC-5 is an outlier)	Variable
Distribution of $CaCO_3$ is : similar / variable	Similar	Variable	—	—
Reduction / Oxidation is : present / absent	Present	Absent	Present	Absent
Barrier structural development: minimal / significant	Somewhat minimal	Significant	Very minimal	Significant

Note: Similar / variable descriptions are based on profile-to-profile comparisons.

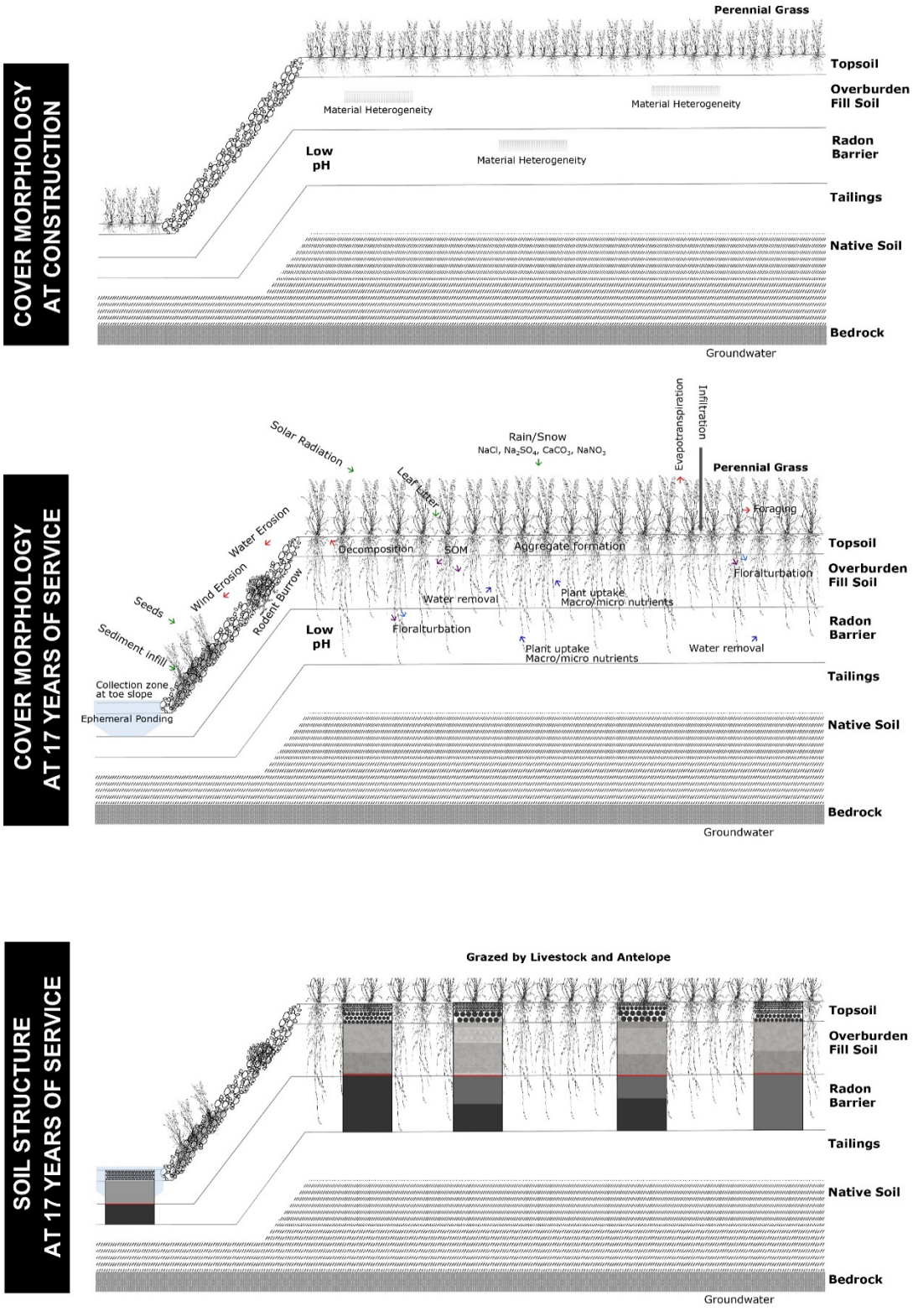

Figure 6-35 Shirley Basin South, Wyoming, Cover Morphology and Soil Development Over Time

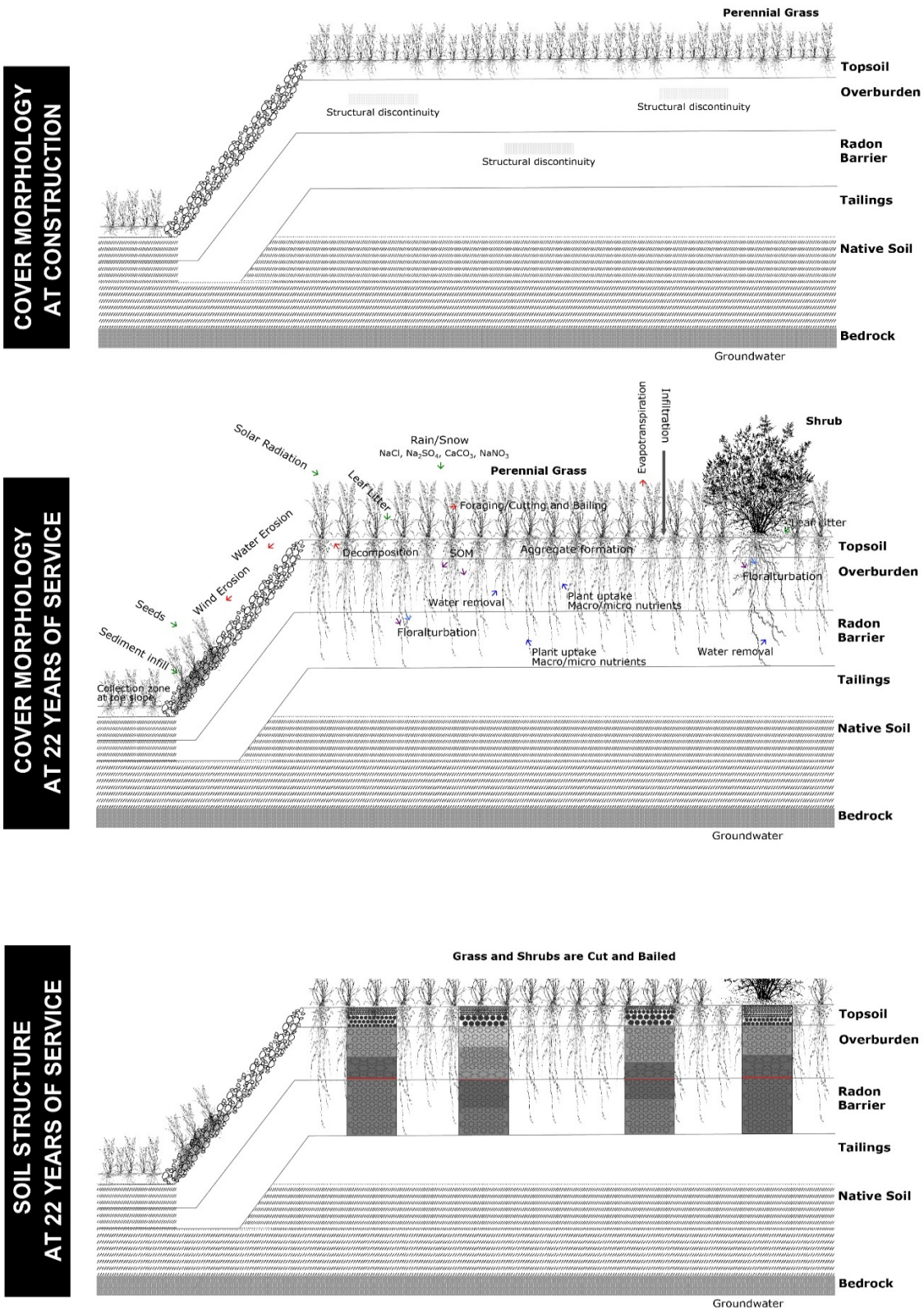

Figure 6-36 Falls City, Texas, Cover Morphology and Soil Development Over Time

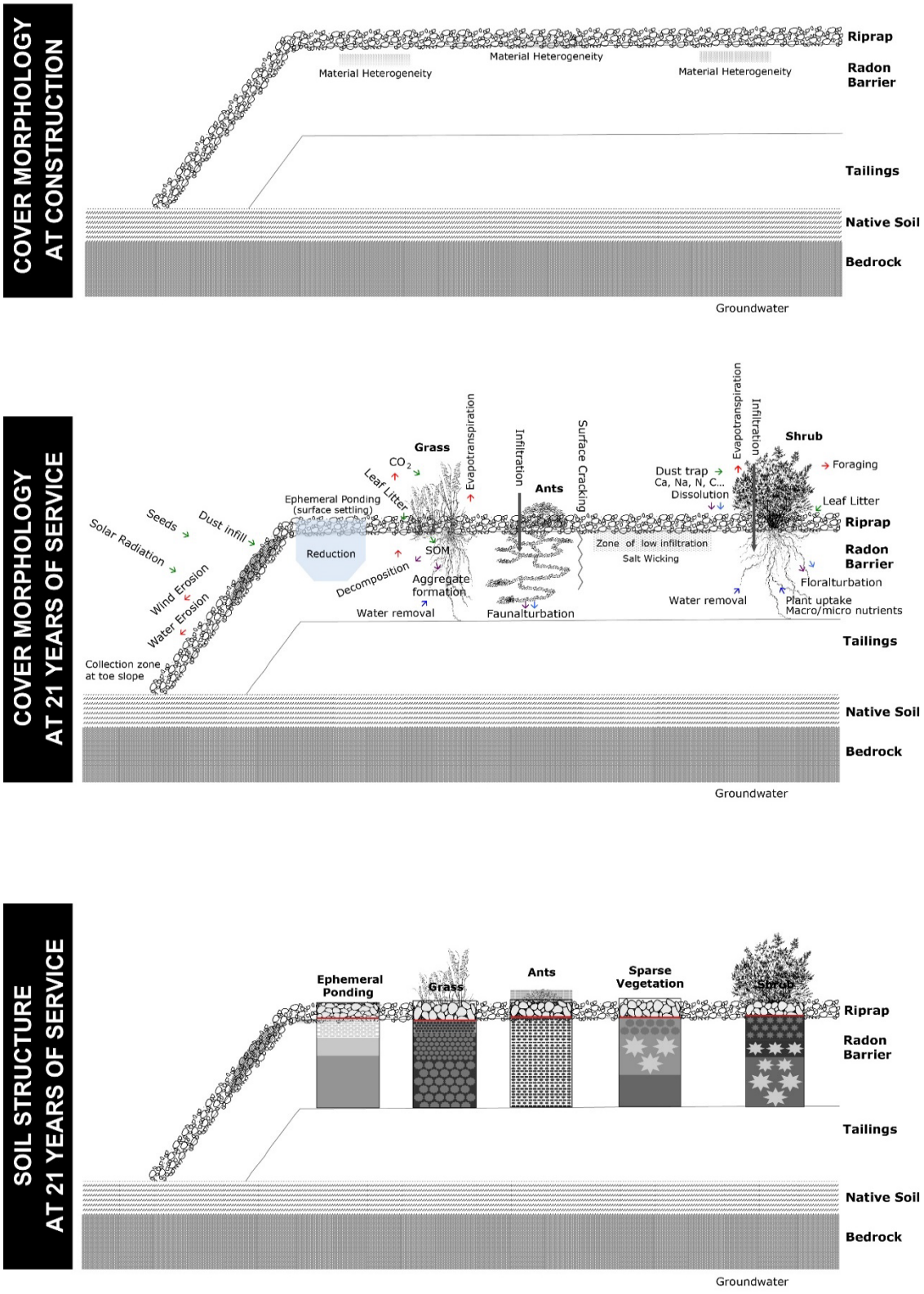

Figure 6-37 Bluewater, New Mexico, Cover Morphology and Soil Development Over Time

6.6 Section Summary and Conclusions

Earth surface processes are occurring across the four waste disposal cells surveyed, altering the as-built radon barrier morphology. A conceptual framework of soil formation in engineered soils for waste containment is proposed to describe the soil morphology in cover systems in the UMTRCA portfolio (see Appendix I for greater detail). The authors find that a combination of factors including cover design, management, climate, vegetation, slope, and depth to ground surface have an impact on the observed differences in the radon barrier morphology.

Profiles associated with downslope areas (e.g., side slopes, toe slopes, and depressions) displayed the least structural development across all cover types and climates. Downslope profiles located in on-cell surface depressions (i.e., Bluewater TP-1), on rock riprap side slopes (i.e., Lakeview DC-4; Falls City DC-6; and Shirley Basin South DC-6), and at rock riprap toe slopes (i.e., Shirley Basin South DC-1) all had radon barriers that were wetter than other profiles on the same cell. The radon barrier observed on the rock riprap side slope at the Falls City site (DC-6) displayed gleyic features, suggesting extended periods of saturation. Concentrations of $CaCO_3$ were also elevated (compared to top deck averages) in downslope profiles at the Falls City site, indicating that water drainage on the cell is likely contributing to sustained saturation of the radon barrier of these profiles. Such conditions result in the maintenance of soil structure, despite observed plant rooting and the presence of remnant soil structure from borrow materials. Consequently, downslope profiles (i.e., Falls City DC-6, Bluewater TP-1, Shirley Basin South DC-1, and Lakeview DC-4) had among the lowest measured radon diffusion coefficients (Section 4). Water movement and collection across an individual cell surface can play a significant role in regulating long-term soil morphological development.

Climate can influence the development of soil morphology through time. The Falls City and Shirley Basin South sites share many of the same design factors (vegetated covers with thick overburden and topsoil layers). However, the climate at Falls City is hot and humid, while Shirley Basin South is cold and semiarid (see Section 2.4.3). Given rainfall and temperature, deep-rooted vegetation is more abundant at the Falls City site than at the Shirley Basin South site, resulting in the need for increased management. High soil pH in the radon barrier at the Shirley Basin South site presumably also contributes to dominance by shallower rooted plants.

Active surface management can increase the profile-to-profile uniformity of radon barrier structure. The Falls City and Shirley Basin South sites vegetated covers with thick overburden and topsoil layers that are managed by grazing, mowing, and spot removal of deep-rooted vegetation show greater resistance to changes in soil structure and plant rooting over decadal time frames compared to the other designs studied. The Falls City site cell requires active management of honey mesquite by periodic mowing. Under such management, rooting in the radon barrier is largely restricted to very fine roots, with some fine to coarse root benching occurring along remnant soil structure in the top section of the radon barrier. Rooting characteristics in the mature mixed woodland analogue (Falls City AN-1) display very fine to medium sized roots in soil materials of similar texture and compaction to the radon barriers at depths exceeding the bottom boundary of the radon barrier at the site. This observation suggests that current vegetation management at the Falls City site is effective at limiting plant rooting to the top sections of the radon barrier. However, if mowing were to be discontinued and management altered to incorporate the establishment of deep-rooted vegetation on the cell (including mesquite), it is likely that the radon barrier would become more structured over time. In a hotter and drier climate, such rooting would likely serve to accelerate the dewatering of the barrier through transpiration, presumably resulting in increased radon diffusion. However, a tradeoff exists as rates of evapotranspiration and water percolation may be reduced under

conditions of greater vegetation cover at the Falls City site. The chances of accelerated structuring under drier conditions or increased evaporative demand from deep-rooted vegetation are increased further given the presence of remnant soil structure (from borrow materials) characterized by hairline fractures in smectite rich materials prone to shrink-swell.

Cover design influences the development of soil morphology. The rock riprap cover at the Bluewater site has changed more over time than the vegetated cover with thick overburden and topsoil layers at the Shirley Basin South site under similar climate (aridic-ustic soil moisture and mesic soil temperature). The main cover at the Bluewater site was unplanted at construction, and the surface is now characterized by an emergent patchwork of vegetation that corresponds to diverse radon barrier morphology resembling the natural analogue under some of the observed surface conditions. Plant rooting and soil structural development varied considerably across the surface features surveyed at the Bluewater site. The emergence of horizontal soil morphological impact gradients at the Bluewater site was also significant. Conversely, the cover at the Shirley Basin South site is characterized by a relatively even stand of mixed grasses, and very infrequent shrubs that match the adjacent natural steppe conditions. Soil morphology is very similar between profiles on the top deck of the disposal cell at the Shirley Basin South site and of the natural analogue.

The development of radon barrier morphology between profiles on the cover of the Bluewater site is significantly influenced by bioturbation by plants and animals. The harvester ant mound profile (MP-2) displayed the greatest soil structural development, followed by the squirreltail grass (TP-2) and fourwing saltbush profiles (TP-5 and TP-7). Sparse annual weed profiles (TP-4 and TP-3) displayed less morphological development, with the downslope, ephemeral lake, collection basin (TP-1) displaying the least development. The natural analogue profile associated with mixed high desert steppe vegetation in the borrow pit area (AN-3) displays soil structuring that very closely resembles the shape, size, grade, and rupture resistance of the highly developed squirrel tail grass profile (TP-2). Additionally, plant rooting in AN-3 represents a sum combination of root characteristics observed in the saltbush (TP-5 and TP-7) and squirreltail grass (TP-2) profiles, with saltbush contributing the greatest root variation and squirreltail grass the greatest rooting density for very fine roots. This observation shows that the Bluewater disposal cell is approaching the soil condition found in the surrounding natural environment.

The development of soil morphology between profiles on the cover of the Lakeview site is also significantly influenced by bioturbation. The profiles associated with bitterbrush (DC-2 and DC-10) display the greatest morphological development, followed by the rabbitbrush (DC-12) and sheep fescue (DC-13). The sparsely vegetated spaces in between shrubs display the least morphological development. These small-scale changes in morphological development result in gradients that are significant contributors to heterogeneity in radon barrier morphology across the cell. Plant rooting in the natural analogue (AN-2) represents a sum combination of root characteristics observed in the sheep fescue (DC-13), rabbitbrush (DC-12), and bitterbrush (DC-2) profiles. This observation shows that the Lakeview disposal cell is approaching the soil condition found in the surrounding natural environment.

The intensity of soil morphological development in radon barriers generally decreases with depth from surface. Such findings were also observed across natural analogue profiles. In general, greater rooting diversity and abundance was observed in natural analogue profiles compared to cover profiles, indicating that further changes to radon barrier morphology are likely to occur over time. Across the profiles surveyed at the Bluewater and Lakeview sites, plant root size and abundance generally decrease with depth. Soil structural unit size increases

with depth and decreases in grade of expression (intensity) across all profiles observed, with few exceptions. The soil structuring in the radon barrier was consistent through the depth of the excavated harvester ant mound (Bluewater, MP-2). Additionally, bands of larger sized structures were found in between bands of smaller sized structures in Lakeview profiles DC-5 and DC-2, suggesting that the structural, textural, or mineralogical conditions of individual barrier lift-and-compaction events also exert some control on patterns of emergent structuring.

The exploration of natural analogue soils can be used to estimate the long-term condition of soil morphology in radon barriers and may serve to validate cover design performance over regulatory time periods. Under some surface conditions, the radon barrier at the Bluewater and Lakeview sites has already approached that of the natural analogue representing considerable change since construction. The active management of deep-rooted vegetation at the Falls City site is presumably keeping the radon barrier from approaching that of the natural analogue.

At the Shirley Basin South site, plant rooting and soil structuring are remarkably similar between on-cell and natural analogue conditions (AN-4); however, this similarity is not connected to the cover equilibrating to the natural environment over time. With exception to infrequent fractures, soil structuring is naturally inhibited in AN-4 at depths that correspond to the top boundary of the radon barrier (1000 mm). Both on-cell and analogue soils (at the depth of the radon barrier) are acidic and may serve to naturally deter deep plant rooting and subsequent soil structuring. On-cell and analogue observations suggest that the cell at the Shirley Basin South site was presumably constructed in a quasi-stable state of equilibrium with the natural environment and will likely be slow to change if soil-forming factors persist through time (e.g., climate and management).

6.1 References

Arthur, W.J., III and O.D. Markham, 1983. "Small Mammal Soil Burrowing as a Radionuclide Transport Vector at a Radioactive Waste Disposal Area in Southeastern Idaho," *Journal of Environmental Quality,* 12, 117–122.

ASTM (American Society for Testing and Materials). *Standard Test Method for Laboratory Determination of Water (Moisture) Content of Soil and Rock by Mass*, ASTM D2216.

Benson, C. H., F.S. Hardianto, and E.S. Motan, 1994. "Representative Specimen Size for Hydraulic Conductivity Assessment of Compacted Soil Liners," In *Hydraulic Conductivity and Waste Contaminant Transport in Soil*, Eds Daniel, D. and Trautwein, T. ASTM International, West Conshohocken, PA, 3-29.

Benson, C.H., T.H. Abichou, M.A. Olson, and P.J. Bosscher, 1995. "Winter Effects on Hydraulic Conductivity of Compacted Clay," *Journal of Geotechnical Engineering,* 121(1), 69–79.

Bryant Jr., V.M., and H.J. Shafer, 1977. "The Late Quaternary Paleoenvironment of Texas: A Model for the Archaeologist," *Bulletin of the Texas Archeological Society*, *48*, 1–25.

Burt, C.J., and S.W. Cox, 1993. "An Assessment of Plant Biointrusion on Six UMTRA Project Disposal Cells," Waste Management Conference 1993, Working Towards a Cleaner Environment, Tucson, Arizona.

Cable, J.M. and T.E. Huxman, 2004. "Precipitation Pulse Size Effects on Sonoran Desert Soil Microbial Crusts," *Oecologia,* 141(2), 317–324.

CNAL (Cornell Nutrient Analysis Laboratory), 2011a. *Determination of Organic, Inorganic, and Total Carbon in Soils by Wet Oxidation,* Procedure Number, S2740-50, revision date January 13, 2011.

CNAL (Cornell Nutrient Analysis Laboratory), 2011b. *Determination of Ammonia Nitrogen in 2N Potassium Chloride Extraction Solution of Soil Using the Bran+Luebbe Automated Ion Analyzer,* Procedure Number, S2503, revision date January 6, 2011.

CNAL (Cornell Nutrient Analysis Laboratory), 2011c. *Determination of Nitrate and Nitrite Nitrogen in 2N Potassium Chloride Extraction Solution of Soil Using the Bran+Luebbe Automated Ion Analyzer,* Procedure Number, S2503 revision date January 6, 2011.

CNAL (Cornell Nutrient Analysis Laboratory), 2011d. *Determination of Calcium Carbonate Equivalent of Soil*, Procedure Number, S2611, revision date, January 27, 2011.

CNAL (Cornell Nutrient Analysis Laboratory), 2013. *Extraction of Soil Using Modified Morgan for Available Nutrients,* Procedure Number, S1100-MM, revision date, November 8, 2013.

CNAL (Cornell Nutrient Analysis Laboratory), 2016a. *Soluble Salts Content,* Procedure Number, S1880, revision date, November 20, 2016.

CNAL (Cornell Nutrient Analysis Laboratory), 2016b. *Determination of Particle Size Analysis by Pipette Method,* Procedure Number, S1885, revision date, March 10, 2016.

CNAL (Cornell Nutrient Analysis Laboratory), 2017. *Determination of Carbon, Nitrogen, and Hydrogen in Soil/Plant Samples Using The Vario EL Cube,* Procedure Number, S2737/P6747, revision date, October 24, 2017.

CNAL (Cornell Nutrient Analysis Laboratory), 2019. *Determination of Soil pH,* Procedure Number, S1820, revision date, December 11, 2019.

Cohen, A., M. Palacios-Fest, R. Negrini, P. Wigand, and D. Erbes, 2000. "A Paleoclimate Record for the Past 250,000 Years from Summer Lake, Oregon, USA: II, Sedimentology, Paleontology and Geochemistry," *Journal of Paleolimnology*, *24*(2), 151–182.

DOE (U.S. Department of Energy), 2021a. *Soil Morphology, Plant Ecology, and Surface Change at the UMTRCA Title I Disposal Cell, Falls City, Texas, LMS/FCT/S30757, Office of Legacy Management, Grand Junction, CO.*

DOE (U.S. Department of Energy), 2021b. *Soil Morphology, Plant Ecology, and Surface Change at the UMTRCA Title II Disposal Cell, Bluewater, New Mexico, document forthcoming, Office of Legacy Management, Grand Junction, CO.*

DOE (U.S. Department of Energy), 2021c. *Soil Morphology, Plant Ecology, and Surface Change at the UMTRCA Title II Disposal Cell, Shirley Basin South, Wyoming, document forthcoming, Office of Legacy Management, Grand Junction, CO.*

DOE (U.S. Department of Energy), 2021d. *Soil Morphology, Plant Ecology, and Surface Change at the UMTRCA Title I Disposal Cell, Lakeview, Oregon, document forthcoming, Office of Legacy Management, Grand Junction, CO.*

Dunbar, N.W., and F.M. Phillips, 2004. "Cosmogenic 36Cl Ages of Lava Flows in the Zuni-Bandera Volcanic Field, North-Central New Mexico, USA," *Tectonics, geochronology, and volcanism in the Southern Rocky Mountains and Rio Grande rift: New Mexico Bureau of Mines and Mineral Resources Bulletin*, *160*, 51–59.

Fuhrmann, M., Benson, C., Waugh, J., Arlt, H., Williams, M., 2019a. *Proceedings of the Radon Barriers Workshop*, NUREG/CP-0312, U.S. Nuclear Regulatory Commission, Washington, D.C.

Fuhrmann, M., A. Michaud, M. Salay, C.H. Benson, W.J. Likos, N. Stefani, W.J. Waugh, and M.M. Williams, 2019b. "Lead-210 Profiles in Radon Barriers, Indicators of Long-Term Radon-222 Transport," *Applied Geochemistry* 110:104434.

Harshman, E.N., 1972. *Geology and Uranium Deposits, Shirley Basin area, Wyoming* (No. 745). U.S. Government Printing Office, Washington D.C.

Kim, W.H. and D.E. Daniel, 1992. "Effects of Freezing on Hydraulic Conductivity of Compacted Clay," *Journal of Geotechnical Engineering* 118(7), 1083–1097.

Lin, H. S., K.J. McInnes, L.P. Wilding, and C.T. Hallmark, 1999. "Effects of Soil Morphology on Hydraulic Properties I. Quantification of Soil Morphology," *Soil Science Society of America Journal*, 63(4), 948–954.

Lin, H.S., 2010. "Linking Principles of Soil Formation and Flow Regimes," *Journal of Hydrology,* 393(1-2), 3–19.

Lin, H.S., 2011. "Three Principles of Soil Change and Pedogenesis in Time and Space," *Soil Science Society of America Journal,* 75(6), 2049–2070.

Link, S.O., L.L. Cadwell, K.L. Petersen, M.R. Sackschewsky, and D.S. Landeen, 1995. *The Role of Plants and Animals in Isolation Barriers at Hanford*, *Washington PNL-10788*, Pacific Northwest Laboratory, Richland, Washington.

Melchior, S., 1997. "In-Situ Studies of the Performance of Landfill Caps (Compacted Soil Liners, Geomembranes, Geosynthetic Clay Liners, Capillary Barriers)," *Land Contamination and Reclamation,* 5(3), 209–216.

Michaud, A.M., 2018. *Long-Term Performance of Radon Barriers in Limiting Radon Flux From Four Uranium Mill Tailings Containment Facilities*, thesis for Master of Science, University of Wisconsin-Madison.

Montgomery, R., and L. Parsons, 1989. "The Omega Hills Final Cover Test Plot Study: Three Year Data Summary," *1989 Annual Meeting of the National Solid Waste Management Association, Washington, DC*.

Robinson, G.R., and S.N. Handel, 1995. "Woody Plant Roots Fail to Penetrate a Clay-Lined Landfill: Management Implications," *Environmental Management*, 19, 57–64.

Rumpel, C., and I. Kögel-Knabner, 2011. "Deep Soil Organic Matter—a Key but Poorly Understood Component of Terrestrial C Cycle," *Plant and Soil*, *338*(1-2), 143-158.

Schwinning, S., O.E. Sala, M.E. Loik, and J.R. Ehleringer, 2004. "Thresholds, Memory, and Seasonality: Understanding Pulse Dynamics in Arid/Semi-Arid Ecosystems," *Oecologia,* 14, 191–193.

Simonson, R. W., 1959. "Outline of a Generalized Theory of Soil Genesis," *Soil Science Society of America Journal*, 23(2), 152–156.

Stefani, N., 2016. *Field and Laboratory Measurement of Radon Flux and Diffusion for Uranium Mill Tailings Cover Systems*, thesis for Master of Science, University of Wisconsin-Madison.

Targulian, V.O. and P.V. Krasilnikov, 2007. "Soil System and Pedogenic Processes: Self-Organization, Time Scales, and Environmental Significance," *Catena, 71*(3), 373–381.

USDA (U.S. Department of Agriculture), 2012. *Field Book for Describing and Sampling Soils*, version 3.0, Natural Resource Conservation Service.

Waugh, W.J., S.J. Morrison, G.M. Smith, M. Kautsky, T.R. Bartlett, C.E. Carpenter, and C.A Jones, 1999. *Plant Encroachment on the Burrell, Pennsylvania, Disposal Cell: Evaluation of Long-Term Performance and Risk*, GJO-99-96-TAR, Environmental Sciences Laboratory, U.S. Department of Energy, Grand Junction, Colorado.

Wells, S. G., J.C. Dohrenwend, L.D. McFadden, B.D. Turrin, and K.D. Mahrer, 1985. "Late Cenozoic Landscape Evolution on Lava Flow Surfaces of the Cima Volcanic Field, Mojave Desert, California," *Geological Society of America Bulletin*, 96(12), 1518–1529.

Williams, M.M., 2019. *Pedogenic Process in Engineered Soils for Radioactive Waste Containment*, University of California, Berkeley, Doctor of Philosophy dissertation.

Zeigler, K.E., C. Cikoski, P. Drakos, and J. Riesterer, 2012. "Preliminary Geologic Map of the Grants Quadrangle, Cibola County, New Mexico," New Mexico Bureau of Geology and Mineral Resources, Open-file Digital Geological Map OF-GM 224.

7 DETERMINATION OF LONG-TERM PERFORMANCE CONDITION OF FOUR WASTE COVERS THROUGH SOIL MORPHOLOGICAL COMPARISON TO NATURAL ANALOGUES

7.1 Introduction

Field studies have shown that structure develops in earthen final covers at waste containment facilities in response to abiotic and biotic interactions between the earthen cover materials and the environment. Volume changes in the earthen materials induced by wet-dry and freeze-thaw cycles result in the formation of initial soil structure. Rooting systems in the cover profile contribute to subsequent structural development through stresses induced by root water uptake and root penetration. Burrowing animals and insects also create structure in the cover. These structural changes alter the engineering properties of cover soils, most notably the hydraulic properties (i.e., saturated hydraulic conductivity [K_{sat}] and the soil water characteristic curve [SWCC]), and therefore the cover hydrology, including water balance.

Changes in hydraulic properties due to structural development are significant in final covers that employ compacted mineral barriers (CMBs) as the primary means to control percolation and gas diffusion (i.e., resistive barrier designs) (Albright et al. 2010; Benson et al. 2011). CMBs are composed of fine-textured soils compacted to remove large pores and other structural features so that the barrier has very low K_{sat}, and an SWCC with high water retention characteristics. These attributes also contribute to low gas diffusion coefficients (D_g). This is particularly true for earthen final covers placed at disposal facilities for uranium mill tailings that rely on a CMB with low K_{sat} to control the downward movement of meteoric water and low D_g to control the upward movement of radon gas emitted from the tailings (Waugh et al. 1999; Waugh et al. 2007; Albright et al. 2010; Benson et al. 2011). These low permeability “radon barriers” are particularly susceptible to alteration by natural processes of soil development (Section 6; Appendix H).

This section describes the K_{sat} reported in Section 3 and the radon diffusion coefficients (D_{Rn}) reported in Section 4 that were measured on the radon barriers at each of the field sites in the context of the degree of soil morphological development that has occurred since the final covers were constructed (Section 6). Depth dependence of soil morphology is also explored. Assessments are also made for natural analogues, which are soil profiles intended to represent the morphology and engineering properties anticipated for the final covers over their period of design performance. Soil morphology is used here in the context of soil structure, pore space, root patterning, and soil texture.

7.2 Methods

Field work was conducted at the Uranium Mill Tailings Radiation Control Act (UMTRCA) waste covers in Falls City, Texas; Bluewater, New Mexico; Shirley Basin South, Wyoming; and Lakeview, Oregon, in 2016–2017. The rationale for selecting these sites is in Section 2 along with a description of the cover profiles at each of these sites as shown in Figure 2.2. Test pit locations were identified at each site where the radon barrier could be exposed and evaluated. These locations were selected to represent a range of cover conditions that can influence soil

morphology and therefore K_{sat} and D_{Rn}. These conditions include variations in cover design (i.e., rock riprap or vegetated top deck and side slopes) and surface condition (i.e., large shrubs, animal burrows, perennial grass stands, sparse vegetation, and surface depressions that result in ephemeral ponds). The selection process identified test locations anticipated to have the greatest changes in cover performance, the worst-case conditions rather than typical conditions.

Radon flux measurements were conducted in each test pit as described in Section 4. After the flux measurements were completed, morphology of cover soils was characterized, and large-diameter intact block samples were collected for laboratory characterization of soil hydraulic properties as described in Section 3. Soil morphological characterization of exposed cover profiles was then conducted as described in Section 6. Similar morphological characterization and block sampling was also conducted at locations adjacent to each disposal facility selected as natural analogues. Six soil profiles were investigated at Falls City, ten at Bluewater, eight at Shirley Basin South, and eight at Lakeview.

7.2.1 Radon Diffusion Coefficients

Radon flux measurements were made with flux chambers of various sizes with radon concentrations in the chambers measured with the RAD7 electronic radon monitors. Methods described in Section 4 and Appendix F were used to determine the radon buildup curves and radon flux. In each test pit, radon fluxes measured on the surface of the radon barrier ("top flux" in Section 4) and on the surface of the tailings directly beneath the radon barrier ("bottom flux" in Section 4). These fluxes are summarized in Tables 4-9 through 4-12.

Radon diffusion coefficients were calculated from the "top" and "bottom" radon fluxes using the "two-flux method" implemented in the RAECOM computer program (Nielson and Rogers 1982; Nielson et al. 1984; NRC 1989), as described in Section 4. RAECOM simulates one-dimensional steady-state radon diffusion through a multilayer porous medium. The "bottom" flux measured in the field was used as the inlet flux at the bottom of the radon barrier in RAECOM. The "exit flux" at the top of the barrier was then computed with RAECOM using an assumed value for D_{Rn}. The assumed D_{Rn} was varied systematically until the exit flux predicted by RAECOM was within 1% of the "top flux" measured in the field on the surface of the radon barrier.

7.2.2 Saturated Hydraulic Conductivity

Block samples were collected from each test pit and from the analogue sites using the procedure described in ASTM D7015. When possible, samples were collected in a vertical profile to capture conditions existing as a function of depth. The intact samples were trimmed directly into PVC sampling rings having an inside diameter and height of 400 millimeters (mm) as described in Section 3. After trimming, each sample was carefully sealed with a plastic sheet, transferred to a protective pallet, and shipped to the laboratory for testing. K_{sat} of each block sample was measured in a large-scale flexible wall permeameter using the procedure in ASTM D5084. Test specimens were trimmed from the samples by hand to a diameter of 305 mm and aspect ratio of 1. Testing was conducted at an effective stress of 21 kilopascals and a hydraulic gradient of 10. SWCC tests were conducted on a subset of the hydraulic conductivity test specimens after permeation was complete. Specimens for SWCC testing were trimmed to a thickness of 25 mm and tested using the procedures in ASTM D6836. The wet end of the SWCC was measured in large-scale (300 mm diameter) pressure plate extractors, and the dry

end was determined using a chilled mirror hygrometer. Additional details on the test methods and data interpretation are presented in Section 3.

7.2.3 Soil Morphological Development Score

The soil morphology of each horizon in each test pit was described using standard soil survey procedures (USDA 2012). Pore shape, size, and quantity was described using the visual observation method in Lin et al (1999a). Soil descriptions focused on texture, moisture content, pedality, porosity, and root density. Morphological features were visually determined in-field, except for texture and moisture. A natural analogue site was also selected in proximity to each waste cover to characterize the morphology of a soil with similar soil forming factors as the final cover and presumably representing a long-term stable state of cover condition (Table 6.10). Full soil characterization and sampling methods are described in Section 6. Descriptions of the soil surveys performed at each site are in their respective soil morphology, plant ecology, and surface change reports (DOE forthcoming).

The point system developed by Lin et al. (1999a) was used to provide a quantitative measure of the morphological attributes in the radon barriers (e.g., moisture, texture, pedality, porosity, and rooting), referred to as the soil morphological development score (SMDS). Lin et al. (1999a) assumed a hypothetical structureless clay as the reference soil. This reference soil was assumed to contain no macropores or roots and to exist in a fully swollen and saturated state. The reference soil is comparable to the intended condition of a radon barrier where the compaction process has eliminated all structure in the soil. Lin et al (1999a) assigned points to each morphological feature based on the impact of that feature on hydraulic conductivity relative to the reference soil. Lin et al. (1999a) assigned the points using a “one-at-a-time” search method to obtain an optimal correlation with measured infiltration rates (Shoup 1982; McCuen and Snyder 1986). Points for morphological soil classes are in Table 7.1.

Points were assigned using the definitions from Lin et al. (1999a) to each feature in each horizon that was apparent in the radon barrier and in the natural analogue. Horizons frequently corresponded to lift-and-compaction interfaces within the radon barrier. For pedality, macroporosity, and root density, which have multiple descriptors (e.g., ped grade, ped size, and ped shape), the score for the feature was computed as the product of the pertinent descriptors using Equations 7.1, as described in Lin et al (1999a):

$$\text{Pedality} = (\text{ped grade}) \times (\text{ped size}) \times (\text{ped shape}) \quad (7.1a)$$

$$\text{Macroporosity} = (\text{pore quantity}) \times (\text{pore size}) \times (\text{pore type}) \quad (7.1b)$$

$$\text{Root density} = (\text{root quantity}) \times (\text{root size}) \quad (7.1c)$$

The individual scores for the morphological feature were then summed to produce the SMDS for the horizon using Equation 7.2:

$$\text{SMDS} = (\text{texture})+(\text{pedality})+(\text{macroporosity})+(\text{root density})+(\text{water content}) \quad (7.2)$$

A total radon barrier SMDS ($_t$SDMS) was calculated to evaluate how soil morphology has affected D_{Rn} by summing the SMDS for each horizon (Equations 7.1) based on their relative contribution of each horizon to the thickness of the radon barrier. A $_t$SMDS was also calculated for the natural analogues, as constrained to the horizons at the same depth as the radon barrier.

$_t$SMDS computed using this approach ranged from as low as 5 (TP-5 at the Falls City site) to as high as 10,688 (MP-2 at the Bluewater site). An optimally constructed radon barrier would have

a low $_t$SMDS (<100) on completion of construction comprising morphological contributions from texture and moisture alone (i.e., no macrostructure or roots). As the barrier evolves through pedogenic processes (e.g., desiccation cracking, plant rooting, development and stabilization of aggregates) the $_t$SMDS will increase and ultimately could approach that of a natural analogue.

A partial SMDS ($_p$SDMS) was calculated to evaluate how soil morphology has affected K_{sat} by constraining scoring to the depth and thickness of the block monolith sample.

7.3 Results and Discussion

The $_t$SMDS for the radon barrier in each test pit at each of the four sites is in Figure 7.1 along with the $_t$SMDS for horizons at similar depths in the natural analogues. The relative contribution of individual morphological features to the $_t$SMDS for the radon barrier and analogue at each site is in Table 7.2. A summary of the morphological features recorded in the field investigation and the corresponding SMDS calculations is in Appendix J.

7.3.1 Comparison of $_t$SMDS Between Sites

A detailed account of soil morphology of the waste covers studied is in Section 6, and a description of factors that contribute to variable morphology in waste covers is in Appendix H. As discussed in detail in Appendix H, the presence of soil morphology can be described by soil forming factors including cover design (e.g., riprap, slope, depth from surface), management (e.g., chopping of shrubs), biota (e.g., vegetation establishment, insect and rodent burrowing), climate (e.g., average precipitation and temperature), and time since construction. Combinations of these factors influence the way a waste cover system intercepts environmental fluxes, with impacts to soil processes that result in the development of soil morphology and subsequent $_t$SMDS values. Lower $_t$SMDS values would generally be associated with soils that have been subjected to low frequency or low intensity soil processes (e.g., infrequent very fine rooting), while higher $_t$SMDS values would generally be associated with soils that have been subjected to a high frequency, long duration, and diverse set of soil processes (e.g., bioturbation by plants and animals, significant desiccation and cracking, freeze-thaw cycling).

Table 7.1 Points for Soil Morphological Classes (Lin et al. 1999a)

Morphological Feature[a]	Descriptor	Class	Points
Texture	No additional descriptors	Clay	1
		Silty clay	2
		Sandy clay	3
		Silty clay loam	4
		Clay loam	5
		Sandy clay loam	6
		Loam	10
		Silt loam	13
		Sandy loam	15
		Silt	19
		Loamy sand	24
		Sand	27
Pedality	Ped grade	Massive	0
		Weak	1
		Moderate	5
		Strong	25
		Single grain	50
	Ped size	Very coarse	1
		Coarse / medium	3
		Fine / very fine	18
	Ped shape	Massive	0
		Platy	1
		Prismatic	10
		Blocky	10
		Granular / single grain	30
Macroporosity[b]	Quantity	Very few	1
		Few	3
		Common	10
		Many	28
		Very many	60
	Size	Very fine	1
		Fine	9
		Medium	49
		Coarse	60
		Very coarse	70
		Extremely coarse	75
	Type	Vugh	1
		Channel	8
		Fracture	10
		Packing void	25
Root Density	Quantity	Few / very few	1
		Common	16
		Many	25
	Root size	Very coarse	1
		Coarse / medium	13
		Fine / very fine	43
Water Content[a]	No additional descriptors	Saturated	1
		Wet	3
		Moist	7
		Dry	30
		Very dry	65

[a] Soil morphology described using standard soil survey procedures (USDA 2012).
[b] Method for pore size and shape characterization described in Lin et al (1999a)
[c] Gravimetric water content was related to saturation by water class state in USDA (2012): saturated (>30%), wet (20–30%), moist (10–20%), dry (7–10%), very dry (<7%).

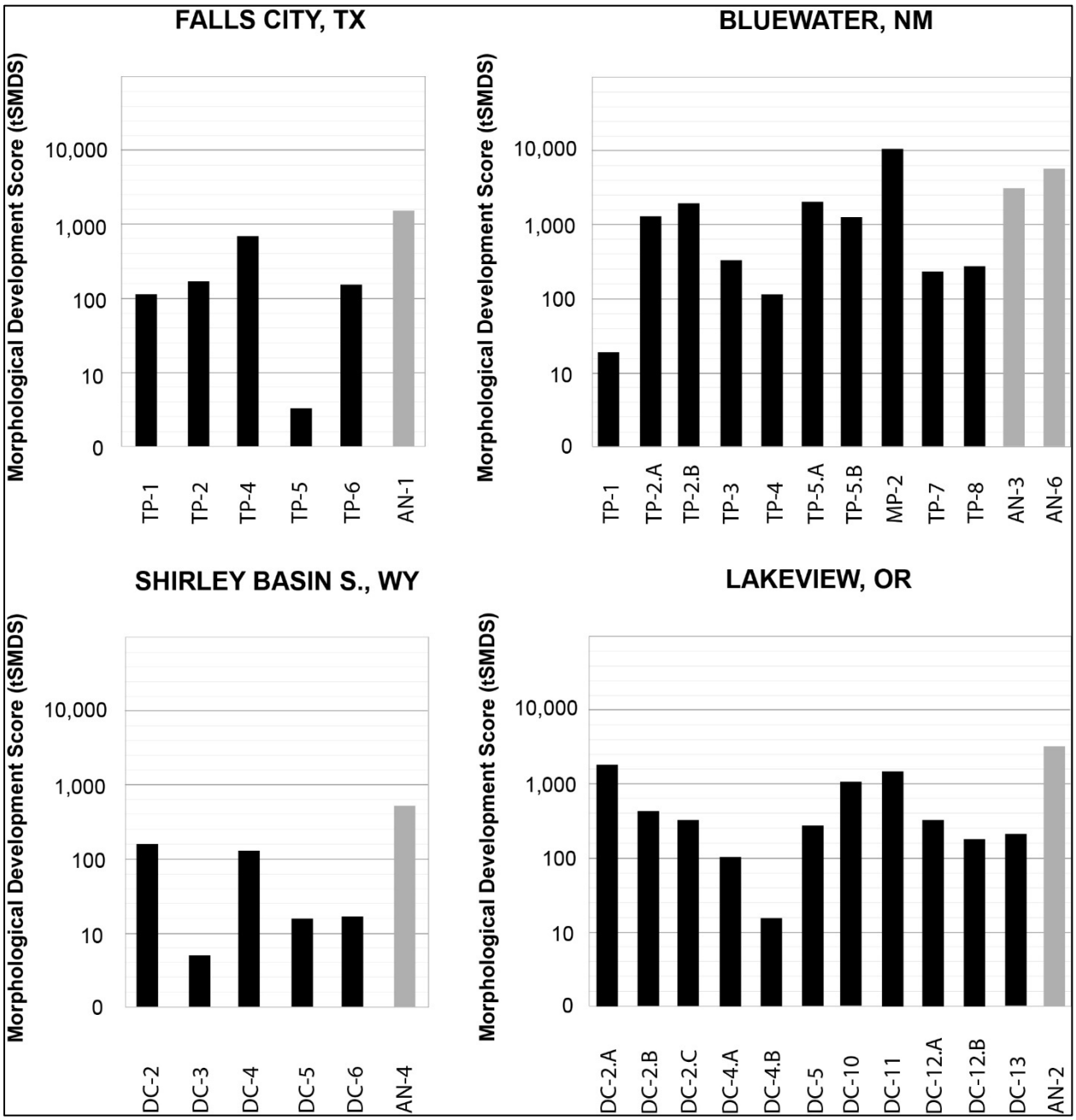

Figure 7-1 $_t$SMDS of the Radon Barrier in Each Test Pit at Each Site and for Horizons at Similar Depth in Natural Analogue Profiles

Table 7.2 Relative Contribution of Individual Soil Morphological Features to $_t$SMDS

Site	Profile	Surface Condition[a]	$_t$SMDS[b]	Relative Contribution to $_t$SMDS[c] (% and value)									
				Moisture		Texture		Pedality		Porosity		Roots	
Falls City, TX	TP-1	Mesquite and mixed grasses	135	1%	1	1%	2	37%	49	24%	32	37%	50
	TP-2	Mixed grasses	253	0%	1	1%	2	78%	197	4%	10	17%	43
	TP-4	Mixed grasses	847	0%	1	0%	3	63%	532	32%	269	5%	43
	TP-5	Rock-apron	5	20%	1	80%	3	0%	0	0%	0	0%	0
	TP-6	Rock-slope	197	1%	1	2%	4	0%	0	2%	4	95%	188
	AN-1[d]	Mixed woodland	1889	0%	1	0%	1	16%	383	7%	166	77%	1338
Bluewater, NM	TP-1	Ephemeral lakebed	31	22%	7	33%	10	3%	<1	1%	<1	41%	13
	TP-2.A	Squirreltail grass (2.0 m)	1558	1%	13	0%	7	78%	1213	8%	118	13%	207
	TP-2.B	Squirreltail grass (0.0 m)	2516	1%	22	0%	5	43%	1080	9%	226	47%	1183
	TP-3	Sparse vegetation	551	6%	30	1%	8	62%	343	0%	1	31%	169
	TP-4	Sparse vegetation	134	13%	17	6%	8	72%	96	1%	<1	9%	12
	TP-5.A	Saltbush (0.0 m)	2861	2%	65	0%	11	12%	346	41%	1159	45%	1280
	TP-5.B	Saltbush (2.0 m)	1410	3%	39	0%	6	15%	206	51%	718	31%	441
	MP-2[e]	Harvester ant mound	10688	1%	65	0%	8	42%	4500	51%	5403	7%	713
	TP-7	Young saltbush	366	10%	35	2%	6	7%	25	8%	28	74%	272
	TP-8	Sparse vegetation	487	5%	26	1%	6	88%	431	1%	5	4%	19
	AN-3[f]	High desert steppe	5205	1%	34	0%	6	57%	2990	19%	1004	23%	1171
	AN-6[g]	Desert pavement	7439	1%	52	0%	4	38%	2837	48%	3568	13%	978
Shirley Basin S., WY	DC-2	Mixed grasses	202	1%	3	1%	1.5	0%	0	0%	0	98%	197
	DC-3	Mixed grasses	7	38%	3	15%	1	0%	0	15%	1	32%	2
	DC-4	Mixed grasses	156	2%	3	1%	1	0%	0	0%	0	98%	153
	DC-5	Saltbush and mixed grasses	24	4%	1	4%	1	0%	0	0%	0	91%	22
	DC-6	Rock-slope / burrow	26	12%	3	4%	1	0%	0	0%	0	84%	22
	AN-4[h]	Black sage steppe	703	0%	3	0%	1	0%	2	1%	10	98%	687
Lakeview, OR	DC-2.A	Bitterbrush (0.0 m)	2350	0%	2	1%	12	5%	125	1%	27	93%	2183
	DC-2.B	Bitterbrush (1.0 m)	615	1%	4	2%	14	20%	122	3%	20	74%	455
	DC-2.C	Bitterbrush (2.0 m)	522	1%	4	3%	14	3%	18	4%	20	89%	466
	DC-4.A	Rock-slope / grass	111	1%	1	17%	19	0%	0	0%	0	82%	91
	DC-4.B	Rock-slope	20	5%	1	95%	19	0%	0	0%	0	0%	0
	DC-5	Rabbitbrush / burrow	444	1%	3	3%	14	16%	71	10%	44	70%	312
	DC-10.A	Sparse vegetation	1086	0%	1	1%	15	8%	88	5%	56	85%	927
	DC-11.A	Bitterbrush	1840	0%	6	1%	16	8%	150	1%	21	90%	1649
	DC-12.A	Rabbitbrush (0.0 m)	560	0%	1	2%	14	41%	232	2%	10	54%	303
	DC-12.B	Rabbitbrush (2.0 m)	253	0%	1	5%	14	32%	80	3%	6	60%	152
	DC-13	Sheep fescue	379	1%	2	4%	16	15%	55	14%	52	67%	248
	AN-2[i]	Big sage steppe	5366	0%	3	0%	17	39%	2071	14%	767	47%	2509

[a] Profiles with 0.0, 1.0, or 2.0 m annotation indicate lateral distance away from surface feature. 0.0 m is directly beneath the feature.
[b] $_t$SMDS calculations are constrained to the radon barrier component of the cover profile.
[c] Relative contribution accounts for the thickness of individual radon barrier horizons, the percent contribution of that horizon to the overall radon barrier thickness, and the scores given to individual morphological features within those horizons.
[d] AN-1. $_t$SMDS and relative contribution % constrained to analogue horizons from 900 mm – 1520 mm to better match radon barrier.
[e] MP-2. Given destructive nature of K_{sat} and D_{Rn} sampling, we could not conduct full profile morphology of TP-6.
[f] AN-3. $_t$SMDS and relative contribution % constrained to analogue horizons from 80 mm – 1780 mm to better match radon barrier.
[g] AN-6. $_t$SMDS and relative contribution % constrained to analogue horizons from 80 mm – 1000 mm to better match radon barrier.
[h] AN-4. $_t$SMDS and relative contribution % constrained to analogue horizons from 850 mm – 1610 mm to better match radon barrier.
[i] AN-2. $_t$SMDS and relative contribution % constrained to analogue horizons from 400 mm – 1170 mm to better match radon barrier.

7.3.1.1 Falls City, Texas

At the Falls City disposal cell, $_t$SMDS for the radon barrier ranges from 5 to 847 representing very low to low development. The top of the radon barrier is roughly 1.0 meter (m) from ground surface, the top deck of the cover is vegetated, while the apron and side slopes are covered with rock riprap. The two profiles associated with riprap (TP-5 and TP6) had the lowest $_t$SMDS values, while the vegetated profiles on the top deck had the highest values (TP1, TP-2, and TP-4). Contrary to initial hypotheses, the mesquite (*Prosopis glandulosa)* profile did not have the highest $_t$SMDS value on the cover, and roots larger than very fine were limited to the top edge of the radon barrier.

Pedality (soil structuring) is the largest contributor to $_t$SMDS values on the top deck of the cover, corresponding to lower moisture saturation versus profiles on rock riprap aprons or side slopes. Pedality also corresponds with the observance of remnant soil structure from borrow materials in the radon barrier (Section 6.4.1; Figure 6.5). Very fine rooting contributes to the desiccation of radon barrier materials and the enlargement of fractures along remnant soil structure. Given remnant soil structure, the Falls City barrier was likely constructed with the highest *initial* $_t$SMDS value of the covers investigated in this study. Given high swell potential of radon barrier materials, variations in weather during field observations (including intermittent rainfall and extreme humidity), time that profile face was exposed prior to observation, and methodological challenges visually classifying remnant soil structure in swollen condition, SMDS values were likely underreported for profiles at the Falls City site, therefore comparisons between Falls City and other sites should be undertaken with added caution.

The $_t$SMDS of the natural analogue is 1889. Plant rooting is the largest contributor to $_t$SMDS in the analogue profile. The active management of vegetation on the cover presumably results in the slow establishment of plant roots in the radon barrier due to frequent chopping of mesquite plants. Should vegetation management on the cover be reduced, plant rooting in radon barrier sections underneath mesquite on the top deck of the cover would likely begin to resemble the analogue $_t$SMDS; a roughly 2–15-fold increase from present $_t$SMDS value.

7.3.1.2 Bluewater, New Mexico

At the Bluewater disposal cell, $_t$SMDS for the radon barrier ranges from 31 to 10,688 representing very low to extremely high development. The top of the radon barrier is roughly 0.1 m from ground surface and has a thin layer of rock riprap for erosion protection. The highest $_t$SMDS value is associated with the harvester ant mound (*Pogonomyrmex spp.*) (MP-2), followed by fourwing saltbush (*Atriplex canescens*) (TP-5), squirreltail grass (*Elymus elymoides*) (TP-2), and annual weeds (TP-3). The lowest $_t$SMDS are associated with the ephemeral lake depression and sparse vegetation (TP-1).

Significant heterogeneity in surface condition exists at the Bluewater site and contributes to a high diversity of soil morphology (Section 6.4.2). Rooting dominates $_t$SMDS values in fourwing saltbush profiles that have coarse and medium roots (e.g., TP-5.A and TP-7). Pedality dominates $_t$SMDS values in grassy or sparsely vegetated profiles with very fine roots (e.g., TP-2.B, TP-3, TP-4, and TP-8), presumably due to fine scale root induced desiccation and cracking. Porosity dominates $_t$SMDS values under harvester ant mounds (MP-2). The saturated nature of the radon barrier under the ephemeral lake (TP-1) results in very limited soil structural development.

The $_t$SMDS of the natural analogues range from 5205 to 7439. A mixture of pedality and porosity are the largest contributors to $_t$SMDS in the analogues, presumably reflecting contributions from many different surface conditions over time (e.g., grasses, shrubs, insects). As the cover continues to age and biotic processes continue to evolve, the average $_t$SMDS on the top deck of the cover will likely approach that of the analogues; a roughly 2–200-fold increase from present $_t$SMDS value.

7.3.1.3 Shirley Basin, Wyoming

At the Shirley Basin South disposal cell, $_t$SMDS for the radon barrier ranges from 7 to 202 representing very low development. The top of the radon barrier is roughly 1.0 m from ground surface. The top deck of the cover is vegetated, while the side slopes are covered with rock riprap. Surface condition (i.e., shrub, grass, or side slope) does not result in systematic variation in $_t$SMDS; radon barrier macromorphological development is negligible across all profiles investigated at the site. Low $_t$SMDS values are attributed to isolation from surface processes, including desiccation cracking and freeze thaw (due to depth of the radon barrier), in addition to the presence of limited roots that would increase desiccation. Low root mass is attributed to acidic soil conditions unfavorable to root development (Section 6.4.5.1).

The $_t$SMDS of the natural analogue is 775, the lowest of the analogues observed in this study. The dominant contributor to $_t$SMDS in the analogue is plant rooting; however, roots are exclusively confined to infrequent fractures at the depths shared by the radon barrier. Analogue soils at the depth of the radon barrier are also acidic, posing constraints to rooting. While the average $_t$SMDS of the top deck of the cover may slowly approach that of the analogue over time, representing a roughly 3–100-fold increase from present $_t$SMDS value, such changes would still represent a relatively low overall $_t$SMDS value.

7.3.1.4 Lakeview, Oregon

At the Lakeview disposal cell, $_t$SMDS for the radon barrier ranges from 20 to 2349 representing very low to high development. The top of the radon barrier is roughly 0.6 m from ground surface. The top deck of the cover is a vegetated multicomponent cover, while the side slopes are covered with rock riprap. The highest $_t$SMDS values are associated with antelope bitterbrush (*Purshia tridentata;* DC-2 and DC-11) on the top deck, while the lowest $_t$SMDS is associated with the unvegetated rock riprap side slope (DC-4).

Plant rooting is the largest contributor to $_t$SMDS values at the Lakeview site, with antelope bitterbrush and rubber rabbitbrush (*Ericameria nauseosa*) having the greatest abundance and diversity of roots. Very fine to coarse roots were commonly observed, in addition to both remnant and emergent soil structure. Plant rooting contributes to desiccation of radon barrier materials and the enlargement of fractures along remnant soil structure from uptake of water by roots.

The $_t$SMDS of the natural analogue is 5366. Plant rooting is the largest contributor to $_t$SMDS in the analogue. As the cover ages and natural succession continues, the average $_t$SMDS of the top deck of the cover will likely approach that of the analogue, a roughly 2–20-fold increase from present $_t$SMDS value.

7.3.2 Soil Morphology, Radon Diffusion Coefficients, and Radon Travel-Time

The relationship between D_{Rn} and $_tSMDS$ is shown in Figure 7.2. Diffusion coefficients for each of the 25 test pits represent an average of the measurements made in that pit. Measurement ranges are indicated as bars in Figure 7.2. For some test pits, D_{Rn} could not be computed due to instrumentation errors or radon fluxes below detection limits. A summary of D_{Rn} and $_tSMDS$ values is provided in Table 7.3.

D_{Rn} increases as $_tSDMS$ increases, indicating that radon barriers with greater structure have higher diffusion coefficients and higher radon fluxes for the same level of activity in the tailings. This relationship can be described by the linear model shown in Figure 7.2, which was obtained by least squares regression ($R^2 = 0.90$). The observance of relatively high D_{Rn} compared to relatively lower $_tSMDS$ at the Falls City site may be attributed to underestimating soil structure, and the site is excluded from the linear regression in Figure 7.2.

In four of the five profiles with the highest D_{Rn}, plant rooting is the dominant contributor to $_tSMDS$, indicating that plants contribute to increased radon diffusion. The Bluewater site has the profiles with the highest D_{Rn}, whereas the Shirley Basin South site has the profiles with the lowest D_{Rn}. The shallow riprap cover at the Bluewater site has undergone a significant amount of change due to biotic processes (Section 7.3.1.2), while the vegetated cover at the Shirley Basin South site has a deep and acidic radon barrier that inhibits root growth and subsequent root induced soil development (Section 7.3.1.3). The Lakeview site also has abundant plant rooting and high D_{Rn}.

Calculations for radon transport times through the barrier material are reported in Section 4.6.4. The number of Rn-222 half-lives required to move through the barrier compared to $_tSMDS$ is summarized in Figure 7.3. As $_tSMDS$ increases travel time decreases, indicating that radon barriers with greater soil structuring have faster radon transport times. This relationship can be described by the logarithmic model shown in Figure 7.3, which was obtained by least squares regression ($R^2 = 0.72$). The Falls City site was excluded from the logarithmic regression in Figure 7.3.

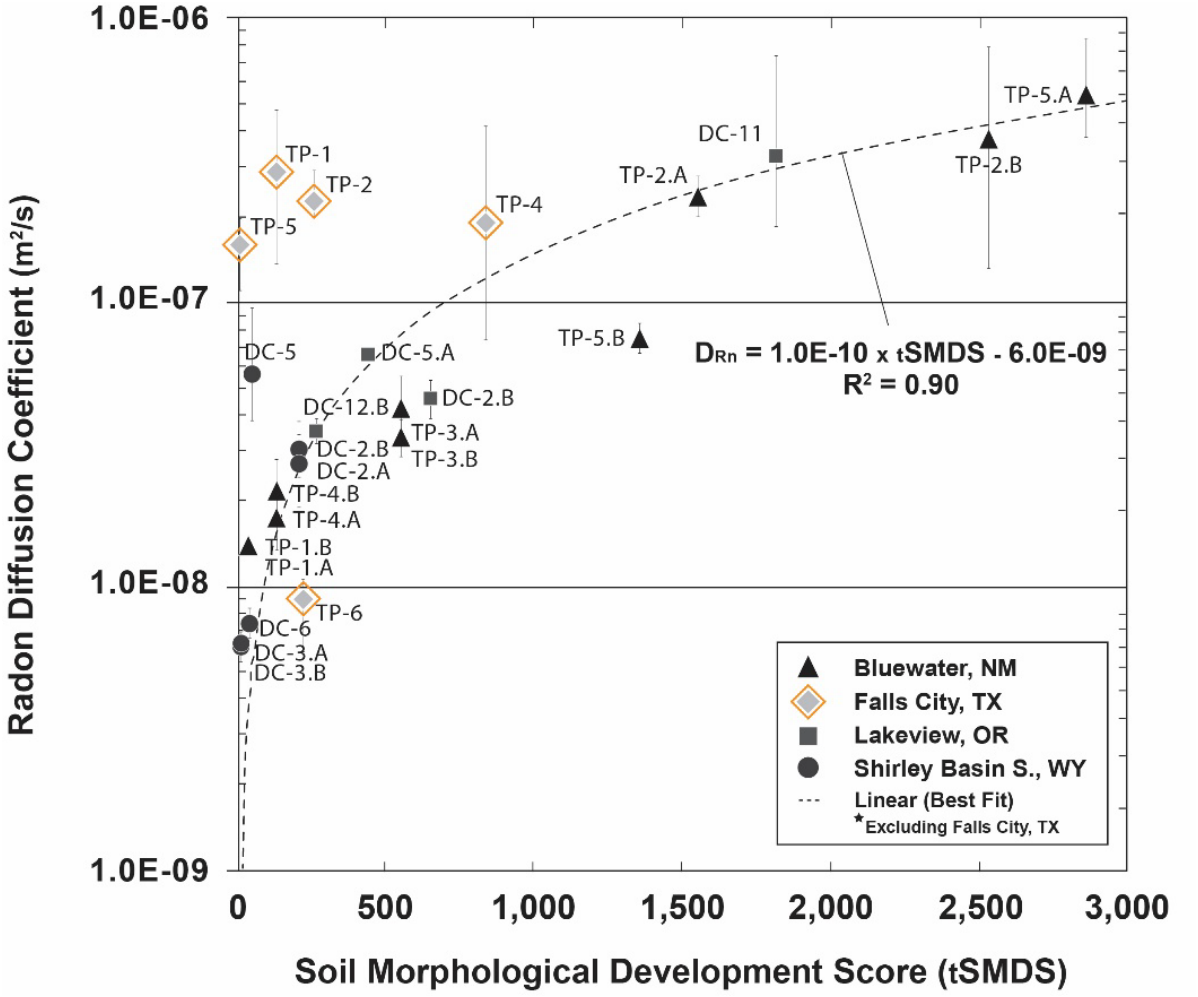

Figure 7-2 Radon Diffusion Coefficients and Radon Barrier tSMDS

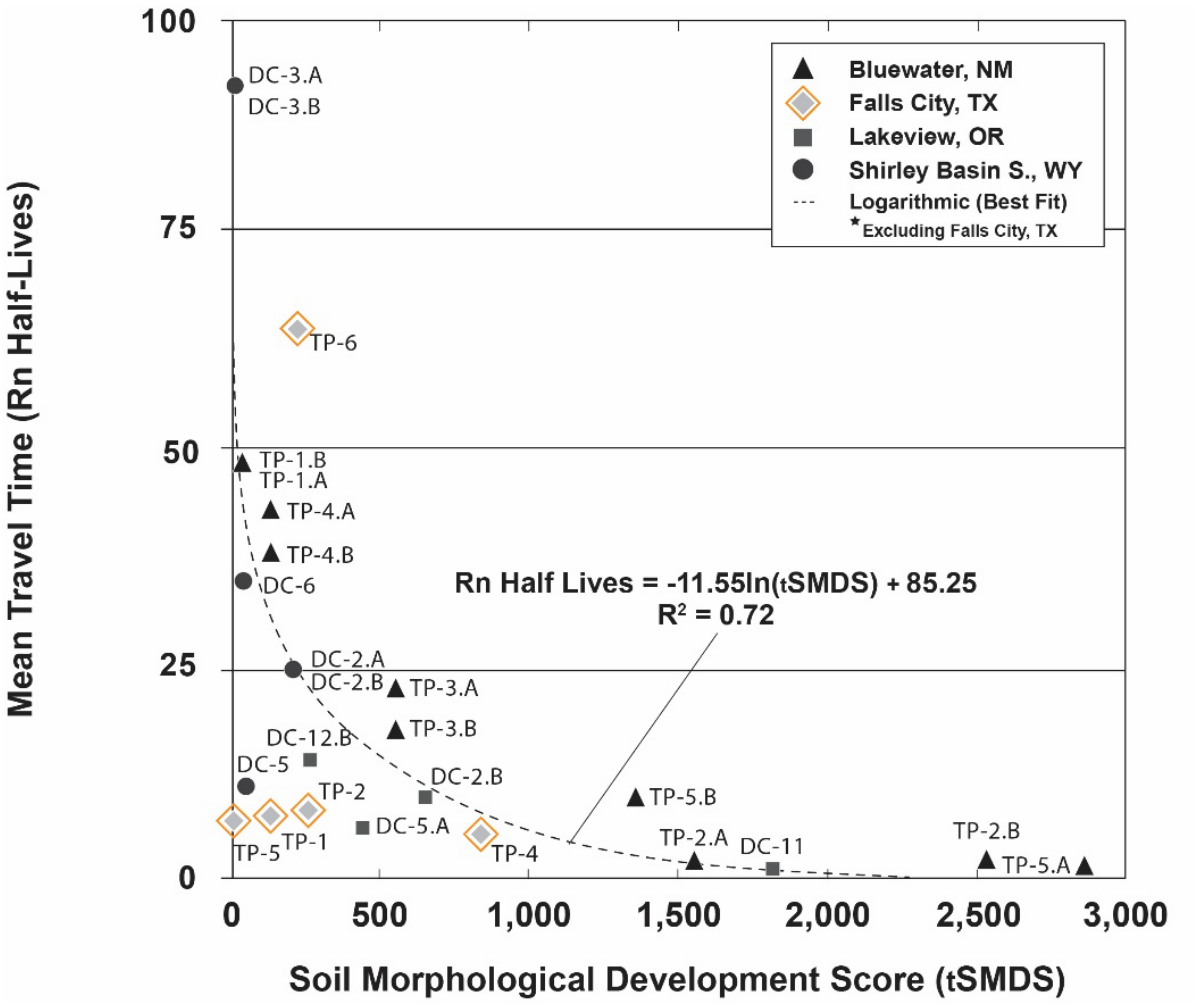

Figure 7-3 Mean Travel Time (Radon Half-Lives) and tSMDS

Table 7.3 Summary of Radon Diffusion Coefficients and Radon Barrier $_t$SMDS

Site	Profile	Surface Condition[a]	$_t$SMDS[b]	Average Saturation %[c]	Mean D_{Rn} (m^2/s)	Range of D_{Rn} Values (m^2/s)	Mean Rn Half-Lives[d]	Rn Barrier Thickness (m)
Falls City, TX	TP-1	Mesquite and mixed grasses	135	79	3.0×10^{-7}	$1.6\times10^{-7} – 4.4\times10^{-7}$	4.9	0.58
	TP-2	Mixed grasses	253	93	2.3×10^{-7}	$2.0\times10^{-7} – 2.7\times10^{-7}$	5.5	0.52
	TP-4	Mixed grasses	847	91	1.8×10^{-7}	$1.9\times10^{-7} – 6.0\times10^{-8}$	4.3	0.46
	TP-5	Rock-apron	5	94	1.6×10^{-7}	$1.3\times10^{-7} – 1.8\times10^{-7}$	6.4	0.71
	TP-6	Rock-slope	197	88	9.5×10^{-9}	$1.0\times10^{-8} – 6.0\times10^{-9}$	63	0.56
	AN-1	Mixed woodland	1889	-	n/a	n/a	n/a	n/a
Bluewater, NM	TP-1.A	Ephemeral lakebed	31	86	1.4×10^{-8}	1.4×10^{-8}	48.6	0.65
	TP-1.B		31	-	1.4×10^{-8}	1.4×10^{-8}	48.6	
	TP-2.A	Squirreltail grass (2.0 m)	1558	60	2.3×10^{-7}	$2.0\times10^{-7} – 3.0\times10^{-7}$	2.8	0.61
	TP-2.B	Squirreltail grass (0.0 m)	2516	-	3.4×10^{-7}	$1.2\times10^{-7} – 6.8\times10^{-7}$	2.7	
	TP-3.A	Sparse vegetation	551	77	3.4×10^{-8}	$1.9\times10^{-8} – 4.9\times10^{-8}$	24.1	0.63
	TP-3.B		551	-	3.2×10^{-8}	$3.1\times10^{-8} – 3.3\times10^{-8}$	20.0	
	TP-4.A	Sparse vegetation	134	69	1.7×10^{-8}	$1.5\times10^{-8} – 2.2\times10^{-8}$	45.3	0.69
	TP-4.B		134	-	2.2×10^{-8}	$1.6\times10^{-8} – 3.0\times10^{-8}$	37.0	
	TP-5.A	Saltbush (0.0 m)	2861	-	4.9×10^{-7}	$3.0\times10^{-7} – 7.4\times10^{-7}$	1.4	0.62
	TP-5.B	Saltbush (1.0 m)	1410	-	7.2×10^{-8}	$6.7\times10^{-8} – 7.7\times10^{-8}$	8.7	
	MP-2.A	Harvester ant mound	10,688	-	-	-	-	0.70
	TP-7.A	Young saltbush	366	59	-	-	-	NM[e]
	TP-8.A	Sparse vegetation	487	65	-	-	-	NM[e]
	AN-3	High desert steppe	5205	-	n/a	n/a	n/a	n/a
	AN-6	Desert pavement	7439	-	n/a	n/a	n/a	n/a
Shirley Basin S., WY	DC-2.A	Mixed grasses	202	88	2.7×10^{-8}	$2.5\times10^{-8} – 3.2\times10^{-8}$	25.0	0.68
	DC-2.B		202	-	3.1×10^{-8}	$1.8\times10^{-8} – 4.1\times10^{-8}$	25.3	
	DC-3.A	Mixed grasses	7	92	7.4×10^{-9}	$7.2\times10^{-9} – 7.7\times10^{-9}$	87.0	0.65
	DC-3.B		7	-	7.4×10^{-9}	$7.2\times10^{-9} – 7.7\times10^{-9}$	87.0	
	DC-4.A	Mixed grasses	156	90	-	-	-	NM[e]
	DC-5.A	Saltbush and mixed grasses	24	97	5.7×10^{-8}	$1.0\times10^{-7} – 2.8\times10^{-8}$	10.1	0.56
	DC.6.A	Rock-slope/rodent burrow	26	97	6.6×10^{-9}	$6.0\times10^{-9} – 7.2\times10^{-9}$	33.6	0.49
	AN-4	Black sage steppe	703	-	n/a	n/a	n/a	n/a
Lakeview, OR	DC-2.A	Bitterbrush (0.0 m)	2350	-	-	-	-	0.43
	DC-2.B	Bitterbrush (1.0 m)	615	84	3.56×10^{-8}	$3.0\times10^{-8} – 4.0\times10^{-8}$	8.2	0.43
	DC-4.A	Rock-slope/grass	111	92	Radon flux below detection limit		-	0.38
	DC-4.B	Rock-slope	20	92	Radon flux below detection limit		-	0.38
	DC-5	Rabbitbrush/burrow	444	81	6.5×10^{-8}	6.5×10^{-8}	4.9	0.46
	DC-10.A	Sparse vegetation	1086	87	Radon flux measurement error		-	0.41
	DC-11.A	Bitterbrush	1840	-	3.0×10^{-7}	$1.8\times10^{-7} – 6.5\times10^{-7}$	1.3	0.43
	DC-12.A	Rabbitbrush (0.0 m)	560	-	-	-	-	0.61
	DC-12.B	Rabbitbrush (2.0 m)	253	-	3.2×10^{-8}	$3.0\times10^{-8} – 3.5\times10^{-8}$	17.3	0.63
	DC-13	Sheep fescue	379	-	Radon flux below detection limit		-	0.66
	AN-2	Big sage steppe	5366	-	n/a	n/a	n/a	n/a

[a] Profiles with 0.0, 1.0, or 2.0 m annotation indicate lateral distance away from surface feature. 0.0 m is directly beneath the feature.
[b] The reported $_t$SMDS values for analogues are constrained to horizons occurring at depths shared by the radon barrier.
[c] Average Percent Moisture Saturation (S_r) is summarized in Section 4 from Stefani (2016) and Michaud (2018).
[d] Mean number of radon half-lives reported in Section 4.6.4.
[e] NM = not measured. The bottom of the radon barrier was not encountered in these profiles.
Abbreviation: m^2/s = meters squared per second

7.3.2.1 Site Specific Trends in Radon Diffusion and the Influence of Moisture Saturation

The relationship between D_{Rn} and $_tSMDS$ within individual sites is presented in Figure 7.4. At the Bluewater and Lakeview sites, as $_tSMDS$ increases, D_{Rn} increases. The relationship between D_{Rn} and $_tSMDS$ at the Bluewater site can be described by the exponential model shown in Figure. 7.4.B, which was obtained by least squares regression ($R^2 = 0.95$). The relationship at the Lakeview site can be described by the exponential model shown in Figure 7.4.D, which was obtained by least squares regression ($R^2 = 0.89$). No relationship exists for the Falls City or Shirley Basin South sites, presumably due to observational challenges encountered during field investigation (7.3.1.1) and very little visually observable soil development (7.3.1.3), respectively.

Higher moisture saturation (S_r) results in lower D_{Rn} as air-filled pores become occluded by water (NRC 1989). However, Section 4.6.6 suggests that even when moisture is retained in the radon barrier, radon may flow along preferential pathways that have presumably developed due to the formation of soil structure (e.g., “dual-porosity” conditions). These preferential pathways are likely large enough that they drain readily, remaining open to gas transport. As a result, values of D_{Rn}, especially when S_r is above about 80%, are often higher than would be expected based on S_r alone. Figure 7.4 shows the relationship between S_r and D_{Rn} at each site. With exception to the Bluewater site, where higher S_r corresponds to lower D_{Rn} (Figure. 7.4B), no relationship exists between D_{Rn} and S_r under the conditions studied. Given higher than expected D_{Rn} based on S_r alone for many radon barriers in this study (Section 4.6.6), this observation further supports the hypothesis of dual-porosity regulation of D_{Rn} due to emergence of soil structure as captured in $_tSMDS$.

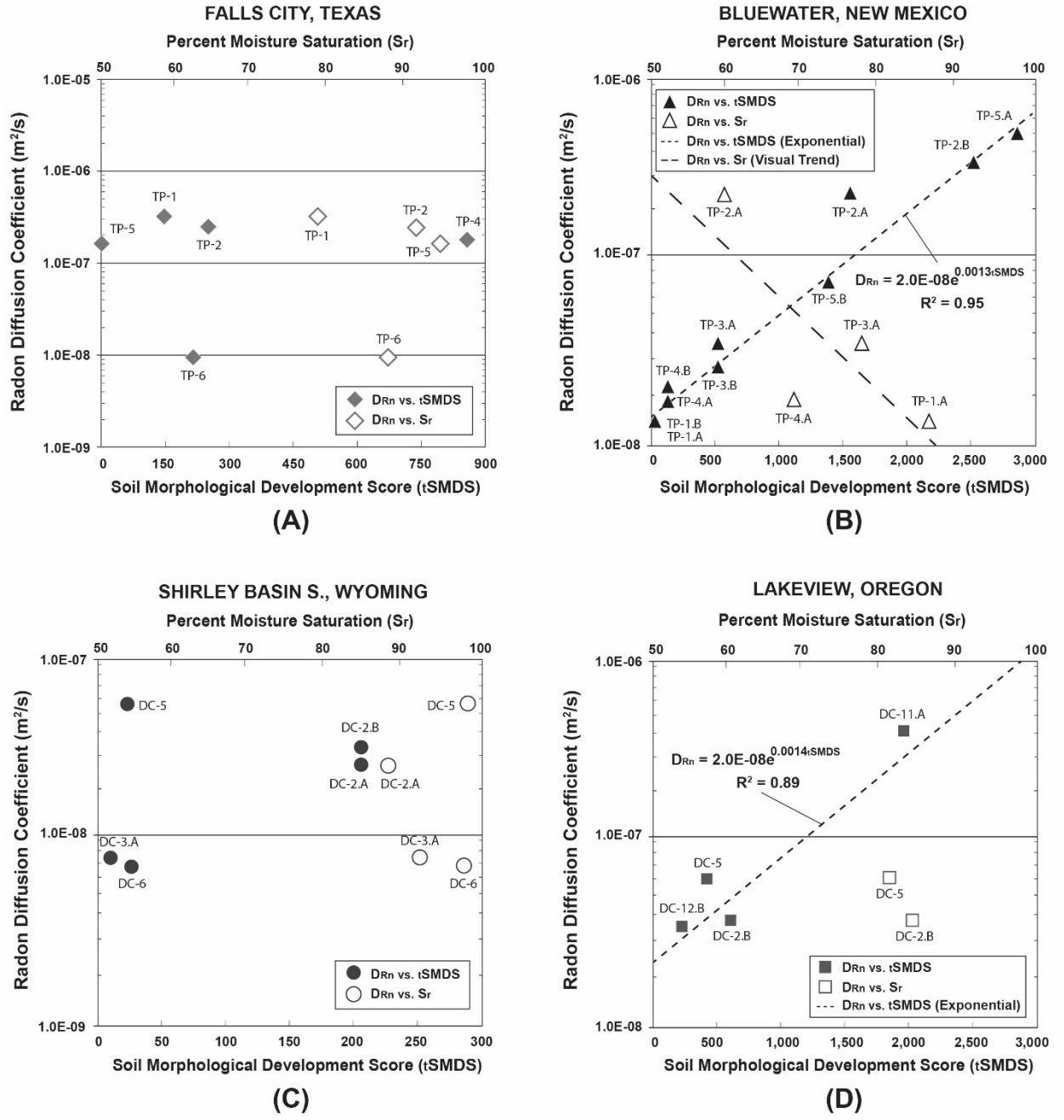

Figure 7-4 Radon Diffusion, Moisture Saturation, and Radon Barrier $_t$SMDS at Each Site

7.3.3 Saturated Hydraulic Conductivity and Soil Morphology

The impact of soil morphological development on K_{sat} is presented in Figure 7.5 and Table 7.5. The $_{p}$SMDS were computed as a weighted average of SMDS for the individual horizons within the depth of the block sample. Given the destructive nature of block sampling and the highly localized morphology of some soil features, K_{sat} and $_{p}$SMDS could not be compared for some profiles.

The highest K_{sat} typically correspond to the highest $_{p}$SMDS and the lowest K_{sat} to low $_{p}$SMDS. Variation in K_{sat} below 1.0×10^{-6} meter per second (m/s) is largely confined to $_{p}$SMDS of less than 1000 (roughly 10% of the range of $_{p}$SMDS values observed), suggesting that K_{sat} and $_{p}$SMDS follow a high-low relationship more than a functional relationship.

With few exceptions, the natural analogue samples, regardless of depth from ground surface, have the highest K_{sat} and $_{p}$SMDS values. The natural analogue at Shirley Basin South has lower K_{sat} and $_{p}$SMDS values compared to analogues at the other sites, which is attributed to acidic soil conditions, the inhibition of rooting, and the maintenance of as-built soil structure (Section 6.4.5.1). The shallowest sample from the Falls City analogue (AN-1.A) was collected in a spatially denser zone associated with coarse rooting resulting in conditionally low K_{sat}. The localized compaction from soil densification around coarse living roots can reduce infiltration rates, particularly at the surface (Guidi et al. 1985; Bruand et al. 1996). Under most conditions, as radon barriers age they begin to resemble the morphology of natural analogues, characterized by high $_{p}$SMDS (between 1879 and 8915) and high K_{sat} (between 1.4×10^{-6} to 4.4×10^{-6} m s^{-1}), representing a plausible range of long-term equilibrium conditions.

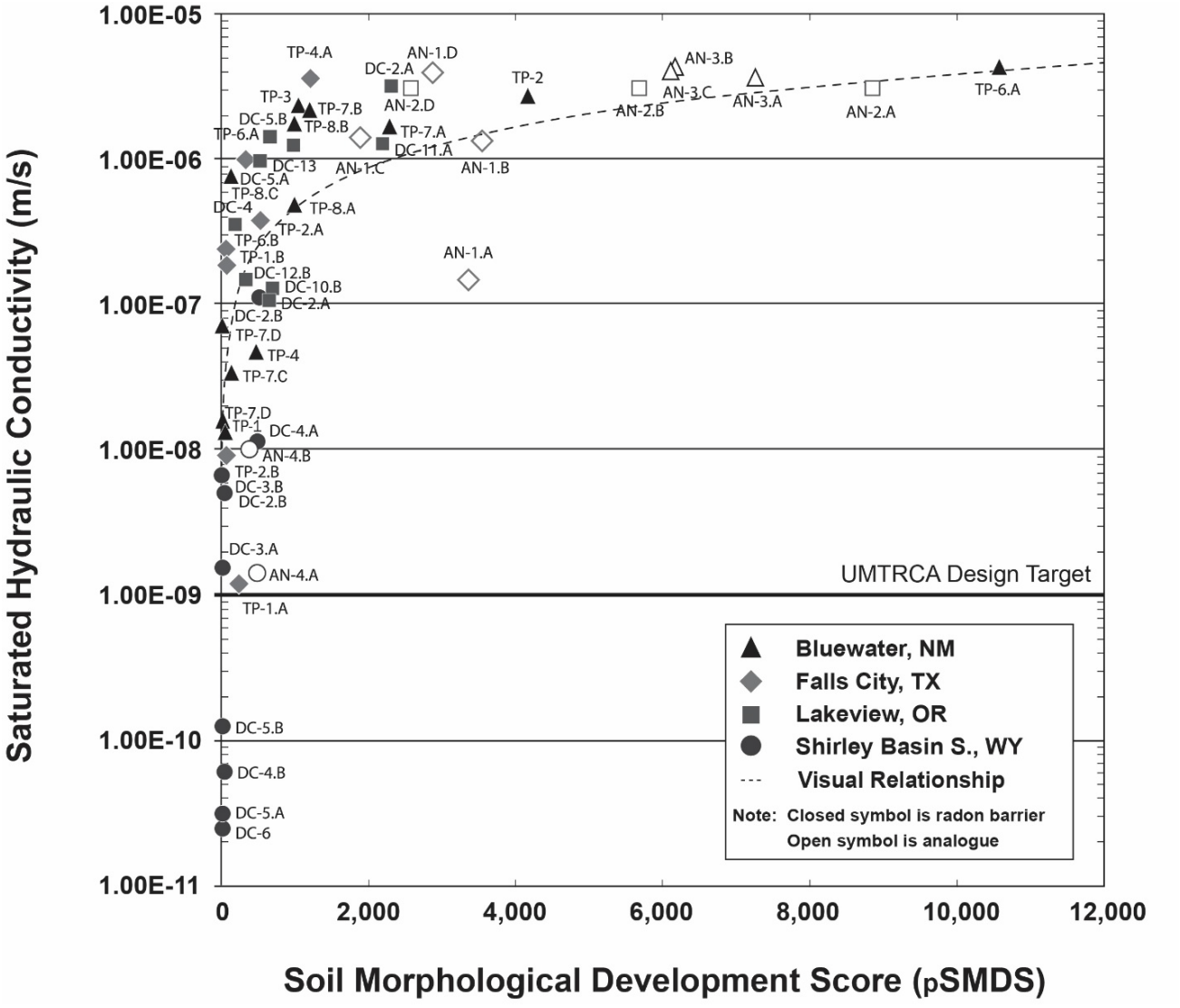

Figure 7-5 Saturated Hydraulic Conductivity and pSMDS

Table 7.4 Summary of Saturated Hydraulic Conductivity and Block Sample $_{p}$SMDS

Site	Block Section ID	Surface Condition[a]	$_{p}$SMDS	K_{sat} (m/s)	Depth (m) to Middle of Section
Falls City, TX	TP-1.A	Mesquite and mixed grasses	247	1.21×10^{-9}	1.12
	TP-1.B		86	2.10×10^{-7}	1.47
	TP-2.A	Mixed grasses	521	4.20×10^{-7}	1.11
	TP-2.B		86	9.37×10^{-9}	1.46
	TP-4.A	Mixed grasses	1485	3.90×10^{-6}	1.03
	TP-5.A	Rock armor apron	4	2.00×10^{-7}	0.92
	TP-6.A	Rock side-slope and mixed vegetation	402	9.97×10^{-7}	0.52
	TP-6.B		48	2.39×10^{-7}	0.87
	AN-1.A[b]	Natural analogue / mixed woodland	3351	1.50×10^{-7}	0.13
	AN-1.B		3547	1.35×10^{-6}	0.48
	AN-1.C		1879	1.40×10^{-6}	1.35
	AN-1.D[c]		2948	4.06×10^{-6}	1.60
Bluewater, NM	TP-1.A	Ephemeral lakebed	50	1.34×10^{-8}	0.24
	TP-2.B	Squirreltail grass (0.0 m)	4165	2.77×10^{-6}	0.22
	TP-3.A	Sparse vegetation	1299	2.38×10^{-6}	0.21
	TP-4.A	Sparse vegetation	471	4.70×10^{-8}	0.19
	TP-5.A	Saltbush (0.0 m)	6034	not collected	0.28
	TP-5.B	Saltbush (1.0 m)	518	not collected	0.47
	TP-6.A[d]	Harvester ant mound (0.0 m)	10,690	4.72×10^{-6}	0.25
	MP-2.A[e]	Harvester ant mound (0.0 m)	10,640	not collected	0.21
	MP-2.B[e]		10,640	not collected	0.53
	MP-2.C[e]		10,601	not collected	0.75
	TP-7.A	Carbonate cell / young saltbush (0.0 m)	2286	1.62×10^{-6}	0.27
	TP-7.B		1310	2.21×10^{-6}	0.60
	TP-7.C		130	3.49×10^{-8}	1.18
	TP-7.D		36	7.48×10^{-8}	1.72
	TP-7.E		13	1.53×10^{-8}	2.33
	TP-8.A	Carbonate cell / sparse vegetation	990	4.90×10^{-7}	0.17
	TP-8.B		990	1.75×10^{-6}	0.58
	TP-8.C		86	7.77×10^{-7}	1.01
	AN-3.A	Natural analogue / high desert steppe	7265	3.69×10^{-6}	0.28
	AN-3.B[f]		6169	4.38×10^{-6}	1.35
	AN-3.C[f]		6127	4.16×10^{-6}	2.06
Shirley Basin S., WY	DC-2.A	Mixed grasses	499	1.12×10^{-7}	1.07
	DC-2.B		30	4.90×10^{-9}	1.39
	DC-3.A	Mixed grasses	21	1.53×10^{-9}	1.02
	DC-3.B		4	6.60×10^{-9}	1.30
	DC-4.A	Mixed grasses	497	1.14×10^{-8}	1.22
	DC-4.B		26	5.90×10^{-11}	1.55
	DC-5.A	Saltbush and mixed grasses	24	3.15×10^{-11}	1.09
	DC-5.B		24	1.24×10^{-10}	1.37
	DC.6	Rock-slope / rodent burrow	26	2.36×10^{-11}	1.38
	AN-4.A	Natural analogue / Black sage steppe	650	1.40×10^{-9}	1.00
	AN-4.B		358	9.81×10^{-9}	1.30
Lakeview, OR	DC-2.A	Bitterbrush (0.0 m)	878	3.21×10^{-6}	0.64
	DC-2.B	Bitterbrush (1.0 m)	103	1.10×10^{-7}	0.76
	DC-4.A	Rock side-slope / grass	226	3.40×10^{-7}	0.61
	DC-5.A	Rodent burrow / rabbitbrush (0.0 m)	960	1.60×10^{-6}	0.64
	DC-5.B		701	1.00×10^{-6}	0.76
	DC-10.B	Sparse vegetation	788	1.30×10^{-7}	0.67
	DC-11.A	Bitterbrush (0.0 m)	2188	1.30×10^{-6}	0.76
	DC-12.B	Rabbitbrush (2.0 m)	46	1.69×10^{-7}	0.55
	DC-13.A	Sheep fescue	1094	1.40×10^{-6}	0.64
	AN-2.A	Natural analogue / Big sagebrush steppe	8915	3.20×10^{-6}	0.60
	AN-2.B		5743	3.06×10^{-6}	0.80
	AN-2.D		2570	3.10×10^{-6}	1.00

[a] Profiles with 0.0, 1.0, or 2.0 m annotation indicate lateral distance away from surface feature. 0.0 m is directly beneath the feature.
[b] Excavated directly adjacent to a tap root, in zone that is spatially denser. Point excluded from regressions.
[c] AN-1.D may be a paleosol (buried soil).
[d] The observation of morphology was only possible for the top block sample in the TP-6 ant mound profile.
[e] MP-2 is an ant mound profile where morphological observation was performed but block sampling not possible.
[f] AN-3.B and AN-3.C may be a paleosol (buried soil).

7.3.4 Saturated Hydraulic Conductivity and Depth from Ground Surface

The relationship between depth from ground surface and K_{sat} has been studied extensively in natural systems, with shallower depths generally displaying higher K_{sat}, and deeper depths lower K_{sat} (e.g., Beven 1982; Beven 1984). Thicker radon barriers have commonly been placed underneath deep layers of overburden and fill soil to resist degradation from freeze thaw, desiccation cracking, and plant intrusion (DOE 1989). A key question in this investigation was to determine if deeper radon barriers maintain low as-built K_{sat} over time.

In the radon barriers studied (all less than 2.5 m from ground surface), the relationship between K_{sat} and depth is conditional (Figures 7.6 and 7.7). After about 20 years of service in a relatively thick radon barrier profile (e.g., the Bluewater TP-7 profile where five stacked radon barrier samples were collected at depths ranging from 0.27 to 2.33 m from ground surface; Figure 7.7.B), K_{sat} values are higher at the surface and decrease with depth. However, individual profiles where two stacked samples were collected from a narrower range of depths show mixed relationships between K_{sat} and depth.

Surface conditions greatly influence K_{sat} and depth relationships. At the Bluewater site, a three order of magnitude variation in K_{sat} is present for radon barrier samples taken at shared depths (0.17 to 0.28 m) under different surface conditions (e.g., ephemeral lake, vegetation type, and harvester ant mound). At the Shirley Basin South site, a five order of magnitude variation in K_{sat} is present for radon barrier samples taken at shared depths (1.02 to 1.39 m) under relatively uniform surface conditions (e.g., mixed steppe vegetation). The mechanisms responsible for the wide variation in relatively low K_{sat} at shared depths at the Shirley Basin South site (1.1×10^{-7} to 2.4×10^{-11} m s^{-1}) are presently unknown.

Except for the previously described natural analogues that display nuanced conditions resulting in lower K_{sat} (e.g., Shirley Basin South AN-4 and Falls City AN-1.A), K_{sat} of the natural analogues occurs within a tight range (1.4×10^{-6} to 4.4×10^{-6} m s^{-1}) at all depths (0.28 to 2.06 m). Therefore, with some exceptions, as radon barriers age (and presumably become more like their natural analogues), depth will likely have less of an impact on K_{sat} within individual profiles resulting in increased K_{sat} at depth with potential impacts for ongoing percolation of meteoric water into tailings.

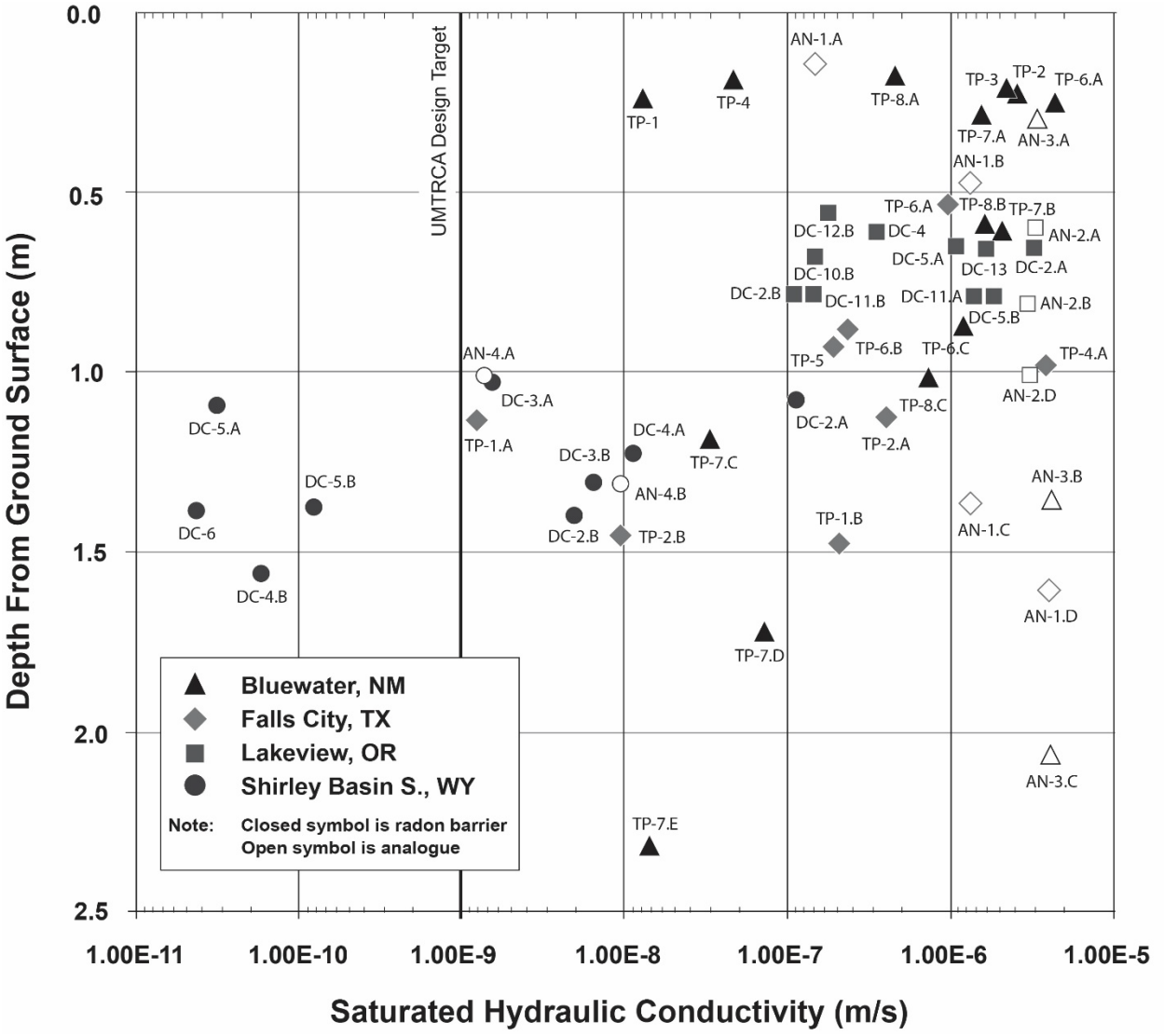

Figure 7-6 Relationship Between Depth from Ground Surface and Hydraulic Conductivity

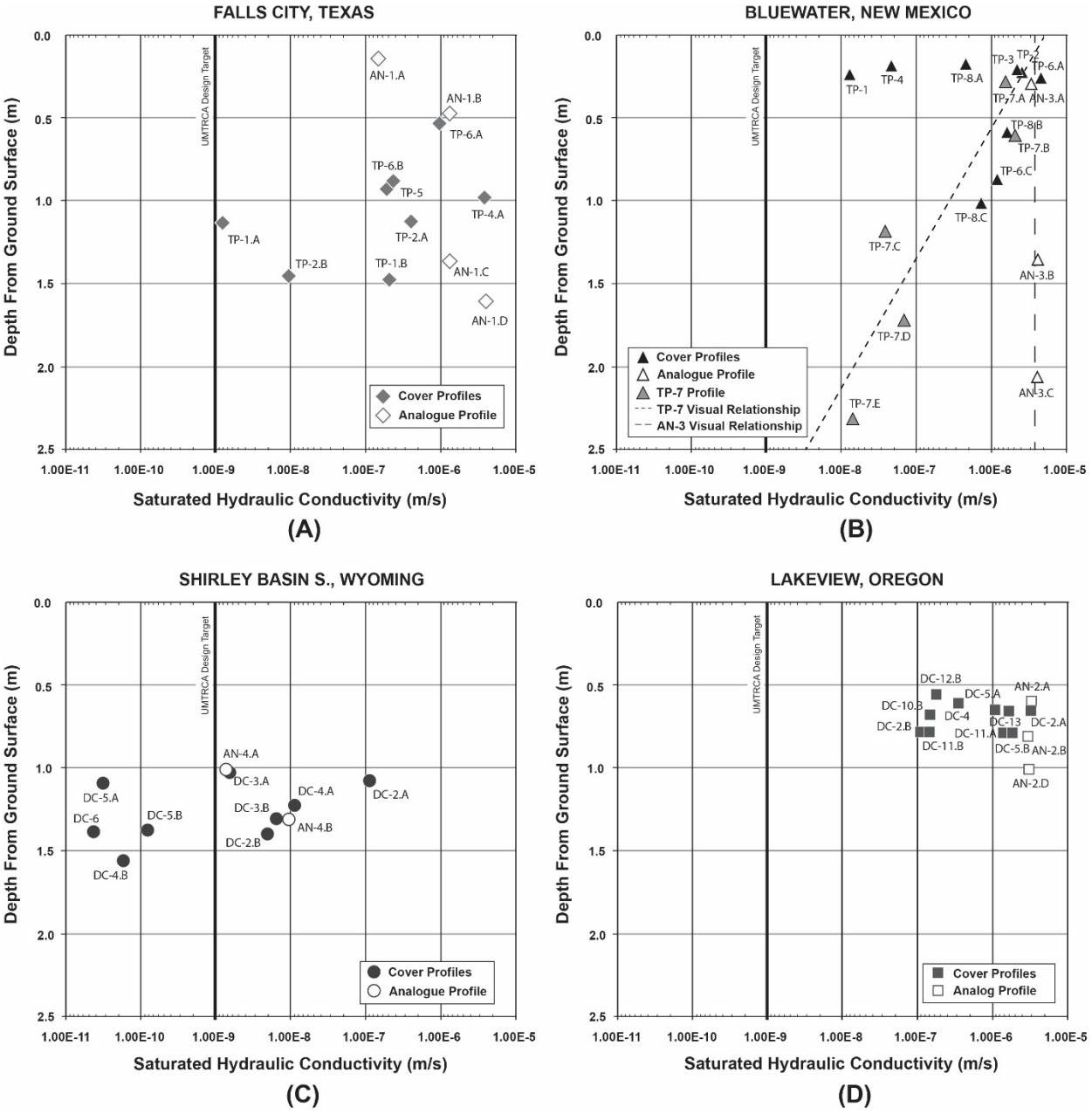

Figure 7-7 Relationship Between Depth from Ground Surface and Hydraulic Conductivity at Each Site

7.4 Summary and Implications

A point system developed by Lin et al. (1999a) was used to provide a quantitative measure of the morphological attributes in the radon barriers (e.g., moisture, texture, pedality, porosity, and root density) based on observations and measurements within the barrier profiles. This Total Soil Morphological Development Score ($_t$SMDS) was used to provide an overall score for each test pit. Lower $_t$SMDS values are associated with soils that have been subjected to low frequency or low intensity soil processes (e.g., infrequent very fine root growth) and therefore little morphological development. Higher $_t$SMDS values are associated with soils that have been subjected to a high frequency, long duration, and diverse set of soil processes (e.g., bioturbation by plants and animals, significant desiccation and cracking, freeze-thaw cycling) and have greater morphological development.

The range of $_t$SMDS among the test pits at Falls City was 5 – 847 while the analogue site was 1889. For Bluewater $_t$SMDS ranged from 31 – 10,688 and the two analogue sites were 5205 and 7439. At Shirley Basin South $_t$SMDS ranged from 7-202 and the analogue site was 703. Lakeview ranged from 20 -2350 and the analogue was 5366. Each site contained at least one pit that was not substantially affected by morphological development while other pits were altered, in some cases dramatically. Plant root growth is the largest contributor to the $_t$SMDS in the radon barriers that were studied. With few exceptions, roots were observed through the depth of the observed radon barrier profiles. Other contributors to a high $_t$SMDS include insect burrowing and desiccation cracking associated with volume change induced by root water uptake. Low $_t$SMDS was associated with wetter conditions induced by surface conditions such as ephemeral ponding, surface depressions and downslope drainages. These inferences are influenced by biased sampling approach that was employed in the study, where sampling locations were associated with surface conditions believed to contribute to development of soil structure. Different inferences may have been obtained had an unbiased sampling methodology been employed.

The radon diffusion coefficient, D_{Rn} increases as $_t$SMDS increases, indicating that radon barriers with greater structure have higher diffusion coefficients and higher radon fluxes for the same level of activity in the tailings. This relationship can be described by the linear model shown in Figure 7.2, which was obtained by least squares regression ($R^2 = 0.90$). In four of the five profiles with the highest D_{Rn}, the presence of plant roots is the dominant contributor to $_t$SMDS, indicating that plants contribute to increased radon diffusion.

A partial SMDS ($_p$SMDS) was calculated to constrain scoring to the depth of block samples for comparison to K_{sat}. K_{sat} and $_p$SMDS follow a high-low relationship more than a functional relationship. With few exceptions, the natural analogue samples, regardless of depth from ground surface, have the highest K_{sat} and $_p$SMDS values.

Under most conditions as radon barriers age, they begin to resemble the morphology of their natural analogue. These analogues are generally characterized by high $_p$SMDS and high K_{sat} (between 1.4×10^{-6} to 4.4×10^{-6} m s^{-1}), representing the upper bounds of K_{sat} proposed in NUREG/CR-7028.

Some cover profiles already display soil morphology matching their natural analogue, indicating that after only two decades of service, some locations on the covers investigated have approached a relative “stable-state” with the surrounding environment. These “stable-state”

radon barrier conditions are all characterized by higher SMDS, K_{sat}, and D_{Rn} compared to those profiles that presumably resemble closer to as-built conditions. Designers and regulators are encouraged to pursue further natural analogue studies to estimate "stable-states" with regards to engineering properties relevant to overall water balance and gas diffusion.

7.5 References

Albright, W.H., C.H. Benson, and W.J. Waugh, 2010. *Water Balance Covers for Waste Containment: Principles and Practice*, American Society of Civil Engineers (ASCE), Reston, Virginia.

Benson, C.H., W.H. Albright, D.O. Fratta, J.M. Tinjum, E. Kucukkirca, S.H. Lee, J. Scalia, P.D. Schlicht, and X. Wang, 2011. *Engineered Covers for Waste Containment: Changes in Engineering Properties and Implications for Long-Term Performance Assessment*, Vol. 1, NUREG/CR-7028, U.S. Nuclear Regulatory Commission Report.

Beven, K.J., 1982. "On Subsurface Stormflow: An Analysis of Response Times," *Hydrological Sciences Journal* 27(4):505–521.

Beven, K.J, 1984. "Infiltration into a Class of Vertically Non-Uniform Soils," *Hydrological Sciences Journal* 29(4):425–434.

Bruand, A., I. Cousin, B. Nicoullaud, O. Duval, and J.C. Begon, 1996. "Backscattered Electron Scanning Images of Soil Porosity for Analyzing Soil Compaction Around Roots," *Soil Science Society of America Journal* 60(3):895–901.

DOE (U.S. Department of Energy), 1989. *Technical Approach Document*, Rev. 2, UMTRA-DOE/AL 050425.0002, Uranium Mill Tailings Remedial Action Program, Albuquerque, New Mexico.

DOE (U.S. Department of Energy), forthcoming. *Soil Morphology, Plant Ecology, and Surface Change at the UMTRCA Title I Disposal Cell, Falls City, Texas,* LMS/FCT/S30757, Office of Legacy Management, to be published.

DOE (U.S. Department of Energy), forthcoming. *Soil Morphology, Plant Ecology, and Surface Change at the UMTRCA Title II Disposal Cell, Bluewater, New Mexico,* Office of Legacy Management, to be published.

DOE (U.S. Department of Energy), forthcoming. *Soil Morphology, Plant Ecology, and Surface Change at the UMTRCA Title II Disposal Cell, Shirley Basin South, Wyoming,* Office of Legacy Management, to be published.

DOE (U.S. Department of Energy), forthcoming. *Soil Morphology, Plant Ecology, and Surface Change at the UMTRCA Title I Disposal Cell, Lakeview, Oregon,* Office of Legacy Management, to be published.

Guidi, G., G. Poggio, and G. Petruzzelli, 1985. "The Porosity of Soil Aggregates from Bulk Soil and from Soil Adhering to Roots," *Plant and Soil* 87(2):311–314.

Lin, H.S., K.J. McInnes, L.P. Wilding, and C.T. Hallmark, 1999a. "Effects of Soil Morphology on Hydraulic Properties I. Quantification of Soil Morphology," *Soil Science Society of America Journal* 63(4):948–954.

Lin, H.S., K.J. McInnes, L.P. Wilding, and C.T. Hallmark, 1999b. "Effects of Soil Morphology on Hydraulic Properties II, Hydraulic Pedotransfer Functions," *Soil Science Society of America Journal* 63(4):955–961.

McCuen, R.H., and W.M. Snyder, 1986. *Hydrologic Modeling—Statistical Methods and Applications,* Prentice-Hall, Englewood Cliffs, New Jersey.

Michaud, A.M., 2018. *Long-Term Performance of Radon Barriers in Limiting Radon Flux from Four Uranium Mill Tailings Containment Facilities*, thesis for Master of Science, University of Wisconsin-Madison.

Nielson, K.K., and V.C. Rogers, 1982. *A Mathematical Model for Radon Diffusion in Earthen Materials*, NUREG/CR-2765; PNL-4301; RAE-18-2, Rogers and Associates Engineering Corporation, Salt Lake City, Utah.

Nielson, K.K., V.C. Rogers, and G.W. Gee, 1984. "Diffusion of Radon Through Soils: A Pore Distribution Model," *Soil Science Society of America Journal* 48(3):482–487.

NRC (U.S. Nuclear Regulatory Commission), 1989. *Calculation of Radon Flux Attenuation by Earthen Uranium Mill Tailings Covers*, Regulatory Guide 3.64, U.S. Nuclear Regulatory Commission, Washington DC.

Shoup, T.E., 1982. *A Practical Guide to Computer Methods for Engineers*, Prentice-Hall, Englewood Cliffs, New Jersey.

Stefani, N., 2016. *Field and Laboratory Measurement of Radon Flux and Diffusion for Uranium Mill Tailings Cover Systems*, thesis for Master of Science, University of Wisconsin-Madison.

USDA (U.S. Department of Agriculture), 2012. *Field Book for Describing and Sampling Soils*, version 3.0, Natural Resource Conservation Service.

Waugh, W.J., S.J. Morrison, G.M. Smith, M. Kautsky, T.R. Bartlett, C.E. Carpenter, and C.A. Jones, 1999. *Plant Encroachment on the Burrell, Pennsylvania, Disposal Cell: Evaluation of Long-Term Performance and Risk*, GJO-99-96-TAR, U.S. Department of Energy.

Waugh, W.J., G. Smith, B. Danforth, G. Gee, V. Kothari, and T. Pauling, 2007. "Performance Evaluation of the Engineered Cover at the Lakeview, Oregon, Uranium Mill Tailings Site," in *Global Accomplishments in Environmental and Radioactive Waste Management: Education and Opportunity for the Next Generation of Waste Management Professionals*, Vol. 6, proceedings of Waste Management Symposium 2007, Tucson, Arizona.

8 SUMMARY AND CONCLUSIONS

This study was conducted to evaluate the impact of in-service conditions on radon (Rn) barriers in earthen final covers. Rn barriers were studied at four uranium mill tailings disposal facilities that had been closed for approximately 20 years. Soil profiles representing natural analogues were also evaluated at each facility to draw an inference regarding the in-service condition that may exist in the very long term. Understanding alterations in the hydraulic conductivity and gaseous diffusivity of radon barriers was the primary objective of the study. Soil structure in the Rn barrier and overlying soil layers was also studied. The influence of features on the surface of a final cover (e.g., vegetation, insects, etc.) on soil structure, hydraulic conductivity, and transmission of radon gas in Rn barriers was also evaluated. Based on this assessment, the following conclusions and recommendations are made.

Soil Morphology of Radon Barriers. Soil structure developed in all of the Rn barriers, apparently in response to plant rooting, volume change due to root water uptake, and biota intrusion (e.g., insect burrowing). With few exceptions, roots and soil structure were observed throughout the depth of the Rn barriers. Deep-rooted woody plants and harvester ants contributed to greater structural development than other biota. These findings indicate that soil structure changes should be anticipated when conducting performance assessments, with engineered properties reflecting structural development when evaluating near term and very long-term conditions.

Cover management can significantly contribute to limiting the impact of deep-rooted woody vegetation on soil structure in the near term. Actively managed vegetated covers generally offered more protection to the radon barrier through time compared to un-managed riprap armored covers. In the very long-term, however, active management likely will not exist. Performance assessments should acknowledge this long-term condition when selecting engineering properties for modeling.

Radon Flux. The overall Rn-222 flux emitted from each Rn barrier was below 0.74 $Bq/m^2/s$ (a sitewide annual average flux requirement) after about 20 years of service. A slight increase over the as-built Rn flux was evident for some of the barriers. However, the intentionally biased sampling procedure and differences between the methods used in this study for measuring Rn flux relative to those used in the as-built condition precluded making inferences regarding sitewide in-service Rn fluxes. Rn fluxes were higher in regions where woody vegetation (mesquite, salt bush, and bitterbrush) or aggressive insects had established on the cover, suggesting that the vegetation and insect instruction affected the performance of the barrier in these locations. These higher fluxes are attributed to soil structure induced by root activity and insect burrowing in the Rn barrier, as well as higher diffusion coefficients associated with lower water saturation in areas influenced by root water uptake.

Computations of Rn diffusion made during design of UMTRCA final covers were based on the assumption that the Rn barrier is a homogenous medium. This assumption is not realized for in-service covers; the Rn flux is spatially variable, with areas of higher flux apparently associated with preferential transport pathways. Models to account for evolving and more complex Rn transport processes should be developed for predicting the long-term performance of Rn barriers in final covers.

A new method involving Pb-210 profiles was developed in this study to quantify average Rn-222 fluxes over decades. This method involves Pb-210 profiles in the Rn barrier, which can be measured on cores obtained at multiple locations using conventional sampling techniques. Rn fluxes interpreted from these profiles can be used to assess how the flux changes as a Rn barrier ages.

Hydraulic Conductivity. The saturated hydraulic conductivity of the Rn barriers at three of the four sites typically fell within the range recommended in NUREG CR-7028 to represent long-term in-service conditions (1.0×10^{-7} to 5.0×10^{-6} m/s), regardless of depth or thickness of the cover or radon barrier. These saturated hydraulic conductivities are 2 to 3 orders of magnitude above the common 1.0×10^{-9} m/s design criterion established for low-conductivity Rn barriers. One Rn barrier was an exception. This barrier was constructed with a naturally occurring montmorillonitic clay analogous to bentonite, and had lower saturated hydraulic conductivity falling below the range identified in NUREG CR-7028. The higher saturated hydraulic conductivities measured at three of the four sites likely were caused by development of soil structure within the Rn barriers.

Saturated hydraulic conductivities measured on block samples collected from the analogue profiles generally were at the upper end of the range of the hydraulic conductivities measured for a given cover, and at the high end of the range identified in NUREG CR-7028. This suggests that additional increases in hydraulic conductivity are likely to occur in the Rn barriers that were evaluated, and that the upper bound of the range in NUREG CR-7028 likely is a reasonable end state to use for saturated hydraulic conductivity when modeling the hydrology of final covers for performance assessments

An additional objective of this investigation was to evaluate whether the in-service saturated hydraulic conductivity was depth dependent, based on the premise that the surface processes that induce soil structure should diminish with greater depth. In the radon barriers that were studied, all of which were < 2.5 m bgs, no relationship between saturated hydraulic conductivity and depth could be identified. In only one case was the hydraulic conductivity at depth lower than at locations closer to the surface, and only for two samples. Moreover, no dependence on depth was identified in the saturated hydraulic conductivity of the analogue profiles. These findings suggest that increases in saturated hydraulic conductivity should be anticipated in Rn barriers at all depths less than 2.5 m bgs, and that performance assessments should not incorporate depth-dependent saturated hydraulic conductivity for Rn barriers.

Natural Analogues. The findings from this study indicated that natural analogues can be effective when assessing the very long-term condition that is likely to exist in final covers, and Rn barriers in particular. A comparison of a proposed design relative to an analogue will provide insight into the changes that are likely to occur as the cover evolves and equilibrates with the surrounding environment. In this study, the natural analogues were provided insight into the long-term hydraulic properties that can be expected for Rn barriers. Similar assessments were not possible for Rn fluxes and gas diffusion coefficients within the scope of the study. Field work using gas tracers at analogue sites could be conducted to assess the efficacy of natural analogues for identifying diffusion coefficients representative of the long-term equilibrium state.

Natural analogues can also be used to identify final cover designs that are more resilient to long-term change. The Rn barrier that maintained lower hydraulic conductivity closely mimics the natural analogue, and was constructed with montmorillonitic clays that are resistant to degradation in the local environment. In effect, the cover was effectively constructed near its

equilibrium condition. The radon barrier in this cover had the lowest saturated hydraulic conductivity and lowest radon diffusion coefficient of all four covers studied. Incorporating natural analogue studies is recommended to identify more resilient cover designs that are more congruent with the natural environment.

Monitoring. The alterations in soil structure, saturated hydraulic conductivity, and radon flux observed in this study are anticipated to occur within all earthen final covers at disposal sites. They were documented in this study because explicit measurements were made to characterize the in-service condition. Similar processes are likely occurring at other sites, with the potential to impact environmental performance of the facility. These findings suggest that performance monitoring programs should be developed to evaluate changes in final covers during the service life, and the potential impact on these changes on the containment system. Performance monitoring can provide an early warning of potential changes in performance, allowing adaptive management before a compliance monitoring system indicates more substantive problems that require corrective action. Performance monitoring systems should be developed during design and incorporated during construction. They should be flexible and adaptable so that the system can evolve as technology changes.

Cross-Disciplinary Expertise. The findings in this study illustrate the value of cross-disciplinary expertise in evaluating and interpreting the performance of final covers at disposal sites. In this study, cross-disciplinary expertise in characterizing hydrologic properties, gas fluxes, plant ecology, and soil morphology was critical to understanding the changes that occur in Rn barriers while in service, and the mechanisms controlling the long-term performance of Rn barriers. Future studies should involve cross-disciplinary teams whenever practical to achieve maximum impact.

Presentations and Publications (To Date)

Benson, C.H., K. Tian, W.H. Albright, M. Fuhrmann, W.J. Likos, N. Stefani, W.J. Waugh, and M.M. Williams, 2017. *Radon Fluxes from an Earthen Barrier Over Uranium Mill Tailings After Two Decades of Service,* Proceedings from the 2017 Waste Management Conference, Phoenix, Arizona.

Benson, C.H., W.H. Albright, W.J. Waugh, and M.M. Davis, 2018. "Field Hydrologic Performance of Earthen Covers for Uranium Mill Tailings Disposal Sites on the Colorado Plateau." Long-Term Stewardship Conference, August 20-23, 2018, U.S. Department of Energy Office of Legacy Management, Grand Junction, CO.

Fuhrmann, M., C. Benson, J. Waugh, H. Arlt, and M. M. Williams, 2019a. *Proceedings of the Radon Barriers Workshop*, NUREG/CP-0312, U.S. Nuclear Regulatory Commission, Washington, D.C.

Fuhrmann, M., C. H. Benson, W. J. Likos, N. Stefani, A. Michaud, W. J. Waugh, and M. M. Williams, 2021, Radon Fluxes at Four Uranium Mill Tailings Disposal Sites after About 20 Years of Service, *Journal of Environmental Radioactivity*, in press.

Fuhrmann, M., A. Michaud, M. Salay, C.H. Benson, W.J. Likos, N. Stefani, W.J. Waugh, and M.M. Williams, 2019b. "Lead-210 Profiles in Radon Barriers, Indicators of Long-Term Radon-222 Transport," *Applied Geochemistry*, 110, 104434.

Fuhrmann, M., A. Michaud, M. Salay, C.H. Benson, W.J. Likos, N. Stefani, W.J. Waugh, and M.M. Williams, 2018. "Lead-210 Profiles in Radon Barriers, Indicators of Long-Term Radon-222 Transport", Long-Term Stewardship Conference, August 20-23, 2018, U.S. Department of Energy Office of Legacy Management, Grand Junction, CO.

Michaud, A.M., 2018. *Long-Term Performance of Radon Barriers in Limiting Radon Flux From Four Uranium Mill Tailings Containment Facilities*, thesis for Master of Science, University of Wisconsin-Madison.

Stefani, N., 2016. *Field and Laboratory Measurement of Radon Flux and Diffusion for Uranium Mill Tailings Cover Systems*, thesis for Master of Science, University of Wisconsin-Madison.

Stefani, N., Michaud, A., Likos, W., Benson, C., Fuhrmann, M., Waugh, J., and Williams, M. (2020), Comparison of Methods to Measure Radon Flux from Earthen Radon Barriers over Uranium Mill Tailings, Geotechnical Testing J., in review.

Waugh, W.J, W.H. Albright, C.H. Benson, D.C. Dander, M. Fuhrmann, C.N. Joseph, W.J. Likos, D.A. Marshall, A.M. Michaud, A. Tigar and M.M. Williams, 2018a. "Evaluating the ecology and performance of conventional and evapotranspiration covers for uranium mill tailings disposal cells." In: Proceedings of Ecological Society of America 2018, August 5-10, 2018; New Orleans, Louisiana.

Waugh, W.J., W.H. Albright, C.H. Benson, C.N. Joseph, D.A. Marshall, and A.D. Tigar, 2018b. "Are Natural Processes Transforming Conventional Disposal Cell Covers into Evapotranspiration Covers? Should We Enhance Beneficial Processes?" Long-Term

Stewardship Conference, August 20-23, 2018, U.S. Department of Energy Office of Legacy Management, Grand Junction, CO.

Williams, M.M., 2018. “The Spatial Development of Soil Architecture at Four UMTRCA Sites: Implications to Hydraulic Conductivity and Long-Term Performance” Long-Term Stewardship Conference, August 20-23, 2018, U.S. Department of Energy Office of Legacy Management, Grand Junction, CO.

Williams, M.M., 2019. *Pedogenic Process in Engineered Soils for Radioactive Waste Containment*, Dissertation for Doctor of Philosophy, University of California, Berkeley.

NRC FORM 335
(12-2010)
NRCMD 3.7

U.S. NUCLEAR REGULATORY COMMISSION

BIBLIOGRAPHIC DATA SHEET

(See instructions on the reverse)

1. REPORT NUMBER

NUREG/CR-7288
Volume 1

2. TITLE AND SUBTITLE

Evaluation of In-Service Radon Barriers over Uranium Mill Tailings Disposal Facilities

3. DATE REPORT PUBLISHED

MONTH	YEAR
March	2022

4. FIN OR GRANT NUMBER

5. AUTHOR(S)

M. Williams, M. Fuhrmann, N. Stefani, A. Michaud, W. Likos, C. Benson, W. Waugh

6. TYPE OF REPORT

Technical

7. PERIOD COVERED (Inclusive Dates)

2019-2021

8. PERFORMING ORGANIZATION - NAME AND ADDRESS (If NRC, provide Division, Office or Region, U. S. Nuclear Regulatory Commission, and mailing address; if contractor, provide name and mailing address.)

Geological Engineering, University of Wisconsin-Madison, 1415 Engineering Drive, Madison, WI 53706 USA

9. SPONSORING ORGANIZATION - NAME AND ADDRESS (If NRC, type "Same as above", if contractor, provide NRC Division, Office or Region, U. S. Nuclear Regulatory Commission, and mailing address.)

Division of Risk Analysis, Office of Nuclear Regulatory Research, U. S. Nuclear Regulatory Commission

10. SUPPLEMENTARY NOTES

11. ABSTRACT (200 words or less)

Earthen final covers over uranium mill tailings and associated wastes were investigated at four sites that had been in service for approximately 20 years: Falls City in Texas, Bluewater in New Mexico, Shirley Basin South in Wyoming, and Lakeview in Oregon. Test pits were excavated, radon fluxes were measured, soil morphological observations made, and samples were collected to determine saturated hydraulic conductivity, soil water characteristic curves, Pb-210 concentrations, and related properties. Saturated hydraulic conductivity of the Rn barriers at three of the four sites typically fell within values of 1.0×10^{-7} to 5.0×10^{-6} m/s, regardless of depth or thickness of the cover or radon barrier. One Rn barrier was an exception, with some hydraulic conductivities as low as 10^{-11}m/s. A slight increase over as-built Rn flux was evident for some of the barriers, but site-wide flux comparisons to as-built values are inappropriate because of different sampling and analytical methods used between current and site closure surveys. These higher fluxes are attributed to soil structure induced by root activity and insect burrowing in the Rn barrier, as well as higher Rn diffusion coefficients associated with lower water saturation in areas influenced by root water uptake. A method to use Pb-210 concentration profiles to quantify long-term (decades) Rn-222 fluxes was developed.

12. KEY WORDS/DESCRIPTORS (List words or phrases that will assist researchers in locating the report.)

UMTRCA, radon barriers, hydraulic conductivity, radon flux, Rn diffusion coefficient, soil morphology, uranium mill tailings, mill tailings covers, Pb-210, Rn-222

13. AVAILABILITY STATEMENT

unlimited

14. SECURITY CLASSIFICATION

(This Page)

unclassified

(This Report)

unclassified

15. NUMBER OF PAGES

16. PRICE

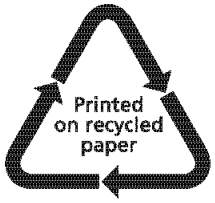

Federal Recycling Program

UNITED STATES
NUCLEAR REGULATORY COMMISSION
WASHINGTON, DC 20555-0001

OFFICIAL BUSINESS

NUREG/CR-7288
Volume 1

Evaluation of In-Service Radon Barriers over Uranium Mill Tailings Disposal Facilities

March 2022